

PAGES 117-228

ISSN 0003-2654



The Analyst

A monthly international journal dealing with all branches of the theory and practice of analytical chemistry, including instrumentation and sensors, and physical, biochemical, clinical, pharmaceutical, biological, environmental, automatic and computer-based methods

Vol.117 No.2 February 1992

The Analyst

The Analytical Journal of The Royal Society of Chemistry

Analytical Editorial Board

Chairman: A. G. Fogg (Loughborough, UK)

K. D. Bartle (Leeds, UK)	S. J. Hill (Plymouth, UK)
D. Betteridge (Sunbury-on-Thames, UK)	D. L. Miles (Keyworth, UK)
J. Egan (Cambridge, UK)	J. N. Miller (Loughborough, UK)
H. M. Frey (Reading, UK)	R. M. Miller (Port Sunlight, UK)
D. E. Games (Swansea, UK)	B. L. Sharp (Loughborough, UK)

Advisory Board

J. F. Alder (Manchester, UK)	E. Pungor (Budapest, Hungary)
A. M. Bond (Victoria, Australia)	J. Růžicka (Seattle, WA, USA)
R. F. Browner (Atlanta, GA, USA)	R. M. Smith (Loughborough, UK)
D. T. Burns (Belfast, UK)	M. Stoeppel (Jülich, Germany)
J. G. Dorsey (Cincinnati, OH, USA)	J. D. R. Thomas (Cardiff, UK)
L. Ebdon (Plymouth, UK)	J. M. Thompson (Birmingham, UK)
A. F. Fell (Bradford, UK)	K. C. Thompson (Sheffield, UK)
J. P. Foley (Villanova, PA, USA)	P. C. Uden (Amherst, MA, USA)
T. P. Hadjiioannou (Athens, Greece)	A. M. Ure (Aberdeen, UK)
W. R. Heineman (Cincinnati, OH, USA)	P. Vadgama (Manchester, UK)
A. Hulanicki (Warsaw, Poland)	C. M. G. van den Berg (Liverpool, UK)
K. Karube (Yokohama, Japan)	A. Walsh, K.B. (Melbourne, Australia)
E. J. Newman (Poole, UK)	J. Wang (Las Cruces, NM, USA)
T. B. Pierce (Harwell, UK)	T. S. West (Aberdeen, UK)

Regional Advisory Editors

For advice and help to authors outside the UK

- Professor Dr. U. A. Th. Brinkman**, Free University of Amsterdam, 1083 de Boelelaan, 1081 HV Amsterdam, THE NETHERLANDS.
- Professor Dr. sc. K. Dittich**, Institute for Analytical Chemistry, University Leipzig, Linnéstr. 3, D-0-7010 Leipzig, GERMANY.
- Dr. O. Osibanjo**, Department of Chemistry, University of Ibadan, Ibadan, NIGERIA.
- Professor K. Saito**, Coordination Chemistry Laboratories, Institute for Molecular Science, Myodaiji, Okazaki 444, JAPAN.
- Professor M. Thompson**, Department of Chemistry, University of Toronto, 80 St. George Street, Toronto, Ontario M5S 1A1, CANADA.
- Professor Dr. M. Valcárcel**, Departamento de Química Analítica, Facultad de Ciencias, Universidad de Córdoba, 14005 Córdoba, SPAIN.
- Professor J. F. van Staden**, Department of Chemistry, University of Pretoria, Pretoria 0002, SOUTH AFRICA.
- Professor Yu Ru-Qin**, Department of Chemistry and Chemical Engineering, Hunan University, Changsha, PEOPLES REPUBLIC OF CHINA.
- Professor Yu. A. Zolotov**, Kurnakov Institute of General and Inorganic Chemistry, 31 Lenin Avenue, 117907, Moscow V-71, USSR.

Editorial Manager, Analytical Journals: Judith Egan

Editor, The Analyst

Harpal S. Minhas

The Royal Society of Chemistry,
Thomas Graham House, Science Park,
Milton Road, Cambridge CB4 4WF, UK
Telephone 0223 420066.
Fax 0223 423623. Telex No. 818293 ROYAL.

US Associate Editor, The Analyst

Dr J. F. Tyson

Department of Chemistry,
University of Massachusetts,
Amherst MA 01003, USA
Telephone 413 545 0195
Fax 413 545 4490

Senior Assistant Editor

Paul Delaney

Assistant Editors

Brenda Holliday, Paula O'Riordan, Sheryl Whitewood

Editorial Secretary: Claire Harris

Advertisements: Advertisement Department, The Royal Society of Chemistry, Burlington House, Piccadilly, London, W1V 0BN. Telephone 071-437 8656. Telex No. 268001. Fax 071-437 8883.

The Analyst (ISSN 0003-2654) is published monthly by The Royal Society of Chemistry, Thomas Graham House, Science Park, Milton Road, Cambridge CB4 4WF, UK. All orders, accompanied with payment by cheque in sterling, payable on a UK clearing bank or in US dollars payable on a US clearing bank, should be sent directly to The Royal Society of Chemistry, Turpin Transactions Ltd., Blackhorse Road, Letchworth, Herts SG6 1HN, United Kingdom. Turpin Transactions Ltd., distributors, is wholly owned by the Royal Society of Chemistry. 1992 Annual subscription rate EC £276.00, USA \$589, Rest of World £310.00. Purchased with Analytical Abstracts EC £604.00, USA \$1299.00, Rest of World £669.00. Purchased with Analytical Abstracts plus Analytical Proceedings EC £712.00, USA \$1527.00, Rest of World £791.00. Purchased with Analytical Proceedings EC £551.00, USA \$749.00, Rest of World £395.00. Air freight and mailing in the USA by Publications Expediting Inc., 200 Meacham Avenue, Elmont, NY 11003.

USA Postmaster: Send address changes to: The Analyst, Publications Expediting Inc., 200 Meacham Avenue, Elmont, NY 11003. Second class postage paid at Jamaica, NY 11431. All other despatches outside the UK by Bulk Airmail within Europe, Accelerated Surface Post outside Europe. PRINTED IN THE UK.

Information for Authors

Full details of how to submit material for publication in The Analyst are given in the Instructions to Authors in the January issue. Separate copies are available on request.

The Analyst publishes papers on all aspects of the theory and practice of analytical chemistry, fundamental and applied, inorganic and organic, including chemical, physical, biochemical, clinical, pharmaceutical, biological, environmental, automatic and computer-based methods. Papers on new approaches to existing methods, new techniques and instrumentation, detectors and sensors, and new areas of application with due attention to overcoming limitations and to underlying principles are all equally welcome. There is no page charge.

The following types of papers will be considered:

Full research papers.

Communications, which must be on an urgent matter and be of obvious scientific importance. Rapidity of publication is enhanced if diagrams are omitted, but tables and formulae can be included. Communications receive priority and are usually published within 5-8 weeks of receipt. They are intended for brief descriptions of work that has progressed to a stage at which it is likely to be valuable to workers faced with similar problems. A fuller paper may be offered subsequently, if justified by later work. Although publication is at the discretion of the Editor, communications will be examined by at least one referee.

Reviews, which must be a critical evaluation of the existing state of knowledge on a particular facet of analytical chemistry.

Every paper (except Communications) will be submitted to at least two referees, by whose advice the Editorial Board of The Analyst will be guided as to its acceptance or rejection. Papers that are accepted must not be published elsewhere except by permission. Submission of a manuscript will be regarded as an undertaking that the same material is not being considered for publication by another journal.

Regional Advisory Editors. For the benefit of potential contributors outside the United Kingdom and North America, a Group of Regional Advisory Editors exists. Requests for help or advice on any matter related to the preparation of papers and their submission for publication in The Analyst can be sent to the nearest member of the Group. Currently serving Regional Advisory Editors are listed in each issue of The Analyst.

Manuscripts (four copies typed in double spacing) should be addressed to:

Harpal S. Minhas, Editor, The Analyst,
Royal Society of Chemistry,
Thomas Graham House,
Science Park, Milton Road,
CAMBRIDGE CB4 4WF, UK or:

Dr J. F. Tyson
US Associate Editor, The Analyst
Department of Chemistry
University of Massachusetts
Amherst MA 01003, USA

Particular attention should be paid to the use of standard methods of literature citation, including the journal abbreviations defined in Chemical Abstracts Service Source Index. Wherever possible, the nomenclature employed should follow IUPAC recommendations, and units and symbols should be those associated with SI.

All queries relating to the presentation and submission of papers, and any correspondence regarding accepted papers and proofs, should be directed either to the Editor, or Associate Editor, The Analyst (addresses as above). Members of the Analytical Editorial Board (who may be contacted directly or via the Editorial Office) would welcome comments, suggestions and advice on general policy matters concerning The Analyst.

Fifty reprints are supplied free of charge.

© The Royal Society of Chemistry, 1992. All rights reserved. No part of this publication may be reproduced, stored in a retrieval system, or transmitted in any form, or by any means, electronic, mechanical, photographic, recording, or otherwise, without the prior permission of the publishers.

Information Should Be A Solution, Not A Problem

STN International helps scientists and engineers solve problems.

Devoted exclusively to scientific and technical information, STN offers more than 100 databases from leading scientific organizations around the world. Our files, command language, and customer support are designed especially to make information retrieval easy and effective. Think of STN for chemistry, physics, bioscience, materials science, engineering, geoscience, health-and-safety, and other technical fields.

Discover STN and uncover a wealth of information for science and technology.

Enquirers from Eire or UK, please return to:

STN International
c/o Royal Society of Chemistry
Thomas Graham House
Science Park
Milton Road
Cambridge CB4 4WF
United Kingdom
STN Help Desk (0223) 420237



Circle 002 for further information

BOOKS FROM WILEY

Principles and Practice of Spectroscopic Calibration

H. MARK, Bran & Luebbe Analyzing Technologies, USA

Clearly linking theory with applications, this unique guide to spectroscopic calibration advances an approach that is understandable, free of the usual uncertainties, and simple to execute. The book details the practical aspects of generating a calibration equation, as well as the basics of recognizing and dealing with different types of problems affecting calibration.

0471546143 190pp 1991 \$59.00/\$89.50

Activation Spectrometry in Chemical Analysis

S.J. PARRY, University of London, UK

In clear, easy-to-read language this book provides a straightforward review of just what activation analysis can do, describing the technique as it is currently applied to analytical problems. With emphasis on activation spectrometry, the book outlines the specifics of the procedure, which, along with other activation analysis methods, have proven critical to the technique's success.

Series: Volume 119 in *Chemical Analysis: A Series of Monographs on Analytical Chemistry and its Applications*
0471638447 258pp 1991 \$63.00/\$95.00

Trace and Ultratrace Analysis by HPLC

S. AHUJA, CIBA-Geigy Corp, NY, USA

The most popular separation technique used for trace and ultratrace analysis is high pressure/performance liquid chromatography (HPLC). For the analyses of DNA and RNA, HPLC is proving extremely useful. Trace and ultratrace analyses could provide potentially helpful data for diagnostic studies. The book deals with both analyses executed at or below ppm level and on-column injection at low microgram or nanogram level.

Series: Volume 115 in *Chemical Analysis: A Series of Monographs on Analytical Chemistry and its Applications*
0471514195 approx 320pp due Feb 1992 approx \$60.00/\$87.00

Structural and Chemical Analysis of Materials

**X-ray, electron and neutron diffraction
X-ray, electron and ion spectrometry
Electron microscopy**

J.P. EBERHART, Louis Pasteur University, Strasbourg, France

This book provides a comprehensive and coherent survey of the theoretical and practical aspects of the more important techniques used in materials analysis. Introductory chapters discuss the way in which X-rays and particle beams interact with matter, followed by a section explaining the generation and measurement of radiation, thus establishing the underlying principles for the techniques described later.

0471929778 576pp 1991 \$95.00/\$202.15

Periodic Table for Chromatographers

M. LEDERER, University of Lausanne, Switzerland

This is a collection of equilibrium constants for both heterogeneous and homogeneous systems which cover the entire periodic table. They are of interest for comparing interactions under different conditions for example, to compare complexing reactions with various acids. The arrangement of data in this way also facilitates the planning of separations for analysis.

0471931497 136pp 1991 \$60.00/\$128.00

Wiley books are available through your bookseller. Alternatively order direct from Wiley (payment to John Wiley & Sons Ltd). Credit card orders accepted by telephone - (0243) 829121. Please note that prices quoted here apply to UK and Europe only.

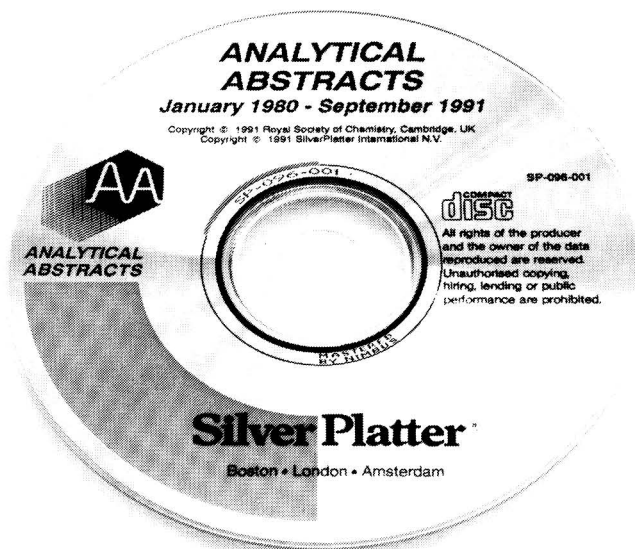
JOHN WILEY & SONS LTD
BAFFINS LANE · CHICHESTER
WEST SUSSEX PO19 1UD · UK



WILEY
Publishers Since 1807

Circle 001 for further information

Analytical Abstracts Now on CD-ROM!



See us on
Stand No. 5429
The Pittsburgh Conference
New Orleans, USA
March 9th–12th 1992

The premier source of current awareness information in analytical chemistry is now available on a single SilverPlatter CD-ROM.

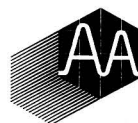
Analytical Abstracts on CD-ROM features:

- Approximately 140,000 items from 1980 onwards
- Easy to use SilverPlatter software
- Quarterly updates with more than 3,000 items
- Unlimited searching – no additional costs

Special Discount for Hardcopy Subscribers

Contact us today for further information and a FREE demo disk.

Judith Barnsby, Royal Society of Chemistry,
Thomas Graham House, Science Park, Milton Road,
Cambridge CB4 4WF, United Kingdom
Tel: +44 (0) 223 420066 Fax: +44 (0) 223 423623
Telex: 818293 ROYAL



ROYAL
SOCIETY OF
CHEMISTRY



Information
Services

On-line Microwave Digestion of Slurry Samples With Direct Flame Atomic Absorption Spectrometric Elemental Detection

Stephen J. Haswell and David Barclay

School of Chemistry, University of Hull, Hull HU6 7RX, UK

A flow injection (FI) system for on-line microwave digestion of slurried samples with direct elemental determinations by flame atomic absorption spectrometry is described. Organically based elemental reference samples were prepared as slurries in 5% v/v HNO_3 and the system was optimized for slurry mass, acid strength and tube and microwave cavity geometry. Bubble formation during digestion was controlled by post-digestion cooling and pressure regulation. Comparison of direct and FI calibrations indicated no apparent loss in sensitivity. Various samples were examined and elemental recoveries for Ca, Fe, Mg and Zn were typically found to be in the range 94–107% with precisions of less than 4.5% relative standard deviation. The major source of error was found to be in the dispersion of solids ($<180\text{ }\mu\text{m}$) as slurries in dilute HNO_3 . The throughput of samples in the system developed was found to be 1–2 min per sample.

Keywords: Microwave digestion; on-line digestion; flame atomic absorption spectrometry; elemental analysis; flow injection

The decomposition of samples by microwave digestion prior to trace elemental determination has now become a popular method with many analysts for a wide range of matrix types.¹ To date, the majority of digestions described have been based upon a batch technique, in which the microwave digestion replaces traditional wet or dry ashing methodology.^{2,3} The move to a microwave digestion approach offers many advantages over the conventional methods including reduction in digestion time, digestion of difficult matrices and dissolution in what is essentially a closed environment, which reduces volatile analyte loss and atmospheric contamination.¹ Despite these obvious advantages, the batch type of approach to sample digestion is still prone to contamination problems associated with the sample, reagent and containment together with analyte loss and potential errors from volumetric transfers. Many of these problems can be overcome or controlled by adopting a flow injection (FI) methodology.⁴ It would seem therefore that the advantages of a microwave digestion approach to sample dissolution could be further improved by incorporating the digestion into an FI manifold. There have been only a few reports of systems based upon this approach^{5–6} to date, and none of the methodologies describes a continuous-flow system with on-line microwave digestion. This paper reports the development of such an FI system with on-line microwave digestion coupled directly to an atomic absorption (AA) spectrometer for elemental determination.

Experimental

Apparatus

A schematic diagram of the on-line digestion system is shown in Fig. 1 and was assembled as follows: (i) an Ismatec pump MV-Z; (ii) a Rheodyne injection valve (Anachem 5020) with a 1 ml sample injection loop; (iii) a CEM MDS81 microwave oven containing 20 m of 0.8 mm i.d. poly(tetrafluoroethylene) (PTFE) tubing; (iv) a 5 m cooling loop in an antifreeze bath cooled by six Peltier devices (MI 1069T-03AC, Marlow Industries, Tadworth, UK); (v) a Rheodyne injection valve (Anachem 5020) with an in-line back-flush filter fitted in the place of the injection loop; (vi) a CEM pressure sensor; and (vii) a 516.75 kPa (75 psi) back-pressure regulator (Anachem P736). The outlet from the back-pressure regulator was coupled directly to the nebulizer of an AA spectrometer (Thermoelectron 357) using 0.8 mm i.d. PTFE tubing (Anachem 33-1331). The same tubing was used throughout the system for all couplings and loops. A magnetic stirrer for

slurry preparation and a chart recorder (Linseis LS52) for data collection were also used.

Reagents

Concentrated nitric acid and all 1000 ppm standards were of AnalaR quality supplied by Merck (Poole, Dorset, UK) and the water used was distilled, de-ionized. The following Certified Reference Materials (CRMs) were used: Chlorella, Mussel, Sargasso and Pepperbush supplied by National Institute for Environmental Studies (NIES), Japan, together with a National Institute of Standards and Technology (NIST) Standard Reference Material (SRM) 1577a Bovine Liver.

Procedure

Calibration was carried out by filling the 1 ml sample loop of the injector with standards prepared in 5% v/v HNO_3 within the linear calibration range for each of the elements studied as follows: Ca, 0–2 ppm; Fe, 0–4 ppm; Mg, 0–0.4 ppm; and Zn, 0–0.8 ppm. In addition, calibration was performed directly

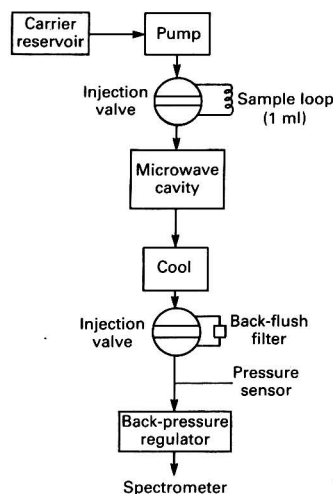


Fig. 1 Schematic diagram of the on-line microwave digestion FI system

with the AA spectrometer, *i.e.*, without the FI system in place. Slurries of the reference materials were prepared by accurately weighing an appropriate mass (50–500 mg) of the solid (<180 μm) into a beaker and adding dilute HNO_3 (5% v/v; 25–250 ml) using a pipette to obtain a slurry in the range 0.005–0.5% m/v. The selection of a suitable percentage slurry was dictated by the elemental concentration in the particular sample but was chosen to give an acceptable minimum mass (not less than 25 mg) without producing a slurry of greater than 1%. It was observed that for some samples a slurry of >1% could cause blockages in the small apertures within the switching plate of the Rheodyne valve. The slurries were agitated by a magnetic stirrer for approximately 30 s, and an aliquot of approximately 2–3 ml was taken using a syringe (10 ml) to fill the 1 ml sample loop. The slurry was found to be stable for at least 10 h. The flow rate throughout the system was adjusted to match the optimum nebulizer uptake rate of the AA spectrometer. The operating parameters of the AA spectrometer were in accordance with the manufacturer's recommended instrument conditions for each element using an air-acetylene flame. Absorption signals for both standards and slurries were recorded on a chart recorder and peak height measurements were taken. Replicate injections were performed for standards and samples in the same experimental run for the appropriate element.

Results and Discussion

Calibration

Calibration using a series of five standards in 5% v/v HNO_3 was carried out within the linear calibration range for each element by using the AA spectrometer in a conventional manner. The results from this direct nebulization were compared with those obtained by processing the same standards through the FI system with the microwave oven at 90% power. This established that no loss in instrumental performance occurred from analyte dispersion or mixing owing to the total length of tubing used and heating in the microwave cavity. The results in Table 1 indicate that, for standards in dilute acid (5% v/v HNO_3), no apparent loss in linearity or sensitivity occurs following the passage of a 1 ml slug of standard through the FI system compared with direct nebulization. During the passage of the standards through the microwave cavity, out-gassing was observed as bubbles but these completely recondensed in the cooling loop. The flow rate through the system was maintained during this out-gassing period. The relevance of gas evolution is discussed in detail in the following section.

Optimization of Digestion Conditions

Given that the flow rate for the FI system was more or less limited to a narrow range (4–6 ml min^{-1}) by the nebulizer uptake rate of the AA spectrometer, the digestion conditions or degree of dissolution in the microwave cavity were governed by three variables, namely, microwave power, tube length and acid slurry strength. As one of the objectives of this work was to minimize the time taken for the digestion whilst maintaining sensitivity, power ratings from 0 to 90% were evaluated for both signal sensitivity and digestion. Signal sensitivity was evaluated by comparing the absorbance response for a standard solution of 4 ppm of Cu in 5% v/v

HNO_3 , over a range of microwave powers (Fig. 2). At microwave powers of below 10%, very little or no out-gassing occurred in the 20 m digestion loop and this led subsequently to a high degree of sample dispersion and a corresponding loss in sensitivity. In the range 10–55% power (stage 2), an increase in gas formation was observed that, by stage 3, led to the sample slug undergoing optimum fragmentation into discrete cells or sample fractions, which on cooling recombined to produce the original sample with minimal dispersion (Table 1). This rather unexpected consequence of bubble formation together with the efficiency of digestion observed for solid samples during the out-gassing process clearly represents an important process in the method described (a point returned to later). The results for slurry samples indicated that, as expected, a high power rating was preferable and that at 90% power (525 W) maximum digestion and sensitivity were achieved for the samples investigated. Selection of 100% power was not found to give any improvement in results over those for 90% and so, in order to minimize heating of the oven components by continuous use, 90% power was selected for the work described. Having selected a fixed microwave power, the geometry of the tubing in the microwave cavity was evaluated. Various lengths (10, 20 and 30 m) and internal diameters (0.3, 0.5 and 0.8 mm) of tubing were examined and these were either knotted into a ball or wrapped around the conventional 12 bomb holder as supplied by CEM for conventional microwave digestion. A satisfactory digestion was identified by observing the passage of the digested 1 ml slug of slurry (for this *Chlorella* was used) for particulates following centrifugation, collected after the back-pressure

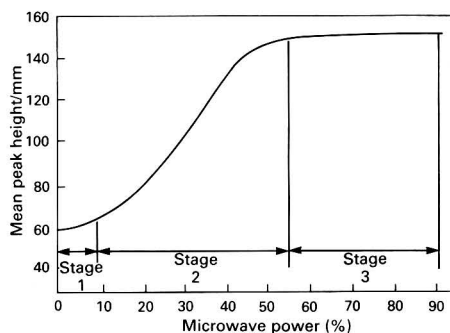


Fig. 2 Plot of microwave power versus signal response for a Cu standard (4 ppm). Stage 1, insufficient power to cause out-gassing therefore little signal improvement; stage 2, increasing power gives increasing out-gassing therefore signal improves; and stage 3, no further increase in out-gassing therefore no further signal improvement, *i.e.*, maximum sensitivity above 55%

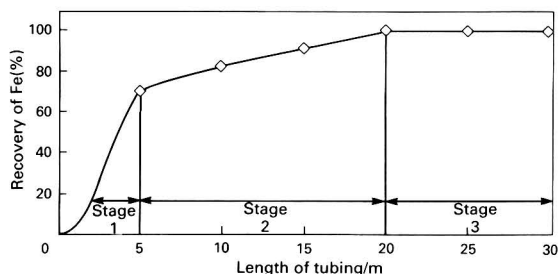


Fig. 3 Percentage recoveries of Fe (*Chlorella* 0.2% slurry in 5% v/v HNO_3) versus length of digestion tubing (0.8 mm i.d.) at a flow rate of 6 ml min^{-1} . Stage 1, increasing time in microwave up to a point where maximum out-gassing occurs and digestion is fully underway; stage 2, increasing time in cavity and hence digestion without increasing dispersion; and stage 3, full digestion is accomplished for sample

Table 1 Comparison of the calibration for Mg of the AA spectrometer with nebulization and an FI system

System	Slope	Intercept	Correlation coefficient
Nebulizer	32.7	0.95	0.9994
FI	32.02	1.04	0.9999

regulator with no in-line filter in place. The 0.3 mm i.d. tubing was found to block readily with slurries. The 0.8 mm i.d. tubing was found to give a longer residence time in the cavity over the 0.5 mm i.d. tubing for the same length with no obvious blocking effects or loss in sensitivity. By using 0.8 mm i.d. tubing it was found that, at lengths greater than 20 m and flow rates of up to 6 ml min⁻¹, total digestion was achieved, *i.e.*, negligible particulates remained (Fig. 3). Some particulates (2–5, visible by eye) were always present probably owing to poor dissolution associated with an unavoidable dilution or

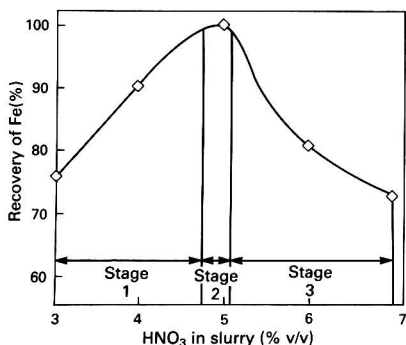


Fig. 4 Percentage recoveries of Fe (chlorococci 0.2% slurry) versus acid strength of the slurry. Stage 1, increasing digestion as out-gassing develops; stage 2, optimum digestion with out-gassing sufficient for digestion without disrupting the flow; and stage 3, flow disrupted and erratic owing to excessively violent out-gassing giving loss in reproducibility and increase in dispersion and sampling time

dispersion effect of the 1 ml slug of 5% v/v HNO₃ at the trailing interface with the water carrier, characteristic of FI peaks. It was decided to place a back-flush filter in the system to protect the back-pressure regulator from possible blockages, and to prepare for the likelihood of residual material with matrices that might be studied at a later date. This filter was constructed in-house from 4 mm diameter stainless-steel mesh (50 µm) housed in a modified zero dead volume coupling packed with acid-washed glass wool to minimize dispersion. As a 20 × 0.8 mm i.d. length of tubing was found to be adequate for digestion of all the samples analysed in this work, it only remained necessary to establish the best geometry for the tubing in the cavity. Knotting of the tubing, in an attempt to minimize dispersion, was found not to be advantageous because it led to local heating of the solid material and eventual blockage of the tubing, as it became physically stuck in the tight curves of the knot. The best geometry for the 20 m tubing was found to be when it was wound around the carousel designed conventionally for holding 12 digestion bombs; a modified version of the carousel was used in subsequent work.

During the digestion of slurries various acid strengths were evaluated (0–70% v/v HNO₃) by investigating the percentage recoveries of Fe from a 0.2% m/v slurry of chlorococci in 5% v/v HNO₃ (Fig. 4). At acid strengths below 5% v/v HNO₃, the production of bubbles or a gas phase in the digestion loop was low which led to poor digestion and consequently lower signal recoveries. As indicated previously, the presence of a gas phase has been found to be essential for the digestion of samples and early attempts to remove the bubbles completely by increasing the back-pressure of the system was found to give poorer digestions of the slurry material. As yet it is not clear what the actual mechanism of digestion is but the

Table 2 Percentage recoveries and precisions for reference materials, *n* = 10

	Mg		Ca		Zn		Fe	
	Recovery (%)	RSD (%)	Recovery (%)	RSD (%)	Recovery (%)	RSD (%)	Recovery (%)	RSD (%)
Chlorococci	96.3	2.3	99.0	3.1	ND*	—	97.5	1.5
Reference value	0.33%		0.49%		20.5 µg g ⁻¹		0.185%	
CRM Mussel	97.2	1.4	100	7.6	102	7.0	96.8	4.0
Reference value	0.21%		0.13%		106 µg g ⁻¹		158 µg g ⁻¹	
CRM Sargasso	102	0.89	93.8	1.9	ND	—	95.4	3.3
Reference value	0.67%		1.41%		16.4 µg g ⁻¹		187 µg g ⁻¹	
CRM Pepperbush	96.5	0.8	103	1.9	93.6	0.7	98.0	3.0
Reference value	0.408%		1.38%		340 µg g ⁻¹		205 µg g ⁻¹	
SRM 1577a Bovine Liver	94.0	4.5	ND	—	95.9	0.7	107	4.3
Reference value	600 µg g ⁻¹		120 µg g ⁻¹		123 µg g ⁻¹		194 µg g ⁻¹	

*ND = Not detectable in a slurry of ≤0.5%.

Table 3 Relative standard deviations and percentage slurries for reference materials, *n* = 10

	Mg		Ca		Zn		Fe	
	RSD (%)	Slurry (% m/v)	RSD (%)	Slurry (% m/v)	RSD (%)	Slurry (% m/v)	RSD (%)	Slurry (% m/v)
CRM Chlorococci	2.3	0.01	3.1	0.01	—	—	1.5	0.2
CRM Mussel	1.4	0.01	7.6	0.01	7.0	0.5	4.0	0.5
CRM No. 9 Sargasso	0.89	0.005	1.9	0.005	—	—	3.3	0.4
CRM Pepperbush	0.8	0.01	1.9	0.01	0.7	0.2	3.0	0.5
SRM 1577a Bovine Liver	4.5	0.01	—	—	0.7	0.5	4.3	0.5

presence of gas, liquid and solid phases in narrow bore tubing under the influence of heat from microwave power is significant and should form the basis of a more fundamental study. If, however, gas production is allowed to become too excessive then controlling the bubble size and flow characteristics through the digestion loop will lead to erratic flows and dispersion effects. These problems, which can be associated with increasing acid strength, led to a loss in signal sensitivity and as a consequence the apparent low recoveries observed in Fig. 4 for the higher acid concentrations. Obviously the degree of gassing will be a function of sample type and volume; the experimental conditions described in this paper were found to be adequate for the range of sample types studied. It may be necessary, however, to review the acid slurry strength, microwave power and pressure and length of the digestion loop in the microwave cavity for alternative sample types.

Analysis of Samples

The results, expressed as percentage recoveries and precision [relative standard deviation (RSD)], for the four elements determined by atomic absorption spectrometry (AAS) are summarized in Table 2. It was necessary to select different slurry masses or dilution factors for the various samples to facilitate obtaining a signal in the linear working range of the spectrometer. It was considered that sample masses below 25 mg would lead to unacceptable precision, and the percentage slurries (m/v) that were selected are summarized in Table 3. The elemental concentrations in some samples, for example Zn in *Chlorella/Sargasso* and Ca in Bovine Liver, were found to be too low, using the maximum slurry concentration of 0.5%, to give a measurable signal. What is apparent from observations taken during experimental work is that it is not just the mass of the sample taken that influences precision but also the wettability or dispersion of the solid as a slurry that affects the results. For example Bovine Liver and Mussel were difficult to disperse in the 5% v/v HNO₃ and gave correspondingly higher RSD values. Surfactants were not used in this work but this is one possible area to investigate further. In general the results obtained were found to be acceptable in terms of recoveries and precision.

Conclusion

The method described offers rapid and efficient sample preparation using on-line microwave digestion of slurries with direct elemental detection by flame AAS. The sample preparation and analysis time for ten replicate samples was approximately 0.5 h for the method described compared with 2 h for the same number of samples prepared by the microwave bomb digestion technique. The elemental levels that can be determined are at present governed by the limited calibration range of the AA spectrometer and the current percentage slurry range used. Clearly this limitation could be overcome by the use of a wider dynamic calibration range such as that offered by inductively coupled plasma atomic emission spectrometry. Problems were experienced with the dispersion or wettability of some of the powdered (<180 µm) organic reference material used but at worst these gave precisions of 4–5% RSD. Samples were processed in approximately 2 min and elemental recoveries for the samples studied were typically in the range 94–107%.

The authors gratefully acknowledge the contribution of Dr. P. Riby and L. Neville to the progress of this work.

References

- 1 *Introduction to Microwave Sample Preparation*, eds. Kingston, H. M., and Jassie, L. B., American Chemical Society, Washington, DC, 1988.
- 2 Fisher, L. B., *Anal. Chem.*, 1986, **58**, 261.
- 3 Millward, C. G., and Kluckner, P. O., *J. Anal. At. Spectrom.*, 1989, **4**, 709.
- 4 Růžicka, J., and Hansen, E. H., *Flow Injection Analysis*, Wiley, New York, 2nd edn., 1988.
- 5 de la Guardia, M., Salvador, A., Burguera, J. L., and Burguera, M., *J. Flow Injection Anal.*, 1988, **5**, 121.
- 6 Burguera, M., Burguera, J. L., and Alarcon, O. M., *Anal. Chim. Acta*, 1986, **179**, 351.

Paper 1/030461

Received June 20, 1991

Accepted September 10, 1991

High-pressure Microwave Digestion for the Determination of Arsenic, Antimony, Selenium and Mercury in Oily Wastes

Milford B. Campbell and George A. Kanert

Laboratory Services Branch, Ministry of the Environment, 125 Resources Road, Rexdale, Ontario, Canada M9W 5L1

The determination of arsenic, antimony and selenium by hydride generation and mercury by the cold vapour technique, following acid digestion of oily waste samples, can be very difficult if there is any residual organic matter. The preparation stage usually requires prolonged digestion to oxidize the organic matter. The situation is exacerbated if these metals are present as the organometallic derivatives. A method has been developed in which the organic matrices of oily waste samples, after solvent extraction, are completely oxidized. This has been achieved through the use of a newly designed microwave system that uses special high-pressure vessels capable of withstanding internal pressures in excess of 82.2 bar (1200 psi) (1 bar = 10^5 Pa). The relative standard deviation using organometallic standards ranged from 5.4 to 6.6% and the recoveries for four spiked oily waste samples ranged from 89 to 105%.

Keywords: *Petroleum-based oily waste; microwave digestion; mercury, arsenic, antimony and selenium determination; cold vapour and hydride-generation atomic absorption spectrometry*

The US Environmental Protection Agency Method 1330 'Extraction Procedure for Oily Wastes' is used to determine the mobile metal concentration in petroleum-based wastes¹ and hence provides a method for screening these types of wastes prior to landfilling. Owing to the expected low concentrations in these types of wastes, arsenic, antimony and selenium are determined by the hydride generation method whereas mercury is determined by the cold vapour method. Both of these methods usually require perchloric acid digestion of the samples in order to destroy any organic matter.^{2,3}

Microwave digestion techniques have been used successfully to digest different types of samples, ranging from geological⁴ to biological⁵ matrices. Fisher⁴ found that by using a low-pressure system, a decrease in the volatility of the more volatile elements led to improved sample to acid contact and hence a more complete digestion of the samples. Very little work, however, has been performed with these types of samples at internal vessel pressures in excess of 13.7 bar (200 psi). In this study, a microwave technique employing specially designed high-pressure digestion vessels was used to digest oily waste samples in a non-perchloric acid medium at pressures in excess of 82.2 bar (12 psi) (1 bar = 10^5 Pa).

Experimental

Microwave Digestion System

The Milestone microwave system (Mandell Scientific, Guelph, Ontario) consists of three separate units: oven, fume extraction module and a capping station. The MLS-1200 oven is capable of producing a maximum power of 1200 W. An actual value of 1100 W was found by monitoring the change in temperature of 1 kg of water. The power can be varied from 1 to 50% in 1% increments and then by 25% increments to 100%. A microprocessor is used to control the power. For the acid digestions, a maximum of 50% power was used.

High-pressure Vessels

The Milestone high-pressure vessels (HPV 80) are constructed of a patented polymer derivative that allows the use of high boiling-point acids such as sulfuric acid at temperatures up to 350 °C. The vessels used had special seal rings and burst discs rated at 100 bar (1460 psi). Four vessels at a time were placed in the oven.

Instrumentation

A Varian Techtron Model 70 atomic absorption spectrometer capable of operating at 193.70, 217.58 and 196.03 nm for the determination of arsenic, antimony and selenium, respectively, was used. The atomizing chamber is a 10 cm long \times 6 mm i.d. quartz tube wound with Chromel C insulated resistance wire (approximately 1 Ω per 0.3 m). The operating temperature of 850 °C was controlled by a Variac transformer.

The sample flow together with various reagents was maintained by use of a Gilson Minipuls 2 proportional pump (Varian Techtron). Tygon tubing of various inner diameters was used to connect the different units. The sample and reagents were mixed in the two mixing coils prior to introduction into the atomizer in a stream of argon *via* a centrally placed 2 mm i.d. quartz tube. The output from the atomic absorption spectrometer was fed into a strip-chart recorder set at an input voltage of 10 mV. A schematic diagram of the analytical system is shown in Fig. 1. An LCD/Milton Roy mercury monitor set at 254 nm was used to determine mercury.

Reagents

All inorganic acids used were of Baker analysed ACS grade, except sulfuric acid which was of BDH analytical-reagent grade. Doubly distilled water was used as a diluent. Toluene and tetrahydrofuran used for the extractions were from Caledon Laboratories (distilled in glass).

Organometallic Standards

No reference materials for metals in oily wastes were available. As the primary area of interest was in the metals that were present as the organometallic derivatives and not simply as particulates in oil, the following organometallic standards obtained from Conostan Division, Conoco (Ponca City, OK, USA) were used: antimony alkyl sulfonate in white mineral oil (5000 ppm); selenium amine sulfonate in white mineral oil (100 ppm); arsenic amine sulfonate in white mineral oil (100 ppm); and mercury alkyl dithiocarbamate in white mineral oil (100 ppm). A working mixed standard solution of 1 ppm was prepared by diluting the standards appropriately with toluene.

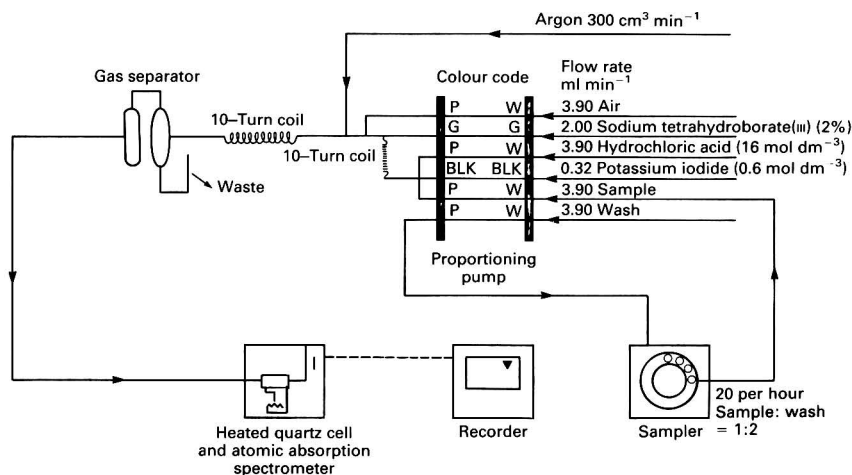


Fig. 1 Atomic absorption spectrometer manifold for the determination of arsenic and antimony

Inorganic Standards

The aqueous inorganic standards for arsenic, antimony and selenium were prepared by diluting 1000 mg dm⁻³ certified atomic absorption stock solutions (Delta Scientific). The mercury stock standard solution (100 mg dm⁻³) was obtained from J. T. Baker and diluted appropriately.

Oily Wastes

The following oily wastes were used: OW-1, oil-saturated clay; OW-2, tank bottom from oil refinery (lumpy solid); OW-3, sludge from oil refining (soft, oily solid); and OW-4, aqueous oily sludge (aqueous brown upper portion and solid lower layer). Owing to the high incidence of volatile petroleum products such as diesel fuel in some of the oily waste samples, the solids were air dried for 24 h in a fume hood prior to use.

Procedure

Duplicate oily wastes were Soxhlet extracted according to the US Environmental Protection Agency Method 1330.¹ These extracts were composed of a mixture of toluene and tetrahydrofuran together with the organics solubilized in them. The combined solvent extracts were filtered through a 0.46 µm glass-fibre filter to remove any large particulates that would pass through the extraction thimble.

A 2 ml aliquot of the mixed solvent extracts was pipetted on to an 8.5 × 5 cm piece of Whatman QA-M quartz microfibre filter horizontally supported at one end. The filter was left at room temperature in a fume hood for approximately 20 min to allow for the bulk of the solvents to evaporate.

It is important that blank determinations are performed on these filters prior to use; they were found to produce fairly high blanks for selenium and arsenic. Therefore, the filters were pre-treated by boiling in 6 mol dm⁻³ hydrochloric acid for approximately 15 min. The excess of acid solution was drained and the filters were then dried in the microwave oven followed by heating in a muffle furnace at 450 °C for at least 5 h. This treatment should produce blank values below 0.1 ppb for these elements.

Each filter was cut into small pieces and then placed in a high-pressure digestion vessel. A 5 ml mixture of sulfuric and nitric acid (3 + 1) was carefully added to each of the vessels. The burst disc was placed in position, then the cap was screwed in place and tightened in the capping station to

10 N m. The vessels were inserted in the rotating safety shield and the whole arrangement was placed in the microwave oven. The samples were digested according to program 1: 20% power for 2 min, 30% power for 3 min and 50% power for 6 min.

[Caution: It is important with these types of samples that a gradual rate of heating is used, otherwise the pressure build-up may be too rapid. It is also important that, if the waste sample is suspected to contain unstable compounds, the bombs are left in their safety shield in the oven long enough to allow adequate cooling and cessation of any chemical reactions. If this is not done, it is possible for one or more of the bombs to vent on removal from the oven.]

At the end of the digestion period, the assembly was removed from the oven and immersed in cold water until the vessels had cooled sufficiently that they could be removed from the safety shield. The vessels were opened carefully with the venting tube in place (according to the manufacturer's instructions). In order to ensure complete digestion, a further 3 ml of the sulfuric-nitric acid mixture were added cautiously to each vessel and they were resealed as above. The samples were further digested according to program 2: 25% power for 2 min and 50% power for 10 min. At the end of this time, the vessels were cooled and opened as described above.

Approximately 5–10 ml of distilled water were added slowly to each of the digests; care was taken at this stage as there was a vigorous reaction with the evolution of brown fumes. The solutions were allowed to stand for 5 min and then gently swirled. The filter pieces were then washed into clean 150 ml glass beakers with doubly distilled water. These solutions and the filters were completely colourless once all the nitrogen dioxide had escaped. The solutions were thoroughly stirred with a glass rod and then filtered through Whatman No. 541 filter-paper into 50 ml calibrated flasks. After the initial solutions had drained from the filters, they were rinsed with small volumes of doubly distilled water. The filters were pressed with a glass rod to remove as much of the rinse solution as possible and the contents of the flasks were then diluted to the mark with doubly distilled water.

It has been found from this work that the nitric acid remaining within the final solution suppresses the arsenic and antimony signals. In order to counteract this, 0.2–0.3 g of urea was added slowly to a 10 ml aliquot of each of the above solutions contained in 15 ml acid-rinsed sample vials. After the effervescence had subsided, the vials were capped and inverted several times to ensure complete mixing. These samples were then analysed for arsenic, antimony and selenium.

For the determination of arsenic, antimony and selenium by the hydride generation atomic absorption method, it is important that these metals are in the correct oxidation state. The results obtained from the work performed by Sinemus *et al.*⁶ show that much better sensitivities are obtained for these elements when they are in their lower oxidation states. In the present study, the reduction to the lower oxidation state was achieved by using 10% m/v potassium iodide for arsenic and antimony and 6 mol dm⁻³ hydrochloric acid for selenium. In each instance these solutions were automatically added by using a proportioning pump and mixed in a ten-turn glass coil as indicated in Fig. 1. Reduction to arsine, stibine and hydrogen selenide was accomplished by the introduction of 2% sodium tetrahydroborate(III) into the flow system prior to the second mixing coil.

Certain transition metals, such as nickel, copper and iron, are known to interfere in the determination of arsenic, antimony and selenium.^{7,8} According to Kirkbright and Taddia,⁹ the interference effect could be due to the reduction of these transition metals to the free metals; these could then absorb the hydride product, thus reducing the signal. It has been found⁸⁻¹⁰ that 5 mol dm⁻³ hydrochloric acid extends the analytical range in which these analytes can be determined in the presence of these interfering metals. Inductively coupled plasma spectrometric studies have shown that one or more of these transition metals can be present, in excess of the concentrations known to cause interference problems,⁸ in oily waste extract samples, especially if the particulate matter is not removed from the extract. For this reason, 6 mol dm⁻³ hydrochloric acid was mixed with the sample solution prior to the reduction stage.

Mercury was determined by pouring the remaining digestate solutions into small glass beakers. Saturated potassium permanganate was added dropwise until a persistent pink colour was obtained (Landi *et al.*¹¹ noted the merits of having a strongly oxidizing environment for the determination of mercury). The beakers were covered with watch-glasses, placed on a rotating platform and then inserted in the microwave oven. These samples were slowly heated at 15% power for 15 min. Samples that became colourless during this time were separately treated with potassium permanganate as above and re-heated. The manganese dioxide formed in this process was dissolved by careful treatment with 35% v/v hydrogen peroxide to the point where a pink colour was just obtained. If the hydrated manganese dioxide is not removed, it can hinder the oxidation of the mercury ions.¹²

The final solution for the determination of mercury was treated with a 20% m/v solution of hydroxylamine sulfate to reduce the potassium permanganate. The ionic mercury was then reduced by tin(II) chloride to its elemental form in an automatic mixing system similar to that shown in Fig. 1.

Digestion recovery studies were carried out in two stages. The first was by evaluating the recovery of the mixed standards only, and the second by evaluating the effects of the different oily waste samples under investigation on the added standards. In each instance, 0.5 ml of the 1 ppm mixed organometallic standard in toluene was pipetted on to the support and left to evaporate. In the second method, the 0.5 ml volume was added to the support after the solvent from the sample had evaporated. These samples were microwave digested in the same manner as the oily waste extracts.

Results and Discussion

The recoveries obtained from the digestion and analysis of mixed 10 ppb organometallic standards are shown in Table 1. The lower values found in the 8 ppb range were attributed to a slight loss of pressure in these particular vessels. The short-term precisions (relative standard deviations) are fairly consistent.

Results of the oily waste spiking study are presented in Table 2. The recoveries ranged from 90 to 100%, indicating

Table 1 Recoveries (%) obtained from the digestion of the mixed 10 ppb organometallic standards

	Mercury	Arsenic	Antimony	Selenium
	9.6	10.0	10.1	10.1
	10.4	9.6	10.3	8.8
	9.1	8.9	8.6	9.5
	8.5	10.8	9.9	10.3
	9.4	9.6	10.1	9.8
Average	9.4	9.8	9.8	9.7
Standard deviation (%)	0.622	0.621	0.613	0.523
Relative standard deviation (%)	6.6	6.3	6.2	5.4

Table 2 Recovery data from the analysis of spiked duplicate oily waste samples

Element	Parameter	Sample			
		OW-1	OW-2	OW-3	OW-4
Mercury	Concentration in extract + spike (ppb)	9.7	11.3	10.3	9.6
	Average extract concentration (ppb)	0.6	1.3	0.8	0.6
	Recovery at the 10 ppb spike level (%)	91	100	95	90
	Concentration in extract + spike (ppb)	9.6	9.4	11.4	10.3
Arsenic	Average extract concentration (ppb)	0.4	0.5	0.9	0.8
	Recovery at the 10 ppb spike level (%)	92	89	105	95
	Concentration in extract + spike (ppb)	10.1	10.5	11.8	9.8
	Average extract concentration (ppb)	0.7	0.8	2.1	0.3
Antimony	Recovery at the 10 ppb spike level (%)	94	97	97	95
	Concentration in extract + spike (ppb)	9.6	10.1	10.5	9.8
	Average extract concentration (ppb)	<0.3*	0.5	0.7	<0.3*
	Recovery at the 10 ppb spike level (%)	96	96	98	98
Selenium	Concentration in extract + spike (ppb)	9.6	10.1	10.5	9.8
	Average extract concentration (ppb)	<0.3*	0.5	0.7	<0.3*
	Recovery at the 10 ppb spike level (%)	96	96	98	98

* Estimated detection limit for selenium made from 3σ ($n = 5$), where σ is the standard deviation of the results obtained from the support and solvent blanks.

that the digestion method was acceptable for the sample types investigated.

Cross-contamination between samples was not a problem owing to the material used in the construction of the high-pressure vessels. Rinsing each vessel with 5% v/v nitric acid followed by rinsing with distilled and doubly distilled water was all that was required.

Conclusions

Petroleum-based oily waste samples are extremely difficult to oxidize completely *via* acid digestion. It has been found from earlier studies carried out under normal atmospheric condi-

tions that residual organic matter in solution will result in numerous problems in the determination of mercury, arsenic, antimony and selenium. With the automated method of analysis used, coating of the mixing tube by an oily film occurs, which results in a gradual decrease in sensitivity. This film also results in drift of the recorder baseline and irregularly shaped peaks. With the high-pressure microwave system and using the method described, all of these problems were eradicated.

One of the main disadvantages of this high-pressure technique is that there is no way of accurately monitoring the internal pressure and temperature inside the high-pressure vessels. It was established, however, that the internal pressures developed in the vessels were between 82.2 and 95.9 bar (1400 psi) by carefully monitoring the conditions under which a burst disc would rupture.

This microwave technique, and other high-pressure systems that are becoming commercially available, will be increasingly used to digest samples with difficult matrices.

The authors thank all those who assisted in this project, particularly T. McIntosh and H. Konstantinou for carrying out the hydride measurements and D. Russell for carrying out the mercury determinations. Special thanks are extended to J. Pimenta for technical support and providing different samples.

References

- 1 *Extraction Procedure for Oily Wastes, Method 1330, Test Methods for Evaluating Solid Waste, SW-846*, United States Environmental Protection Agency, Washington, DC, 1986.
- 2 May, K., and Stoeppler, M., *Fresenius Z. Anal. Chem.*, 1984, **317**, 127.
- 3 *Official Methods of Analysis of the Association of Official Analytical Chemists*, Association of Official Analytical Chemists, Washington, DC, 13th edn., 1980, sect. 25, p. 110.
- 4 Fisher, L. B., *Anal. Chem.*, 1986, **58**, 261.
- 5 Abu-Samra, A., Morris, J. S., and Koirtiyohann, S. R., *Anal. Chem.*, 1975, **47**, 1475.
- 6 Sinemus, H. W., Melcher, M., and Welz, B., *At. Spectrosc.*, 1981, **2**, No. 3, 81.
- 7 Welz, B., and Melcher, M., *Analyst*, 1984, **109**, 569.
- 8 Welz, B., and Melcher, M., *Analyst*, 1984, **109**, 573.
- 9 Kirkbright, G. F., and Taddia, M., *Anal. Chim. Acta*, 1978, **100**, 145.
- 10 Welz, B., and Melcher, M., *Analyst*, 1984, **109**, 577.
- 11 Landi, S., Fagioli, F., Locatelli, C., and Vecchiotti, R., *Analyst*, 1990, **115**, 173.
- 12 Stainton, M. P., *Anal. Chem.*, 1971, **43**, 625.

Paper 1/02546E

Received May 30, 1991

Accepted August 6, 1991

Critical Evaluation of Three Analytical Techniques for the Determination of Chromium(VI) in Soil Extracts

Radmila Milačič, Janez Štupar, Nevenka Kožuh and Janez Korošič

Jožef Stefan Institute, University of Ljubljana, 61000 Ljubljana, Jamova 39, Slovenia, Yugoslavia

Three different analytical techniques [1,5-diphenylcarbazide spectrophotometry, chelating ion-exchange chromatography (Chelex-100), and ion-pairing reversed-phase high-performance liquid chromatography (RP-HPLC) combined with electrothermal atomic absorption spectrometry (ETAAS)] were critically evaluated for the determination of Cr^{VI} in soil extracts. Spectrophotometry was not applicable to the analysis of most soil extract samples owing to its high limit of detection (LOD = 30 ng cm⁻³), and the possibility of the instantaneous reduction of Cr^{VI} under the acidic conditions employed. A Chelex 100 column, although adequately sensitive (LOD = 1.5 ng cm⁻³), is inclined to give higher results as inert and moderately labile Cr^{III} complexes partially passed through the resin together with Cr^{VI}. In addition, very small particles (<0.45 µm) carrying chromium can produce severe positive systematic errors. In order to avoid this, filtration employing a 0.1 µm filter is recommended. Ion-pairing RP-HPLC was found to be the most sensitive technique (LOD = 0.3 ng cm⁻³). It might also give high chromatate results if negatively charged Cr^{III} complexes form ion pairs with tetrabutylammonium phosphate and their elution partially coincided with that of Cr^{VI}. Fulvate ligands showed this type of interference. Reversed-phase HPLC is not suitable for analysis of extracts obtained from soils with freshly added tannery waste owing to the effects of the undestroyed tannery waste matrix. This study showed that each method investigated was vulnerable to some type of interference.

Keywords: Chromate; spectrophotometry; chromatography; electrothermal atomic absorption spectrometry; soil extracts

Chromium appears frequently as a pollutant in terrestrial systems. The hexavalent form is of prime concern because of its high toxicity. Studies by several workers of the formation and fate of Cr^{VI} in soil have produced controversial results. This may be owing to the lack of reliable analytical data on Cr^{VI} in soil extracts. A number of different analytical techniques are available for the determination of Cr^{VI};¹⁻²⁶ however, most of them cannot be applied efficiently to complex samples such as soil extracts. Samples containing Cr^{VI} and Cr^{III} at nanogram levels have been concentrated on anion- and/or cation-exchange resins.¹⁻⁴ Investigations based on various extraction techniques^{5,6} combined with atomic absorption spectrometry (AAS) or inductively coupled plasma atomic emission spectrometry (ICP-AES) have also been carried out. Coprecipitation of Cr^{VI} with lead sulfate⁷ is satisfactory for water and waste water samples which are low in chloride and sulfate ions (found to produce severe negative interferences). A flow injection method for the determination⁸ of CrO₄²⁻ and Cr^{III} was also reported. The 1,5-diphenylcarbazide spectrophotometric method was used for the determination of Cr^{VI} in soil extract samples,⁹⁻¹⁴ but high positive interferences were also observed.¹⁴ Several papers have been published on the determination of trace amounts of Cr^{VI} and Cr^{III} in water samples using reversed-phase high-performance liquid chromatography (RP-HPLC) combined with AAS.¹⁵⁻¹⁹

A method has been developed²⁰ for the determination of Cr^{VI} in aqueous samples or sample extracts using ion chromatography coupled with ICP mass spectrometry or colorimetry. Trace amounts of Cr^{VI} and Cr^{III} in water samples have also been determined using chelating ion-exchange resins.²¹⁻²⁵ The main advantage of these resins is their high purity. A comparative study²⁶ of the lead sulfate coprecipitation, the 1,5-diphenylcarbazide spectrophotometric and the chelation-extraction methods was carried out for the determination of Cr^{VI} in the presence of a large excess of Cr^{III}.

The aim of this work was to develop a reliable analytical technique for the determination of Cr^{VI} in soil extract samples. The 1,5-diphenylcarbazide spectrophotometric method and chelating ion-exchange chromatography (Chelex 100) and ion-pairing RP-HPLC separation, both combined off-line with electrothermal AAS (ETAAS) as a Cr specific detector, were critically evaluated. In addition, various interferences asso-

ciated with the sample matrix were carefully investigated for each method examined.

Experimental

Apparatus and Procedures

Detection systems

A Varian Cary Model 16 spectrophotometer adjusted to a wavelength of 540 nm was used for the determination of Cr^{VI} by the 1,5-diphenylcarbazide spectrophotometric method.⁹

Separated chromium species (chelating ion exchange, RP-HPLC) were determined on a Varian AA 575 atomic absorption spectrometer with a Perkin-Elmer HGA 76B graphite furnace. The spectral bandpass of the monochromator was 0.2 nm. A Varian Techtron hollow cathode lamp was operated at a current of 5 mA. The integrated absorbance of chromium was measured at the 357.9 nm line by injecting 15 mm³ of the sample. The atomization temperature was 2773 K. Background absorption was largely eliminated by careful control of the ashing conditions (ashing temperature between 1673 and 1873 K, time 10–30 s) and/or by a deuterium background corrector. Platform atomization was found to be superior to wall atomization. High chromate concentrations, employed in some RP-HPLC separations (interference studies), were measured by flame AAS (Varian AA-5, N₂O-acetylene flame).

Separation system

All soil extract samples were centrifuged with a Heraeus Model 17S Sepatech Biofuge at 10 000 rev min⁻¹ for 20 min and filtered through 0.1 µm membrane filters, unless stated otherwise.

Chelating ion exchange. A system was developed for the separation of chromium species employing Chelex 100 (50–100 mesh) resin. The batch procedure of Isozaki *et al.*²³ was modified into a column technique to obtain a better separation and lower limits of detection (LODs). Chelex 100 (Na form) resin was first transformed to the NH₄ form²³ and approximately 0.3 g of the resin was slurried with water and transferred into the column (using a 1 cm³ plastic pipette tip) without prior purification. Quartz wool was placed at each end of the column, and the column was connected to a peristaltic

pump (Ismatec MS4 Reglo) through which the flow rates could be varied between 0.2 and 4.5 cm³ min⁻¹. The column resin was first treated with 10 cm³ of buffer solution,²⁷ followed by passage of a buffered sample (5 cm³ of sample and 5 cm³ of buffer) at a flow rate of 1 cm³ min⁻¹ and then washed with 15 cm³ of buffer at a flow rate of 4.5 cm³ min⁻¹. The sample eluent was collected in a beaker, acidified with 0.2 cm³ of nitric acid (1 + 1), evaporated to approximately 2 cm³, transferred into a 5 cm³ calibrated flask and diluted with water to the calibration mark. Chromium not retained by the column was then measured by ETAAS. The same procedure was applied to the blank solution. Although the column capacity was not exceeded by performing 20 consecutive separations (solutions containing 80 ng cm⁻³ of Cr³⁺ and 40 ng cm⁻³ of Cr⁶⁺), the multiple use of the same column for the separation of chromium in soil extracts resulted in an increased blank value. Therefore, the column was refilled with fresh resin for each sample analysis.

Ion-pairing RP-HPLC. Separation of chromium species was accomplished on a column (150 × 4.6 mm i.d.) packed in-house with LiChrosorb RP C₁₈ particles (5 µm). The eluent was pumped through the column at a rate of 1.0 cm³ min⁻¹ by a gradient Merck-Hitachi 6200 intelligent pump. The sample was introduced onto the column by a Rheodyne injector equipped with a laboratory-built 5 cm³ loop. The minimum volume for reproducible injection of samples on the loop was found to be 12 cm³. Chromium(vi) was separated from other chromium species by the formation of an ion pair with the reagent, tetrabutylammonium phosphate (PIC A). The soil extract (2–10 cm³) was mixed with the reagent and diluted with water to 15 cm³ so that the final reagent concentration was 1 × 10⁻² mol dm⁻³. Standard and blank solutions were prepared in the same way and injected into the loop. The pump (operated at a flow rate of 1 cm³ min⁻¹) was programmed in the following steps, which were determined experimentally to ensure quantitative and reproducible separation. (i) The prepared sample (15 cm³) was injected into the loop and washed with water onto the column for 15 min (inject position). (ii) The injector was then turned to the load position to ensure the direct elution of the retained chromate by 50% v/v methanol-water. This phase was completed in 12 min. (iii) The column was rinsed with water for 33 min and was then ready for the next separation. The Cr^{VI} peak appeared 19 min after injection in a volume of 0.2–0.4 cm³. The retention time depended on the pH and sample matrix and could vary; therefore, ten fractions of 0.2 cm³ were collected from the eighteenth minute after injection. Chromium(vi) was then determined in collected fractions 'off-line' by ETAAS. A typical chromatogram for Cr^{VI} is presented in Fig. 1.

Reagents

Merck Suprapur acids and doubly distilled water were used for the preparation of samples and standard solutions. All other chemicals were of analytical-reagent grade.

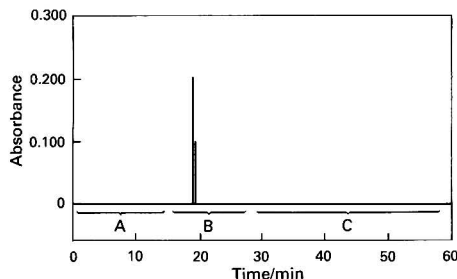


Fig. 1 Typical chromatogram for chromium(vi), as 2 ng ml⁻¹ of Cr^{VI}, separated on a 15 cm RP C₁₈ column and detected 'off-line' by ETAAS. Stage: A, sample; B, 50% v/v methanol-water; and C, rinse

A standard Cr^{III} stock solution (1000 µg cm⁻³) was prepared by dissolving 1.0 g of Cr metal powder (99.99%) in 20 cm³ of HCl (6 mol dm⁻³) followed by dilution to 1000 cm³ with water.

Chromium(III) citrate, maleate, oxalate and fulvate complexes (1000 µg cm⁻³) were prepared by mixing CrCl₃ stock solution with an appropriate amount (3:1 ligand to Cr ratio) of citric, maleic and oxalic acid, respectively. Solid fulvic acid isolated from peat soil (relative molecular mass about 1000) was used to form chromium(III) fulvate. The concentration of fulvic acid in the solution (145 µg cm⁻³) was more than adequate for complexation of added Cr^{III}.

A standard Cr^{VI} stock solution (1000 µg cm⁻³) was prepared by dissolving 2.828 g of potassium dichromate in 1000 cm³ of water. Chelating resin Chelex 100, Na form, 50–100 mesh was obtained from Sigma. Tetrabutylammonium phosphate (PIC A) (0.5 mol dm⁻³, Supelco) stock solution was used as an ion-pairing reagent. Methanol (Merck) for chromatography was employed in HPLC measurements.

Formic acid-potassium hydroxide buffer solutions were applied²⁷ for the pH range 2.5–5.0 and cellulose nitrate membrane filters, 0.45–0.05 µm, and 25 mm diameter (Sartorius), were used in the filtration procedure.

Sample Preparation

Soil samples were prepared by shaking 2.00 g of moist soil for 2 h with 20 cm³ of KH₂PO₄ (1.5 × 10⁻² mol dm⁻³), then centrifuging and decanting. The KH₂PO₄ solution (1.5 × 10⁻² mol dm⁻³) was used to extract efficiently water-soluble chromate and chromate sorbed on various oxides and clay particles.⁹ Samples were then filtered through 0.1 µm membrane filters and the concentration of total soluble chromium was determined by ETAAS. Aliquots of these solutions were used for the determination of different chromium species. It was found experimentally that filtering through 0.45 µm membrane filters did not remove particles from the solution efficiently. These fine particles containing chromium might produce large positive systematic errors if separation is performed on ion-exchange columns. This problem is virtually eliminated by filtering through 0.1 µm filters.

Results and Discussion

Parameters Influencing Chromium Speciation and the Study of Interferences

Spectrophotometry

Two similar procedures were tested: addition of acidified 1,5-diphenylcarbazide reagent to the sample⁹ (Procedure I), and addition of 1,5-diphenylcarbazide reagent to the sample before acidification¹⁴ (Procedure II). Procedure I: a 1 cm³ aliquot of azide reagent was added to 10 cm³ of soil extract and the magenta colour was compared with standard Cr^{VI} solutions at 540 nm after 20 min. For preparation of the azide reagent, 120 cm³ of 85% v/v H₃PO₄ were diluted with 280 cm³ of distilled water and added to 0.4 g of 1,5-diphenylcarbazide dissolved in 100 cm³ of 95% v/v ethanol. Procedure II: a 0.4 cm³ aliquot of 1,5-diphenylcarbazide solution (0.1 g of 1,5-diphenylcarbazide dissolved in 10 cm³ of acetone) was added to 10 cm³ of soil extract. Then, 0.2 cm³ of H₂SO₄ (20 g of 95% H₂SO₄ dissolved in 80 cm³ of distilled water) was added to the sample. The magenta colour was compared with standard Cr^{VI} solutions at 540 nm after 20 min. Analysis of soil extract matrices to which Cr^{VI} had been added indicated that both procedures produced similar results.

The reproducibility of measurement for six parallel determinations of Cr^{VI} (50 ng cm⁻³) was found to be ±2%. The LOD (3σ) for Cr^{VI} in aqueous standard solutions was 10 ng cm⁻³. In soil extracts, the matrix influenced the sensitivity of the measurements. The LOD in soil extracts was found to be 30 ng cm⁻³, and therefore analysis of most soil extracts was not possible employing this technique. The

method could only be applied in particular situations where soils heavily polluted with Cr were investigated.

Parameters influencing the determination of Cr^{VI} in soil extracts. The influence of organically complexed Cr^{III} present in soil extract samples on the determination of Cr^{VI} was studied. To $1 \mu\text{g cm}^{-3}$ of Cr^{VI} , $2.5 \mu\text{g cm}^{-3}$ of Cr^{III} complexes were added and Cr^{VI} was determined by Procedure I and Procedure II. The results are presented in Table 1.

It can be seen from Table 1 that interferences from organically complexed Cr^{III} species were almost negligible in Procedure II. The slightly lower results obtained by Procedure I can be explained by partial reduction of chromate in the presence of reductants under low pH conditions.

Influence of particles and soil matrix on the determination of Cr^{VI} in soil extracts. Clay and peat soil extracts were prepared as described previously. After centrifugation, the supernatant was separated from the solid residue either by decanting, decanting and filtering through a $0.45 \mu\text{m}$ filter or filtering through a $0.1 \mu\text{m}$ filter. The total concentration of soluble chromium in these soil extracts was below 1 ng cm^{-3} . A 500 ng cm^{-3} concentration of Cr^{VI} was added to each soil extract and Cr^{VI} was determined by spectrophotometry (Procedure I). The influence of particles in the soil extracts and the influence of the soil matrix were studied. The results are presented in Table 2.

Two effects influencing the results in Table 2 could be observed. The first is light scattering caused by particles in solution, which contributes to severe positive interferences, particularly in soils with a high clay fraction. It is therefore reasonable to expect that the results previously reported by Bartlett and James⁹ overestimate the oxidation of Cr^{III} to chromate in soils with a high content of MnO_2 . The formation of chromate from soluble Cr^{III} species in soils due to the presence of MnO_2 was actually confirmed in our laboratory but the levels of chromate found in the soils were significantly lower. In addition, Heringer Donmez and Kalenberger¹⁴ by not performing filtration actually reported anomalously high Cr^{VI} levels in soil (28.7% clay) leachates, which is consistent with our observation. The second effect observed from Table 2 is a slightly lower recovery in filtered extracts. This is probably due to the partial reduction of chromate in the acidic medium of the 1,5-diphenylcarbazide reagent by reducing substances in the soil extract.

Chelating ion exchange-ETAAS

Influence of pH on the sorption of chromium. The resin and standard solutions of Cr^{III} (CrCl_3) (200 ng cm^{-3}) and Cr^{VI} (40 ng cm^{-3}) were prepared at pH 3–5 in formic acid–potas-

sium hydroxide buffer solutions.²⁷ The efficiency of sorption as a function of pH is shown in Fig. 2. A quantitative sorption of Cr^{III} was obtained in the pH range examined, while most of the Cr^{VI} passed through the column resin. Optimum conditions for the separation of Cr^{III} and Cr^{VI} were found at pH 3.5–4.5. A pH of 4.0 was chosen for further work, owing to the increased possibility of Cr^{VI} reduction in the lower pH range. Even at this pH, about 15% of added Cr^{VI} (40 ng cm^{-3}) was retained on the resin column.

Separation of Cr^{III} and Cr^{VI} ions in synthetic mixtures. Synthetic mixtures of Cr^{III} (CrCl_3) and Cr^{VI} ($\text{K}_2\text{Cr}_2\text{O}_7$) solutions were prepared at pH 4.0 in various concentration ratios. Chromium(vi) was measured in the eluate. The results are presented in Table 3. The proposed separation of Cr^{III} from Cr^{VI} is satisfactory for Cr^{VI} concentrations not exceeding 20 ng cm^{-3} , probably because of the efficient elution from the resin column. Most of the soil extracts analysed were in this concentration range; at higher concentrations of Cr^{VI} , samples should be diluted prior to separation.

The reproducibility of measurement, tested for six parallel determinations of Cr^{VI} (10 ng cm^{-3}), was found to be $\pm 5.5\%$. The LOD (3σ) for Cr^{VI} in aqueous standard solutions and soil extracts was 1.5 ng cm^{-3} .

Influence of Cr^{III} complexes on the separation and determination of Cr^{VI} in soil extracts. The existence of negatively charged low relative molecular mass organic complexes of chromium has been demonstrated in soil pore waters.²⁸ Similarly, water-soluble Cr^{III} in the soil solution is expected to be bound to some of the soil borne organic ligands. The presence of these Cr^{III} complexes in soil extracts might affect the determination of chromate. For this reason, the influence of negatively charged low and high relative molecular mass organic complexes of Cr^{III} on the determination of Cr^{VI} was studied in the concentration range expected in soil extracts. The results are presented in Table 4.

It is evident that moderately labile and inert Cr^{III} organic complexes passed partially through the resin column and apparently yielded higher Cr^{VI} values. Chromium(III) citrate and fulvate produced the most severe positive interferences. As these ligands can be found in most soils and waste materials

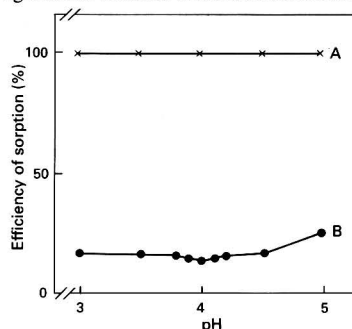


Fig. 2 Efficiency of sorption of: A, chromium(III) (200 ng cm^{-3} of Cr^{3+}) and B, chromium(VI) (40 ng cm^{-3} of Cr^{6+}), on Chelex 100 resin (50–100 mesh) as a function of pH

Table 1 Influence of organically complexed Cr^{III} on the determination of Cr^{VI} by the 1,5-diphenylcarbazide spectrophotometric method

Added/ $\mu\text{g cm}^{-3}$		Procedure I		Procedure II	
		Cr^{VI} found/ $\mu\text{g cm}^{-3}$	Recovery (%)	Cr^{VI} found/ $\mu\text{g cm}^{-3}$	Recovery (%)
Cr^{III}	Cr^{VI}				
2.5 (Citrate)	1.0	0.94	94	0.94	94
2.5 (Oxalate)	1.0	0.85	85	0.94	94
2.5 (Maleate)	1.0	0.98	98	1.00	100
2.5 (Fulvate)	1.0	0.89	89	0.95	95

Table 2 Influence of particles in soil extracts and soil matrix on the spectrophotometric determination of Cr^{VI} (Procedure I)

Particle size/ μm	Sample characteristic	Cr^{VI} added/ ng cm^{-3}	Cr^{VI} found/ ng cm^{-3}	Recovery (%)
>0.45	Clay soil	500	907	181
	Peat soil	500	503	101
<0.45	Clay soil	500	471	94
	Peat soil	500	472	94
<0.1	Clay soil	500	469	94
	Peat soil	500	463	93

Table 3 Separation of Cr^{III} (CrCl_3) and Cr^{VI} ($\text{K}_2\text{Cr}_2\text{O}_7$) ions in synthetic mixtures on Chelex 100 chelating resin (50–100 mesh) at pH 4.0 and determination of Cr^{VI} by ETAAS

Added/ ng cm^{-3}		Cr^{VI} found/ ng cm^{-3}	Recovery of Cr^{VI} (%)
Cr^{III}	Cr^{VI}		
200	200	172	86.0
200	100	86	86.0
200	40	35.8	89.5
200	20	19.9	99.6
200	4	4.1	103.0
200	2	1.9	95.0

Table 4 Influence of organically complexed Cr^{III} on the determination of Cr^{VI} by chelating ion exchange-ETAAS

Added/ng cm ⁻³		Cr ^{VI} found/ ng cm ⁻³	Recovery (%)
Cr ^{III}	Cr ^{VI}		
70 (Citrate)	30	75.0	250
70 (Oxalate)	30	42.5	142
70 (Maleate)	30	32.5	108
70 (Fulvate)	30	58.2	194

in measurable amounts, analysis of soil extracts employing the separation technique described here will tend to give higher chromatate results.

Influence of particles on the determination of Cr^{VI} in soil extracts. Extracts of clay soils contain considerable numbers of particles below 0.45 µm, which pass through normal liquid chromatography columns. Therefore, the presence of such particles would lead to serious errors in chromatate results if such columns were employed for separation. This effect was carefully examined. After centrifugation, soil extracts were filtered through 0.45, 0.2 and 0.1 µm membrane filters and the concentration of chromatate was determined in these filtrates. Decreasing Cr^{VI} values were observed. With KH₂PO₄ (1.5 × 10⁻² mol dm⁻³) extracts, no further change in the Cr^{VI} results was observed by the use of a 0.05 µm filter. Thus, filtering through a 0.1 µm membrane filter was found to be satisfactory for efficient removal of particles from KH₂PO₄ (1.5 × 10⁻² mol dm⁻³) soil extracts. On the other hand, aqueous soil extracts in the absence of electrolytes contain substantially more fine particles (light yellow colour). A 0.05 µm membrane filter should be employed in this instance if accurate Cr^{VI} results are to be obtained.

Ion-pairing reversed-phase HPLC-ETAAS

Influence of pH on the separation of Cr^{VI}. The variation of pH between 4.0 and 7.0 in aqueous standard solutions of chromatate resulted in a slightly shifted retention time of Cr^{VI} during elution, but had no influence on the separation of Cr^{VI}. At pH values lower than 3, a substantial reduction of chromatate ion concentration in the presence of electron donors was observed.

Influence of Cr^{III} on the separation of Cr^{VI}. A standard solution of chromium(III) chloride (400 ng cm⁻³) was prepared alone or in synthetic mixtures containing 200–400 ng cm⁻³ of Cr^{VI}. Positively charged Cr^{III} species did not form ion pairs with the PIC A reagent and showed no influence on the determination of Cr^{VI}. In addition, the calibration graph for Cr^{VI} in the presence of 400 ng cm⁻³ of chromium(III) chloride was found to be linear in the concentration range 200–400 ng cm⁻³.

The reproducibility of measurement tested for six parallel determinations of Cr^{VI} (1 ng cm⁻³) was found to be ±4.5%. The LOD (3σ) for aqueous standard solutions was 0.2 ng cm⁻³ and for soil extracts, 0.3 ng cm⁻³.

Influence of Cr^{III} on the separation and determination of Cr^{VI} in soil extracts. Negatively charged complex species of Cr^{III} might form ion pairs with the PIC A reagent analogous to chromatate. If the elution of these species coincides with that of chromatate, an interference in the determination of the latter would result. These effects were therefore investigated carefully by employing several organic complexes of Cr^{III} typical of the soil environment. The results are presented in Table 5. It is evident that citrate, oxalate and maleate complexes of Cr^{III} had no influence on the determination of Cr^{VI}. In contrast, fulvate complexes formed ion pairs with the PIC A reagent that partially coincided with Cr^{VI} elution. The severe positive interference of chromium(III) fulvate on the determination of Cr^{VI} (Table 5) was similar to that observed in the use of the chelating ion-exchange separation technique (Table 4). The complexation of Cr^{III} with fulvic acid ligands in

Table 5 Influence of organically complexed Cr^{III} on the determination of Cr^{VI} by ion-pairing RP-HPLC-ETAAS

Added/ng cm ⁻³		Cr ^{VI} found/ ng cm ⁻³	Recovery (%)
Cr ^{III}	Cr ^{VI}		
70 (Citrate)	30	29.4	98.0
70 (Oxalate)	30	29.5	98.3
70 (Maleate)	30	29.3	97.6
70 (Fulvate)	30	55.7	185

Table 6 Effect of PIC A reagent concentration on the determination of Cr^{VI} in soil extracts (KH₂PO₄, 1.5 × 10⁻² mol dm⁻³) by ion-pairing RP-HPLC-ETAAS

Concentration of PIC A reagent/ mol dm ⁻³	Cr ^{VI} added/ ng cm ⁻³	Peat soil		Clay soil	
		Cr ^{VI} found/ ng cm ⁻³	Recovery (%)	Cr ^{VI} found/ ng cm ⁻³	Recovery (%)
5 × 10 ⁻⁴	500	19	3.7	50	6.3
2 × 10 ⁻³	500	210	41.1	330	65.4
1 × 10 ⁻²	500	580	116.0	490	98.0
2 × 10 ⁻²	500	580	116.0	491	98.2

soil solution, therefore, leads to an overestimate of the chromatate content of these soils.

Influence of particles on the determination of Cr^{VI} in soil extracts. It was found experimentally that small particles present in soil extracts did not influence the results of the determination of Cr^{VI} when separation was performed on the HPLC column. Obviously, the dense packing of the HPLC column, in contrast to the Chelex 100 column, retained particles of <0.45 µm. However, deposition of these particles in the column during consecutive determinations results in a continuous increase of the blank values and in column pressure. Consequently, the lifetime of the column was drastically reduced. The lifetime of the HPLC column was prolonged when soil extracts were filtered through 0.1 µm membrane filters.

Influence of the concentration of PIC A reagent on the determination of Cr^{VI} in soil extracts. The PIC A reagent was used to form an ion pair with the chromatate ions for preconcentration from natural pond-water samples.¹⁸ The optimum concentration of the reagent in the sample solution was reported to be 5 × 10⁻⁴ mol dm⁻³. Extraction of water-soluble chromatate from a soil sample was performed using 1.5 × 10⁻² mol dm⁻³ KH₂PO₄. Owing to the similarity of CrO₄²⁻ and H₂PO₄⁻ ions, the latter should also form an ion pair with the PIC A reagent. Additionally, some similar ions that could react with the reagent might be present in the soil solution. Thus, the optimum concentration of PIC A reagent in soil extracts for quantitative formation of an ion pair with the chromatate ion in soil should exceed 1 × 10⁻² mol dm⁻³. In order to prove this assumption, the following experiment was carried out. Chromium(VI) (500 ng cm⁻³) was added to each of two soil extracts (peat and clay soil extracted with KH₂PO₄, 1.5 × 10⁻² mol dm⁻³) in which the contents of total soluble chromium were below 1 ng cm⁻³. Various concentrations of PIC A reagent were added to 10 cm³ of these solutions and the samples were diluted to 15 cm³ with water. The concentrations of PIC A in the final solutions for HPLC separation were between 5 × 10⁻⁴ and 2 × 10⁻² mol dm⁻³. Aqueous standard solutions of 500 ng cm⁻³ of Cr^{VI} were prepared with these concentrations of PIC A reagent. Recovery for the aqueous standard solutions of Cr^{VI} was found to be between 98 and 100% for all concentrations of PIC A examined. The effect of the PIC A reagent concentration on the determination of Cr^{VI} in soil extracts (extracted with KH₂PO₄, 1.5 × 10⁻² mol dm⁻³) is presented in Table 6.

An additional experiment with aqueous extracts of the same soils indicated about 90% recovery for added Cr^{VI} at a concentration of PIC A of 5 × 10⁻⁴ mol dm⁻³. From these

observations and the data in Table 6, it was concluded that KH_2PO_4 formed ion pairs with the PIC A reagent. The optimum concentration of the reagent depends on the KH_2PO_4 concentration in the solution. A concentration of $1 \times 10^{-2} \text{ mol dm}^{-3}$ of PIC A reagent was found to be optimum when $1.5 \times 10^{-2} \text{ mol dm}^{-3} \text{ KH}_2\text{PO}_4$ is used as the extractant solution.

Analysis of Soil Extracts

In order to evaluate the capability of the methods for the determination of chromium in soil extracts, various types of soil samples were selected and analysed for total soluble and hexavalent soluble chromium. The selection of soils was such as to provide a wide variety of sample matrices characterized either by the physico-chemical nature of the soil or by the soil and waste material together. The first group represented natural soils of different characteristics (clay, sandy, peat and acid soils) with a low and medium concentration of total chromium ($40\text{--}120 \mu\text{g g}^{-1}$) and three natural serpentine soil samples with a high concentration of total chromium ($480\text{--}1300 \mu\text{g g}^{-1}$). The total chromium was determined by the procedure described previously.²⁹ The second group constituted some natural soils mixed with tannery waste, which were left to settle for 6 months under atmospheric conditions. The total chromium contents of these soils were $2300\text{--}3800 \mu\text{g g}^{-1}$. Finally, a clay field soil, which had been treated continuously

for 17 years with tannery waste, was sampled 4 years after the last waste application. The total chromium concentration of this field was between 1000 and $1400 \mu\text{g g}^{-1}$, while the concentration on a nearby meadow, which was indirectly contaminated by tannery waste (wind), was $170 \mu\text{g g}^{-1}$. Samples were prepared in triplicate as described under Experimental and analysed by the appropriate method. All of the samples were extracted with KH_2PO_4 ($1.5 \times 10^{-2} \text{ mol dm}^{-3}$), but some of the contaminated soils were also extracted with water in order to demonstrate the effects of chromate adsorption and the presence of colloidal particles in the extract solution on the results of the determination of chromium. The results of these measurements are summarized in Tables 7–9.

The concentration of soluble (KH_2PO_4 , $1.5 \times 10^{-2} \text{ mol dm}^{-3}$) hexavalent chromium in natural soils was generally below the detection limit for spectrophotometry and chelating ion exchange-ETAAS. The RP-HPLC-ETAAS technique, being the most sensitive, was therefore used (Table 7).

It is evident that the concentrations of soluble (KH_2PO_4 , $1.5 \times 10^{-2} \text{ mol dm}^{-3}$) chromate in natural soil samples are very low, with the exception of the serpentine soil samples. Despite the sensitive technique used ($\text{LOD} = 0.3 \text{ ng cm}^{-3}$) some of the concentrations were below the LOD. The inconsistency in the LOD shown in Table 7 reflects the differences in moisture contents of the soil samples considered. The pH of all the soil extracts was between 5.5 and 6.3 with the exception of the acid soil samples No. 10 ($\text{pH} = 3.8$) and No. 11 ($\text{pH} = 4.2$).

When these two samples were analysed by RP-HPLC-ETAAS, the Cr^{VI} peak did not appear either in the soil extracts or in the soil extracts to which Cr^{VI} was added due to a low pH and the presence of reducing substances in these soils. Chromium(vi) added to the sample extract was reduced immediately. Despite the relatively high total soluble chromium concentration in acid soils (Table 7) the expected chromate concentration should be extremely low owing to the nature of these soils.

Chromium(vi) was also added to the extracts of other soil matrices. Recoveries obtained were between 98 and 115%, which indicated that RP-HPLC-ETAAS was a suitable technique for the determination of soluble (KH_2PO_4 , $1.5 \times 10^{-2} \text{ mol dm}^{-3}$) hexavalent chromium in natural soils with normal pH values.

Table 7 Determination of total Cr, total soluble Cr and soluble Cr^{VI} in KH_2PO_4 ($1.5 \times 10^{-2} \text{ mol dm}^{-3}$) extracts of various natural soils by RP-HPLC-ETAAS, $n = 3$

Soil sample No.	Sample characteristic	Total Cr/ $\mu\text{g g}^{-1}$	Total soluble Cr/ ng g^{-1}	Soluble Cr^{VI} (RP-HPLC-ETAAS)/ ng g^{-1}	pH of extract
1	Sandy soil	45	2.4	<5	6.0
2	Clay soil	115	4.5	<5	5.5
3	Peat soil	40	2.9	<8	6.3
4	Clay soil	93	17.0	10	5.7
5	Sandy soil	75	5.6	<5	5.6
6	Clay soil	92	16.5	8.8	5.7
7	Serpentine soil	1324	75.4	53.9	5.4
8	Serpentine soil	485	46.1	27.2	5.6
9	Serpentine soil	825	43.4	36.9	5.9
10	Acid soil	127	35.3	—	3.8
11	Acid soil	85	30.5	—	4.2

Table 8 Determination of total Cr, total soluble Cr and soluble Cr^{VI} in KH_2PO_4 ($1.5 \times 10^{-2} \text{ mol dm}^{-3}$) extracts of various soils contaminated by tannery waste using spectrophotometry, chelating ion exchange-ETAAS and RP-HPLC-ETAAS, $n = 3$

Soil sample No.	Sample characteristic	Total Cr/ $\mu\text{g g}^{-1}$	Total soluble Cr/ ng g^{-1}	Soluble $\text{Cr}^{\text{VI}}/\text{ng g}^{-1}$			pH of extract
				Spectrophotometry	Chelating ion exchange-ETAAS	RP-HPLC-ETAAS	
I	Sandy soil*	2360	776	482	517	434	6.1
II	Clay soil*	2470	1621	1245	1389	909	5.3
III	Peat soil*	3730	960	<750	658	822	6.4
IV	Clay soil†	1400	384	<450	290	297	6.0
V	Clay soil†	1050	233	<450	169	184	5.8
VI	Clay soil†	169	37	—	33	34	5.4

* Tannery waste treated, analysed 6 months after waste application.

† Seventeen years of continuous tannery waste application, analysed in the fourth year after the last application.

Table 9 Determination of total Cr, total soluble Cr and soluble Cr^{VI} in aqueous soil extracts of various soils contaminated by tannery waste using chelating ion exchange-ETAAS and RP-HPLC-ETAAS, $n = 3$

Soil sample No.	Sample characteristic	Total Cr/ $\mu\text{g g}^{-1}$	Total soluble Cr/ ng g^{-1}	Soluble $\text{Cr}^{\text{VI}}/\text{ng g}^{-1}$		pH of extract
				Chelating ion exchange-ETAAS	RP-HPLC-ETAAS	
IV	Clay soil*	1400	238	183	143	6.7
V	Clay soil*	1050	140	92	62	6.8
VI	Clay soil*	169	48	38	<5	5.7

* Seventeen years of continuous tannery waste application, analysed in the fourth year after the last application.

Contaminated soil samples were analysed in triplicate by all three techniques (Table 8). Spectrophotometry could not be applied generally to the analysis of some of the contaminated soil extracts because of the poor LODs (30 ng cm^{-3} for Cr^{VI}). Results for the determination of Cr^{VI} obtained by RP-HPLC-ETAAS and chelating ion exchange-ETAAS agreed very well for soil samples treated with tannery waste, analysed 4 years after the last application (samples IV, V and VI). It was found experimentally that after consecutive RP-HPLC-ETAAS analyses of these samples, the blank value was constant but a slight broadening of the chromate peak appeared.

When extracts of soil samples freshly treated with tannery waste are analysed (samples I, II and III), the influence of the waste matrix should be taken into account. Tannery waste is a protein-based matrix with a high content of Cr^{III} , organic polymers and reducing substances which could produce interferences in the determination of Cr^{VI} . In order to suppress these effects, the soil extracts were diluted 1 + 7.5 prior to RP-HPLC determinations and 1 + 2 prior to chelating ion exchange. The samples were not diluted for spectrophotometric analyses because of the poor LOD of the technique. It should be emphasized that with these types of soil extracts excessively high and variable blanks appeared when using RP-HPLC-ETAAS, making the results uncertain and in disagreement with those given by the other two techniques. In addition, the lifetime of the RP-HPLC columns was drastically reduced.

Results using spectrophotometry and chelating ion exchange-ETAAS correlated well for these samples, provided that the concentration of chromate in the soil extracts was $>30 \text{ ng cm}^{-3}$. This good agreement indicates that the concentrations of organic ligands forming relatively inert Cr complexes, present in the samples should be low, otherwise much higher results would be obtained by chelating ion exchange-ETAAS. The accuracy of the result for the freshly treated peat soil sample (sample III) obtained by chelating ion exchange-ETAAS is questionable as no reliable comparison could be made using the other two techniques. According to the expected interference effects of chromium(III) fulvate, the reported value might be too high.

A comparison of the results from samples IV, V and VI (Tables 8 and 9) obtained by RP-HPLC-ETAAS reflected the effect of chromate adsorption on clay minerals, which was reported by Bartlett and James.⁹ On the other hand, from the results obtained by chelating ion exchange-ETAAS two effects were superimposed: the effect due to adsorption and the effect produced by the colloidal particles present in the aqueous extract.

Conclusions

Light scattering on colloidal particles can produce severe positive systematic errors in the spectrophotometric determination of Cr^{VI} in soils containing a high clay fraction. Similarly, particles passing through the ion-exchange column contribute to higher results for Cr^{VI} . In HPLC separation, particles had no direct influence but reduced the lifetime of the RP columns. A KH_2PO_4 ($1.5 \times 10^{-2} \text{ mol dm}^{-3}$) extraction solution efficiently released adsorbed chromate⁹ and prevented formation of colloidal solutions. Nevertheless, filtering through a $0.1 \mu\text{m}$ membrane filter was found to be necessary.

A low LOD for Cr^{VI} in soil extracts (0.3 ng cm^{-3}) using RP-HPLC-ETAAS enabled the determination of soluble hexavalent chromium in most natural soils. For soil samples contaminated by tannery waste, spectrophotometry was found to be suitable only for heavily contaminated soils. This technique may produce lower chromate results probably owing to partial reduction of Cr^{VI} during the measuring procedure in acidic media and a reducing environment. Analysis of samples treated with tannery waste, 4 years after the last application, showed very good agreement in the determination of soluble (KH_2PO_4 , $1.5 \times 10^{-2} \text{ mol dm}^{-3}$) Cr^{VI} between RP-HPLC-ETAAS and chelating ion exchange

-ETAAS techniques, taking into account soil characteristics. Analysis of freshly treated tannery waste soil samples employing RP-HPLC-ETAAS gave uncertain results because of the influence of the waste matrix and the variable blank. Spectrophotometry and chelating ion exchange-ETAAS results for these samples agreed well when the chromate concentration in the soil extracts was above 30 ng cm^{-3} .

Despite the considerable experimental efforts associated with the preparation of this paper, the reliable determination of chromium in soil extracts still remains a problem at least for some particular situations. Nevertheless, the experimental evidence presented demonstrates the complex nature of the effects of soil and tannery waste.

This work was supported by the Research Council of Slovenia and US Environmental Protection Agency (project JF 908). The authors thank Professor S. A. Katz for valuable suggestions in preparing this manuscript and Dr. A. R. Byrne for assistance with linguistic correction. The authors also thank Marko Zupan, for providing some soil samples and their physical characterization.

References

- 1 Fajgelj, A., and Kosta, L., *Vestn. Slov. Kem. Drus.*, 1987, **34**, 175.
- 2 Pankow, J. F., and Januer, G. E., *Anal. Chim. Acta*, 1974, **69**, 97.
- 3 Naranjit, D., Thomassen, Y., and Van Loon, J. C., *Anal. Chim. Acta*, 1979, **110**, 307.
- 4 Minoia, C., Mazzucotelli, A., Cavalleri, A., and Minganti, V., *Analyst*, 1983, **108**, 481.
- 5 Bergmann, H., and Hardt, K., *Fresenius Z. Anal. Chem.*, 1979, **297**, 381.
- 6 Donaldson, E. M., *Talanta*, 1980, **27**, 779.
- 7 Vos, G., *Fresenius Z. Anal. Chem.*, 1985, **320**, 556.
- 8 de Andrade, J. C., Rocha, J. C., and Baccan, N., *Analyst*, 1985, **110**, 197.
- 9 Bartlett, R., and James, B., *J. Environ. Qual.*, 1979, **8**, 31.
- 10 James, B. R., and Bartlett, R. J., *J. Environ. Qual.*, 1983, **12**, 169.
- 11 James, B. R., and Bartlett, R. J., *J. Environ. Qual.*, 1983, **12**, 173.
- 12 James, B. R., and Bartlett, R. J., *J. Environ. Qual.*, 1983, **12**, 177.
- 13 James, B. R., and Bartlett, R. J., *J. Environ. Qual.*, 1984, **13**, 67.
- 14 Heringer Donmez, L. A., and Kalenberger, W. E., *J. Am. Leather Chem. Assoc.*, 1989, **84**, 110.
- 15 Krull, I. S., Bushue, D., Savage, R. N., Schleicher, R. G., and Smith, S. B., *Anal. Lett., Part A*, 1982, **15**, 267.
- 16 Krull, I. S., Panaro, K. W., and Gershmann, L. L., *J. Chromatogr. Sci.*, 1983, **21**, 460.
- 17 Lawrence, K. E., Rice, G. W., and Fassel, W. A., *Anal. Chem.*, 1984, **56**, 292.
- 18 Syty, A., Christensen, R. G., and Rains, T. C., *At. Spectrosc.*, 1986, **7**, 89.
- 19 Syty, A., Christensen, R. G., and Rains, T. C., *J. Anal. At. Spectrom.*, 1988, **3**, 193.
- 20 Roehl, R., and Alforque, M. M., *At. Spectrosc.*, 1990, **11**, 210.
- 21 Mayazaki, A., and Barnes, R. M., *Anal. Chem.*, 1981, **53**, 364.
- 22 Colella, M. B., Siggia, S., and Barnes, R. M., *Anal. Chem.*, 1980, **52**, 967.
- 23 Isozaki, A., Kumagai, K., and Utsumi, S., *Anal. Chim. Acta*, 1983, **153**, 15.
- 24 Florence, T. M., and Batley, G. E., *Talanta*, 1976, **23**, 179.
- 25 Knudtsen, K., and O'Connor, G. A., *J. Environ. Qual.*, 1987, **16**, 85.
- 26 Nazario, C. L., and Menden, E. E., *J. Am. Leather Chem. Assoc.*, 1990, **85**, 212.
- 27 Perrin, D. D., *Aust. J. Chem.*, 1963, **16**, 572.
- 28 Brown, L., Haswell, S. J., Rhead, M. M., O'Neill, P., and Bancroft, K. C. C., *Analyst*, 1983, **108**, 1511.
- 29 Ajlec, R., Čop, M., and Štupar, J., *Analyst*, 1988, **113**, 585.

Paper 1/01559A

Received April 3, 1991

Accepted September 2, 1991

[illegible]

miniature cups were heated to 2600 °C before use to remove any contamination.

The powder mill was an Ishikawa Model AGA grinder with an agate mortar and pestle. The powder mixer was an Iwaki Model MA-1 mill with a polyethylene cylinder (24 mm × 12 mm i.d.) and a single polyethylene ball (9 mm diameter).

Powdered samples (0.5–1.0 mg) weighed on a Mettler Model M3 microbalance were introduced into the miniature cup using paper. The miniature cup was handled with titanium or brass tweezers. Liquid samples were injected into the cup within the graphite furnace with a Model 4700 Eppendorf micropipette (10 µl). Particle size distributions were measured with a Shimadzu Model SA-CP3L centrifugal particle size analyser.

Reagents and Samples

Graphite powder of about 50 µm particle size was prepared from spectroscopic graphite (Nippon Carbon) by grinding in an agate mortar. Standard solutions for calibration were prepared from commercially available 1000 ppm standard solutions (Junsei Kagaku) by dilution before use. All reagents used were of analytical-reagent grade and water was de-ionized.

The samples were nine geochemical standard reference rock samples issued by the Geological Survey of Japan: JG-1, JGb-1, JP-1, JR-1, JR-2, JA-1, JB-1a, JB-2 and JB-3.

Procedure

Rock samples were ground in order to make the average particle radius less than 2 µm (with no particles exceeding 10 µm). A portion of the powdered sample was mixed with the same amount of graphite powder. A 1.0 mg amount of the

mixture was weighed in the tared miniature graphite cup and inserted into the graphite furnace. The mixture was dried, pyrolysed and atomized according to the heating programme described later. Absorbance was determined by integration of the spectral lines in the absorbance–time spectrum. Analyte concentrations were determined by comparison with calibration graphs for standard solutions. For Rb and Cs, 20 ppm of K were added to each calibration standard solution to suppress the ionization interference.

Results and Discussion

Particle Size and Rock Sample

Minor elements are present in rocks forming solid solutions with rock-forming minerals or at the boundary of the minerals as oxides, sulfides, etc. They are heterogeneously distributed in rocks. Therefore, sufficient grinding of samples to fine powders is required to make the sample powders homogeneous for better reproducibility.

Wilson¹⁵ reported that it is desirable for the number of particles to exceed 1×10^5 to obtain favourable analytical repeatability (*i.e.*, relative standard deviations of less than 10%) in the analysis of solid samples. His calculation showed that 1 mg of powder contains 7×10^3 particles for a particle size of 50 µm and 8×10^5 particles for a particle size of 10 µm. At a size of 5 µm, the number of particles in 1 mg of powder is 7×10^6 , and sampling errors become less important.

Fig. 1 shows the variation in absorbance of Cu, Rb and Pb with grinding time for a 3.0 g rock sample (JG-1). The variation in the associated relative standard deviations for each element is shown in Fig. 2. The absorbance of Be, Co, Ni, Cu, Pb and Bi increased abruptly in the first 20 min of grinding, which was followed by a gradual increase up to 160 min. For Li, Rb and Cs, the absorbance was constant and essentially independent of grinding time. The relative standard deviation decreased slightly for the first 20 min, then levelled off. Both the median and the mode of the particle size distribution also decreased abruptly in the first 5 min and levelled off up to 160 min. The variation in the relative standard deviations of the absorbance showed a similar trend. The optimum grinding time was longer than 20 min for Be,

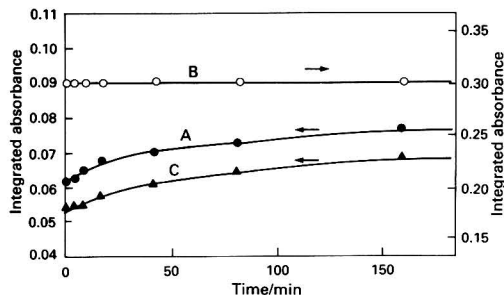


Fig. 1 Variation in the absorbance of A, Cu; B, Rb; and C, Pb in silicate rock samples with grinding time. A 0.50 mg amount of rock powder (JG-1) mixed with 0.50 mg of graphite powder was atomized. The rock powder (3 g) was ground with an Ishikawa grinder (Type AGA)

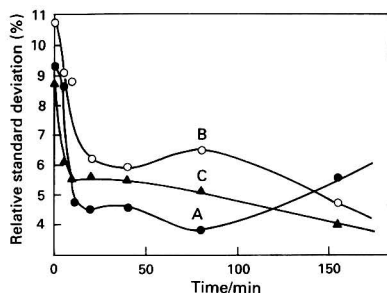


Fig. 2 Variation in relative standard deviation ($n = 5$) of the absorbance of A, Cu; B, Rb; and C, Pb in silicate rock powder (JG-1) with grinding time

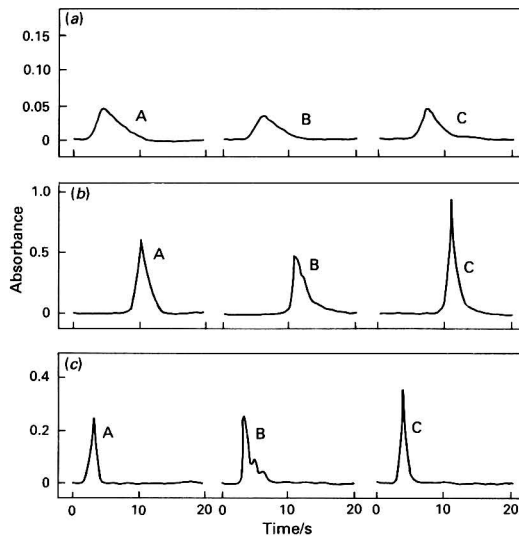


Fig. 3 Absorbance–time profiles for (a) Cu; (b) Rb; and (c) Pb in A, aqueous solution; B, silicate rock powder (JG-1); and C, a mixture of rock powder and graphite powder

Co, Ni, Cu, Pb and Bi, although 20 min was sufficient for Li, Rb and Cs for good reproducibility. Based on data obtained so far, the following grinding conditions are considered to be applicable: a 3.0 mg rock sample is ground for 20 min and the particle size range of the powder is 0.3–25 μm (median 2.4 μm ; mode 2.0 μm), 12% of the particles being larger than 10 μm . According to Wilson,¹⁵ this size distribution is suitable for obtaining sufficiently accurate results.

Addition of Graphite Powder

Mixing of graphite powder with solid powders in the graphite furnace gives a sharp spectral line^{12,13} owing to the improved atomization. This is because the total effective surface area of bulk samples is made larger and the heat conductivity is improved. Fig. 3 shows the change in the profiles of spectral lines with the addition of graphite powder. Fig. 4 shows the variation in the absorbance of Cu, Rb and Pb with amount of graphite powder added. Stable and maximum absorbance was obtained with 0.5 mg of rock powder mixed with 0.5 mg of graphite powder.

Fig. 5 shows the secondary electron images of rock powder (JR-1) after heating at 2400 °C with and without graphite powder. The presence of graphite powder gives a sharp spectral line and enhances the intensity of the spectral lines for Li, Be, Ni, Cs, Pb and Bi. No change in the half-width of the spectral lines of Co, Cu and Rb was observed, although the absorbances of these elements were intensified. The mixing ratio of graphite powder to sample powder for maximum absorbance for each element is as follows: Li, >0.8; Be, 1.5–3.0; Co, 1.0–1.5; Ni, 1.0–1.5; Cu, 0.0–1.0; Rb, 0.8–1.0; Cs, 0.8–2.0; Pb, 1.0–1.5; and Bi, 0.8–1.5. A mixing ratio of graphite powder of 1.0 appeared to be suitable, although for Be the value was 2.0.

The proposed method is effective even for a sample with a concentration that is too high for the dynamic range; a sample containing elements at levels as high as a few hundred ppm can be analysed simply by increasing the amount of graphite powder.

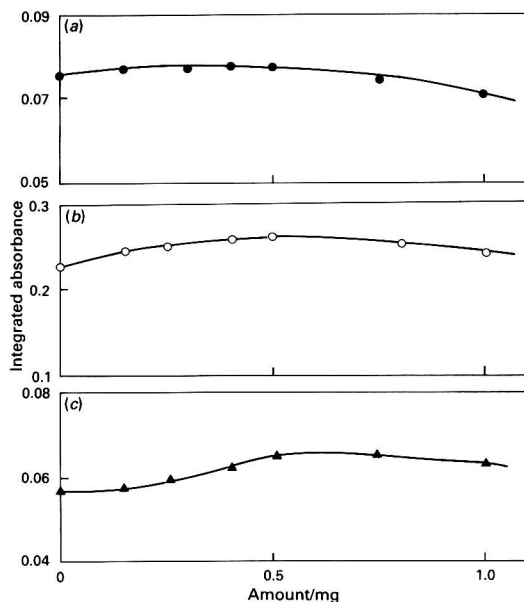


Fig. 4 Variation in the absorbance of (a) Cu; (b) Rb; and (c) Pb in silicate rock powder (JR-1) with the amount of graphite powder added to 0.50 mg of silicate rock powder

Heating Programme

Optimum temperatures for the drying, pyrolysis and atomization steps for each element were determined with JG-1 and for Pb with JB-1a. Fig. 6 shows the variation in absorbance for Cu, Rb and Pb with temperature. The heating programme established is given in Table 2.

Sample Amount

Fig. 7 shows the variation in absorbance with amount of sample. The absorbances for Li, Be, Ni, Cu, Cs, Pb and Bi are proportional to sample amount from 0.2 to 1.0 mg and for Co and Rb up to 0.7 and 1.5 mg, respectively. When the sample amount exceeds the upper limit or the content of the element is more than 2–3 ng, the proportionality no longer holds. However, when aqueous standard solutions are atomized, proportionality holds up to 10–30 ng. This result implies that an increase in sample amount inhibits the diffusion of atomic vapour. Hence, the optimum sample amounts for Li, Ni, Cu, Rb, Cs, Pb and Bi are 1.0 mg and those for Be and Co, which are more sensitive than other elements, are 0.2 and 0.5 mg, respectively.

Suppression of Ionization Interference

For an element with an ionization potential higher than 4.6 eV, the ionization interference can be ignored.¹⁶ The ionization potentials of Rb and Cs are 4.2 and 3.9 eV, respectively, hence suppression of the interference is required. Potassium, with a low ionization potential, is usually added to suppress the interference. Rock samples usually contain significant amounts of Na and K which suppress the interference, but those elements are not present in standard solutions.

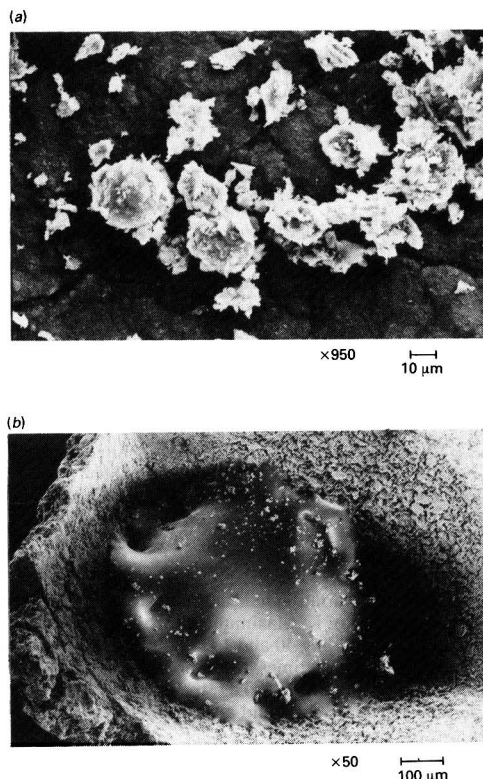


Fig. 5 Secondary electron images of rock powder (JR-1) after heating at 2400 °C (a) with and (b) without graphite powder

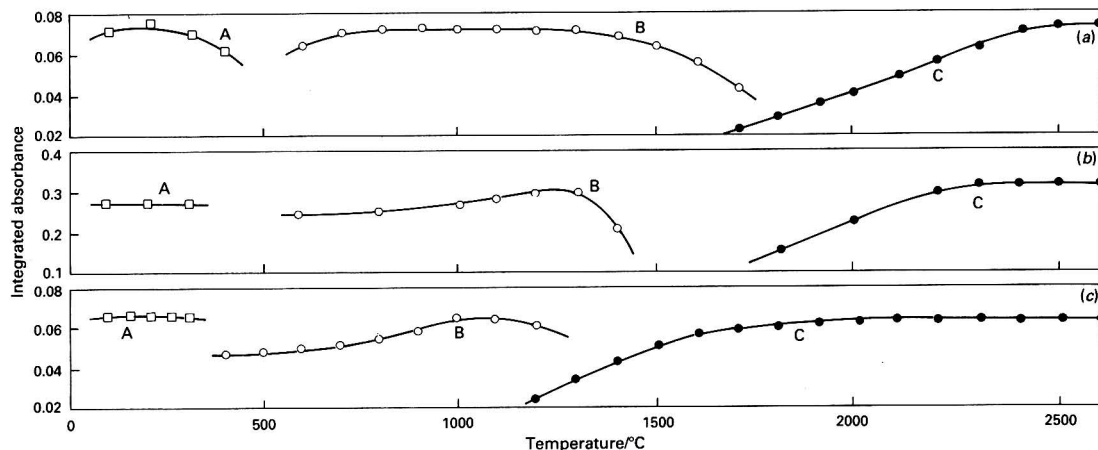


Fig. 6 Variation in the absorbance of (a) Cu; (b) Rb; and (c) Pb in silicate rock samples (JG-1) with A, drying; B, pyrolysis; and C, atomization temperature

Table 2 Analytical conditions for the determination of Li, Be, Co, Ni, Cu, Rb, Cs and Pb in silicate rock samples

Parameter	Li	Be	Co	Ni	Cu	Rb	Cs	Pb	Bi
Sample amount/mg	1.0	0.2	0.5	1.0	1.0	1.0	1.0	1.0	1.0
Grinding time*/min					20				
Particle size†/μm					2.0 (0.3–25)				
Mixing ratio of sample to graphite powder	1:1	1:2	1:1	1:1	1:1	1:1	1:1	1:1	1:1
Atomization conditions:									
Drying	120,30‡	120,30	150,30	150,30	200,30	120,30	120,30	150,30	120,30
Pyrolysis	1400,30	1900,30	900,30	900,30	700,30	1300,30	1600,30	1000,30	1500,30
Atomizing	2600,20	2600,20	2600,20	2600,20	2600,20	2400,30	2600,10	2600,15	2600,10

* 3.0 g of silicate rock samples ground with an Ishikawa type AGA grinder.

† Mode diameter.

‡ The first value in each pair is temperature in °C and the second is time in seconds.

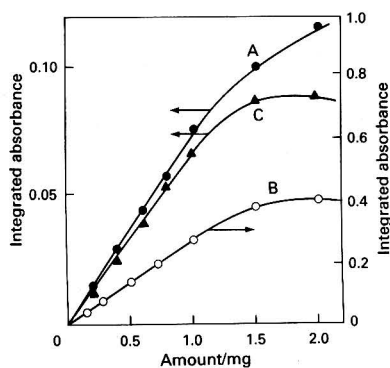


Fig. 7 Variation in the absorbance of A, Cu; B, Rb; and C, Pb in silicate rock powder with amount of sample

Fig. 8 shows the variation in absorbance for 5 ng of Rb and Cs with the amount of K. Maximum absorbance was obtained for Rb and Cs by adding 40 and 100 ng of K (eight times the amount of Rb and 20 times the amount of Cs) or more, respectively. For more than 500 ng, the data processor cannot compensate for the background absorbance.

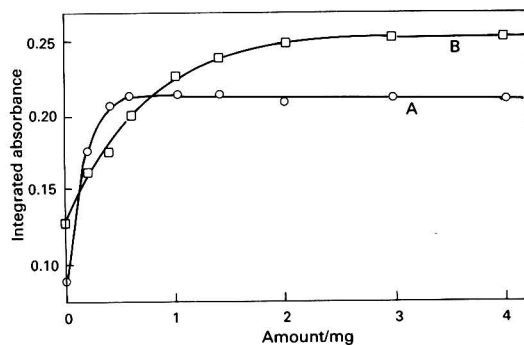


Fig. 8 Variation in the absorbance of 5 ng of A, Rb; and B, Cs in 10 μl of aqueous solution with amount of K added as an ionization suppressor

Application to Geochemical Standard Rock Samples

The results for nine geochemical standard rock samples

obtained under the proposed conditions are given in Table 3. The calibration standard solutions for Rb and Cs contain K in a 30-fold excess. Each value in Table 3 is the average of five measurements; the relative standard deviations are less than 10%. Values recommended by Ando *et al.*¹⁷ are also given in Table 3 for comparison. Fig. 9 shows the correlation between the found and the recommended values. The correlation coefficient of 0.9993 indicates that the present results agree well with the recommended values, and that an aqueous standard solution is effective for the calibration in the direct atomization AAS of solid rock samples.

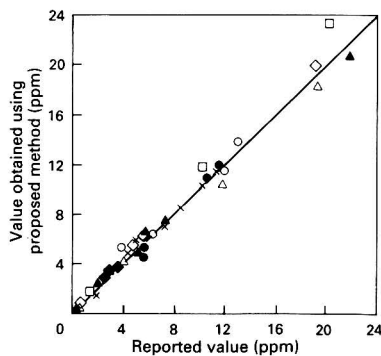
Table 3 Results for the determination of Li, Be, Co, Ni, Cu, Rb, Cs, Pb and Bi in GSJ standard reference rock samples (in ppm), and literature values¹⁷

Sample	Li			Be			Co			Ni			Cu		
	This work	RSD* (%)	Ref. 17	This work	RSD* (%)	Ref. 17	This work	RSD* (%)	Ref. 17	This work	RSD* (%)	Ref. 17	This work	RSD* (%)	Ref. 17
JG-1	84.1	2	85.9	3.3	4	3.1	4.2	5	4.0	6.1	6	6.0	5.2	3	5.6
JGb-1	4.6	4	4.3	0.37	8	0.36	60.3	11	61.6	25.9	6	25.4	85.6	2	86.8
JP-1	1.5	4	1.8	N.D.†		<1	127	9	116	—	—	2460	4.4	6	5.7
JR-1	63.6	6	62.3	3.2	4	3.1	0.70	5	0.65	0.60	5	0.66	1.4	8	1.4
JR-2	87.5	3	83	3.8	3	3.4	0.36	8	0.4	0.93	6	0.84	1.4	12	1.4
JA-1	10.8	2	10.5	0.57	7	0.50	10.2	8	11.8	5.9	2	5	42.4	10	42.4
JB-1a	11.9	7	11.5	1.5	5	1.4	39.5	9	39.5	128.9	0.3	135	56.5	5	55.5
JB-2	8.3	3	8.0	0.28	5	0.27	36.1	8	39.8	19.9	6	19	222	5	227
JB-3	6.8	0.4	7.2	0.74	5	0.74	33.4	5	36.3	38.6	9	38.8	195	1	198

Sample	Rb			Cs			Pb			Bi		
	This work	RSD* (%)	Ref. 17	This work	RSD* (%)	Ref. 17	This work	RSD* (%)	Ref. 17	This work	RSD* (%)	Ref. 17
JG-1	173.2	0.3	181	11.8	2.0	10.2	25.1	3	26.2	0.48	19	0.52
JGb-1	5.1	6	4	N.D.		0.27	2.2	7	1.9	N.D.		0.014
JP-1	N.D.		<1	N.D.		>0.1	N.D.		0.11	N.D.		—
JR-1	260	0.7	257	23.1	2.4	20.2	17.9	6	19.1	0.48	11	0.51
JR-2	286	3	297	26.6	4.1	26	20.4	1	21.9	0.65	8.9	0.65
JA-1	11.6	3	11.8	N.D.		0.64	6.1	4	5.8	N.D.		0.009
JB-1a	41.2	1	41	1.8	12	1.2	7.2	4	7.2	0.95	5.9	—
JB-2	6.2	9	6.2	N.D.		0.90	5.1	6	5.4	N.D.		0.033
JB-3	13.7	5	13	N.D.		1.1	5.0	4	5.5	N.D.		0.020

* Relative standard deviation (%), $n = 5$.

† N.D. = not detected.

**Fig. 9** Correlation between reported values and those obtained with the proposed method for \times , Li; \blacklozenge , Be; \triangle , Co; \bullet , Ni; \circ , Cu; \square , Rb; \blacktriangle , Cs; \blacksquare , Pb; and \blacksquare , Bi in GSJ standard rock samples. The correlation coefficient is 0.9993

The authors thank S. Morita, H. Moriya and S. Miyamoto for technical assistance, and the Machine Shop, Meiji University, for making the miniature cup.

References

- 1 Brooks, R. R., and Boswell, C. R., *Anal. Chim. Acta*, 1965, **32**, 339.

- 2 Reeves, R. D., and Brooks, R. R., *Trace Element Analysis of Geological Materials*, Wiley-Interscience, New York, 1978, p. 151.
- 3 Govindaraju, K., Mevelle, G., and Chouard, C., *Anal. Chem.*, 1974, **46**, 1972.
- 4 Katskov, D. A., L'vov, B. V., and Polzik, L. K., *Zh. Prikl. Spektrosk.*, 1974, **20**, 739.
- 5 Katskov, D. A., Kruglikova, L. P., and L'vov, B. V., *Zh. Anal. Khim.*, 1975, **30**, 238.
- 6 Karyakin, A. V., Pchelintsev, A. M., Shidlovskii, A. I., Vul'fson, E. K., and Tsimigarelli, M. N., *Zh. Prikl. Spektrosk.*, 1973, **18**, 610.
- 7 Vul'fson, E. K., Karyakin, A. V., and Shidlovskii, A. I., *Zh. Anal. Khim.*, 1973, **28**, 1253.
- 8 Katskov, D. A., and L'vov, B. V., *Zh. Prikl. Spektrosk.*, 1969, **10**, 382.
- 9 Leucke, W., Eschermann, F., Lennartz, U., and Papastamat-aki, A. J., *Neues Jahrb. Mineral. Abh.*, 1974, **120**, 178.
- 10 Fuller, C. W., and Thompson, I., *Analyst*, 1977, **102**, 141.
- 11 Isozaki, A., Morita, Y., and Utsumi, S., *Bunseki Kagaku*, 1990, **39**, 605.
- 12 Langmyhr, F. J., Stubergh, J. R., Thomassen, Y., Hassen, J. E., and Dolezal, J., *Anal. Chim. Acta*, 1974, **71**, 35.
- 13 Siemer, D. D., and Wei, H. Y., *Anal. Chem.*, 1978, **50**, 147.
- 14 Atsuya, L., and Itoh, K., *Bunseki Kagaku*, 1982, **31**, 708.
- 15 Wilson, A. D., *Analyst*, 1964, **89**, 416.
- 16 Suzuki, M., and Ohta, K., *Bunseki*, 1984, **125**, 416.
- 17 Ando, A., Mita, N., and Terashima, S., *Geostand. Newsl.*, 1987, **11**, 159.

Paper 1/03891E

Received July 29, 1991

Accepted September 25, 1991

Determination of Lanthanum in Food and Water Samples by Zeeman-effect Atomic Absorption Spectrometry Using a Graphite Tube Lined With Tungsten Foil

Shen Miao-Kang

Hangzhou Health and Anti-Epidemic Station, Hangzhou 310006, People's Republic of China

Shi Yin-Yu

Department of Chemistry, Zhejiang University, Hangzhou 310027, People's Republic of China

A sensitive, selective method for the determination of lanthanum in food and water samples by atomic absorption spectrometry using a graphite tube lined with tungsten foil is described. The atomization of lanthanum from the tungsten surface gives better analytical sensitivity, a lower atomization temperature and negligible memory effects. The characteristic mass and detection limit of the method were 8.1×10^{-9} and 7.85×10^{-9} g, respectively. The precision (relative standard deviation in the range 5.9–9.9%), accuracy and interferences of the method were also investigated. The method can be used directly for the determination of trace amounts of lanthanum in food and water without pre-dissociation of the matrices. The results obtained by this method are in good agreement with those obtained from inductively coupled plasma atomic emission spectrometry.

Keywords: Lanthanum determination; food and water; atomic absorption spectrometry; tungsten atomizer

Atomic absorption analysis with electrically heated graphite atomizers has found widespread acceptance as a routine method in many research and application laboratories. Atomization of the sample in a graphite tube heated to 3000 °C gives a method of good sensitivity, capable of determining a large number of trace elements directly in diverse sample matrices. However, the determination of lanthanum by atomic absorption spectrometry (AAS) has always been difficult because of the poor sensitivity and strong memory effect for the element. These problems are generally attributed to carbide formation resulting from the interaction of lanthanum with carbon from the atomizer. The graphite itself has been improved to overcome these problems. Although a pyrolytic graphite coated graphite tube has been used,^{1–5} this atomizer does not give adequate sensitivity for lanthanum which forms refractory carbides with graphite at high temperatures resulting in incomplete vaporization of the lanthanum. Attempts have also been made to use a graphite tube pre-coated with a salt of tantalum, zirconium or tungsten.^{6–8} Other attempts have been made to use a tantalum or tungsten–tantalum lining inserted inside the graphite furnace.^{9–17} These atomizers can eliminate physical contact and, hence, reaction between the graphite surface and analytes, and significantly increase the analytical sensitivity. However, the lifetime of the atomization surfaces is not very long and the reproducibilities are not satisfactory because of the deformation of the metal at high temperatures.

This paper describes the determination of lanthanum in food and water samples by Zeeman-effect background-corrected AAS using a graphite tube lined with tungsten foil.

Experimental

Apparatus

A Perkin-Elmer Zeeman 5000 AA spectrometer with a hollow cathode lamp operating at 30 mA and with a slit-width of 0.4 nm was used. Measurements were made at 550.1 nm. Zeeman-effect background correction was used. A Perkin-Elmer HGA-500 graphite furnace atomizer was operated under the conditions given in Table 1. Samples were injected using a Perkin-Elmer AS-40 autosampler. The volume injected was 20 µl. Signals were recorded on a Perkin-Elmer Model 100 recorder. The height of the absorbance peak was measured.

Preparation of the Furnace Lined With Tungsten Foil

The tungsten lining was prepared from a rectangular strip (12 × 15 mm) of tungsten foil of purity 99.967% and thickness 0.1 mm and formed by winding a tungsten strip around a glass rod of diameter slightly less than that of the graphite tube. The lining was inserted into the centre of a new pyrolytic graphite coated graphite tube and a metal rod was placed into the tube and firmly rolled inside it to attach the tungsten foil smoothly to the inner lining of the graphite tube. In order to prevent distortion of the foil on heating, the tube lined with foil was pre-treated in the HGA 500 atomizer, by heating several times to a high temperature in a current of argon according to the following programme: (i) the tube was heated to 500 °C in 10 s, held at that temperature for 5 s, and then cooled down in 10 s; and (ii) the operation was repeated for temperatures of 1000, 1500, 2000 and 2500 °C, followed by blank firings according to the heating programme in Table 1. The lifetime of the tungsten-surface atomizer was about 130 firings.

Reagents

All reagents for the interference study were of analytical-reagent grade and all solutions were prepared with doubly distilled, de-ionized water.

Lanthanum oxide stock standard solution, 1000 µg ml⁻¹. Accurately weigh 0.1000 g of lanthanum oxide (99.99%) and dissolve by gently heating in 10 ml of concentrated hydrochloric acid. Wash the solution into a 100 ml calibrated flask and dilute to the mark with water. Store the solution in a stoppered polyethylene bottle.

Lanthanum working standard solution. Prepare working solutions to cover a wide concentration range by mixing an

Table 1 Graphite furnace conditions for the determination of lanthanum

Step	Temperature/°C	Ramp time/s	Hold time/s	Argon flow rate/ml min ⁻¹
Dry	100	5	10	300
Dry	200	5	10	300
Ash	1300	5	10	300
Atomize	2400	0	4	0
Clean	2500	1	3	300

aliquot of the stock solution with water (final acidity approximately 4% hydrochloric acid) and store in polyethylene bottles.

Concentrated hydrochloric acid, Suprapur grade.

Concentrated nitric acid, Suprapur grade.

Procedure

The lanthanum content of food and water samples is usually small and therefore it is often necessary to concentrate the element in a small volume.

Preparation of food samples for analysis

Samples of food *e.g.*, rice, wheat, maize, milk powder, vegetable and tea were oven-dried and ground. An accurately weighed sample (5–10 g) was placed in a porcelain crucible and covered. The crucible was heated for 1 h on a hot-plate, then several drops of concentrated nitric acid were added to aid charring and the heating was continued. The temperature was increased gradually in order to avoid sputtering of the sample. After charring was complete, the crucible was heated in a muffle furnace at 400 °C for 30 min and 600 °C for a further 6 h. The crucible was removed, cooled and, after the addition of 0.5 ml of concentrated nitric acid, heated in the same manner as described above for 6 h. The sample ash was treated with 0.2 ml of concentrated hydrochloric acid and 0.2 ml of water (warming may be necessary). The solution was transferred quantitatively into a 5 ml calibrated flask and diluted to the mark with water. In this ashing method, the preparation of a blank was necessary.

Preparation of water samples for analysis

A suitable volume of water sample (250–500 ml) was transferred into a 500 ml beaker and 0.2 ml of concentrated hydrochloric acid was added. The beaker was heated in a water-bath and the solution was evaporated to 2–3 ml. The concentrated solution was transferred quantitatively into a 5 ml calibrated flask and diluted to the mark with water.

Determination

The treated solutions were decanted into the sampling cups of the autoanalyser and measurements of lanthanum were made using the conditions given in Table 1. The absorbances were recorded on chart paper.

Results and Discussion

Optimization of the Graphite Furnace Programme

Experiments were carried out to ascertain the best temperature and time for the drying, ashing and atomization steps. A mirror was used to observe the drying of the sample in the

furnace. It was found that a temperature of >150 °C allowed uniform drying with no sputtering, and that the drying time was dependent on the volume of solution injected into the furnace; a time of 20 s was required for 20 µl of a sample. In order to optimize the ashing and atomization temperatures, graphs were constructed for an aqueous solution containing 10 µg ml⁻¹ of lanthanum and the optimum concentration of hydrochloric acid; the results are shown in Fig. 1. The optimum ashing temperature was 1300 °C (the dip in the ashing curve probably related to the volatilization of lanthanum) and the optimum atomization temperature was 2400 °C. The internal gas-stop mode and maximum power were used during the atomization stage. The use of the gas-stop mode in the atomization step can produce tube memory effects, therefore, in order to overcome this, the tube was fired at 2500 °C for 3 s with the internal gas at the maximum flow rate of 300 ml min⁻¹.

The ashing time for the sample in the hydrochloric acid matrix was 10 s. The atomization temperature was maintained for only 4 s, as longer atomization times did not effectively reduce the peak height of the blank solution further, but only reduced the usable life span of the graphite tube.

Effect of Hydrochloric Acid Concentration

In a hydrochloric acid matrix, the chloride complex is usually present before atomization. However, lanthanum chloride hydrolyzes to oxychlorides on evaporation and, at a higher temperature, these decompose to the oxide. Therefore, the lanthanum oxide intermediate can be expected to form before atomization in a hydrochloric acid medium. The effect of hydrochloric acid concentration on the determination of lanthanum is shown in Fig. 2. The peak height absorbance increased slightly as the concentration of hydrochloric acid increased from 0.5 to 1.0% v/v, but remained constant at concentrations of >1.0%. Therefore, a hydrochloric acid concentration of 4.0% v/v was selected.

Calibration and Standard Additions Graphs

In order to obtain a calibration graph, standard solutions containing 0–10 µg ml⁻¹ of lanthanum with the optimum concentration of hydrochloric acid were subjected to the furnace programme. When using the standard additions method, 0, 1, 2, 4 and 8 µg ml⁻¹ of lanthanum and the optimum concentration of hydrochloric acid were added to a sample. The correlation coefficient of the calibration graph for absorbance *versus* concentration of lanthanum was 0.9991. The slopes of the calibration and standard additions graphs were in close agreement, which illustrated that the matrix effect was negligible.

Sensitivity and Detection Limit

The sensitivity can be conveniently measured in terms of 'characteristic mass'. In this work, the proposed method has a characteristic mass of 8.1×10^{-9} g, which is similar to that given by L'vov and Pelieva.⁹ The detection limit, *i.e.*, the

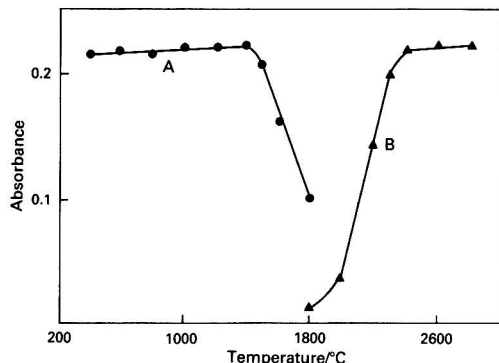


Fig. 1 A, Ashing and B, atomization graphs for lanthanum

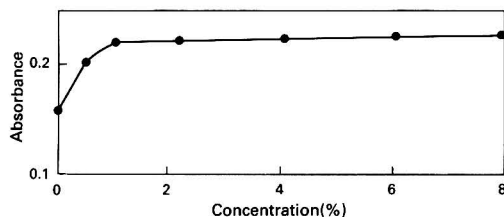


Fig. 2 Effect of concentration of hydrochloric acid on absorbance of lanthanum

Table 2 Precision of the results for the determination of lanthanum

Sample No.	Concentration/ $\mu\text{g ml}^{-1}$	Mean absorbance	Standard deviation/ $\mu\text{g ml}^{-1}$	Relative standard deviation (%)
1	2.0	0.0238	0.00237	9.9
2	4.0	0.0426	0.00374	8.8
3	20.0	0.214	0.01270	5.9

Table 3 Recovery of lanthanum from food and water samples

Sample No.	Lanthanum/ $\mu\text{g ml}^{-1}$			Recovery (%)
	Present*	Added	Found	
1	1.55	2.5	3.90	94.0
2	1.60	2.5	3.65	82.0
3	2.10	2.5	4.30	88.0
4	2.30	2.5	4.40	84.0
5	2.85	2.5	4.70	74.0
6	1.10	3.0	3.80	90.0
7	1.85	3.0	4.95	103.0
8	1.95	3.0	4.40	82.0
9	2.70	3.0	4.85	73.0
10	1.70	5.0	5.87	83.0

* Preconcentrated samples.

Table 4 Interference of other ions on the determination of lanthanum

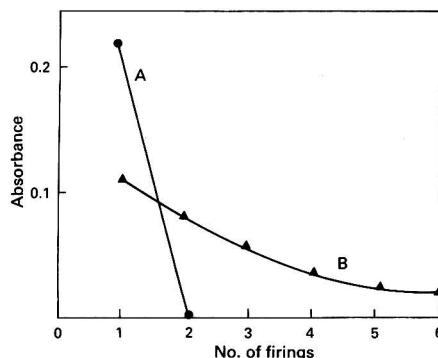
Ion	Added as	Amount added (ppm)	Relative absorbance
None	—	—	1.00
Ca^{2+}	CaCO_3	500	0.97
Mg^{2+}	MgCO_3	200	0.97
K^+	KCl	500	0.89
Na^+	NaCl	500	1.05
Cu^{2+}	$\text{Cu}(\text{NO}_3)_2$	10	1.00
Fe^{3+}	$\text{Fe}(\text{NO}_3)_3$	100	0.89
Zn^{2+}	$\text{Zn}(\text{NO}_3)_2$	10	0.97
Pb^{2+}	$\text{Pb}(\text{NO}_3)_2$	10	0.98
Cr^{6+}	$\text{K}_2\text{Cr}_2\text{O}_7$	10	0.91
Cd^{2+}	$\text{Cd}(\text{NO}_3)_2$	10	0.90
Mn^{2+}	MnSO_4	10	0.99
Al^{3+}	$\text{Al}(\text{NO}_3)_3$	5	0.93
Sn^{4+}	SnCl_4	5	0.94
Si^{2+}	Na_2SiO_2	100	1.09
Se^{4+}	$\text{Se}(\text{NO}_3)_4$	2	1.00
Cl^-	NaCl	300	1.05
NO_3^-	$\text{Fe}(\text{NO}_3)_3$	80	0.89
SO_4^{2-}	MnSO_4	100	0.99

lowest concentration level that can be determined to be statistically different from a blank, is defined as three times the within-batch standard deviation of a single blank determination (*i.e.*, the standard deviation was obtained from replicate analyses of a single blank sample), corresponding to a 99% confidence level. In this study, the detection limit of lanthanum was 7.85×10^{-9} g.

Precision and Accuracy

The precision (relative standard deviation) of the method was obtained for replicate analyses of one sample during the same run and the results are shown in Table 2. The within-batch precision of the method, obtained for replicates of three synthetic samples with 2.0, 4.0 and $20.0 \mu\text{g ml}^{-1}$ lanthanum added, varied over the range 5.9–9.9%.

In order to study the accuracy of the method, the recovery of standard additions of lanthanum to the samples was investigated over the entire sample preparation procedure. Each addition was performed in duplicate. The results obtained gave recoveries ranging from 73 to 103% of lanthanum (Table 3).

**Fig. 3** Memory effects of atomizers: A, lined tube; and B, unlined tube**Table 5** Comparison of results for the determination of lanthanum

Sample No.	Lanthanum concentration/ $\mu\text{g ml}^{-1}$	
	Proposed method	ICP-AES method
1	0.155	0.142
2	0.210	0.221
3	0.230	0.213
4	0.285	0.298
5	0.110	0.123
6	0.185	0.213
7	0.195	0.198
8	0.085	0.104
9	0.063	0.078
10	0.050	0.052

Interference Study

Different amounts of other ions were added to a test solution containing $10 \mu\text{g ml}^{-1}$ of lanthanum and lanthanum was determined using the proposed procedure. The absorbance data were compared with the value obtained for $20 \mu\text{l}$ of a $10 \mu\text{g ml}^{-1}$ pure lanthanum standard solution. The results obtained are given in Table 4, which shows that not all the elements tested interfered with the determination of lanthanum. The interference caused by other rare earth elements was also investigated and appeared negligible. This illustrates that the selectivity of the method is very good.

Memory Effect

Lanthanum in the presence of carbon is considered to form a non-volatile carbide that may result in a memory effect. This memory effect was reduced when a pyrolytic graphite coated graphite tube lined with tungsten foil was used (Fig. 3). After injection of a $20 \mu\text{l}$ aliquot of a $10 \mu\text{g ml}^{-1}$ solution into a graphite tube lined with tungsten foil, a return to background levels was obtained without any blank firings. However, after injection of a $20 \mu\text{l}$ aliquot of a $10 \mu\text{g ml}^{-1}$ solution into an unlined graphite tube, a significant memory effect remained even after five blank firings. Therefore, the atomization surface plays an important role in the determination of lanthanum.

Comparison of Two Analytical Methods

A comparison of the results obtained by the proposed method with those obtained using inductively coupled plasma atomic emission spectrometry (ICP-AES) is shown in Table 5. The results show that there is satisfactory agreement and no significant difference ($P > 0.05$) between the two methods.

References

- 1 Zvonimir, G., *Fresenius' Z. Anal. Chem.*, 1978, **289**, 337.
- 2 Horsky, S. J., *At. Spectrosc.*, 1980, **4**, 129.
- 3 Horsky, S. J., and Fletcher, W. K., *Chem. Geol.*, 1981, **32**, 335.
- 4 Sen Gupta, J. G., *Anal. Chim. Acta*, 1982, **138**, 295.
- 5 Sicinska, P., and Michalewska, M., *Fresenius' Z. Anal. Chem.*, 1982, **312**, 530.
- 6 Sastry, M. D., Bhide, M. K., Savitri, K., Babu, Y., and Joshi, B. D., *Fresenius' Z. Anal. Chem.*, 1979, **298**, 367.
- 7 Sneddon, J., and Fuavao, V. A., *Anal. Chim. Acta*, 1985, **167**, 317.
- 8 Zatk, V. J., *Anal. Chem.*, 1978, **50**, 538.
- 9 L'vov, B. V., and Pelieva, L. V., *Zavod. Lab.*, 1978, **44**, 173.
- 10 Chen, Y.-W., and Li, J.-X., *Fenxi Huaxue*, 1979, **7**, 7.
- 11 Wahab, H. S., and Chakrabarti, C. L., *Spectrochim. Acta, Part B*, 1981, **36**, 475.
- 12 Wahab, H. S., and Chakrabarti, C. L., *Spectrochim. Acta, Part B*, 1981, **36**, 463.
- 13 Sen Gupta, J. G., *Talanta*, 1984, **31**, 1053.
- 14 L'vov, B. V., and Pelieva, L. V., *Zh. Anal. Khim.*, 1979, **34**, 1744.
- 15 Sen Gupta, J. G., *Talanta*, 1985, **32**, 1.
- 16 Sen Gupta, J. G., *Talanta*, 1987, **34**, 1043.
- 17 Ma, Y.-Z., and Wu, Z.-K., *Huaxue Tongbao*, 1982, **1**, 22.

Paper 1/04144D

Received August 8, 1991

Accepted October 2, 1991

Rapid and Simple Method for the Determination of Copper, Manganese and Zinc in Rat Liver by Direct Flame Atomic Absorption Spectrometry

Svetlana Luterotti

Department of Chemistry, Faculty of Pharmacy and Biochemistry, University of Zagreb, 1, A. Kovačića, Zagreb, Croatia

Tihana Žanić-Grubišić and Dubravka Juretić

Department of Medical Biochemistry, Faculty of Pharmacy and Biochemistry, University of Zagreb, 1, A. Kovačića, Zagreb, Croatia

An acidic homogenate method, which includes simple homogenization pre-treatment of tissue material and direct nebulization flame atomic absorption spectrometry (FAAS), is successfully applied to the simultaneous determination of copper, manganese and zinc in rat liver. The proposed method involves only a few steps for sample pre-treatment at room temperature, making the risk of systematic errors very small. Because recoveries of 101% for copper, 98% for manganese and 100% for zinc could be achieved using aqueous standards, matrix-matched standards were redundant. Favourable results obtained in biological media, including limits of detection of 0.04, 0.03 and 0.04 mg l⁻¹ for Cu, Mn and Zn, respectively, together with accuracies of 0–3%, and relative standard deviations ranging from 2 to 10% are further evidence of the suitability of the method.

Keywords: Copper, manganese and zinc determination; rat liver; direct flame atomic absorption spectrometry; sample pooling and homogenization; direct standardization

Tissue analyses are generally time-consuming and prone to error, mainly because sample preparation is tedious and includes the risk of contamination or loss of analyte. Dry and wet decomposition methods have been used frequently as procedures for the treatment of tissue samples¹ prior to determinations using atomic absorption spectrometry (AAS).² Wet ashing is generally quicker than dry ashing and has been applied to various types of tissue at room or elevated temperature.^{3–10} However, the hazardous nature of the reagents requires constant vigilance, and high purity reagents must be used in order to avoid high blank values. Digestion time was, however, reduced to as little as 1 h by solubilizing the tissue with a quaternary ammonium hydroxide.^{11,12} Chelation of vanadium(v) with hydroxamic acid and subsequent extraction into an organic solvent has recently been applied to wet digested samples of sera and urine.¹³

Dry ashing of samples is time-consuming, and some metals can be volatilized.^{1,14} Low-temperature dry ashing¹⁵ gives less likelihood of loss of volatile metals but the method is slow and requires expensive apparatus. However, Failla and Kiser,¹⁶ and Parker⁴ reported the successful dry ashing pre-treatment of tissues, plasma and feed prior to measurements using AAS of copper, zinc, manganese, iron and magnesium.

Pre-treatment requiring a minimum of handling and glassware has been described by Jackson and Mitchell,¹⁷ who simply homogenized the sample material with water producing a uniform suspension; suitable dilutions of the homogenate were introduced into the Delves cups for direct determination of cadmium by AAS.

The necessity for a simple method of hepatic metal quantification has served as a stimulus for a detailed analytical validation of a method where final measurement by flame AAS (FAAS) of trace metals in the liver of experimental animals is preceded by a simple homogenization procedure.

Experimental

Reagents

Analytical-reagent grade chemicals were used. Ultrapure HCl was purchased from J. T. Baker. All-glass apparatus was used

to produce doubly distilled water, which was used throughout the study.

Standard solutions. In addition to aqueous standards, solutions matched to corresponding samples, with respect to biological matrix, concentration of acid and major inorganic salts content *i.e.*, synthetic samples, were also prepared.

Matrix modifier. As liver is a complex matrix, synthetic samples corresponding to 1 + 5 (by mass) liver homogenates were prepared as 1.1% m/v solutions of human albumin, enriched with inorganic salts to contain 163 mg l⁻¹ Na⁺, 489 mg l⁻¹ K⁺, 226 mg l⁻¹ Cl⁻ and 1390 mg l⁻¹ H₂PO₄⁻ in the final solution. For liver homogenates diluted 1 + 29 synthetic samples diluted similarly were used.

A solution of human albumin for intravenous application, stabilized with 0.16 mmol sodium octanoate per gram of protein was used.

Standard reference material (SRM). Lyophilized Bovine Liver (SRM 1577a) purchased from The National Institute of Standards and Technology (NIST), was used.

Apparatus

Atomic absorption spectrometer, Perkin-Elmer 305B, with a Hitachi 56 recorder, was used throughout for the determination of metal ions.

Liver samples were homogenized using an Ultra-Turrax homogenizer, type Janke and Kunkel GK, and the homogenates were centrifuged using a Sorvall S-34 centrifuge.

A Radiometer Model PHM 85 digital pH meter with a combination glass electrode (Radiometer GK 2322 C) was used for pH readings.

Acid-washed polyethylene laboratory accessories were used where possible, such as spatulas, spoons, bottles for storing samples and standard solutions. Tubes with tight-fitting caps were used for centrifugation of samples and for storing the centrifuged samples.

Analytical Procedures

Sampling

Several female Wistar rats were used in each experimental group. The animals were anaesthetized and killed by decapita-

Table 1 Instrumental parameters

Element	Lamp type	Wavelength/nm	Lamp current/mA	Lamp power/W	Slit setting (band pass)/nm	Scale expansion factor
Cu	HCL*	325.2	15	—	4 (0.7)	1
Mn	HCL	280.3	20	—	4 (0.7)	3
Zn	EDL†	214.6	—	6	4 (0.7)	1

* Hollow cathode lamp.

† Electrodeless discharge lamp.

Table 2 Internal quality control of AHM; values given for dry mass of sample

SRM 1577a Bovine Liver				
Analyte	Certified value/ $\mu\text{g g}^{-1}$	Value found, CI/ $\mu\text{g g}^{-1}$	RSD (%)	Accuracy (%)
Cu	158 ± 7	154.3 ± 3.0 (12)*	2.0	3
Mn	9.9 ± 0.8	9.9 ± 0.5 (13)	5.1	0
Zn	123 ± 8	124.6 ± 5.5 (13)	4.6	2

* Number of individual samples in parentheses, $p = 0.995$.

tion. The livers were rapidly removed, rinsed with ice-cold saline ($0.15 \text{ mol dm}^{-3} \text{ NaCl}$), gently blotted dry, cut into small pieces using stainless-steel surgical scissors and mixed with a plastic spoon. The pooled material was then randomly divided into several sample portions each of them being weighed accurately ($1 \times 10^{-4} \text{ g}$). The remaining portion was used for the determination of the dry mass content.

The pooled material was immediately frozen at -20°C in polyethylene bottles and thawed prior to use.

Acidic homogenate method (AHM)

In order to obtain a homogeneous tissue sample, a portion of pooled rat liver was homogenized with an exact five-fold amount (by mass) of water for $3 \times 1 \text{ min}$. The aqueous homogenate was then adjusted to be 1 mol dm^{-3} in HCl. The suspension obtained was shaken for 30 min, and centrifuged at $12000g$. The original supernatant ($1 + 5$ by mass), served for the direct measurement of copper and manganese; an additional dilution to give a final dilution of $1 + 29$ was prepared for the measurement of zinc.

The lyophilized NIST Bovine Liver sample required a hydration treatment ($\geq 70 \text{ h}$) prior to homogenization. The same dilution ratios were applied for the determination of manganese and zinc in the SRM as for native liver; however, for the measurement of copper a $1 + 29$ dilution was needed.

FAAS measurements

Liquid samples were aspirated directly into the nebulizer system of the instrument. The analytical signals were processed in the peak height mode. The deuterium arc background corrector was used throughout.

Instrumental parameters are given in Table 1. All the measurements were performed under standard pressure and flow rate conditions for both air ($2.1 \times 10^5 \text{ Pa}$, 22.5 l min^{-1}) and acetylene ($5.5 \times 10^4 \text{ Pa}$, 3.9 l min^{-1}).

Estimation of dry mass content

An accurately weighed portion of the pooled tissue material was dried for 24 h at $20\text{--}25^\circ \text{C}$ at a pressure of $<30 \text{ Pa}$.

Evaluation of analytical results

Analytical data are presented as confidence intervals, $\text{CI} = \bar{x} \pm t\sigma/n^{1/2}$, at the stated probability level p (\bar{x} = mean value, t = tabulated t -value, σ = standard deviation and n = number of results).

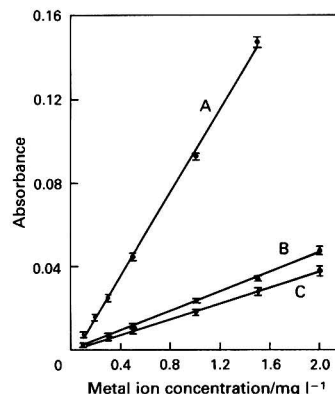


Fig. 1 Regression analysis applied to the total calibration data for: A, zinc: $y = 0.099574x - 0.004428$, $r = 0.9995$, $n = 6$ (7); B, copper: $y = 0.023521x + 0.000080$; $r = 0.9996$, $n = 6$ (6); and C, manganese: $y = 0.019102x - 0.00037$; $r = 0.9998$, $n = 6$ (6). The individual points refer to mean absorbance $\pm \sigma$. Number of parallels denoted in parentheses

Limits of detection (c_L) are expressed as the concentration derived from the smallest measure x_L that can be detected with a reasonable certainty for a given analytical procedure: $x_L = \bar{x}_b + 3\sigma_b$; $c_L = f(x_L)$ (\bar{x}_b = mean of the blank measurements and σ_b = standard deviation of the blank measurements), according to IUPAC recommendations.¹⁸

Results and Discussion

It is known⁶ that procedural errors are very much smaller than the biological variations that can arise if a tissue sample is not representative of a whole organ. Any objective validation of an analytical method applied to tissue material requires that the analytical results be free from the influence of biological variations. Therefore, the present investigations were performed on pooled rat liver material treated as several independent samples, thus fluctuations of results indicate only the imperfections of the method.

By limiting the number of manipulations and reagents employed, the risk of contamination is considerably reduced. From this point of view the proposed simple and direct determination of metal-ions from liver homogenates appears to be very promising.

Acidic Homogenate Method

Comprehensive preliminary studies directed us to propose an acidic extraction of metal ions, applicable to the aqueous homogenates of both the native rat liver and the lyophilized SRM Bovine Liver.

Internal quality control and analytical performances

The results of the AHM internal quality control presented in Table 2, indicate that the application of deuterium arc background correction assures interference-free results and excellent accuracy of the method for all three analytes.

Table 3 Analytical performances of AHM

Analyte	Calibration sensitivity*/l mmol ⁻¹		Recovery* (%)	Limit of detection†/mg l ⁻¹	Characteristic concentration/mg l ⁻¹
	Aqueous standards	ASA standards†			
Cu	1.49 ± 0.08	1.50 ± 0.01	101.30 ± 5.21 (97.34–107.20)§	0.04	0.15
Mn	1.27 ± 0.05	1.18 ± 0.07	98.29 ± 2.42 (96.83–101.09)	0.03	0.21
Zn	6.51 ± 0.19	6.45 ± 0.13	99.57 ± 3.0 (96.54–103.03)	0.04	0.06

* $\bar{x} \pm \sigma$.† $p = 0.996$.

‡ Matrix-matched standards (acid–salt–albumin).

§ Range of values given in parentheses.

Table 4 AHM in analysis of rat liver; values given for dry mass of sample

Sample group	Performance characteristic	Cu	Mn	Zn
I	CI/ $\mu\text{g g}^{-1}$	12.4 ± 1.2 (9)*	5.4 ± 0.5 (12)	105.8 ± 4.6 (11)
	$\sigma/\mu\text{g g}^{-1}$	1.0	0.5	4.0
	SEM/ $\mu\text{g g}^{-1}$	0.3	0.1	1.3
	RSD (%)	7.6	8.8	3.8
II	CI/ $\mu\text{g g}^{-1}$	19.8 ± 2.0 (6)	6.2 ± 1.0 (7)	122.7 ± 5.8 (6)
	$\sigma/\mu\text{g g}^{-1}$	1.0	0.6	3.0
	SEM/ $\mu\text{g g}^{-1}$	0.4	0.2	1.2
	RSD (%)	5.1	9.8	2.4
III	CI/ $\mu\text{g g}^{-1}$	20.4 ± 2.4 (6)	9.0 ± 1.0 (7)	136.9 ± 5.0 (6)
	$\sigma/\mu\text{g g}^{-1}$	1.2	0.6	2.6
	SEM/ $\mu\text{g g}^{-1}$	0.5	0.2	1.1
	RSD (%)	6.1	6.5	1.9

* Number of individual samples in parentheses; $p = 0.995$.

† Standard error of the mean.

The high conformity of calibration graphs for aqueous and matrix-matched standards together with the mean recoveries (Fig. 1 and Table 3) make the use of aqueous standards sufficient, and is further confirmation of the selectivity of the method. The results for aqueous and matrix-matched standards were treated together, resulting in the mean values and standard deviations shown in Fig. 1.

Values obtained for the limits of detection and characteristic concentrations, indicating acceptable sensitivity of the method are summarized in Table 3.

Homogenization of the pooled livers was found to be critical. Repeatability of the results obtained through the application of the method to the analysis of native rat liver (Table 4) confirm that effective homogenization of the tissue material has been achieved.

Precision studies were completed by calculation of day-to-day relative standard deviations (RSDs) (Table 5). The precision seems to be independent of run type (within-run, Table 2; day-to-day run, Table 5) for manganese and zinc. These results, together with those from Table 4 and nearly 100% recoveries for all three metals, indicated that both the precision and accuracy of the proposed method were satisfactory.

Conclusion

An acidic homogenate method for the direct quantification of copper, manganese and zinc in rat liver, with negligible risk of contamination or analyte loss, has been developed. The method is simple and rapid, as no time-consuming procedures are employed for either standardization or sample preparation. Accurate and precise analyses can be performed using

Table 5 Day-to-day precision of AHM; values given for dry mass of sample

Analyte	SRM 1577a Bovine Liver			
	CI/ $\mu\text{g g}^{-1}$	$\sigma/\mu\text{g g}^{-1}$	SEM/ $\mu\text{g g}^{-1}$	RSD (%)
Cu	148.8 ± 4.2 (25)†	6.7	1.4	4.5
Mn	10.3 ± 0.4 (25)	0.6	0.1	5.8
Zn	126.6 ± 4.0 (25)	6.4	1.3	5.1

* Standard error of the mean.

† Number of individual samples in parentheses, $p = 0.995$.

aqueous standards. Reliability together with simplicity and speed make the proposed method suitable for use in clinical chemistry research, where the relationship between hepatic trace metal status and metabolic disorders are dealt with.

References

- 1 Analytical Methods Committee, *Analyst*, 1960, **85**, 643.
- 2 *Analytical Methods for Atomic Absorption Spectrophotometry*, Perkin-Elmer, Norwalk, CT, USA, March 1971, BC-13.
- 3 Jacob, R. A., Klevay, L. M., and Logan, G. M., Jr., *Am. J. Clin. Nutr.*, 1978, **31**, 477.
- 4 Parker, H. E., *At. Absorpt. Newsl.*, 1963, **2**, 23.
- 5 Cheek, D. B., Graystone, J. E., Willis, J. B., and Holt, A. B., *Clin. Sci.*, 1962, **23**, 169.
- 6 Parker, M. M., Humoller, F. L., and Mahler, D. J., *Clin. Chem.*, 1967, **13**, 40.
- 7 Kahnke, M. J., *At. Absorpt. Newsl.*, 1966, **5**, 7.
- 8 Clegg, M. S., Keen, C. L., Loennerdal, B., and Hurley, L. S., *Biol. Trace Element Res.*, 1981, **3**, 107.
- 9 Uriu-Hare, J. Y., Stern, J. S., Raeven, G. M., and Keen, C. L., *Diabetes*, 1985, **34**, 1031.
- 10 Sprenger, K. B. G., and Franz, H. E., *Clin. Chem.*, 1983, **29**, 1522.
- 11 Murthy, L., Menden, E. E., Eller, P. M., and Petering, H. G., *Anal. Biochem.*, 1973, **53**, 365.
- 12 Gross, S. B., and Parkinson, E. S., *At. Absorpt. Newsl.*, 1974, **13**, 107.
- 13 Ishida, O., Kihira, K., Tsukamoto, Y., and Marumo, F., *Clin. Chem.*, 1989, **35**, 127.
- 14 Thiers, R. E., in *Trace Analysis. Symposium on Trace Analysis N. Y. Acad. Med. 1955*, eds. Yoe, J. H., and Koch, H. J., Wiley, New York, 1957, pp. 637–666.
- 15 Sanui, H., *Anal. Biochem.*, 1971, **42**, 21.
- 16 Failla, M. L., and Kiser, R. A., *J. Nutr.*, 1981, **111**, 1900.
- 17 Jackson, K. W., and Mitchell, D. G., *Anal. Chim. Acta*, 1975, **80**, 39.
- 18 IUPAC, *Pure Appl. Chem.*, 1976, **45**, 99.

Paper 1/03455C

Received July 9, 1991

Accepted September 2, 1991

Synthesis of a Morin Chelating Resin and Enrichment of Trace Amounts of Molybdenum and Tungsten Prior to Their Determination by Inductively Coupled Plasma Optical Emission Spectrometry

Xing-yin Luo,* Zhi-xing Su,* Wen-yun Gao, Guang-yao Zhan and Xi-jun Chang

Department of Chemistry, Lanzhou University, Lanzhou 730000, People's Republic of China

A morin chelating resin was synthesized using aminated poly(vinyl chloride) as the starting material, and the optimum conditions for the synthesis were established. The parameters governing the characteristics of the resin for the adsorption of Mo^{VI} and W^{VI} including acidity, flow rate, rate constant, saturated capacity of adsorption, effect of re-use, interfering ions and desorption were investigated. The Mo^{VI} and W^{VI} concentrations in standard samples were determined by using inductively coupled plasma optical emission spectrometry, with satisfactory results. For concentrations of Mo^{VI} and W^{VI} of 0.4 mg l^{-1} , the relative standard deviation was 2.8% for Mo^{VI} and 2.6% for W^{VI} . The structure of the chelating resin was deduced by infrared spectrometry, and the mechanism of the enrichment of Mo^{VI} and W^{VI} is discussed.

Keywords: Morin chelating resin; synthesis; enrichment; molybdenum and tungsten determination; inductively coupled plasma optical emission spectrometry

Morin (2',3,4',5,7-pentahydroxyflavone) is amongst the most sensitive reagents used for the spectrophotometric and spectrofluorimetric determination of a number of metal ions,^{1,2} particularly $\text{Mo}^{3,4}$. In the present work this reagent was attached to an aminated macroporous poly(vinyl chloride) resin by means of the Mannich reaction to give a chelating resin containing morin as the functional group. This chelating resin is resistant to the action of strong acid or base. The conditions for the synthesis of the resin and its ability to absorb trace amounts of Mo^{VI} and W^{VI} were studied. The resin was used in the analysis of several standard samples with satisfactory results.

Experimental

Apparatus and Instruments

An ICP 6500 inductively coupled plasma optical emission spectrometer (Perkin-Elmer), a Nicolet 170-sx Fourier transform infrared (FTIR) spectrometer, a Model pHs-3A digital pH meter and an electrodynamic oscillator were used.

The adsorption column consisted of 0.2 g of chelating resin, which was kept in distilled water for 8–10 h before use, in a glass tube (20 cm long, 0.46 cm i.d., 0.15 cm i.d. at the lower end), in which a small pad of cotton-wool had been placed at the lower end beforehand.

Materials and Reagents

The aminated macroporous poly(vinyl chloride) resin (N content: 10%; particle diameter: 0.36–0.45 mm) was synthesized by the procedure described in ref. 5. All the reagents used were of analytical-reagent grade and distilled water was used throughout.

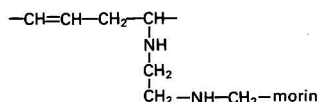
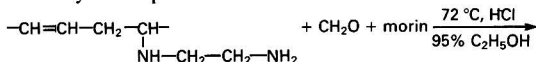
The stock solution of Mo^{VI} or W^{VI} , at a concentration of 1.0 g l^{-1} , was prepared by dissolving 0.4610 g of $(\text{NH}_4)_6\text{Mo}_7\text{O}_{24} \cdot 4\text{H}_2\text{O}$ or 0.4486 g of $\text{Na}_2\text{WO}_4 \cdot 2\text{H}_2\text{O}$ in distilled water and diluting to 250 ml with distilled water. The mixed standard solution of Mo^{VI} and W^{VI} , each at a concentration of 20 mg l^{-1} , was prepared by diluting the stock solution with distilled water.

Synthesis of the Morin Chelating Resin

A 0.5 g amount of morin was placed in a three-necked 250 ml flask fitted with a condenser and agitator. Then, 100.0 ml of

95% ethanol, 20.0 ml of formaldehyde solution (40%), 2.5 ml of concentrated HCl and 1.0 g of aminated poly(vinyl chloride) resin were added. After heating the mixture at 72°C for 10 h, the chelating resin was washed with distilled water until the washings were of neutral pH and dried under IR radiation. The dried resin was then placed in an extractor and extracted with 95% ethanol in order to wash off the free morin. The resin was then dried for later use. The procedure described in ref. 6 was used to determine whether there was any morin in the extracting agent.

The synthesis procedure can be described as follows:



Procedure

A 0.2 g amount of the morin chelating resin, which had been stored in distilled water for 8–10 h, was loaded onto the adsorption column. Then, 2.0 ml of the mixed stock standard Mo^{VI} and W^{VI} solution were transferred by pipette into beakers and diluted with distilled water to 100.0 ml. The solutions were adjusted to pH 2.0 and then passed through the adsorption column at a flow rate of 1.0 ml min^{-1} . Molybdenum(VI) and W^{VI} were desorbed quantitatively with 25 ml of 0.1 mol l^{-1} NaOH, and the desorption solutions were evaporated to about 5 ml, then transferred into 10 ml flasks and diluted to the mark with distilled water. Molybdenum(VI) and W^{VI} were determined by inductively coupled plasma optical emission spectrometry (ICP-OES) using the following instrument settings: forward power, 1100 W; viewing height, 14 mm; plasma gas (argon) flow rate, 14 l min^{-1} ; auxiliary gas (argon) flow rate, 0.6 l min^{-1} ; nebulizer gas (argon) flow rate, 1.0 l min^{-1} ; and wavelengths, 204.598 nm for Mo^{VI} and 209.475 nm for W^{VI} .

Results

Effect of Acidity on Adsorption

Equal concentrations of mixed Mo^{VI} and W^{VI} standards were diluted to equal volumes, and the solutions concentrated using

* Authors to whom correspondence should be addressed.

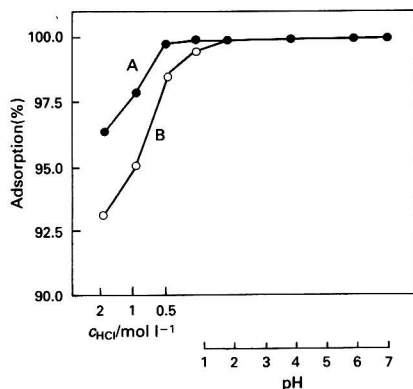


Fig. 1 Effect of acidity on adsorption for: A, Mo; and B, W

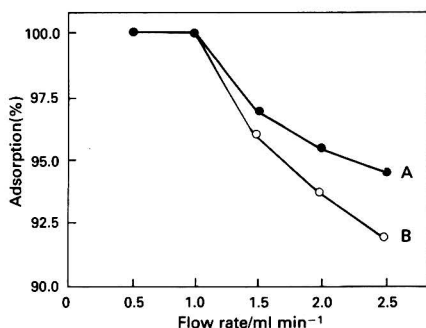


Fig. 2 Effect of flow rate on adsorption for: A, Mo; and B, W

the adsorption column. The acidity was maintained in the range from 2.0 mol l⁻¹ HCl to pH 7.0. The results (Fig. 1) show that Mo^{VI} is adsorbed quantitatively at all the acidities, whereas W^{VI} is not adsorbed completely in 2.0 mol l⁻¹ HCl. As W^{VI} forms WO₃·H₂O at pH ≤ 1.0,⁷ the adsorption of Mo^{VI} and W^{VI} at pH 2.0 is considerable.

Adsorption Rate

By using the procedure described above, the flow rates of the Mo^{VI} and W^{VI} solutions through the column were varied from 0.5 to 2.5 ml min⁻¹. The results, given in Fig. 2, show that Mo^{VI} and W^{VI} are adsorbed quantitatively at a flow rate of 0.5–1.0 ml min⁻¹. Hence a flow rate of 1.0 ml min⁻¹ was selected for the adsorption of Mo^{VI} and W^{VI}.

Dynamic Saturated Capacity of Adsorption

A 0.05 g amount of chelating resin was weighed accurately and, after storing in distilled water for 8–10 h, it was loaded onto the adsorption column. Then, a 100 mg l⁻¹ Mo^{VI} solution (pH 2.0) was passed through the column at a flow rate of 1.0 ml min⁻¹ and the eluate was collected in 10 ml fractions in order to determine the concentration of Mo^{VI}, until $c = c_0$, where c_0 is the initial concentration of Mo^{VI} in the solution and c is the concentration of Mo^{VI} in the eluate. The results, given in Fig. 3, show that the dynamic saturated capacity of adsorption of the resin for Mo^{VI} was 4.17 mmol per gram of dry resin.

A 0.1000 g amount of resin was weighed accurately and, using a similar method, the dynamic saturated capacity of adsorption of the resin for W^{VI} was determined. The value obtained was 0.762 mmol per gram of dry resin; the results are given in Fig. 3.

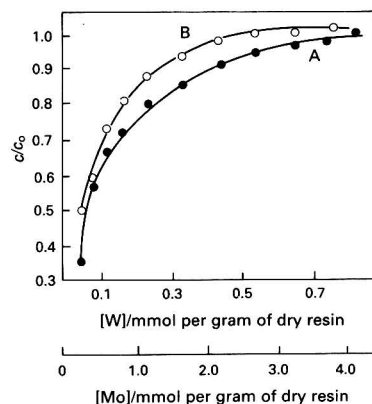


Fig. 3 Dynamic saturated capacity of adsorption for: A, Mo; and B, W

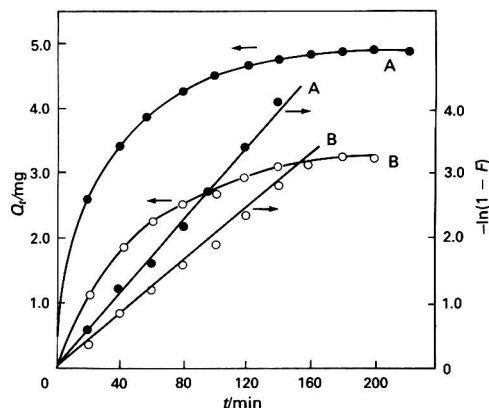


Fig. 4 Rate constant of adsorption for: A, Mo; and B, W

Determination of Rate Constant

A 0.1000 g portion of resin was placed in each of two 100 ml conical flasks. A 50.0 ml volume of a Mo^{VI} solution of pH 2.0 (Mo = 100 mg l⁻¹) was added to one of the flasks and 50.0 ml of a W^{VI} solution of pH 2.0 (W = 100 mg l⁻¹) were added to the other. Both flasks were attached to the electrodynamic oscillator and shaken at normal speed (100 cycles min⁻¹). The metal uptake was determined at intervals of 20 min until equilibrium was reached (about 160 min). The results are shown in Fig. 4. According to Brykina *et al.*,⁸ the isothermal adsorption equation for a low concentration of ions can be expressed as $-\ln(1-F) = kt$, where $F = Q_t/Q_\infty$, and t is the reaction time, Q_t is the adsorption capacity at reaction time t , Q_∞ is the adsorption capacity at equilibrium and k is the rate constant. The values of k obtained from the slope of a linear calibration graph were $4.58 \times 10^{-4} \text{ s}^{-1}$ for Mo^{VI} and $3.88 \times 10^{-4} \text{ s}^{-1}$ for W^{VI}. The results are given in Fig. 4.

Desorption Conditions and Desorption Curves

After Mo^{VI} and W^{VI} had been adsorbed by the resin following the above procedures, the columns were desorbed with 0.01, 0.05, 0.10, 0.25 and 0.50 mol l⁻¹ NaOH solution, respectively. The results, given in Fig. 5, show that Mo^{VI} and W^{VI} are desorbed quantitatively when the concentration of NaOH solution is higher than 0.1 mol l⁻¹. Hence 0.1 mol l⁻¹ NaOH solution was selected for the desorption of Mo^{VI} and W^{VI}.

By using the eluent selected above, the desorption curves of Mo^{VI} and W^{VI} were obtained. The results, given in Fig. 6, show that 25 ml of eluent were sufficient for desorption.

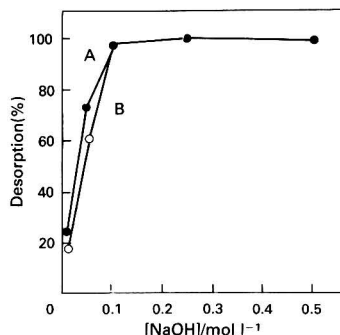


Fig. 5 Effect of concentration of NaOH (25 ml) on desorption efficiency of: A, Mo; and B, W

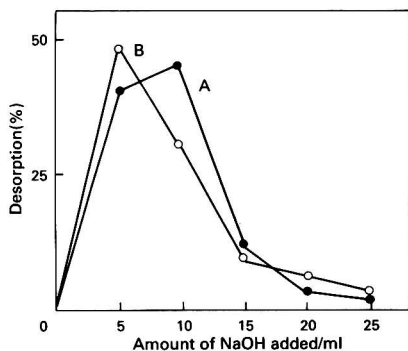


Fig. 6 Desorption curves of: A, Mo; and B, W, using 0.1 mol l⁻¹ NaOH as eluent

Table 1 Results of the re-use of the resin

No. of times resin used	Adsorption (%)	
	Mo ^{VI}	W ^{VI}
1	99.8	100.0
2	100.0	100.5
3	100.5	100.0
4	99.3	99.9
5	99.6	99.3
6	99.5	100.1

Stability and Re-use of the Resin

After the resin has been treated with strong acid or base, it can still be used for the adsorption of Mo^{VI} and W^{VI}, with recoveries in the range 95.4–100%. Experiments were also carried out to determine the number of times the resin could be used. A column containing adsorbed Mo^{VI} and W^{VI} was eluted with 3 mol l⁻¹ NaOH or 6 mol l⁻¹ HCl and then washed with 20 ml of 0.1 mol l⁻¹ HCl and distilled water until the washings were of neutral pH. This enrichment, desorption and neutralization procedure was repeated six times and the absorbing ability of the resin for Mo^{VI} and W^{VI} was virtually unchanged. The results are given in Table 1.

Interfering Ions

Various interfering ions were added, respectively, to the diluted standard solutions of Mo^{VI} and W^{VI} (0.4 mg l⁻¹) at a 100-fold excess over Mo^{VI} and W^{VI}. The Mo^{VI} and W^{VI} were then enriched and determined. Table 2 shows that a 100-fold excess of concomitant ions causes little interference and that a 50-fold excess of Fe^{III} interferes seriously. However, if 0.1 g of ascorbate is used to reduce a 250-fold excess of Fe^{III} to Fe^{II}, the

Table 2 Effect of interfering ions on Mo^{VI} and W^{VI} at a concentration of 0.4 mg l⁻¹

Interfering ion	Concentration/mg l ⁻¹	Recovery (%)	
		Mo ^{VI}	W ^{VI}
Mg ^{II}	40.0	100.6	97.7
Ca ^{II}	40.0	100.1	97.6
Al ^{III}	40.0	98.8	100.5
Fe ^{III}	20.0	20.7	21.3
Cr ^{III}	40.0	98.9	91.7
Zn ^{II}	40.0	97.8	97.7
Ni ^{II}	40.0	96.6	97.1
Co ^{II}	40.0	94.0	96.6
Cd ^{II}	40.0	92.7	97.7
V ^V	40.0	91.1	106.3
Cu ^{II}	40.0	97.2	105.1
Cr ^{VI}	40.0	93.3	91.4
Fe ^{II}	250.0	101.2	100.2
Fe ^{III}	250.0	98.6*	96.7*

* The recoveries were obtained after 250 mg l⁻¹ of Fe^{III} had been masked with 5000 mg l⁻¹ of ascorbate.

Table 3 Lowest limits of adsorption

Amount added/mg		Volume/l	Concentration (ppb)		Recovery (%)	
Mo ^{VI}	W ^{VI}		Mo ^{VI}	W ^{VI}	Mo ^{VI}	W ^{VI}
0.010	0.0125	0.50	20.0	25.0	95.7	73.3
0.010	0.025	0.50	20.0	50.0	95.3	91.8

interference from Fe^{III} can be eliminated and the recoveries of Mo^{VI} and W^{VI} are 98.1 and 96.3%, respectively.

Lowest Limits of the Resin for Adsorption of Mo^{VI} and W^{VI}

Mixed solutions of Mo^{VI} and W^{VI} of lower concentration (ppb level) were determined as described under Procedure. The results, given in Table 3, show that the morin chelating resin possesses a fairly strong absorbing ability for Mo^{VI} and W^{VI}: 20 ppb of Mo^{VI} and 50 ppb of W^{VI} can be absorbed quantitatively.

Precision and Analysis of Standard Samples

Eight portions of a standard solution containing equal concentrations of Mo^{VI} and W^{VI} were accurately transferred by pipette into beakers and diluted with distilled water to give a concentration of 0.4 mg l⁻¹. The diluted solutions were analysed as described under Procedure; the average results for eight determinations were 0.393 mg l⁻¹ for Mo^{VI} and 0.398 mg l⁻¹ for W^{VI} and the relative standard deviations were 2.8% for Mo^{VI} and 2.6% for W^{VI}. The four standard samples were dissolved as follows: a 0.1000 g amount of a standard sample was weighed accurately and dissolved in 10 ml of an acid mixture [HCl–HNO₃ (3 + 1)] with heating (the undissolved residue was removed by filtration). The solution was then transferred into a 100 ml flask and diluted to the mark with distilled water. A 5.0 ml aliquot of the solution was transferred by pipette into a 100 ml beaker and the contents of Mo and W in the standard sample were determined as described under Procedure. The results are given in Table 4. It can be seen that the contents of Mo and W determined are in agreement with the certified values.

Discussion

Conditions for the Synthesis of the Morin Chelating Resin

The effects of the conditions used for the synthesis on the morin content of the chelating resin were investigated. The

Table 4 Results of the analysis of standard samples using the proposed method

Sample	Element	Certified value (%)	Concentration (%)				Relative standard deviation (%)
			Found			Average	
1. 20Cr ₃ MoWV (No. 192)*	Mo	0.64	0.63	0.61	0.62	0.62	3.0
	W	0.38	0.40	0.40	0.38	0.39	2.6
2. CrMoWV (No. H34)*	Mo	0.46	0.45	0.44	0.45	0.45	2.2
	W	0.43	0.41	0.43	0.43	0.42	2.3
3. 38CrWVAI (No. 169-2)*	W	0.32	0.32	0.33	0.30	0.32	0
	Mo	0.26	0.25	0.27	0.25	0.26	0
4. Standard steel†							

* Certified reference materials supplied by the Central Iron and Steel Research Institute of the Department of Metallurgical Industry of China.

† Certified reference material supplied by the Iron and Steel Factory at Chongqin, Sichan province.

Table 5 Effect of the conditions of the synthesis on the morin content of the resin

Reaction temperature/°C	Morin content* (%)	Reaction time/h	Morin content† (%)	HCHO/ml	Morin content‡ (%)	Morin/g	Morin content§ (%)
30	9.1	4.0	21.9	1.0	9.6	0.05	25.6
50	21.9	6.0	28.6	2.0	13.8	0.1	35.5
72	32.6	8.0	31.0	4.0	35.5	0.2	21.9
		10.0	32.6	6.0	25.9	0.3	16.7

* Aminated resin, 0.2 g; HCHO, 2.0 ml; morin, 0.1 g; 95% C₂H₅OH, 20 ml; concentrated HCl, 0.5 ml; and reaction time, 10 h.

† Aminated resin, 0.2 g; HCHO, 2.0 ml; morin, 0.1 g; 95% C₂H₅OH, 20 ml; concentrated HCl, 0.5 ml; and reaction temperature, 72 °C.

‡ Aminated resin, 0.2 g; morin, 0.1 g; 95% C₂H₅OH, 20 ml; reaction time, 10 h; reaction temperature, 72 °C; and concentrated HCl, 0.5 ml.

§ Aminated resin, 0.2 g; HCHO, 4.0 ml; 95% C₂H₅OH, 20 ml; reaction time, 10 h; reaction temperature, 72 °C; and concentrated HCl, 0.5 ml.

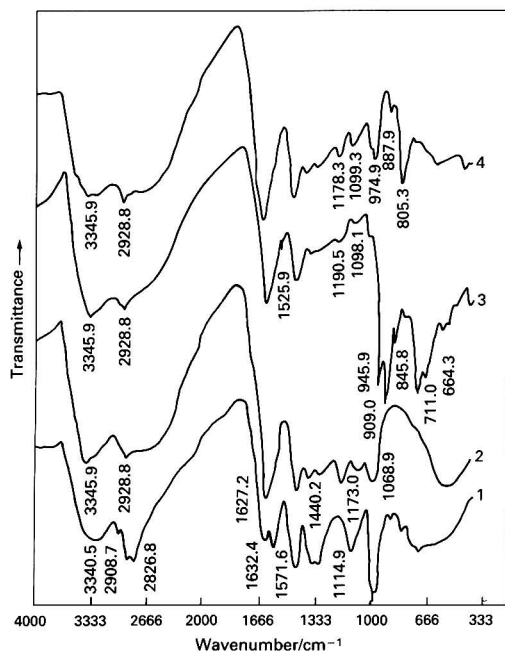
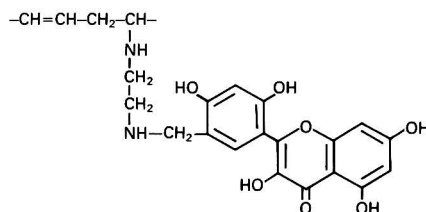


Fig. 7 IR spectra of aminated poly(vinyl chloride) resin (spectrum 1), morin chelating resin (spectrum 2), morin chelating resin saturated with Mo^{VI} (spectrum 3) and morin chelating resin saturated with W^{VI} (spectrum 4)

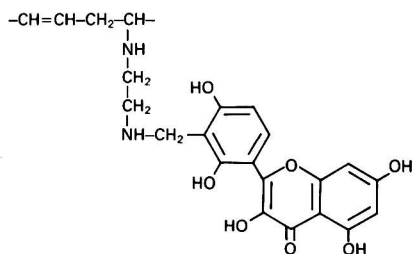
results, shown in Table 5, indicate that a higher content of morin can be obtained. However, if the proportion of materials used is incorrect and the reaction time is too long, the mechanical strength of the chelating resin obtained is affected; moreover, the catalytic effect of acid in the Mannich reaction must be taken into account. Hence, the following optimum conditions were selected for the synthesis: aminated poly(vinyl chloride) resin, 0.2 g; formaldehyde, 4.0 ml; morin, 0.1 g; ethanol, 20.0 ml; concentrated HCl, 0.5 ml; reaction time, 10 h; and reaction temperature, 72 °C.

Structure of the Morin Chelating Resin and Adsorption Mechanism

Fig. 7 shows the IR spectra of the aminated resin (spectrum 1), the morin chelating resin (spectrum 2) and the morin resin saturated with Mo^{VI} (spectrum 3) or W^{VI} (spectrum 4). The peaks in Fig. 7 can be analysed as follows^{9,10} ($\nu_{\max}/\text{cm}^{-1}$). Spectrum 1: 3340.5 ($\nu\text{N-H}$); 2908.7 and 2826.8 (δCH_2 and $\nu\text{C-H}$); 1632.4 [$\nu\text{C=C}$ of the highly conjugated system resulting from the dehydrochlorination reaction in the course of the amination of poly(vinyl chloride)⁵ and $\delta\text{N-H}$]; 1571.6 ($\delta\text{N-H}$); and 1114.9 ($\rho\text{N-H}$). Spectrum 2: 3345.9 ($\nu\text{N-H}$); 2928.8 ($\nu\text{C-H}$); 1627.2 ($\nu\text{C=C} + \nu\text{C=O}$); 1440.2 ($\nu\text{C=C}$ of the aromatic rings); the two peaks that were present in spectrum 1, at 1571.6 and 1114.9 cm^{-1} , were not visible and this showed that the reaction was essentially complete. The additional peak at 1173.0 cm^{-1} in spectrum 2 may be due to the $\nu\text{C-O}$ of phenol and that at 1068.9 cm^{-1} to $\rho\text{N-H}$. Hence, according to the principle of the Mannich reaction and the IR spectra, the structure of the resin might be as shown below:



or



On comparing spectrum 3 with spectrum 2 in Fig. 7, it can be seen that the peaks at 3345.9 and 2928.8 cm^{-1} change slightly. At 1525.9 cm^{-1} a new but weak peak appears; this is due to the reaction of Mo^{VI} with the $>\text{C}=\text{O}$ function of the resin, which causes the peak for $>\text{C}=\text{O}$ to be shifted from 1627.2 to 1525.9 cm^{-1} . Two other peaks at 1173.0 and 1068.9 cm^{-1} become weaker and are shifted to 1190.5 and 1098.1 cm^{-1} , respectively; this shows that Mo^{VI} can also react with the $-\text{OH}$ and $-\text{NH}-$ groups of the resin. Some obvious changes can be seen below 1000 cm^{-1} and the peaks can be assigned as follows¹¹ ($\nu_{\text{max}}/\text{cm}^{-1}$): 945.9 and 909.0 ($\nu_{\text{asym}}\text{Mo}=\text{O}$); 845.8 ($\nu_{\text{asym}}\text{Mo}=\text{O}$); 711.0 and 664.3 ($\nu_{\text{asym}}\text{Mo}-\text{O}-\text{Mo}$). Therefore, it can be concluded that the mechanism of the adsorption of Mo^{VI} onto the resin consists of two parts: the first is a chelating mechanism, *i.e.*, Mo^{VI} reacts with $>\text{C}=\text{O}$ and $-\text{OH}$ in position 3 or 5 to form a chelating structure with a five- or six-membered ring; the second part is an association mechanism, *i.e.*, Mo^{VI} reacts with the $-\text{NH}-$ group to form an ion associate.

On comparing spectrum 4 with spectrum 2 in Fig. 7, it can also be seen that there is only a slight change in the peaks at 3345.9 and 2928.8 cm^{-1} ; no peak appears at 1525 cm^{-1} and the peak at 1173.3 cm^{-1} is smaller and is shifted to 1178.3 cm^{-1} . This is a small change and might indicate that W^{VI} reacts weakly with $>\text{C}=\text{O}$ and $-\text{OH}$ to form a chelating structure. That the peak at 1068.9 cm^{-1} becomes weaker and is shifted to 1099.3 cm^{-1} shows that the reaction between W^{VI} and the $-\text{NH}-$ group of the resin is fairly strong. Compared with spectrum 3, some obvious changes can be seen in spectrum 4 below 1100 cm^{-1} and the peaks can be assigned as follows¹² ($\nu_{\text{max}}/\text{cm}^{-1}$): 974.9 ($\nu_{\text{asym}}\text{W}=\text{O}$); 887.9 ($\nu_{\text{asym}}\text{W}=\text{O}$); 805.3 ($\delta\text{O}-\text{W}-\text{O}$). Therefore, it can be concluded that the mechanism of the adsorption of W^{VI} onto the resin also consists of two parts: the main part is an association mechanism, *i.e.*, W^{VI} reacts with the $-\text{NH}-$ group to form an ion associate; the minor part is a chelating mechanism, *i.e.*, W^{VI} reacts with the $>\text{C}=\text{O}$ function and the OH group in position 3 or 5 of the resin to form a chelating structure with a five- or six-membered ring.

Conclusion

The proposed method using a morin chelating resin to adsorb trace amounts of Mo^{VI} and W^{VI} from sample solutions selectively is satisfactory. The proposed method was also found to be efficient for the determination of trace amounts of Mo^{VI} and W^{VI} in standard samples. The method is rapid, accurate and convenient. In addition, the chelating resin is stable and its synthesis is also simple and rapid.

References

- 1 Goppelsroeder, F., *Fresenius Z. Anal. Chem.*, 1868, 7, 195.
- 2 Sanz-Medel, A., and Garcia Alonso, J. I., *Anal. Chim. Acta*, 1984, 165, 159.
- 3 Almasy, G., and Viyvari, M., *Magy. Kem. Foly.*, 1956, 62, 332.
- 4 Murata, A., and Yume Muchi, F., *Shizuoka Daigaku Kagakubu, Kenkyu Hokoku*, 1958, 9, 97.
- 5 Guo, X. W., Zhang, J. F., Su, Z. X., and Cao, D. R., *Guangpuxue Yu Guangpu Fenxi*, 1990, 10(3), 48.
- 6 *Spot Tests in Organic Analysis*, Publishing House of Fuel Chemistry Industry, Beijing, 1972, pp. 315–316.
- 7 Cotton, F. A., and Wilkinson, G., *Advanced Inorganic Chemistry*, Wiley, New York, 3rd edn., 1972, pp. 545–583.
- 8 Brykina, G. D., Marchak, T. V., Krysina, L. S., and Velyavskaya, T. A., *Zh. Anal. Khim.*, 1980, 35, 2294.
- 9 Zhong, H. Q., *Elementary IR Spectral Methods*, Publishing House of Chemistry Industry, Beijing, 1984, pp. 118–132.
- 10 Ning, Y. C., *Structure Identification of Organic Compounds and Organic Spectroscopy*, Qin Hua University Press, Beijing, 1989, pp. 329–351.
- 11 Cousius, M., and Green, M. L. H., *J. Chem. Soc.*, 1964, 1567.
- 12 Sengupta, A. K., and Nath, S. K., *Indian J. Chem., Sect. A*, 1981, 20(2), 203.

Paper 1/04722A

Received September 11, 1991

Accepted September 26, 1991

High-performance Liquid Chromatographic Study of Nickel Complexation With Humic and Fulvic Acids in an Environmental Water

Peter Warwick and Tony Hall

Department of Chemistry, Loughborough University of Technology, Loughborough, Leicestershire LE11 3TU, UK

A high-performance liquid chromatographic method was developed to determine cation-exchange capacities and conditional association constants for metal interactions with humic and fulvic materials present in environmental waters. The method does not require prior extraction of the humic and/or fulvic compounds. A salt-gradient is used, which exploits the size-exclusion and adsorption properties of a coated porous silica stationary phase, in order to separate and permit the measurement of the free and complexed metal concentrations. The results are subjected to a weak and strong binding site interpretation.

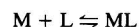
Keywords: Humic acid; fulvic acid; nickel complexation; high-performance size-exclusion chromatography; water

There is increasing interest in the fate and behaviour of trace metals in the environment and humic and fulvic acids, present in natural waters, play an important role. Humic and fulvic acids bind (complex) with metal pollutants and thereby affect such diverse phenomena as transport mechanisms, toxicity, bioavailability and the effectiveness of recovery and clean-up procedures.¹ The acids generally occur as complex heterogeneous mixtures of polymeric anions showing local and seasonal variations in composition. Probably every structural analytical technique, from classical elemental and functional group analysis to advanced instrumental analytical methods, including infrared (IR), nuclear magnetic resonance (NMR) and mass spectrometry, have been applied to these compounds but owing to their complexity full structural elucidation has not been achieved. However, much information has been gained;^{2,3} for example, it has been discovered that humic and fulvic acids often contain aromatic backbones carrying a variety of functional groups, *e.g.*, phthalate, salicylate and amine functions. With metals, humic and fulvic acids form anionic complexes, whereas with organic pollutants, molecular association or covalently bound species can be produced. One particular environmental concern is the interaction of humic and fulvic acids with radionuclides. Radionuclides can enter the environment as a result of accidental or controlled releases of effluent. In addition, in the future it may be envisaged that over prolonged time periods eventual ingress of groundwater into planned radioactive waste repositories is likely. Consequently, a full understanding of possible complexation and transport mechanisms is highly desirable.

The speciation of a metal (*i.e.*, distribution amongst the various possible physico-chemical forms) determines its overall geochemical and biological behaviour. In order to assess the amount of 'free' metal species present, both the inorganic and organic complex speciation must be known, which requires a knowledge of the relevant stability constants. Also with humic and fulvic acids it is desirable to have a measure of the maximum amount of metal uptake that is likely under any given set of environmental conditions. This requires the determination of the maximum cation complexing capacity (C_c) of the material.

In order to explain the mechanism of metal binding with humic and fulvic acids, several models have been developed. In a review, Falck⁴ categorizes the models into two main types, either discrete ligand models or continuous distribution models. A survey of the literature suggests that the discrete ligand model is accepted by most workers. The model proposes that major binding sites (L), such as salicylate and

phthalate, act as ligands towards the metals (M). The stoichiometry at a ligand site is 1 : 1, but of course the denticity may be higher. Hence the complexation reaction may be simply represented as



for which the conditional association value (site binding constant) is given by

$$K = \frac{[ML]}{[M][L]} \quad (1)$$

where the brackets denote concentrations and in particular [L] is the concentration of free binding sites, *i.e.*, not the concentration of humic or fulvic compounds.

The number of ligand sites present determines the maximum complexing capacity of the substance, *i.e.*,

$$C_c = [ML]_{\max} \quad (2)$$

Therefore,

$$K = \frac{[ML]}{[M]([ML]_{\max} - [ML])} \quad (3)$$

The mathematical interpretation of experimental data depends, of course, on the model adopted and no model has escaped criticism.

A large number of analytical techniques have been applied to the determination of association and capacity values and are described in several texts.^{5,6} However, in general, in order to simplify the chemistry involved investigations have been carried out using extracted humic and fulvic materials. Diethylaminoethyl (DEAE)-cellulose or XAD resins are commonly used as the extraction media.⁷ The adsorbed organics are eluted from these extractants using alkaline solutions in which they are readily soluble. However, such extraction procedures can be expected to change the properties and structures of the organic compounds. States of aggregation, stereochemistry, inherent metal content and over-all purity are likely to be affected. Measured values of K and C_c could well then be different to those applicable to the *in situ* material. Accordingly, this paper describes a high-performance liquid chromatographic technique which has been developed primarily to study *in situ* materials, *i.e.*, direct investigation of the environmental water, without any prior treatment, apart from 0.45 μm filtration, which is employed to remove most of the colloidal clays and micro-organisms which may be present and mild rotary evaporation when preconcentration is necessary. The technique involves high-performance size-exclusion chromatography (HPSEC) and by means of

salt-gradient elution exploits cationic absorption, which is normally considered to be a disadvantage of HPSEC. A separation of anionically complexed metal from free metal is achieved, so that the relative amounts in an equilibrium mixture can be measured. During the time of the separation (≤ 10 min), the dissociation of the previously formed complex must be negligible. The method was developed from work previously reported using Sephadex gels,⁸ but the gel technique was rejected in favour of the higher speed and resolution of the high-performance technique.

Accordingly, this investigation was conducted using nickel, a typical divalent transition metal, which is known to form complexes with humic and fulvic materials, and for which the kinetics of association and dissociation are slow, several days being required for the attainment of equilibrium. Nickel complexation has been studied extensively by various workers using extracted humic and fulvic materials.⁹⁻¹¹ Nickel-63 ($t_{1/2} = 100$ years, $\beta, E_{\max} = 66$ keV) was used to label the nickel mixtures so that the chromatographically separated complexed and free nickel could be assayed using liquid scintillation counting. Currently the technique is being modified to study europium complexation using europium-152 ($t_{1/2} = 13$ years, $\gamma, 0.122$ MeV, 62%) and solid-state counting.

Experimental

Apparatus

The HPSEC experiments were carried out using a Philips PU 4000 Series liquid chromatograph fitted with a PU 4100 gradient pumping system, a PU 4021 diode-array detector (DAD), a Rheodyne injection valve with a 100 μ l loop and PU 6000 and PU 6003 integration and control software. SynChro-Pak GPC-60 guard (50×4.6 mm i.d.) and analytical (250×4.6 mm i.d.) size-exclusion columns were used, which contained a 5 μ m porous silica stationary phase, coated with a glyceryl propyl bonded phase. This material has a stated linear relative molecular mass separation range of 300–20 000 for dextrans and 300–30 000 for proteins and is suitable for humic and fulvic acid fractionation.

In exploratory experiments, the eluate emerging from the DAD was passed into a Waters Model 420 fluorescence detector, which was used to help to confirm the identity of the humic and fulvic fractions. In the complexation experiments the eluate emerging from the DAD passed through a Canberra Packard Flo-One/Beta (A140) radioactivity detector, fitted with an 800 μ l flow cell. A scintillation cocktail (Ecoscint A; National Diagnostics) was mixed with the column eluate before the flow-through cell. The experimental arrangement is shown schematically in Fig. 1.

Environmental Water Sample

A surface water was taken from moorland in the Derbyshire Peak District, near the village of Moscar. The water was subjected to 0.45 μ m filtration, which was commenced 3 h after collection, and this was followed by the rotary evaporation of a 1000 ml sample to 250 ml at 30°C, the resulting sample henceforth being referred to as $\times 4$ moorland water. Rotary evaporation is a mild process and the 4-fold increase in concentration was undertaken to increase the ease of detection of the humic and fulvic material.

The rotary evaporation lowered the pH from the original *in situ* value of 3.8 to 3.5. As the extent of nickel complexation increases with increase in pH, a very small amount of concentrated NaOH solution was added to adjust the pH to 6.3. The estimated concentration of the humic and fulvic acid species from both the TOC (total organic carbon) and ultraviolet (UV) absorption data was about 52 mg l⁻¹. The results of the analysis of the $\times 4$ moorland water are given in Table 1.

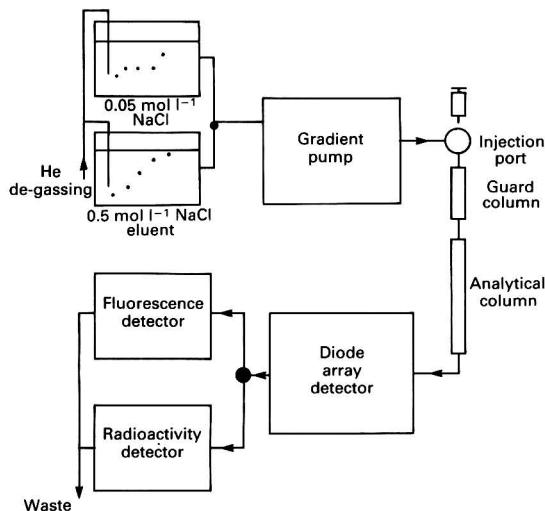


Fig. 1 HPSEC experimental arrangement

Table 1 Analyses of working solutions

Parameter	Units	$\times 4$ Water	Sodium humate
pH	—	6.3	6.3
Chloride	mg l ⁻¹	86	33
Bromide	mg l ⁻¹	—	—
Alkalinity as CaCO ₃	mg l ⁻¹	—	10
Ammonia as N	mg l ⁻¹	0.130	0.090
Nitrite as N	mg l ⁻¹	0.013	0.057
Calcium	mg l ⁻¹	21	<1
Magnesium	mg l ⁻¹	14	<0.1
Sodium	mg l ⁻¹	48	25
Potassium	mg l ⁻¹	4.1	<0.1
Total hardness as CaCO ₃	mg l ⁻¹	107	<1
Sulfate	mg l ⁻¹	122	123
Phosphate as P	mg l ⁻¹	<0.05	<0.05
Silica	mg l ⁻¹	40	<0.1
Fluoride	mg l ⁻¹	0.33	<0.05
Total oxidized nitrogen	mg l ⁻¹	0.5	<0.5
Total organic carbon	mg l ⁻¹	26	25.0
Total inorganic carbon	mg l ⁻¹	—	—
Boron	mg l ⁻¹	51	<10
Molybdenum	mg l ⁻¹	<0.01	<0.01
Uranium	mg l ⁻¹	<0.5	—
Lithium	mg l ⁻¹	<0.1	<0.1
Strontium	mg l ⁻¹	0.08	<0.01
Iron	μ g l ⁻¹	3200	510
Manganese	μ g l ⁻¹	1780	<10
Aluminium	μ g l ⁻¹	330	204
Vanadium	μ g l ⁻¹	<10	<10
Lead	μ g l ⁻¹	<5	<5
Chromium	μ g l ⁻¹	<2	<2
Copper	μ g l ⁻¹	63	20
Nickel	μ g l ⁻¹	10.3	<5
Zinc	μ g l ⁻¹	65	<10
Cadmium	μ g l ⁻¹	0.53	<0.5
Barium	μ g l ⁻¹	300	<10
Cobalt	μ g l ⁻¹	<10	<10
Electrical conductivity at 20 °C	μ S cm ⁻¹	420	108

Purified Humic Acid Sample

For comparison purposes, duplicate experiments were conducted using humic acid (HA) prepared from the semi-reference material sodium humate purchased from Aldrich. This material is well characterized, with capacity and complexation data readily available.^{12,13} The purified HA was

produced by lowering the pH of a solution of Aldrich sodium humate to below 1 and then filtering off the precipitated HA. After washing and drying, 57.7 mg of the precipitated HA were dissolved in 1 l of high-performance liquid chromatography (HPLC)-grade water. Finally, the pH was adjusted to 6.3 by the addition of a small amount of NaOH solution. The results of the analysis are given in Table 1.

Preparation of Sample Mixtures

Solutions of $\text{Ni}(\text{NO}_3)_2$ were prepared in the range from 1 to $1 \times 10^{-5} \text{ mol l}^{-1}$ from the analytical-reagent grade salt and then either 25 or 50 μl aliquots of these solutions were added to 5 ml samples of the $\times 4$ moorland water and the purified humic acid solution. Mixtures were produced containing total nickel concentrations ranging from about 5.0×10^{-8} to $1.0 \times 10^{-2} \text{ mol l}^{-1}$. Also, to each mixture either 25 or 50 μl of nickel-63 solution were added. The larger amount of nickel-63 was necessary for the more concentrated nickel solutions to permit detection of the complex in the presence of a large excess of free nickel. The nickel-63 solution was prepared by adding 135 μl of stock NiCl_2 solution (37 MBq ml^{-1} ; supplied by Amersham International) to 5 ml of HPLC-grade water. The total nickel concentrations of the mixtures were corrected for dilution effects, added nickel-63 and, for the $\times 4$ water, the original nickel content.

Characterization of the Dissolved Organic Matter

The presence of humic and fulvic compounds in the moorland water was established as follows.

A chromatographic separation of the filtered $\times 4$ water was carried out using the GPC-60 column and the chromatogram obtained at 230 nm is shown in Fig. 2 (A). The elution volumes of the early peaks demonstrated the presence of large organic molecules. The UV absorption spectra of peaks 1, 2 and 3 showed a gradual increase in absorption, with decreasing wavelength, and the absence of specific absorption bands, properties which are typical of humic and fulvic materials. The narrow UV absorption spectrum of peak 4 indicated the presence of inorganic species, *e.g.*, NO_3^- , whereas the UV absorption spectrum of the low-intensity final peak (peak 5) suggested that small organic species were also present.

A sample of the filtered $\times 4$ moorland water was treated with DEAE-cellulose, which, as stated above, is known to extract humic and fulvic anions, and the chromatographic separation was repeated. The effect on the UV absorption monitored at 230 nm is shown in Fig. 2 (chromatogram B). The macromolecular organic species have been removed.

Humic and fulvic compounds are generally fluorescent, hence the effect of the DEAE-cellulose treatment on the

fluorescence of the eluted species was determined. The results are shown in Fig. 3 (chromatograms A1 and B1). Surprisingly, the first UV peak with a retention time of 9.3 min was not associated with fluorescence (*cf.*, Figs. 2 and 3); however, the major UV peak exhibited fluorescence, which was removed by the DEAE-cellulose treatment. The fluorescent low relative molecular mass organic peak 5 was not completely removed. The fluorescence associated with the low relative molecular mass organic species may have indicated either fragmentation of the humic/fulvic materials or the presence of precursors. The lack of fluorescence associated with the largest molecules may be attributable to either the absence of appropriate aromatic groups or quenching caused by impurities and/or aggregation.

Humic acid is by definition insoluble in very acidic solutions, *i.e.*, pH < 1. Accordingly, a sample was acidified and precipitation was observed. From measurements of the decrease in UV absorption a 70% fulvic–30% humic composition was deduced (the precipitated humic material was separately tested and found to complex nickel in another series of experiments).

From the above evidence, a knowledge of the source of the water, its light-brown colour and its acidity (pH = 3.8) when collected and the TOC content, it was concluded that the presence of humic and fulvic compounds had been established.

Further corroborating evidence resulted from the nickel complexation experiments which, taking into account the time delay between the DAD and the radioactivity detector,

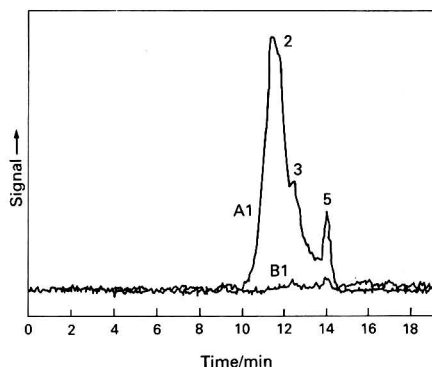


Fig. 3 Fluorescence chromatogram of $\times 4$ moorland water: A1, before and B1, after treatment with DEAE-cellulose. (For designation of peaks see Fig. 2 and text)

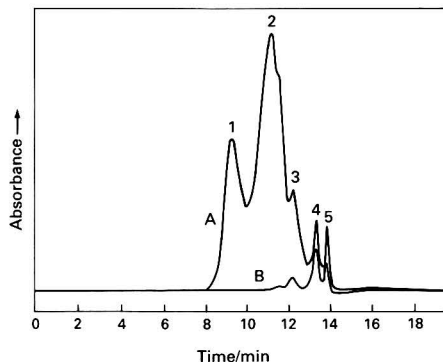


Fig. 2 UV chromatogram of $\times 4$ moorland water monitored at 230 nm: A, before and B, after treatment with DEAE-cellulose. (Peaks 1, 2 and 3 are due to large organic species, peak 4 is attributable to inorganic nitrate and peak 5 results from small organic species)

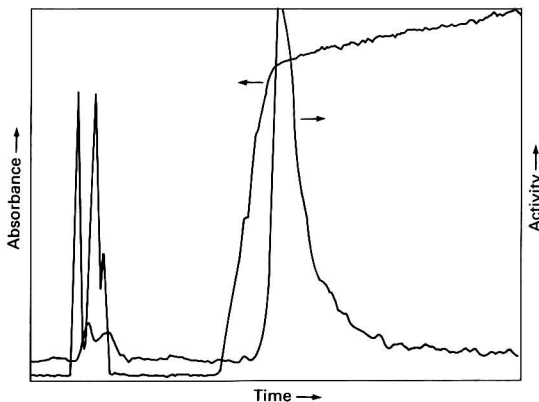


Fig. 4 Simultaneous UV absorbance (230 nm) and ^{63}Ni activity (counts min^{-1}) chromatograms versus time (min) for $\times 4$ moorland water containing labelled $\text{Ni}(\text{NO}_3)_2$ solution

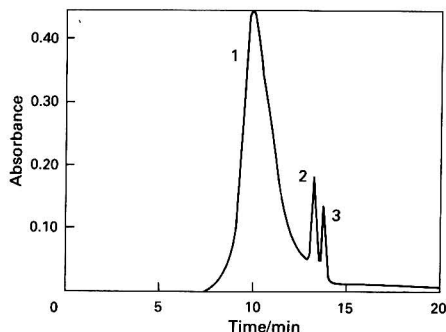


Fig. 5 UV absorbance chromatogram (230 nm) of purified Aldrich HA containing labelled $\text{Ni}(\text{NO}_3)_2$ solution. (Peak 1 is due to large organic species, peak 2 is due to nitrate and peak 3 results from small organic species)

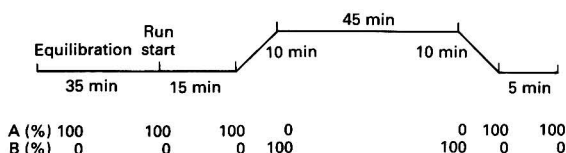


Fig. 6 Salt-gradient elution profile. Flow rate, $0.230 \text{ ml min}^{-1}$; A, $0.05 \text{ mol l}^{-1} \text{ NaCl}$; and B, $0.5 \text{ mol l}^{-1} \text{ NaCl}$

showed that nickel complexed with the species responsible for the early peaks (see Fig. 4).

Chromatographic separation of the purified Aldrich HA yielded a simpler chromatogram. A typical result is shown in Fig. 5. The species producing peaks 1 and 3 are organic and fluorescent whereas peak 2 is due to added nitrate. Again, peak 3 is considered to be due to either humic fragments or precursors.

Complexation Experiments

After allowing 9 d for the mixtures to reach equilibrium, at 20°C , $100 \mu\text{l}$ samples of the mixtures were subjected to chromatographic analysis, using the salt-gradient technique, detailed in Fig. 6.

Results

In all instances the nickel activity eluted in two main fractions, as shown in Figs. 7 and 8, which show typical $\times 4$ moorland water and purified HA chromatograms. The nickel humate/fulvate complexes being partially excluded were eluted first with the $0.05 \text{ mol l}^{-1} \text{ NaCl}$ and were identifiable with the early peaks in the corresponding DAD spectra, whereas the free $\text{Ni}^{2+}(\text{aq})$ which suffered adsorption was eluted much later by the $0.5 \text{ mol l}^{-1} \text{ NaCl}$. The nickel-63 chromatographic peak areas were used in conjunction with the known total nickel concentration to calculate the amounts of free and complexed nickel in each mixture. The assumption was made that the contribution of other nickel species to either peak was negligible. The results are given in Tables 2 and 3.

A control experiment employing quench correction was conducted. Sample quenching was found to be insignificant, as peak area calculations employing disintegrations min^{-1} instead of counts min^{-1} gave identical results.

Maximum Complexing Capacities

In order to determine the maximum complexing capacities (C_c values) of the $\times 4$ moorland water and the purified HA, logarithmic plots of complexed versus free nickel concentrations were constructed (Figs. 9 and 10).

By using curve-fitting software (Macintosh Plus computer; Cricket Graph, polynomial order 2), best fit equations were

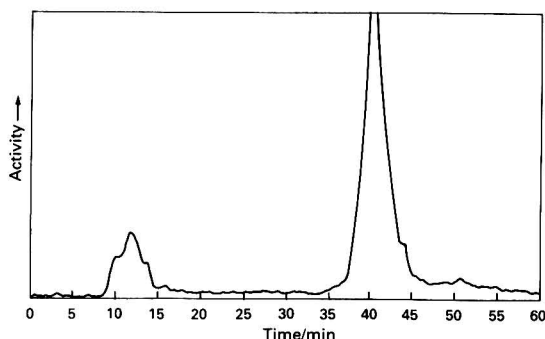


Fig. 7 Activity chromatogram of a typical $\times 4$ moorland water sample containing labelled $\text{Ni}(\text{NO}_3)_2$ solution

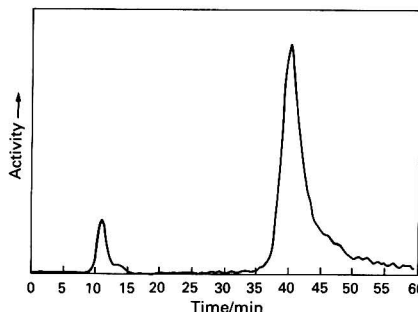


Fig. 8 Activity chromatogram of a typical HA sample containing labelled $\text{Ni}(\text{NO}_3)_2$ solution

obtained and differentiated to calculate the maximum complex concentrations theoretically achievable under the conditions used if precipitation is ignored. In this way the $\times 4$ moorland water was determined to have a C_c value of $3.70 \times 10^{-6} \text{ mol l}^{-1}$ at a free nickel concentration of $3.18 \times 10^{-3} \text{ mol l}^{-1}$, whereas the purified Aldrich HA yielded a C_c value of $4.20 \times 10^{-6} \text{ mol l}^{-1}$ at a free nickel concentration of $5.14 \times 10^{-3} \text{ mol l}^{-1}$. In both instances precipitation occurred at about $1 \times 10^{-3} \text{ mol l}^{-1}$ of added nickel, which precluded precise experimental location of the maxima.

Conditional Association Constant Determinations

By using the appropriate maximum complexing capacity and eqn. (3), the individual values of the conditional association constants were determined for each mixture. The log K values are included in Tables 2 and 3. For the moorland water the average log K was 4.40 [standard deviation (SD) = 0.41 ($n = 9$)] and for the purified Aldrich HA log $K = 4.1$ [SD = 0.25 ($n = 10$)].

Discussion

This investigation was conducted at pH 6.3 to ensure a significant degree of complexation, as the exact nickel speciation of the original water was not an objective of this study. The results given in Table 4 cover a range of pH values. Generally, stability constants and maximum complexing capacities are found to decrease with decreasing pH, which is attributable to increased competition from H^+ ions for binding sites. However, these experiments were conducted below pH 7 to avoid complications arising from the formation of hydroxy species. It can be seen that the log K values found are similar to those reported by other workers for similar systems.

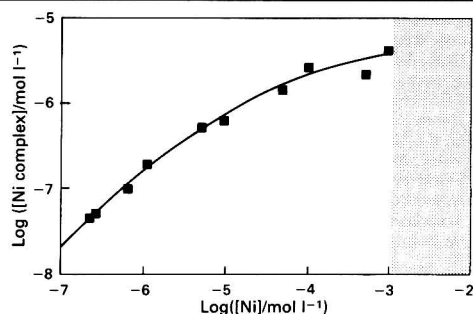
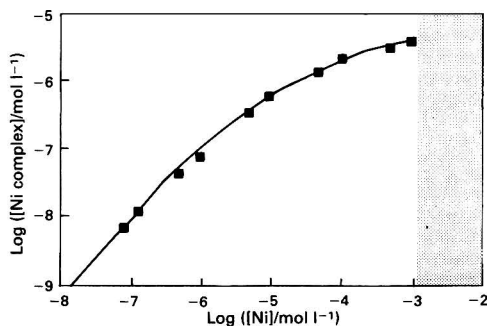
Preconcentration results in pH changes, hence assessment of the nickel speciation in an original *in situ* water would need to take this into account. However, the inherent sensitivity of

Table 2 Nickel complexation with $\times 4$ moorland water ($C_c = 3.72 \times 10^{-6} \text{ mol l}^{-1}$)

[Ni total]/ mol l^{-1}	[Ni complex] (% area)	[Ni] (% area)	[Ni complex]/ mol l^{-1}	[Ni]/ mol l^{-1}	Log [Ni complex]	Log [Ni]	Log K^*
2.619×10^{-7}	16.01	83.99	4.193×10^{-8}	2.200×10^{-7}	-7.378	-6.658	4.72
3.107×10^{-7}	15.69	84.31	4.875×10^{-8}	2.620×10^{-7}	-7.312	-6.582	4.71
7.075×10^{-7}	13.41	86.59	9.488×10^{-8}	6.126×10^{-7}	-7.023	-6.213	4.63
1.197×10^{-6}	16.05	83.95	1.921×10^{-6}	1.005×10^{-6}	-6.716	-5.998	4.74
5.163×10^{-6}	10.26	89.74	5.297×10^{-7}	4.633×10^{-6}	-6.276	-5.334	4.56
1.006×10^{-5}	5.85	94.15	5.885×10^{-7}	9.472×10^{-6}	-6.230	-5.024	4.30
4.973×10^{-5}	2.86	97.14	1.422×10^{-6}	4.831×10^{-5}	-5.847	-4.316	4.11
9.829×10^{-5}	2.67	97.33	2.624×10^{-6}	9.567×10^{-5}	-5.581	-4.019	4.41
4.927×10^{-4}	0.443	99.557	2.183×10^{-6}	4.905×10^{-4}	-5.661	-3.309	3.46
9.805×10^{-4}	0.443	99.557	4.344×10^{-6}	9.762×10^{-4}	-5.362	-3.011	—

* Average log $K = 4.40$ [SD = 0.41 ($n = 9$)].**Table 3** Nickel complexation with purified Aldrich HA ($C_c = 4.2 \times 10^{-6} \text{ mol l}^{-1}$)

[Ni total]/ mol l^{-1}	[Ni complex] (% area)	[Ni] (% area)	[Ni complex]/ mol l^{-1}	[Ni]/ mol l^{-1}	Log [Ni complex]	Log [Ni]	Log K^*
8.692×10^{-8}	7.40	92.60	6.432×10^{-9}	8.049×10^{-8}	-8.191	-7.094	4.28
1.357×10^{-7}	8.99	91.01	1.220×10^{-8}	1.235×10^{-7}	-7.914	-6.908	4.37
5.325×10^{-7}	7.32	92.68	3.898×10^{-8}	4.935×10^{-7}	-7.409	-6.307	4.28
1.022×10^{-6}	7.11	92.89	7.266×10^{-8}	9.493×10^{-7}	-7.139	-6.023	4.27
4.988×10^{-6}	6.46	93.54	3.222×10^{-7}	4.666×10^{-6}	-6.492	-5.331	4.25
9.889×10^{-6}	5.61	94.39	5.548×10^{-7}	9.334×10^{-6}	-6.256	-5.030	4.21
4.955×10^{-5}	2.60	97.40	1.288×10^{-6}	4.826×10^{-5}	-5.890	-4.316	3.96
9.811×10^{-5}	2.15	97.85	2.109×10^{-6}	9.600×10^{-5}	-5.676	-4.018	4.02
4.927×10^{-4}	0.58	99.43	2.833×10^{-6}	4.899×10^{-4}	-5.548	-3.310	3.60
9.805×10^{-4}	0.37	99.63	3.628×10^{-6}	9.769×10^{-4}	-5.440	-3.010	3.81

* Average log $K = 4.10$ [SD = 0.25 ($n = 10$)].**Fig. 9** Ni- $\times 4$ moorland water binding. $y = -6.1289 - 0.55856x - 0.11186x^2$ and $r^2 = 0.986$. Shaded area shows precipitation region**Fig. 10** Ni-humate binding. $y = -6.0161 - 0.55820x - 0.12192x^2$ and $r^2 = 0.998$. Shaded area shows precipitation region

the technique can be exploited for direct measurements on *in situ* waters when the level of dissolved organic material is appropriately high, *i.e.*, about 10 mg l^{-1} TOC or higher. It is worth noting that the high SD of the current results is due in part to the wide concentration range studied, *i.e.*, six orders of magnitude (see later), and the use of individual experimental results rather than the averaging of the means of several replicate series of experiments.

Table 4 Over-all log K values

Sample	pH	Log K	Ref.
Soil fulvic acid	5.0	4.20	2
Ground water fulvic acid	6.5	5.2	13
Stream fulvic acid	7.0	4.63	3
Lake water fulvic acid	8.0	5.14	4
$\times 4$ Moorland water	6.3	4.40	This work
Purified Aldrich HA	6.3	4.10	This work

The apparent difference between the average log K values obtained for the moorland water and purified HA is not statistically significant. The capacities show about a 10% difference. The increased capacity of the purified material is arguably due to the freeing of metal sites during the dissolution and re-acidification stages.

The values of K and C_c obtained must be regarded only as operational values. They are not thermodynamic constants and cannot even be described as stoichiometric constants. The reasons are easily demonstrated by returning to eqn. (3). Rearrangement of this equation gives

$$\frac{[\text{ML}]}{[\text{M}]} = K[\text{ML}]_{\text{max}} - K[\text{ML}] \quad (4)$$

Hence a graph of $[\text{ML}]/[\text{M}]$ against $[\text{ML}]$ should be a straight line with a slope of $-K$ and an intercept on the abscissa of $[\text{ML}]_{\text{max}}$.

The graphs obtained by treating the data in this way are presented in Figs. 11 and 12. The lack of linearity is immediately apparent. However, the C_c values obtained from the intercepts on the abscissa are comparable to the previously produced values, *i.e.*, $3.9 \times 10^{-6} \text{ mol l}^{-1}$ for the Ni-HA (previous value $4.20 \times 10^{-6} \text{ mol l}^{-1}$) and $4.8 \times 10^{-6} \text{ mol l}^{-1}$ for the $\times 4$ moorland water (previous value $3.70 \times 10^{-6} \text{ mol l}^{-1}$). It should be noted that Perdue¹⁴ stated that maximum capacities determined by adding excess of metal ion may be in error, especially at low ligand concentrations, and suggested that the H^+ ion capacity should be used as an upper limit for the site capacity. This approach is precluded with an *in situ* water sample, but Kim *et al.*,¹⁵ for example, used one third of the H^+ ion capacity as a measure of humic concentration in Am^{3+} complexation studies. However, the

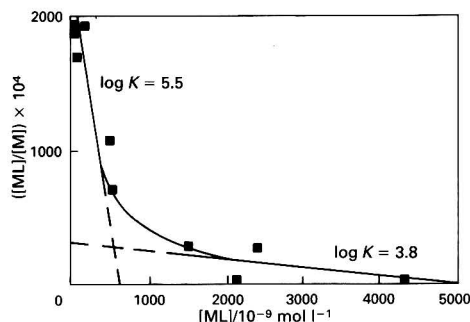


Fig. 11 Ni-×4 moorland water complexation

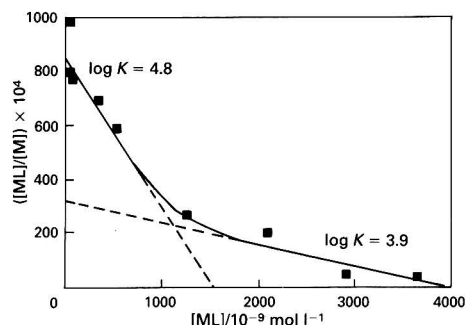


Fig. 12 Ni-humate complexation

lack of linearity is because within humic and fulvic materials, there are a variety of ligand sites with different binding strengths. In more refined treatments of the ligand site model, capacities of each type of site are determined in order to derive individual binding site constants. Methods usually involve the Scatchard analysis technique, an approach much used by biochemists in drug-receptor binding studies.¹⁶ Figs. 11 and 12 can be interpreted in this way. If the simplifying assumption is made that only two types of site are present, A-sites, which are strongly binding, and B-sites, weakly binding, then from eqn. (4)

$$\frac{[ML]_A + [ML]_B}{[M]} = K_A[ML]_{A,\max} - K_A[ML]_A + K_B[ML]_{B,\max} - K_B[ML]_B$$

Now, during the early stages of metal addition $[ML]_B = 0$ because the added metal binds preferentially to the A-sites, and therefore the initial slope is $-K_A$, and in the latter stages of the titration $[ML]_A = [ML]_{A,\max}$, and therefore the final slope is $-K_B$.

The log K values thus determined are presented in Table 5 and again over-all similarity is observed. However, this approach can be criticized: the location of the linear sections is arbitrary and co-operativity and stereochemical effects may, in reality, cause the binding strengths and capacities to change continually as complexation progresses, i.e., the tenets of the continuous distribution model.³ In yet another approach, Klotz¹⁷ recommended the use of so-called stepwise stoichiometric constants. Accordingly, it is emphasized that the values given in Tables 2 and 3 are based on total capacities whereas the values in Table 5 are based on the weak and strong site approach.

Conclusion

Within the 'analytical window' of the technique and under the conditions used, only minor differences have been discovered between the nickel complexation properties of the dissolved humic and fulvic components of the ×4 moorland water and

Table 5 Approximate strong and weak site log K values

Site	×4 Moorland water	Purified Aldrich HA
Strong	5.5	4.8
Weak	3.8	3.9

the purified HA material. However, the ×4 water apparently possesses a proportion of stronger sites than the purified HA.

The main objective of the study was achieved, namely to demonstrate that, when the rate of dissociation is slow, this form of HPSEC can be used in complexation studies to measure both complexed and free metal concentrations in environmental waters without prior extraction of the humic and fulvic materials. The technique is now being applied to compare extracted humic and fulvic materials from the same moorland water. A full account of the comparison will be reported elsewhere.¹⁸

The authors thank the UK Department of Environment for funding this work. The results of this work will be used in the formulation of government policy, but the views expressed in this paper do not necessarily represent government policy. The Analytical Laboratories of the National Rivers Authority, Meadow Lane, Nottingham, are also thanked for the water analysis, as is Christine Bartrop for typing the manuscript.

References

- Patterson, J. W., and Passino, R., *Metals Speciation, Separation and Recovery*, Lewis, Chelsea, MI, 1987.
- Flaig, W., Beutelspacher, H., and Rietz, E., in *Soil Components*, ed. Gieseking, J. E., Springer-Verlag, New York, 1975, vol. 1, pp. 1-211.
- Humic Substances in Soil, Sediment and Water*, eds. Aiken, G. R., McKnight, D. M., Wershaw, R. L., and MacCarthy, P., Wiley, New York, 1985.
- Falck, W. E., *A Review of Modelling the Interaction Between Natural Organic Matter and Metal Cations*, British Geological Technical Report WE/88/49, British Geological Survey, Nottingham, 1988.
- Buffle, J., *Complexation Reactions in Aquatic Systems*, Ellis Horwood, Chichester, 1988.
- Christman, R. F., and Gjessing, E. T., *Aquatic and Terrestrial Humic Materials*, Ann Arbor Science Publishers, Ann Arbor, MI, 1983.
- Miles, C. J., Tuschall, J. R., Jr., and Brezonk, P. L., *Anal. Chem.*, 1983, **55**, 410.
- Warwick, P., Shaw, P., Williams, G. M., and Hooker, J. P., *Radiochim. Acta*, 1988, **44/45**, 59.
- Schnitzer, M., and Hansen, E. H., *Soil Sci.*, 1970, **109**, 333.
- Mantoura, R. F. C., and Riley, J. P., *Anal. Chim. Acta*, 1975, **78**, 193.
- Haworth, D. T., Pitluck, M. R., and Pollard, B. P., *J. Liq. Chromatogr.*, 1987, **10**, 2877.
- Kim, J. I., Buckau, G., Li, G. H., Duschner, H., and Psarros, N., *Fresenius J. Anal. Chem.*, 1990, **338**, 245.
- Smith, B., Higgs, J. J. W., Moodie, P., Davis, J., Williams, G. M., and Warwick, P., *Comparative Study of Humic Substances in Groundwaters: 1. The Extraction of Humic Material from Drigg Groundwater and a Study of its Ability to Form Complexes with Cobalt and Nickel*, DOE Report No. DOE/HMIP/R/90/087, DOE, London, 1990.
- Perdue, M. E., in *Metal Speciation: Theory, Analysis and Application*, eds. Kramer, J. R., and Allen, E. H., Lewis, Chelsea, MI, 1988.
- Kim, J. I., Rhee, D. S., and Buckau, G., *Radiochim. Acta*, 1991, **52/53**, 49.
- Scatchard, G., *Ann. N.Y. Acad. Sci.*, 1949, **51**, 660.
- Klotz, I. M., *Acc. Chem. Res.*, 1974, **7**, 162.
- Warwick, P., and Hall, A., *Radiochim. Acta*, submitted for publication.

Paper 1/04583K

Received September 4, 1991

Accepted September 30, 1991

Simultaneous Determination of Theophylline and Guaiphenesin by Third-derivative Ultraviolet Spectrophotometry and High-performance Liquid Chromatography

Mohamed H. Abdel-Hay,* Mohie Sharaf El-Din† and Mustafa A. Abuirjeie

Department of Medicinal Chemistry, Faculty of Pharmacy, Jordan University of Science and Technology, Irbid, Jordan

Two methods are described for the simultaneous determination of theophylline and guaiphenesin in combined pharmaceutical dosage forms. The first method depends on third-derivative ultraviolet spectrophotometry, with the zero crossing technique of measurement. Third-derivative amplitudes at 222 and 278 nm were selected for the assay of guaiphenesin and theophylline, respectively. The second method is based on high-performance liquid chromatography on a reversed-phase column using a mobile phase of 0.01 mol dm⁻³ sodium dihydrogen phosphate-methanol-acetonitrile (8 + 2 + 1) (pH 5.5) with detection at 245 nm. Both methods showed good linearity, precision and reproducibility. The proposed methods were successfully applied to the determination of these drugs in laboratory-prepared mixtures and in capsules or elixir.

Keywords: *Theophylline and guaiphenesin determination; high-performance liquid chromatography; third-derivative ultraviolet spectrophotometry; pharmaceutical formulations*

Theophylline is a xanthine derivative that relaxes smooth muscles, relieves bronchospasm and has a stimulant effect on respiration.¹ Guaiphenesin (glyceryl guaicolate) is reported to reduce the viscosity of tenacious sputum and is used as an expectorant.¹ Theophylline and guaiphenesin in combination induce bronchodilation and assist the patient in coughing up viscid mucus,² and have been used in the symptomatic treatment of bronchial asthma and other bronchospastic conditions.

Theophylline and guaiphenesin together with their dosage forms, including combinations with other drugs, have been listed in various pharmacopoeias.³⁻⁵ The official compendia describe non-aqueous titrimetry, spectrophotometry and high-performance liquid chromatography (HPLC) for the determination of theophylline as the bulk drug and in dosage forms. Titrimetric, spectrophotometric and gas chromatographic (GC) procedures are described in various pharmacopoeias for guaiphenesin in the bulk drug and in dosage forms. In combination with other drugs, guaiphenesin has been determined using second-derivative⁶ and differential⁷ spectrophotometry, colorimetry,⁸ spectrofluorimetry,^{9,10} densitometry,¹¹ GC¹² and HPLC.¹³⁻¹⁶ Theophylline in combination with other drugs has been determined by conventional ultraviolet (UV),¹⁷ differential¹⁸ and derivative spectrophotometry,^{19,20} colorimetry,²¹ differential thermal analysis,²² densitometry,²³ thin-layer chromatography,²⁴ GC²⁵ and HPLC.²⁶⁻²⁹ Some of the reported methods are not specific for the two drugs and some require extensive sample manipulation. To our knowledge, no methods have been described for both drugs in pharmaceutical dosage forms, except the assay method reported in the United States Pharmacopeia (USP),³ which involves the HPLC determination of theophylline and guaiphenesin in capsules.

Hence it was considered desirable to develop a simpler and faster procedure that would serve as an alternative to the current official method.³ In this work two methods, based on selective derivative UV spectrophotometry and HPLC, are reported and the optimum experimental parameters for each method are described.

Experimental

Materials

Authentic samples of theophylline monohydrate, guaiphenesin and phenacetin (employed as an internal standard) were kindly donated by Alexandria Co. for Pharmaceuticals and Chemical Industries (Alexandria, Egypt) and were used as received. Methanol and acetonitrile (Carlo Erba, Milan, Italy) were of HPLC grade; water was de-ionized and doubly distilled. All other chemicals were of analytical-reagent grade.

Apparatus

Spectrophotometric analysis was carried out on a Shimadzu UV-240 recording spectrophotometer in 1 cm matched quartz cells. The instrument parameters were spectral slit-width 2 nm, scan speed 10 nm s⁻¹, recorder chart speed 10 nm cm⁻¹, wavelength range 190-320 nm and ordinate maximum and minimum settings ± 0.03 . Third-derivative UV spectra were obtained with a Shimadzu attachment (optional programme/interface, Model OPI-2) giving from first to fourth derivatives. Wavelength calibration was checked by using a holmium oxide filter, against air.

The high-performance liquid chromatograph was composed of a Model 114 M single-piston pump (Beckman, Geneva, Switzerland), a Model 165 variable-wavelength UV detector (Beckman), an injector with a 20 μ l loop (Beckman) and an SP 4270 integrator-plotter (Spectra-Physics, Basle, Switzerland). The detector wavelength was set at 245 nm at 0.1 a.u.f.s.

Procedure for Derivative Spectrophotometry

Calibration

Standard solutions of theophylline and guaiphenesin were prepared in distilled water (10-30 μ g ml⁻¹). The third-derivative spectra were recorded over the wavelength range 190-320 nm, and appropriate third-derivative amplitudes were measured graphically (Table 1) and plotted against the corresponding concentration to obtain the calibration graph.

Analysis of capsules and elixir

An accurately weighed portion of the powder (mixed contents of 20 capsules) or an accurately measured volume of elixir, equivalent to about 150 mg of theophylline (90 mg of guaiphenesin), was transferred into a 100 ml calibrated flask

* On leave from the Department of Pharmaceutical Analytical Chemistry, Faculty of Pharmacy, Alexandria University, Alexandria, Egypt.

† On leave from the Department of Analytical Chemistry, Faculty of Pharmacy, Mansoura University, Mansoura, Egypt.

and extracted (or diluted for elixir) by shaking for 10 min with 50 ml of distilled water. The resulting suspension was filtered, by washing through a filter-paper, into a 100 ml calibrated flask and then diluted to volume with distilled water (solution A). Then, 1.50 ml of solution A were pipetted into a 100 ml calibrated flask and the resulting solution was subjected directly to spectrophotometric analysis using distilled water as a reference.

Procedure for HPLC

Chromatographic conditions

Routine analysis was carried out isocratically on a 5 μ m reversed-phase Alltech-Macrosphere 300 C_{18} column (250×4.6 mm i.d.) using a mobile phase of 0.01 mol dm^{-3} sodium dihydrogen phosphate-methanol-acetonitrile (8 + 2 + 1), adjusted to pH 5.5 with phosphoric acid, pumped at a flow rate of 1.2 ml min^{-1} .

Calibration

Standard solutions of theophylline and guaiphenesin ($2.5\text{--}15 \mu g\ ml^{-1}$) containing a fixed concentration ($5 \mu g\ ml^{-1}$) of phenacetin (internal standard) were prepared in the mobile phase. Triplicate 20 μ l injections were made for each solution and the peak area ratio of each drug to the internal standard was plotted against the corresponding concentration to obtain the calibration graph.

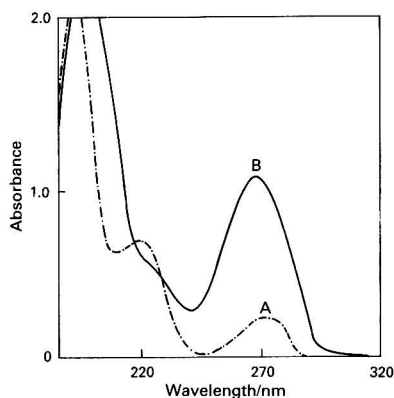


Fig. 1 Zero-order spectra of A, guaiphenesin ($20 \mu g\ ml^{-1}$) and B, theophylline ($20 \mu g\ ml^{-1}$) in distilled water

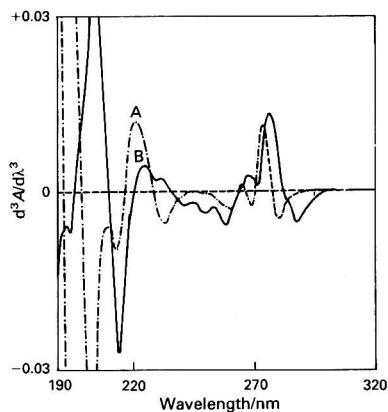


Fig. 2 Third-derivative spectra of A, guaiphenesin ($20 \mu g\ ml^{-1}$) and B, theophylline ($20 \mu g\ ml^{-1}$) in distilled water

Analysis of capsules and elixir

A 0.750 ml aliquot of solution A (prepared as above) was added to 1.0 ml of internal standard solution ($500 \mu g\ ml^{-1}$) and the volume was adjusted to 100 ml with mobile phase. A 20 μ l volume of the final solution was injected into the chromatograph.

Results and Discussion

Derivative Spectrophotometry

The absorption (zero-order) UV spectra of theophylline and guaiphenesin in the 190–320 nm wavelength region are shown in Fig. 1. Theophylline exhibits a peak and a shoulder at about 270 and 225 nm, respectively. Guaiphenesin, however, also absorbs over this wavelength region, with two peaks at about 270 and 220 nm. Because of the extensive overlap of the spectral bands of the two drugs, conventional UV spectrophotometry cannot be used for their individual determination in a mixture. When third-derivative UV spectra are recorded, sharp bands of large amplitudes (Fig. 2) are produced, which may permit more selective identification and determination of the two drugs. As discussed elsewhere,^{30–32} the choice of the optimum wavelength is based on the fact that the contribution of each component to the over-all derivative signal is zero at the wavelength at which the other component has the maximum absorption. Therefore, the third-derivative amplitudes at 278 nm (zero crossing of guaiphenesin) and at 222 nm (zero crossing of theophylline) were chosen for the simultaneous determination of theophylline and guaiphenesin, respectively, in a binary mixture. Fig. 3 shows the third-derivative spectra of theophylline and guaiphenesin at several different concentrations; as can be seen, the position of the iso-differential point for each component is as stated above.

Linear relationships between selected amplitudes from the third-derivative spectra and drug concentration were observed (Table 1). Least-squares regression analysis was carried out on the slope, the intercept and the correlation coefficient (r). The

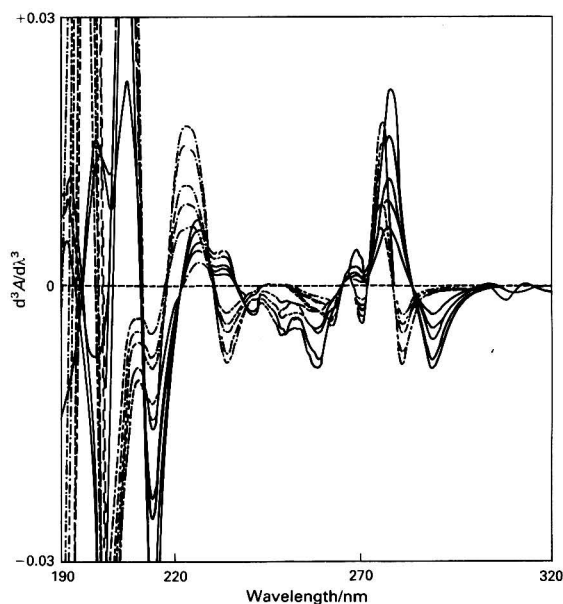


Fig. 3 Third-derivative spectra of guaiphenesin (broken lines) and theophylline (solid lines) at several different concentrations in distilled water: guaiphenesin, 10, 15, 20, 25 and $30 \mu g\ ml^{-1}$; theophylline, 10, 15, 20, 25 and $30 \mu g\ ml^{-1}$

Table 1 Analytical data for the calibration graphs ($n = 5$) for the determination of theophylline and guaiphenesin by third-derivative UV spectrophotometry and HPLC

Drug	Method	Linearity range/ $\mu\text{g ml}^{-1}$	Regression equation		Correlation coefficient, r	RSD (%)*
			Slope	Intercept		
Theophylline	$^3\text{D}_{278}\dagger$	10–30	0.152	–0.011	0.9998	0.89
	HPLC	2.5–15	0.066	–0.007	0.9998	1.13
Guaiphenesin	$^3\text{D}_{222}\dagger$	10–30	0.148	–0.009	0.9996	1.11
	HPLC	2.5–15	0.056	0.008	0.9993	1.53

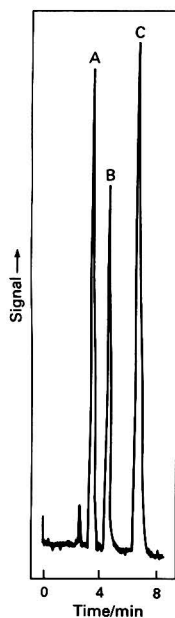
* Relative standard deviation.

 \dagger Third-derivative amplitude measured at 278 or 222 nm for theophylline and guaiphenesin, respectively.**Table 2** Determination of theophylline and guaiphenesin in laboratory-prepared mixtures by third-derivative UV spectrophotometry

Theophylline to guaiphenesin ratio (m/m)	Theophylline			Guaiphenesin		
	Taken/ $\mu\text{g ml}^{-1}$	Found/ $\mu\text{g ml}^{-1}$	Relative error (%)	Taken/ $\mu\text{g ml}^{-1}$	Found/ $\mu\text{g ml}^{-1}$	Relative error (%)
1:2	10	9.86	–1.4	20	20.70	+3.50
2:3	20	20.20	+1.0	30	29.10	–3.00
3:4	15	14.54	–3.07	20	19.40	+3.00
1:1	20	19.64	–1.80	20	20.00	0.00
5:4	25	25.39	+1.56	20	19.50	–2.50
3:2	30	30.33	+1.10	20	20.09	+0.45

Table 3 Determination of theophylline and guaiphenesin in laboratory-prepared mixtures by HPLC

Theophylline to guaiphenesin ratio (m/m)	Theophylline			Guaiphenesin		
	Taken/ $\mu\text{g ml}^{-1}$	Found/ $\mu\text{g ml}^{-1}$	Relative error (%)	Taken/ $\mu\text{g ml}^{-1}$	Found/ $\mu\text{g ml}^{-1}$	Relative error (%)
1:6	2.5	2.52	+0.80	15.0	14.91	–0.60
1:2	5.0	5.04	+0.80	10.0	9.83	–1.70
1:1.67	7.5	7.34	–2.13	12.5	12.78	+2.24
1.67:1	12.5	12.82	+2.56	7.5	7.39	–1.47
2:1	10.0	9.98	–0.20	5.0	5.07	+1.40
6:1	15.0	15.21	+1.40	2.5	2.47	–1.20

**Fig. 4** HPLC trace of a 20 μl injection containing A, 10 $\mu\text{g ml}^{-1}$ of theophylline (3.37 min); B, 10 $\mu\text{g ml}^{-1}$ of guaiphenesin (4.52 min); and C, 5 $\mu\text{g ml}^{-1}$ of phenacetin (6.61 min)

relative standard deviation calculated for the separate determination of each drug was 0.89–1.11%, indicating good precision and reproducibility. In order to assess the validity of the proposed method for assaying each drug in the presence of the other, synthetic mixtures with different proportions of the two drugs were prepared and then assayed using the proposed derivative method. Satisfactory results were obtained for the recovery of both drugs (Table 2).

Chromatography

In order to effect the simultaneous elution of the two component peaks under isocratic conditions, the mobile phase composition was optimized. Phosphate buffer was chosen as the aqueous component. A satisfactory separation was obtained with a mobile phase consisting of the ternary mixture phosphate buffer (0.01 mol dm^{-3})–methanol–acetonitrile (8 + 2 + 1). The pH for the optimum resolution of the two drugs was 5.5. At lower pH values (3 or 4.5) a slight reduction in peak symmetry was observed, and the partial replacement of methanol with acetonitrile improved the resolution. Under the described chromatographic conditions, the analyte peaks were well defined, resolved and almost free from tailing. At a flow rate of 1.2 ml min^{-1} , the retention times for theophylline, guaiphenesin and phenacetin (internal standard) were 3.37, 4.52 and 6.61 min, respectively (Fig. 4). Initial studies were performed while the effluent was monitored at 280 nm; the detector response (theophylline : guaiphenesin) was found to be in the ratio 10 : 1 for equal concentrations of the two drugs. Other wavelengths were therefore tried, and it was observed that on decreasing the wavelength below 280 nm the detector response for theophylline was decreased whereas that for guaiphenesin was increased. The optimum wavelength for detection was 245 nm, at which much better detector responses for both drugs were obtained (Fig. 4).

The proposed method allows the determination of both drugs in capsules (labelled to contain 150 mg of theophylline and 90 mg of guaiphenesin per capsule) using the same dilution and the same injection volume and with reasonable responses for the two well resolved peaks. This is an advantage over the current USP³ procedure, which involves monitoring of the effluent at 280 nm, where the detector response of theophylline was found to be still much higher than that of guaiphenesin despite the different chromatographic conditions adopted in the USP procedure. For quantitative applications, linear calibration graphs were obtained with correlation coefficients better than 0.999 (Table 1). The good precision of the HPLC procedure was indicated by the relative standard deviation (1.13–1.53%). Results for the HPLC analysis of laboratory-prepared mixtures with different proportions of the two drugs are given in Table 3.

Table 4 Results for the determination of theophylline and guaiphenesin in commercial formulations by third-derivative UV spectrophotometry and HPLC methods

Method	Theophylline*				Guaiphenesin*			
	Capsules†		Elixir†		Capsules†		Elixir†	
	Found (%)	RSD (%)	Found (%)	RSD (%)	Found (%)	RSD (%)	Found (%)	RSD (%)
Third-derivative								
UV spectrophotometry	100.02	0.95	100.34	1.13	100.15	1.54	100.97	1.03
HPLC	101.43	1.94	101.27	2.33	100.97	2.18	98.08	2.68

* Mean and relative standard deviation of five determinations given as a percentage of the claimed content.

† Capsules were prepared in the laboratory to contain 150 mg of theophylline and 90 mg of guaiphenesin per capsule. Quibron elixir was claimed to contain 150 mg of theophylline and 90 mg of guaiphenesin per 15 ml.

Analysis of Pharmaceutical Formulations

The validity of the proposed methods for pharmaceutical preparations and the effect of possible interferences were studied by assaying Quibron elixir (labelled to contain 150 mg of theophylline and 90 mg of guaiphenesin per 15 ml) and laboratory-prepared capsules. The latter contained 150 mg of theophylline and 90 mg of guaiphenesin together with common additives and excipients, *e.g.*, lactose, starch, talc and magnesium stearate. The results are given in Table 4. The results are accurate and precise, as indicated by the recovery (98.08–101.43%) and the relative standard deviation (0.95–2.68%).

Conclusions

Derivative UV spectrophotometry and HPLC are suitable techniques for the reliable analysis of commercial formulations containing combinations of theophylline and guaiphenesin. The most striking features of the derivative method are its simplicity, sensitivity and rapidity, which render it suitable for routine analysis in control laboratories.

The HPLC method was shown to be a versatile reference method and may offer advantages over the derivative method for the selective determination of the two intact drugs in the presence of their degradation products or in a variety of matrices.

The authors gratefully acknowledge the Deanship of Research at Jordan University of Science and Technology for financial support of this work through project No. 15/91.

References

- Reynolds, J. E. F., *Martindale: the Extra Pharmacopoeia*, Pharmaceutical Press, London, 29th edn., 1989, pp. 910 and 1532.
- Gennaro, A. R., *Remington's Pharmaceutical Sciences*, Mack, Easton, PA, 17th edn., 1985, p. 874.
- The United States Pharmacopoeia, Twenty-First Revision, The National Formulary, XVI Edition*, US Pharmacopoeial Convention, Rockville, MD, 1985, pp. 473 and 1042.
- British Pharmacopoeia*, HM Stationery Office, London, 1988, vol. 1, pp. 278 and 564.
- European Pharmacopoeia, II*, Maisonneuve, France, 1971, p. 382.
- Yang, Q., Meng, Y., and Zhang, G., *Yaowu Fenxi Zazhi*, 1984, 4, 148; *Anal. Abstr.*, 1985, 47, 10E70.

- Tan, H. S. I., and Salvador, G. C., *Anal. Chim. Acta*, 1985, 176, 71.
- Rao, G. R., Avadhanulu, A. B., Giridhar, R., and Kokta, C. K., *East. Pharm.*, 1988, 31, 141; *Anal. Abstr.*, 1989, 51, 6E69.
- El-Yazbi, F. A., and Korany, M. A., *Spectrosc. Lett.*, 1985, 18, 543.
- Wahbi, A. A. M., and El-Omar, S. S., *Alexandria J. Pharm. Sci.*, 1988, 2, 125.
- Tomankova, H., and Vasatova, M., *Pharmazie*, 1989, 44, 197.
- Bambagiotti-Alberti, M., Pinzauti, S., and Vincieri, F. F., *Pharm. Acta Helv.*, 1987, 62, 175.
- McSharroy, W. O., and Savage, I. V. E., *J. Pharm. Sci.*, 1980, 69, 212.
- Muhammad, N., and Bodnar, J. A., *J. Liq. Chromatogr.*, 1980, 3, 113.
- Carnevale, L., *J. Pharm. Sci.*, 1983, 72, 196.
- Heidemann, D. R., *LC-GC*, 1987, 5, 422.
- Nowakowska, Z., *Farm. Pol.*, 1987, 43, 141; *Anal. Abstr.*, 1988, 50, 5E11.
- Saushkina, A. S., Vergeichik, E. N., Kompantseva, E. V., and Kilyakova, G. M., *Farmatsiya*, 1980, 29, 63; *Anal. Abstr.*, 1981, 41, 3E16.
- Arnoudse, P. B., and Pardue, H. L., *J. Autom. Chem.*, 1986, 8, 75.
- Hu, J., Wang, Y., and Kong, Q., *Yaowu Fenxi Zazhi*, 1988, 8, 217; *Anal. Abstr.*, 1989, 51, 3D40.
- Aliev, A. M., and Guseinov, B. M., *Farmatsiya*, 1983, 32, 75; *Anal. Abstr.*, 1984, 46, 4E15.
- Wesolowski, M., *Int. J. Pharm.*, 1982, 11, 35.
- Salama, O. M., and Walash, M. I., *Anal. Lett.*, 1989, 22, 827.
- Gaitonde, R. V., and Rivankor, U., *Indian Drugs*, 1987, 24, 486.
- Majlat, P., *Pharmazie*, 1984, 39, 325.
- Juenge, E. C., Gurka, D. F., and Kreienbaum, M. A., *J. Pharm. Sci.*, 1981, 70, 589.
- Chem, T.-M., and Chafetz, L., *J. Pharm. Sci.*, 1981, 70, 804.
- Roberts, S. E., and Delaney, M. F., *J. Chromatogr.*, 1982, 242, 364.
- Low, G. K. C., Haddad, P. R., and Duffield, A. M., *J. Chromatogr.*, 1983, 261, 345.
- Garcia, S. F., Carnero, R. C., Marquez, G. T. C., Hernandez, L. M., and Heredia, B. A., *Analyst*, 1990, 115, 1121.
- Carnero, R. C., Heredia, B. A., and Garcia, S. F., *J. Agric. Food Chem.*, 1990, 38, 178.
- Abdel-Hay, M. H., Elsayed, M. A., Barary, M. H., and Hassan, E. M., *J. Pharm. Belg.*, 1990, 45, 259.

Paper 1/02751D

Received June 10, 1991

Accepted August 26, 1991

Determination of Tricarbonyl(2-methylcyclopentadienyl)manganese in Gasoline and Air by Gas Chromatography With Electron-capture Detection

Virindar S. Gaind, Kusum Vohra and Fong Chai

Occupational Health Laboratory, Ontario Ministry of Labour, 101 Resources Road, Weston, Ontario, Canada M9P 3T1

Gas chromatography with electron-capture detection provides a highly sensitive technique for quantifying tricarbonyl(2-methylcyclopentadienyl)manganese (MMT). Airborne MMT can be collected by drawing a known volume of air through tubes containing XAD-2, and MMT concentrations as low as 0.001 mg m^{-3} can be monitored using a 10 l sample. No significant breakthrough was observed when 60 l of air were sampled at 1.0 l min^{-1} in the presence of a large excess of gasoline. The MMT in gasolines or other hydrocarbon fuels can be quantified by direct injection after dilution (1 + 99 or more) with hexane.

Keywords: Tricarbonyl(2-methylcyclopentadienyl)manganese determination; gas chromatography with electron-capture detection; gasoline; air samples

Tricarbonyl(2-methylcyclopentadienyl)manganese (MMT), $\text{CH}_3\text{C}_5\text{H}_4\text{Mn}(\text{CO})_3$ (Fig. 1), is an organometallic additive that improves the octane rating of gasoline. It is also used as a smoke abatement additive in fuels used for conventional reciprocating internal combustion engines and gas turbine engines, where 10–100 mg of MMT per litre of oil reduces smoke and particulate emissions by as much as 50–90%.¹

Tricarbonyl(2-methylcyclopentadienyl)manganese is highly toxic by all routes of exposure, *i.e.*, inhalation, ingestion and skin absorption. Experimental data on animals have shown that exposure to MMT produces severe injury to the kidneys, liver, lungs and central nervous system.^{2–4}

The American Conference of Governmental Industrial Hygienists (ACGIH) has adopted a Threshold Limit Value–Time Weighted Average (TLV–TWA) of 0.2 mg m^{-3} for MMT, determined as Mn.⁵ The TLV–TWA for other Mn compounds and Mn dust, however, is 5 mg m^{-3} as Mn. The considerable difference between the TLV–TWA of MMT and those of other Mn compounds suggested the need for a specific and sensitive analytical procedure capable of determining low concentrations of MMT in workplace atmospheres and in gasoline and other fuels.

A number of analytical procedures have been reported for the determination of MMT, *i.e.*, simple determination of total elemental Mn by atomic absorption⁶ or gas chromatographic separation followed by flame-ionization detection.⁷ Gas chromatography (GC) coupled with an atmospheric pressure helium microwave plasma emission system has been shown to provide highly sensitive analytical capabilities⁸ as has gas chromatographic separation followed by atomic absorption from a d.c. argon plasma⁹ or atomic absorption in a slotted quartz tube analyser.¹⁰ Aue *et al.*¹¹ have described the application of atomic emission through a modified flame-photometric detection system in which the chemiluminescence from Mn is measured in order to quantify MMT. High-performance liquid chromatography coupled with a laser-excited atomic fluorescence spectrometric detector has also been described recently.¹²

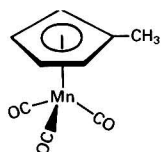


Fig. 1 Structure of MMT

Although some of these procedures are specific and sensitive, their usage entails considerable modifications or interfacing of the available analytical systems, some of which are beyond the capabilities of many environmental analytical laboratories.

This paper describes a simple, highly sensitive and specific gas chromatographic analytical procedure based on the use of electron-capture detection (ECD) for the quantification of MMT in gasoline and air. The unequivocal confirmation of the MMT peak was carried out by gas chromatography–mass spectrometry (GC–MS) in the electron impact (EI) or chemical ionization (CI) mode.

Experimental

Chemicals

Tricarbonyl(2-methylcyclopentadienyl)manganese was obtained from Pfaltz & Bauer (Waterbury, CT, USA). Hexane and isooctane were of pesticide grade and the other chemicals were of analytical-reagent grade from Caledon Chemicals (Georgetown, Ontario, Canada).

Apparatus

The gas chromatograph used was a Hewlett-Packard (Avondale, PA, USA) Model 5840 instrument equipped with a ^{63}Ni electron-capture detector. The mass spectrometer was a Hewlett-Packard Model 5985 instrument with an HP 7920 data system. The column in the GC–MS system was a fused silica capillary column ($25 \text{ m} \times 0.32 \text{ mm i.d.}$) with a chemically bonded DB-5 methylphenylsilicone stationary phase, $1 \mu\text{m}$ thick, from J & W Scientific (Rancho Cordova, CA, USA).

The air sampling pumps were portable Bendix (Ronceverte, WV, USA) Model 44 pumps, and the sorbent sampling tubes were from SKC (Eighty Four, PA, USA). The Tenax tubes had a front section with 50 mg of sorbent and a back-up section with 35 mg of sorbent. The XAD-2 sampling tubes had a front section containing 80 mg of sorbent and a back-up section with 40 mg of sorbent. The Test Atmosphere Generating System (TAGS) was from SRI (Menlo Park, CA, USA).

Gas Chromatographic Conditions

Calibration standards were prepared by diluting a known amount of MMT with isooctane and were prepared daily.

The conditions used for the gas chromatographic separation of MMT were as follows: column, $10 \text{ ft} \times \frac{1}{8}$ in stainless steel

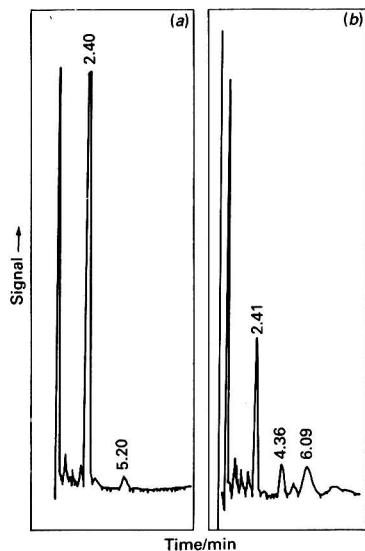


Fig. 2 Gas chromatogram for (a) injection of 2 ng of MMT; and (b) gasoline containing 30 mg l⁻¹ of MMT injected (2 µl) after a 1 + 249 dilution with hexane

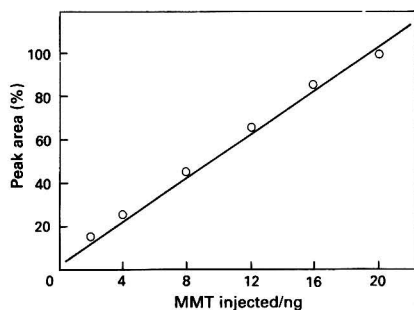


Fig. 3 Linearity of electron-capture detector response [peak area (%) (peak area for a 20 ng injection = 100%)] versus amount of MMT injected (2 µl injection from a solution containing 0.1–10 µg ml⁻¹ of MMT). Correlation coefficient = 0.9986

with 10% FFAP on Chromosorb W, 80–100 mesh; oven temperature, 130 °C; injector temperature, 220 °C; and detector temperature, 240 °C.

A typical chromatogram obtained by injecting 2 µl of MMT solution with a concentration of 1.0 µg ml⁻¹ (2 ng of MMT) is shown in Fig. 2(a).

The linearity of the detector response to MMT was established by carrying out replicate injections ($n = 6$) of serially diluted standard solutions at various concentrations. The average area obtained for each concentration was plotted against the amount of MMT injected in order to establish the linearity of the electron-capture detector response in the range likely to be encountered in samples (Fig. 3).

The lower detection level was calculated by serial dilution of standard solutions until the area of the peak obtained was three times the background noise level.

Mass Spectra of MMT

The EI mass spectrum of MMT [Fig. 4(a)] was obtained at 70 eV and scanned from 35 to 400 u. The CI mass spectrum was obtained at 2400 eV, scanning from 100 to 400 u and using

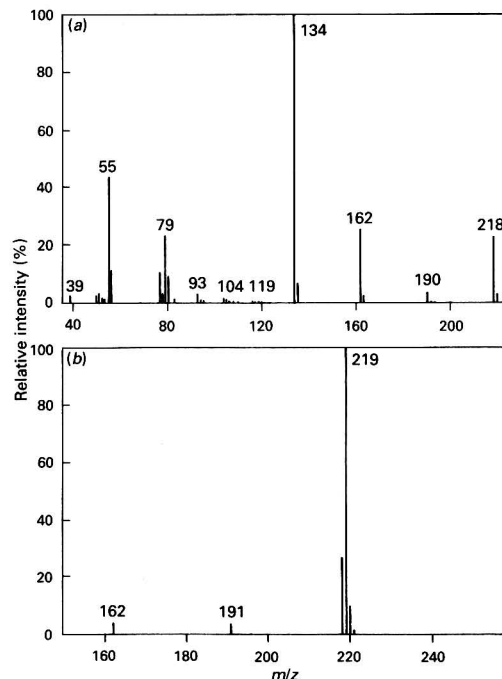


Fig. 4 (a) EI mass spectrum of MMT; and (b) CI mass spectrum of MMT

methane as the reagent gas [Fig. 4(b)]. The oven temperature was held at 100 °C for 1 min and then raised to 150 °C at 10 °C min⁻¹.

Preliminary Evaluation of Sample Collection Media for Spiked MMT

Five common air sampling media were evaluated for the collection of MMT, *i.e.*, (1) glass or stainless-steel sampling bulbs; (2) sorbent tubes containing charcoal; (3) sorbent tubes containing Tenax; (4) sorbent tubes containing XAD-2; and (5) impingers containing isooctane.

A known amount of MMT was spiked onto each of the sampling media. After equilibration for 10 min, an aliquot of air was withdrawn from the glass and stainless-steel bulbs with a glass syringe and 0.1 ml of the air sample was injected into the gas chromatograph in order to quantify MMT.

The MMT in the sorbent tubes was extracted by placing the front and back-up sections in separate vials, adding 1.0 ml of hexane, sealing the vials with PTFE-lined caps and shaking for 30 min. The MMT spiked in the impingers containing isooctane was quantified by injecting 2 µl of the solution.

Through a second set of spiked sorbent tubes and impingers, containing identical amounts of MMT, a measured volume of air was drawn for 50 min at 0.2 l min⁻¹, using a sampling pump. The amount of MMT remaining in each sample was quantified in order to compare the effect of passage of air on the MMT collected.

The percentage recovery in all of the above experiments was calculated by comparing the peak areas against freshly prepared standard solutions of MMT in hexane or isooctane.

Stability of MMT Spiked on Sampling Tubes

The stability of MMT spiked on XAD-2 sorbent tubes was evaluated by spiking replicate tubes with a known amount of

MMT and storing them, wrapped in aluminium foil, at 4 °C in the dark. Duplicate tubes were analysed at various intervals in order to evaluate the stability of MMT adsorbed onto the tubes.

Evaluation of Sample Collection Procedure for Airborne MMT

The actual sample collection was evaluated by using a dynamically generated atmosphere of MMT in a TAGS having multiple sampling ports. The MMT (10% v/v) mixed with gasoline and maintained at room temperature in the sampling bulb of the TAGS was vaporized with a carrier stream of nitrogen at 0.1 l min⁻¹ and further diluted with air at 61 l min⁻¹ in a mixing chamber. The sampling ports were fitted with critical orifices, which allowed a precise sampling flow rate of 1.0 ± 0.05 l min⁻¹. The XAD-2 and Tenax sampling tubes (which showed promising recovery of adsorbed MMT in the spiking experiments) were connected to the sampling ports. Each tube had a front section separated from a back-up section in order to assess whether there was any breakthrough during sample collection.

Quantification of MMT in Gasoline

Gasoline was diluted with hexane (1 + 99 or more) and 2.0 µl of the solution were injected into the gas chromatograph. The MMT furnished a distinct peak, usually without interferences.

Results and Discussion

Linearity, Precision and Minimum Detectable Amount of MMT Using ECD

The electron-capture detector response was linear in the range tested, *i.e.*, 0.2–20 ng of MMT. Fig. 3 shows a plot of the average peak area *versus* the amount of MMT injected (2.0 µl injections of solutions containing 0.1–10 µg ml⁻¹ of MMT). The correlation coefficient of the plot was 0.9986.

The relative standard deviations for replicate injections of the above solutions ranged from 2.4 to 5.07%, showing the fairly good repeatability of the electron-capture detector response to MMT.

The minimum detectable amount (MDA) of MMT using ECD was calculated to be 0.02 ng (2.0 µl injection of a 0.01 µg ml⁻¹ MMT solution). This makes it possible to detect airborne MMT at a concentration of 0.001 mg m⁻³ with a 10 l air sample.

The MDA for MMT when using ECD compares favourably with those reported for other analytical techniques, *i.e.*, 12 ng of MMT by atomic emission from a d.c. plasma; 0.8 ng of MMT for atomic absorption in a slotted quartz tube atomizer; and 2 ng of MMT for atomic emission from the modified flame-photometric detector developed recently by Aue *et al.*¹¹

Stability of MMT Solutions and Spiked Sampling Tubes

The standard solutions of MMT, at concentrations of 1.0–10.0 µg ml⁻¹, were stable for a period of 4 d when kept in a refrigerator and protected from light by wrapping the containers in aluminium foil. These solutions were, however, not very stable on exposure to strong daylight at room temperature and solid particles separated overnight, indicating decomposition of MMT.

Ten XAD-2 sampling tubes, each spiked with 5.0 µg of MMT, showed no significant change in the amount of MMT present when kept in the dark at 4 °C for up to 7 d. This implies that when MMT samples collected on XAD-2 tubes are protected from strong light by wrapping them in aluminium foil and stored in a refrigerator, they can be kept for up to 7 d without any deterioration in the integrity of the samples. However, the calibration standards should be freshly prepared before analysing each batch of samples.

Mass Spectra of MMT

The mass spectrum of MMT in the EI mode [Fig. 4(a)] detected the molecular ion (*m/z* 218) with a relative abundance of 45%. The other expected fragments, *m/z* 190, 162 and 134, representing loss of three successive carbonyl (CO) fragments, were also present. The base peak had *m/z* 134, indicating loss of all three CO functions.

The CI mass spectrum of MMT [Fig. 4(b)] showed *M* + 1 (*m/z* 219) as the only significant ion with very minor ions at *m/z* 191 and 162, representing loss of two CO units.

Either of the two ionization modes can be used for quantifying MMT levels as low as 0.1 ng using the ion at *m/z* 218 or 219 with selected ion monitoring.

Evaluation of Sample Collection Media for Spiked MMT

The addition of MMT to a glass bulb produced erratic results; the MMT was not stable and showed a 90% loss over a period of 48 h. The stability of MMT in air did not improve when the samples were kept in a stainless-steel sampler, and attempts at direct sampling were abandoned.

The results of recovery experiments on MMT spiked on various other sampling media are summarized in Table 1. The charcoal tubes gave erratic recoveries in the range 33–51%. These were considered unacceptable. The recovery of MMT spiked on Tenax tubes was better, ranging from 60 to 85%, and showed little change after the passage of air. The XAD-2 tubes and the impingers containing isooctane, however, gave nearly quantitative recovery of the spiked MMT. The passage of air did not affect the recovery of MMT from Tenax, XAD-2 or the impingers containing isooctane.

This suggests that tubes containing XAD-2, and impingers containing isooctane, are suitable for the collection of

Table 1 Recovery of spiked MMT from various sampling media before and after passage of air

MMT spiked/µg	MMT recovered (%)							
	Sampling medium							
	Charcoal		Tenax		Isooctane impinger		XAD-2	
	NA*	A†	NA*	A†	NA*	A†	NA*	A†
10	50	51	85	81	100‡	103	100	100
1.0	35	33	60	62	100‡	101	100	93
0.1	35	35	80	78	100‡	108	95	93

* NA: Not aerated.

† A: After passage of 10 l of air.

‡ Solutions used for calibration.

Table 2 Comparison of the amount of MMT collected on XAD-2 and Tenax tubes from a dynamically generated atmosphere

Sample No.	MMT collected/ μg					
	XAD-2			Tenax		
	Front	Back	Total	Front	Back	Total
1	18.5	0.7	19.2	2.4	1.1	3.5
2	16.4	0.6	17.0	1.6	0.8	2.4
3	17.4	0.6	18.0	2.5	1.3	3.8
4	16.7	0.5	17.2	1.7	0.7	2.4
5	15.4	0.5	15.9	2.7	1.4	4.1
6	15.2	0.5	15.7	3.1	1.4	4.5
Mean:			17.2			3.5
SD:			1.3			0.9
RSD:			7.6%			25.5%

airborne MMT samples. However, as the sorbent sampling tubes are preferable for personal sampling, Tenax and XAD-2 tubes were subjected to further evaluation for sample collection from dynamically generated atmospheres of MMT as both showed adequate recoveries of spiked MMT.

Evaluation of Sample Collection on XAD-2 and Tenax From a Dynamically Generated MMT Atmosphere

Table 2 shows the amounts of MMT found on XAD-2 and Tenax sampling tubes when a dynamically generated MMT atmosphere was used for multiple sample collection at a flow rate of 1.0 l min^{-1} for a period of 60 min. The total amount of MMT collected on XAD-2 ranged from 15.7 to 19.2 μg , with an average value of 17.2 μg , a standard deviation (SD) of 1.3 μg and a relative standard deviation (RSD) of 7.6%, indicating fairly good precision.

The amount of MMT detected in the back-up section of the XAD-2 sampling tubes was less than 4% of that detected in the front section in all instances, showing that there was no breakthrough even with an air sampling rate of 1 l min^{-1} and in the presence of a large excess of gasoline vapour and an MMT loading of up to 17 μg .

The Tenax tubes, however, showed poor efficiency for sampling airborne MMT as evidenced by the small amounts of MMT collected, the high RSD and the very high breakthrough to the back-up sections for all the samples (Table 2). This discrepancy between the fairly good adsorption efficiency of MMT spiked on Tenax tubes (Table 1) and the very poor collection efficiency of MMT from a dynamically generated atmosphere is probably due to poor adsorption and overloading of Tenax with gasoline vapour.

The air concentration of MMT in the dynamically generated atmosphere was about 0.3 mg m^{-3} . The ACGIH adopted TLV-TWA concentration of MMT is 0.2 mg m^{-3} (expressed as Mn) and corresponds to about 0.7 mg m^{-3} of MMT.

The results of sampling a dynamically generated MMT atmosphere show that XAD-2 tubes with two sections are the most suitable for the collection of airborne MMT.

Determination of MMT in Gasoline

The maximum permissible amount of MMT in unleaded gasolines is 18 mg l^{-1} (as Mn), which corresponds to approximately 72 mg l^{-1} as MMT. As MMT can be detected at very low concentrations through the use of ECD, the gasoline samples were diluted ($1 + 99$ to $1 + 499$) with hexane in order to monitor the level of MMT in gasoline. The chromatogram shown in Fig. 2(b) represents a gasoline with an MMT level of 30 mg l^{-1} and was obtained after a $1 + 249$ dilution of the gasoline with hexane. The peaks due to most of the other constituents of the gasoline show little interference.

However, in some gasolines containing excessively large concentrations of sulfur compounds, the peak due to MMT might be subject to interference from the sulfur-containing components if these are not completely separated. For such samples, it is necessary to quantify the amount of MMT by using a mass spectrometer in the CI mode in order to confirm the identity of the peak unequivocally.

Conclusions

Gas chromatography with ECD provides a simple and highly sensitive analytical procedure for quantifying MMT in air or gasoline. Airborne MMT can be collected by drawing air at 1.01 min^{-1} through XAD-2 sampling tubes for 10–60 min. The MMT in gasoline can be quantified by appropriately diluting the gasoline with hexane or isooctane and injecting the solution directly into a gas chromatograph equipped with an electron-capture detector. An unequivocal confirmation of the presence of MMT can be carried out by GC-MS in either the EI or CI mode.

References

- 1 Craig, P. J., *Organometallic Compounds in the Environment: Principles and Reactions*, Longman, London, 1986, ch. 10.
- 2 McGinley, P. A., Morris, J. B., Clay, R. J., and Gianutsos, G., *Toxicol. Lett.*, 1987, **36**, 137.
- 3 Browning, E., *Toxicology of Metals*, Butterworth, London, 1966, pp. 185–196.
- 4 Hanzlik, R. P., Bhatia, P., Stitt, R., and Traiger, G. J., *Drug Metab. Dispos.*, 1980, **8**, 428.
- 5 *Threshold Limit Values and Biological Exposure Indices, for 1990–1991*, American Conference of Governmental Industrial Hygienists, Cincinnati, OH, 1990, p. 26.
- 6 Smith, G. W., and Oalmby, A. K., *Anal. Chem.*, 1959, **31**, 1798.
- 7 DuPuis, M. D., and Hill, H. H., *Anal. Chem.*, 1979, **51**, 292.
- 8 Quimby, B. D., Uden, P. C., and Barnes, R. M., *Anal. Chem.*, 1978, **50**, 2112.
- 9 Uden, P. C., Barnes, R. M., and DiSanzo, F. P., *Anal. Chem.*, 1978, **50**, 852.
- 10 Coe, M., Cruz, R., and van Loon, J. C., *Anal. Chim. Acta*, 1980, **120**, 171.
- 11 Aue, W. A., Miller, B., and Sun, X.-Y., *Anal. Chem.*, 1990, **62**, 2453.
- 12 Walton, A. P., Wei, G.-T., Liang, Z., Michel, R. G., and Morris, J. B., *Anal. Chem.*, 1991, **63**, 232.

Paper 1/00869B

Received February 22, 1991

Accepted October 16, 1991

Fourier Transform Infrared Spectroscopic Studies on the Interaction Between Copper(II), Amino Acids and Marine Solid Particles

Wang Xiulin

Department of Chemistry, Fudan University, Shanghai 200433, People's Republic of China

Fourier transform infrared (FTIR) spectroscopy was employed to characterize the interaction between Cu^{II}, amino acids (AAs) and solid particles. The ion exchange between Cu^{II} and marine solid particles causes a stepwise change in $\nu(\text{OH})$ of surface H-bonding hydroxyl groups with an increase of the 'ion-exchange amount' of Cu^{II} at room temperature. The bands of the COO^- and NH_3^+ vibrational modes of adsorbed AA and Cu^{II}-AA surface complexes in a solid matrix are first isolated from the overlapping solid particle matrix by use of the spectral subtraction approach. With respect to the corresponding free AA, $\nu(\text{NH}_3^+)$ and $\delta(\text{NH}_3^+)$ of the adsorbed AA shift 10–39 and 13–49 cm^{-1} , respectively, toward higher and lower frequencies, whereas the variation of $\nu(\text{COO}^-)$ (as) and $\nu(\text{COO}^-)$ (s) is less than 4 cm^{-1} , nearly equal to the resolution of the IR spectrometer. This indicates that the surface hydroxyl group associates with the amino group of the amino acid in a solid matrix rather than with the carboxyl group. Similarly, not only do the $\nu(\text{NH}_3^+)$ and $\delta(\text{NH}_3^+)$ of the Cu^{II}-AA surface complex in the solid matrix shift 16–27 and 34–42 cm^{-1} , respectively, toward higher and lower frequencies, but also $\nu(\text{COO}^-)$ (as) and $\nu(\text{COO}^-)$ (s) shift 15–32 and 10–25 cm^{-1} , respectively, toward higher and lower frequencies, indicating that as a 'bridging' reagent the AA joins Cu^{II} and the surface hydroxyl group, respectively, through the amino group and the carboxyl group to form a Model II ternary surface complex (TSC). The IR bands at 287–360 cm^{-1} , due to the Cu–O stretching mode, were detected and thus further confirmed the formation of the TSC model between Cu^{II}, AAs and marine solid particles.

Keywords: Fourier transform infrared spectroscopy; marine solid particle; copper(II); amino acid; adsorption

Marine solids include suspended particles and surface sediment, and consist mainly of oxides (such as Mn, Fe, Si and Al oxide), clays (such as montmorillonite, illite and kaolinite), and calcium carbonate.^{1–3} In general, bare metal ions and hydroxyl groups are two examples of the types of sites on the surface of solid particles.⁴ It has been observed^{5–7} that the isotherms of the ion exchange between trace metal ions and solid particles in sea-water can be classified as the 'plateau' type. Zhang and Liu⁶ suggested that the plateau isotherms can be interpreted in terms of the interfacial stepwise ion-exchange theory they have proposed.^{6,7} However, so far the interfacial stepwise ion-exchange theory has not been demonstrated experimentally.

Amino acids (AAs), which are found at a concentration of about 0.06 mg l^{-1} in sea-water,⁸ are one of the most important marine organic materials identified so far. It appears that AAs react with surface hydroxyl groups on oxides mainly through the amino group.⁹ However, infrared (IR) spectra have rarely been reported for AAs in a solid particle matrix, although IR spectra of simple organic compounds, such as NH_3 , carboxylic acids and amines, in a solid matrix have been measured.^{10–14} Further, there are major limitations in the spectrometric examination of AAs in a solid matrix, including low concentration of AAs, and spectral interferences from the solid particle matrix.

It is generally accepted that the formation of a ternary surface complex (TSC) causes some organic substances to promote the ion exchange between trace metal ions and solid particles when there is an interaction between trace metal ions, solid particles and organic matter.^{6,15–17} However, the IR spectra have rarely been reported for the same reasons as those given above for the amino acid-solid particle system. Leckie and co-workers^{16,18} proposed three models of TSC and Bowers and Huang¹⁹ suggested that these models can be distinguished by comparing the graph of percentage adsorption of metal ions *versus* pH with that of percentage adsorption of organic compound *versus* pH. However, the method of Bowers and Huang may be without value because neither of the pH curves was simple and both varied with the experimental conditions.²⁰ In the present work, emphasis is placed on the IR spectroscopic evidence for the interfacial

stepwise ion-exchange theory,^{6,7} and obtaining, by use of the spectral subtraction approach, the distinctive IR bands of AAs in a solid matrix for 'amino acid-solid particles' and 'amino acid-copper(II)-solid particles' systems.

Experimental

Reagents and Materials

The $\text{CuCl}_2 \cdot 2\text{H}_2\text{O}$ used was of analytical-reagent grade and all AAs used were of spectroscopic grade. The $\alpha\text{-SiO}_2$ was supplied by Beijing Chemical Reagent Co. (Beijing, China). Solid particle samples were prepared as described previously for goethite,⁵ $\gamma\text{-AlOOH}$ ⁶ and CaCO_3 .³ The natural clays of montmorillonite and illite (Zhejiang Mineral Co., Hangzhou, China) were re-purified and transformed from calcium-clay to sodium-clay according to a previous method.⁶ All the solid particle samples were identified by using X-ray diffraction graphs. The specific surface area of these solid particles in aqueous solution, determined by the approach developed by Wang,²⁵ are 742 $\text{m}^2 \text{g}^{-1}$ for $\gamma\text{-AlOOH}$, 451 $\text{m}^2 \text{g}^{-1}$ for goethite, 58 $\text{m}^2 \text{g}^{-1}$ for SiO_2 , 39 $\text{m}^2 \text{g}^{-1}$ for illite, 59 $\text{m}^2 \text{g}^{-1}$ for montmorillonite and 296 $\text{m}^2 \text{g}^{-1}$ for CaCO_3 .

Pre-treatment

Approximately 50 mg of the solid sample powder were accurately weighed and placed in an 80 ml centrifuge tube containing 50.0 ml of a solution of either Cu^{II}, or AA, or Cu^{II}-amino acid of known concentration. The mixture was shaken for 3 h at 25.0 °C, and then the solid powder was separated from the supernatant by using an LXJ-64-01 centrifuge (Beijing Medicine Instrument Factory, Beijing, China). Measurements of pH in the supernatant were made with a Corning combined pH-reference electrode with the use of a Radiometer pHM84 meter (Copenhagen, Denmark). The concentration of Cu^{II} in the supernatant was determined by using a PE-3030 atomic absorption spectrometer (Perkin-Elmer, Norwalk, CT, USA), and of the AA by using a Hitachi 801 amino acid autoanalyser (Hitachi, Tokyo, Japan). In order to obtain a relatively reliable spectrum, revealing the actual surface species in aqueous solution, the solid powder

was dried by evacuation at ambient temperature from atmospheric pressure to 8.8×10^4 Pa for 24 h. This procedure was carried out because some change in the IR spectra arose when the solid powder was pre-desiccated by evacuating to high vacuum, as occurred by heating in air at higher temperatures.^{11,13,22}

Sample Preparation and Infrared Spectral Measurements

The desiccated solid powder (about 20 mg) was mixed with dry potassium bromide (about 100 mg), ground in an agate mortar and subjected to a pressure of 8×10^6 Pa in an evacuated die, to produce a clear transparent disc with a diameter of 12 mm. Infrared spectra of the discs were obtained with 4 cm^{-1} resolution and a medium interscan correlation, using a Nicolet 10-DX Fourier transform (FT) IR spectrometer (Nicolet, Madison, WI, USA), equipped with a Model 1280 acquisition system. Fifty-four cumulative scans yielded an adequate signal-to-noise ratio in the spectra.

Results and Discussion

FTIR Spectra of the Copper(II)-Marine Solid Particle System

Fig. 1 shows FTIR spectra of illite with various ion-exchange amounts (IEAs) of Cu^{II} . Absorption, observed at 3441 cm^{-1} for all copper(II)-illite samples (Table 1), had the same band as the $\nu(\text{OH})$ of the surface H-bonding hydroxyl group (SHHG) on pure illite. The only band at 3441 cm^{-1} appears for an IEA of Cu^{II} of $0.52 \mu\text{mol m}^{-2}$. The bands at 3523, 3574, 3316 and 3361 cm^{-1} appear consecutively with a gradually increasing IEA of Cu^{II} from 18.1 to $158 \mu\text{mol m}^{-2}$, while the band at 3361 cm^{-1} disappears when the IEA of Cu^{II} increases up to $202 \mu\text{mol m}^{-2}$. These bands may be assigned to $\nu(\text{OH})$ of SHHG as has been done in similar earlier analyses.^{12,23,24} It should be noted that the weaker band at 3316 cm^{-1} could be overlapped by the band at 3574 cm^{-1} , which only appears as the IEA of Cu^{II} is somewhat smaller (Fig. 1). These are the characteristic bands of $\nu(\text{OH})$ of surface hydroxyl groups on hydrous CuO (Fig. 2). The hydroxyl bands were chosen to examine the influence of Cu^{II} ion exchange upon hydroxyl

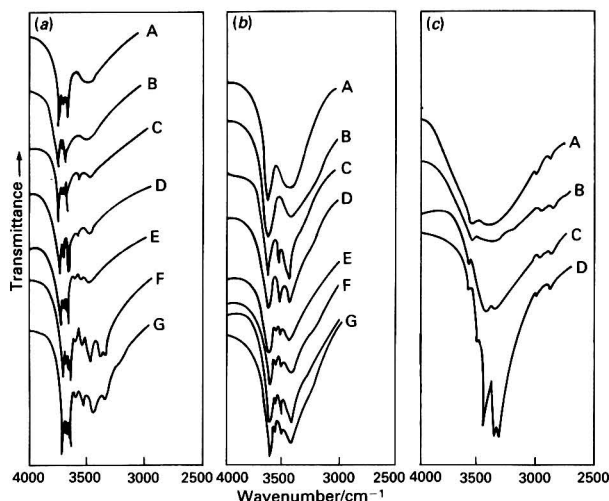


Fig. 1 Stepwise change in $\nu(\text{OH})$ of SHHG with the increase of the IEA of Cu^{II} at room temperature for: (a) Cu^{II} -illite systems with an IEA of Cu^{II} of: A, 0 (pure illite); B, 0.52; C, 18.1; D, 20.1; E, 49.5; F, 158; and G, $202 \mu\text{mol m}^{-2}$; (b) Cu^{II} -montmorillonite systems with an IEA of Cu^{II} of: A, 0 (pure montmorillonite); B, 1.87; C, 10.8; D, 11.9; E, 13.1; F, 14.6; G, 18.8; and H, $22.9 \mu\text{mol m}^{-2}$; (c) Cu^{II} - CaCO_3 systems with an IEA of Cu^{II} of: A, 0 (pure CaCO_3); B, 1.70; C, 10.6; and D, $26.1 \mu\text{mol m}^{-2}$

Table 1 Stepwise change in $\nu(\text{OH})$ of SHHG on clays and CaCO_3 due to the ion exchange between Cu^{II} , clays and CaCO_3

Solid particle	pH	IEA of $\text{Cu}^{II}/\mu\text{mol m}^{-2}$	$\nu(\text{OH})^*/\text{cm}^{-1}$				
Illite	6.38	0.52	3441 m,br	—	—	—	—
	6.05	20.1	3441 m	3523 m	—	—	—
	5.97	49.5	3441 m	3523 w	3574 vw	—	—
	5.57	158	3441 m	3523 m	3574 m	3316 m	3361 m
	8.11	202	3441 m	3523 m	3574 m	3316 m	—
Montmorillonite	2.04	1.87	3427 s,br	—	—	—	—
	5.56	10.8	3427 m	3523 m	—	—	—
	4.76	11.9	3427 m	3523 m	—	—	—
	5.76	13.1	3427 m	3523 m	—	—	—
	5.95	14.6	3427 m	3523 m	3574 w	—	—
	6.06	18.8	3427 m	3523 m	3574 w	—	—
	5.74	22.9	3427 m	3523 m	3574 w	—	—
CaCO_3	6.15	1.70	3427 m,br	—	—	—	—
	5.82	10.6	3427 m	3359 m	—	—	—
	5.65	26.1	3427 s	3359 m	3574 w	3316 s	—

* br = Broad, s = strong, m = medium, w = weak, and vw = very weak.

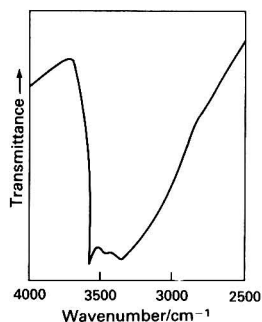


Fig. 2 Characteristic bands at 3316 and 3574 cm^{-1} due to surface hydroxyl groups on hydrous CuO

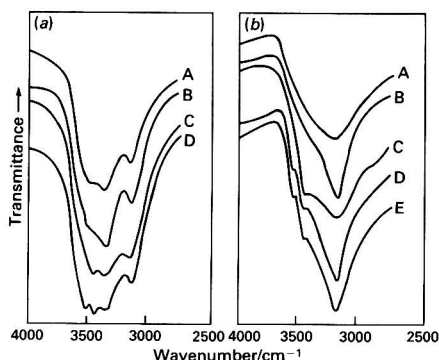


Fig. 3 Stepwise change in $\nu(\text{OH})$ of SHHG with an increase of the IEA of Cu^{II} at room temperature for: (a) Cu^{II} - γ -AlOOH systems with an IEA of Cu^{II} of: A, 0 (pure γ -AlOOH); B, 1.32; C, 3.61; and D, 8.06 $\mu\text{mol m}^{-2}$; (b) Cu^{II} -goethite systems with an IEA of Cu^{II} of: A, 0 (pure goethite); B, 2.37; C, 3.56; D, 4.01; and E, 8.38 $\mu\text{mol m}^{-2}$

groups on illite, indicating that with an increase in the IEA of Cu^{II} , copper(II)-illite ion exchange results in a stepwise change in the $\nu(\text{OH})$ of SHHG on illite, but no change in $\nu(\text{OH})$ of the free surface hydroxyl group (FSHG). Similarly, owing to the copper(II)-montmorillonite ion exchange, a stepwise change in $\nu(\text{OH})$ of SHHG on montmorillonite was observed, but no change in $\nu(\text{OH})$ of FSHG [Fig. 1(b)]. The band, observed at 3427 cm^{-1} for all copper(II)-montmorillonite samples with various IEAs of Cu^{II} (Table 1), had the same IR absorption as the $\nu(\text{OH})$ that was assigned to SHHG on pure montmorillonite.²⁵ Only the band at 3427 cm^{-1} appears for an IEA of 1.87 $\mu\text{mol m}^{-2}$ of Cu^{II} . Bands at 3523 and 3574 cm^{-1} , due to $\nu(\text{OH})$ of SHHG, appear consecutively with gradually increasing IEAs of Cu^{II} , i.e., the band at 3523 cm^{-1} appears when the IEA of Cu^{II} is 10.8, 11.9 and 13.1 $\mu\text{mol m}^{-2}$, while the bands at 3523 and 3574 cm^{-1} appear when the IEA of Cu^{II} increases to 14.6, 18.8 and 22.9 $\mu\text{mol m}^{-2}$.

It was shown from FTIR spectra²⁵ that CaCO_3 had similar bands of surface hydroxyl groups to clays. Fig. 1(c) reveals that Cu^{II} - CaCO_3 ion exchange results in a stepwise change in $\nu(\text{OH})$ of SHHG but no change in $\nu(\text{OH})$ of FSHG on CaCO_3 . The description for the spectra [Fig. 1(c)] is similar to that for the copper(II)-illite and copper(II)-montmorillonite systems, i.e., the bands at 3427, 3359, 3574 and 3316 cm^{-1} appear consecutively when the IEA of Cu^{II} gradually increases from 10.6 to 26.1 $\mu\text{mol m}^{-2}$ (Table 1).

Fig. 3(a) shows FTIR spectra of γ -AlOOH with different IEAs of Cu^{II} , indicating that Cu^{II} - γ -AlOOH ion exchange causes a stepwise change in $\nu(\text{OH})$ of SHHG rather than framework hydroxyl groups (FHG) in γ -AlOOH, and that a

Table 2 Stepwise change in $\nu(\text{OH})$ of SHHG on oxides due to the ion exchange between Cu^{II} and oxides

Oxide	pH	IEA of Cu^{II} / $\mu\text{mol m}^{-2}$	$\nu(\text{OH})^*/\text{cm}^{-1}$		
γ -AlOOH	5.73	1.32	3312 s,br	—	—
	4.95	3.61	3312 s,br	3427 w	—
	5.53	8.06	3312 s,br	3427 w	3512 w
Goethite	5.18	2.37	—	—	—
	4.46	3.56	—	3427 w	—
	5.17	4.01	—	3427 w	3512 w
	5.54	8.38	—	3427 w	3512 w

* br = Broad, s = strong, and w = weak.

band at 3312 cm^{-1} , due to $\nu(\text{OH})$ of SHHG on γ -AlOOH,²⁵ appears for all Cu^{II} - γ -AlOOH samples with various IEAs of Cu^{II} (Table 2). Only the band at 3312 cm^{-1} was detected for a smaller IEA of Cu^{II} (1.32 $\mu\text{mol m}^{-2}$); however, bands at 3427 and 3512 cm^{-1} appear consecutively when the IEA of Cu^{II} gradually increases, i.e., the band at 3427 cm^{-1} appears when the IEA of Cu^{II} is 3.61 $\mu\text{mol m}^{-2}$, while bands at 3427 and 3512 cm^{-1} occur when the IEA of Cu^{II} increases up to 8.06 $\mu\text{mol m}^{-2}$. Fig. 2(b) shows FTIR spectra of goethite with various IEAs of Cu^{II} , indicating that the bands at 3427 and 3523 cm^{-1} , due to $\nu(\text{OH})$ of SHHG,^{12,23,24} appear consecutively when the IEA of Cu^{II} gradually increases from 3.56 to 8.38 $\mu\text{mol m}^{-2}$ (Table 2), and that the intense and broad band at 3133 cm^{-1} , due to $\nu(\text{OH})$ of FHG in goethite,²⁵ appears in the spectrum. However, as the IEA of Cu^{II} was 2.37 $\mu\text{mol m}^{-2}$ only an intense and broad band at 3133 cm^{-1} was detected, consistent with the finding that the band due to $\nu(\text{OH})$ of SHHG on goethite was overlapped by its intense and broad band at 3133 cm^{-1} .²⁵

Summarizing the spectra described above, it can be concluded that with an increase of the IEA of Cu^{II} , Cu^{II} ion exchange causes a stepwise change in $\nu(\text{OH})$ of SHHG on solid particles, but no change in $\nu(\text{OH})$ of either FSHG on illite, montmorillonite and CaCO_3 , or FHG in goethite and γ -AlOOH, and that over the range of the IEA of Cu^{II} , two stepwise changes in $\nu(\text{OH})$ of SHHG were detected except that four were observed for the copper(II)-illite system, presumably due to different IEAs of Cu^{II} . Further, illite, montmorillonite and CaCO_3 had essentially the same stepwise change in $\nu(\text{OH})$ of SHHG due to copper(II)-solid particle ion exchange. The band at 3523 cm^{-1} for clays or 3359 cm^{-1} for CaCO_3 appears first, then the bands at both 3574 and 3316 cm^{-1} and finally the band at 3316 cm^{-1} , and then disappears. Similarly, goethite and γ -AlOOH had essentially the same stepwise change in $\nu(\text{OH})$ of SHHG due to the ion exchange between Cu^{II} and oxides. The first stepwise change is indicated by the appearance of a band at 3427 cm^{-1} , and then at 3512 cm^{-1} . The second change for oxides is different from that for clays and CaCO_3 , i.e., a band at 3512 cm^{-1} appears for oxides, whereas bands at 3574 and 3316 cm^{-1} , due to the characteristic $\nu(\text{OH})$ of SHHG on CuO, appear for clays and CaCO_3 . Consequently, these results provide the first IR evidence for the interfacial stepwise ion-exchange theory,⁶ and have elucidated the mechanism of the stepwise ion exchange between Cu^{II} and marine solid particles more clearly.

FTIR Spectra of Adsorbed Amino Acids in a Solid Matrix for Amino Acid-Marine Solid Particle Systems

The FTIR spectra were measured for free glycine, alanine, histidine, glutamic acid and aspartic acid, and subsequently some band frequencies were assigned to the $-\text{NH}_3^+$ stretching and bending modes $\nu(\text{NH}_3^+)$ and $\delta(\text{NH}_3^+)$, and the $-\text{COO}^-$ symmetric and asymmetric stretching modes $\nu(\text{COO}^-)$, s) and $\nu(\text{COO}^-)$, as) (Table 3) according to a similar study.²⁶⁻²⁹

It is difficult to recognize the IR bands of adsorbed AAs in a solid particle matrix from the IR spectra of amino acid-solid particle systems due to the low concentration of AAs and spectral interferences from the solid matrix. In order to obtain the distinctive AA bands, particularly $\nu(\text{NH}_3^+)$, $\delta(\text{NH}_3^+)$, $\nu(\text{COO}^-)$, as) and $\nu(\text{COO}^-)$, s), the spectral subtraction approach was used to isolate the adsorbed AA bands. The spectrum of the amino acid-solid system was obtained first and then the solid particle background absorption was subtracted. The IR spectra of adsorbed AAs are given in Fig. 4(a) for the glycine-, glutamic acid- and alanine-illite systems, in Fig. 4(b) for the glycine-, histidine-, glutamic acid- and alanine-montmorillonite systems, and in Fig. 4(c) for the amino acid- CaCO_3 and $\gamma\text{-AlOOH}$ systems and the

glycine- SiO_2 system at different pH values. Note that $\delta(\text{NH}_3^+)$ and $\nu(\text{COO}^-)$, s) of an amino acid in a CaCO_3 matrix are difficult to obtain owing to very strong IR interference from the CaCO_3 matrix near 1500 cm^{-1} , and also $\nu(\text{NH}_3^+)$ of AAs in the $\gamma\text{-AlOOH}$ matrix because of very strong interference from the $\gamma\text{-AlOOH}$ matrix in the range $3000\text{--}3500\text{ cm}^{-1}$.

The FTIR spectra of adsorbed AAs (Fig. 4) are different from those of the corresponding free AA; therefore, for amino acid-clay, amino acid-oxide and amino acid- CaCO_3 systems, $\nu(\text{NH}_3^+)$, $\delta(\text{NH}_3^+)$, $\nu(\text{COO}^-)$, s) and $\nu(\text{COO}^-)$, as) of the adsorbed AAs were assigned as in a similar analysis²⁶⁻²⁹ and chosen to examine the interaction between AAs and solid particles, as the main IR absorption comes from amino and carboxyl groups. Their frequency shifts with respect to free AAs, $\Delta\nu(\text{NH}_3^+)$, $\Delta\delta(\text{NH}_3^+)$, $\Delta\nu(\text{COO}^-)$, s) and $\Delta\nu(\text{COO}^-)$, as), are listed in Table 4. For the amino acid-illite, amino acid-montmorillonite, amino acid- $\gamma\text{-AlOOH}$ and amino acid- CaCO_3 systems, $\Delta\nu(\text{COO}^-)$, as) and $\Delta\nu(\text{COO}^-)$, s) are less than 4 cm^{-1} , nearly equal to the resolution of the IR spectrometer (4 cm^{-1}), whereas the variations of $\nu(\text{NH}_3^+)$ and $\delta(\text{NH}_3^+)$ are $10\text{--}39$ and $13\text{--}49\text{ cm}^{-1}$, respectively, moderately more than the resolution. For the glycine- SiO_2 system, the variations of $\nu(\text{NH}_3^+)$, $\delta(\text{NH}_3^+)$, $\nu(\text{COO}^-)$, s) and $\nu(\text{COO}^-)$, as) are similar to those of the above systems when the pH (≈ 6.59) is more than the pH_{pzc} of SiO_2 , which can be defined as the pH value at zero net adsorption of H^+ and OH^- ions as these ions are presumably the potential-determining species,

Table 3 Infrared vibrational bands generated from --NH_3^+ and --COO^- groups of free amino acids

Amino acid	$\nu(\text{NH}_3^+)/\text{cm}^{-1}$	$\nu(\text{COO}^-)$, as)/ cm^{-1}	$\delta(\text{NH}_3^+)/\text{cm}^{-1}$	$\nu(\text{COO}^-)$, s)/ cm^{-1}
Glycine	3186	1592	1522	1413
Alanine	3086	1594	1506	1413
Histidine	3130	1578	1539	1409
Aspartic acid	3141	1617	1501	1420
Glutamic acid	3059	1616	1516	1422

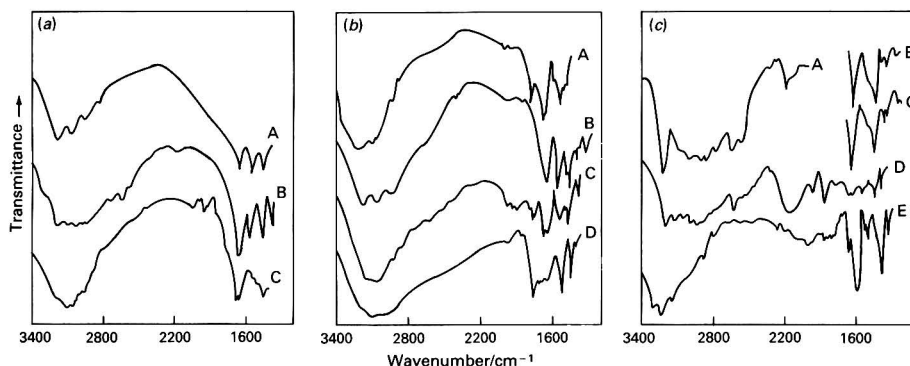


Fig. 4 FTIR spectra of adsorbed amino acids in a solid particle matrix at room temperature for: (a) A, illite-histidine; B, illite-glycine; and C, illite-glutamic acid systems; (b) A, montmorillonite-glycine; B, montmorillonite-histidine; C, montmorillonite-glutamic acid; and D, montmorillonite-alanine systems; (c) A, CaCO_3 -glycine; B, $\gamma\text{-AlOOH}$ -glycine; and C, $\gamma\text{-AlOOH}$ -aspartic acid systems, and SiO_2 -glycine system with D, pH 6.59 and E, pH 5.23

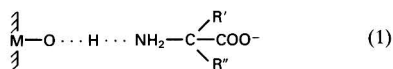
Table 4 Infrared bands of adsorbed amino acids in a solid particle matrix, and the frequency shifts (cm^{-1}) with respect to the corresponding free amino acid

Solid particle	Amino acid	Amount of amino acid adsorbed/ $\mu\text{mol m}^{-2}$	pH	$\nu(\text{NH}_3^+)$	$\Delta\nu(\text{NH}_3^+)$	$\nu(\text{COO}^-)$, as)	$\Delta\nu(\text{COO}^-)$, as)	$\delta(\text{NH}_3^+)$	$\Delta\delta(\text{NH}_3^+)$
Illite	Glycine	1.79	6.26	3178	10	1596	4	1509	-13
	Histidine	0.82	7.64	3148	18	1582	4	1496	-46
	Glutamic acid	0.84	3.22	3098	39	1620	4	1498	-18
Montmorillonite	Glycine	0.93	8.30	3180	12	1596	4	1497	-24
	Histidine	0.59	7.92	3160	30	1581	3	1494	-45
	Glutamic acid	0.52	3.35	3072	13	1620	4	1497	-19
	Alanine	0.58	6.53	3121	35	1596	2	1480	-26
CaCO_3	Glycine	0.33	7.87	3148	16	1596	4		
$\gamma\text{-AlOOH}$	Glycine	0.084	6.60	—	—	1596	4	1487	-35
	Aspartic acid	0.049	2.98	—	—	1619	2	1459	-49
SiO_2	Glycine	0.99	6.59	3180	12	1596	4	1501	-21
	Glycine	1.08	5.23	3164	—	1596	4	1488	-34
				3266*					
				3332*					

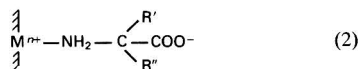
*: $\nu(\text{NH}_2)$.

whereas $\Delta\nu(\text{COO}^-, \text{s})$ and $\Delta\nu(\text{COO}^-, \text{as})$ are also less than 4 cm^{-1} . However, three bands at 3164, 3266 and 3332 cm^{-1} , due to $\nu(\text{NH}_2)$, were detected when the pH (≈ 5.23) is less than pH_{pzc} .

Compared with the resolution of the IR spectrometer the variations of the COO^- stretching modes are meaningless for interpreting the surface species of carboxyl groups in a solid matrix. In contrast, the change of the NH_3^+ stretching and bending modes is sufficiently large to be detected, indicating its great value to elucidation of the interaction mechanism of the AA with the solid matrix. Therefore, it is reasonable to infer that the amino group of an amino acid in a solid matrix, rather than the carboxyl group, reacts with the solid particle. Sokoll and co-workers^{13,30} found that when the N-H bending mode shifts toward lower frequencies, by, e.g., $13\text{--}49 \text{ cm}^{-1}$, as has been observed in this work, the amino acid presumably reacts with the surface hydroxyl groups on a solid particle through its amino group in the following manner:



If this is the mechanism, the N-H bond is reinforced and $\nu(\text{NH}_3^+)$ should shift to higher frequencies. Actually, the increase in $\nu(\text{NH}_3^+)$ by $10\text{--}39 \text{ cm}^{-1}$ (Table 4) further supports the mechanism illustrated in eqn. (1). When $\text{pH} > \text{pH}_{\text{pzc}}$ the mechanism of the interaction between glycine and SiO_2 is the same as the other systems. However, when $\text{pH} < \text{pH}_{\text{pzc}}$ three characteristic (N-H) bands of the metal ion-amino acid complex^{28,31} were observed. It can be inferred that the amino group of an AA in the SiO_2 matrix coordinates with the bare metal ion on the surface of SiO_2 :



Furthermore, for AA- SiO_2 systems (Table 4), the decrease in $\nu(\text{NH}_3^+)$, owing to the formation of the surface complex at $\text{pH} < \text{pH}_{\text{pzc}}$ [eqn. (2)], is 13 cm^{-1} , more than that of the surface species at $\text{pH} > \text{pH}_{\text{pzc}}$ [eqn. (1)]. This is consistent with the finding that the amount of surface hydroxyl groups on SiO_2 is the lowest in the marine solid particles (such as Al, Fe, Mn and Si oxides, clays and CaCO_3) and so its surface hydration level is assumed to be much weaker.²⁵

FTIR Spectra of the Copper(II)-Amino Acid Complex in a Solid Matrix for Amino Acid-Copper(II)-Clay and Oxide Systems

Similarly, owing to the low copper(II)-amino acid complex concentration and the spectral interferences from the solid particle matrix, IR spectra of the copper(II)-amino acid

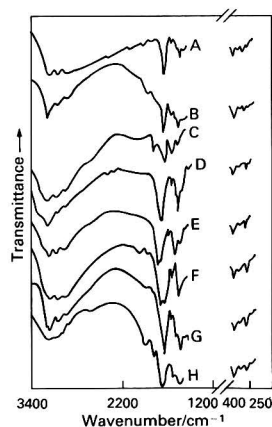


Fig. 5 FTIR spectra of copper(II)-amino acid complexes in a clay matrix at room temperature for the copper(II)-histidine-illite system with an IEA of Cu^{II} of: A, 0.20; and B, $5.56 \mu\text{mol m}^{-2}$; for the copper(II)-histidine-montmorillonite system with an IEA of Cu^{II} of: C, 0; D, 1.07; E, 2.40; F, 6.67; and G, $7.14 \mu\text{mol m}^{-2}$; and for the copper(II)-glycine-montmorillonite system with H, an IEA of Cu^{II} of $5.39 \mu\text{mol m}^{-2}$

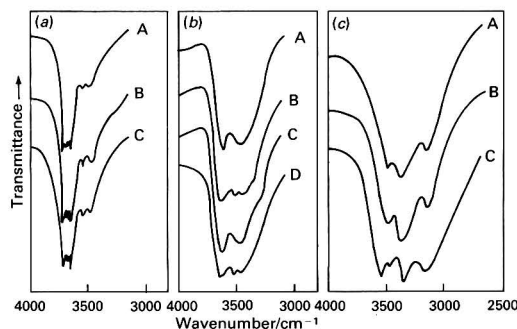


Fig. 6 Change in $\nu(\text{OH})$ of SHHG due to the interaction among copper(II), AAs and marine solid particles at room temperature for: (a) copper(II)-illite-histidine with an IEA of Cu^{II} of: A, $15.0 \mu\text{mol m}^{-2}$; B, copper(II)-illite-glycine with an IEA of Cu^{II} of $16.3 \mu\text{mol m}^{-2}$; and C, $17.4 \mu\text{mol m}^{-2}$; (b) A, copper(II)-montmorillonite-glycine with an IEA of Cu^{II} of $1.57 \mu\text{mol m}^{-2}$; and B, $6.72 \mu\text{mol m}^{-2}$; C, copper(II)-montmorillonite-aspartic acid with an IEA of Cu^{II} of $1.28 \mu\text{mol m}^{-2}$; and D, $6.59 \mu\text{mol m}^{-2}$; (c) Cu^{II} - γ -AlOOH-histidine with: A, an IEA of Cu^{II} of $4.09 \mu\text{mol m}^{-2}$; B, Cu^{II} - γ -AlOOH-aspartic acid with an IEA of Cu^{II} of $3.33 \mu\text{mol m}^{-2}$; and C, $6.79 \mu\text{mol m}^{-2}$

Table 5 Infrared bands of the copper(II)-amino acid complex in a clay matrix for copper(II)-amino acid-clay systems, and the frequency shifts (cm^{-1}) with respect to free amino acid

	Illite-histidine			Montmorillonite-histidine			Montmorillonite-glycine	
pH	4.16	3.58	2.31	4.91	7.04	9.00	3.57	3.06
IEA of $\text{Cu}^{II}/\mu\text{mol m}^{-2}$	0.20	5.56	0	1.07	2.40	6.67	7.14	5.39
Amino acid-copper(II)/ mol mol^{-1}	1.00	1.20	2.54	2.54	12.6	0.06	1.20	11.8
$\nu(\text{NH}_3^+)$	3148	3146	3156	3152	3148	3148	3156	3187
$\Delta\nu(\text{NH}_3^+)$	18	16	27	23	18	18	26	19
$\nu(\text{COO}^-, \text{as})$	1610	1603	1582	1606	1610	1610	1599	1607
$\Delta\nu(\text{COO}^-, \text{as})$	32	25	4	28	32	29	21	15
$\delta(\text{NH}_3^+)$	1501	1504	1501	1504	1497	1497	1504	1483
$\Delta\delta(\text{NH}_3^+)$	-38	-35	-38	-34	-42	-42	-39	-39
$\nu(\text{COO}^-, \text{s})$	1392	1393	1409	1395	1399	1399	1391	1388
$\Delta\nu(\text{COO}^-, \text{s})$	-17	-16	0	-14	-10	-10	-18	-25
$\nu(\text{Cu}-\text{O}, \text{as})$	355	355	—	356	356	356	356	360
$\nu(\text{Cu}-\text{O}, \text{s})$	295	295	—	287	287	287	287	314

Table 6 Stepwise change in $\nu(\text{OH})$ of surface hydroxyl groups due to the interaction among Cu^{II} , amino acid and marine solid particles

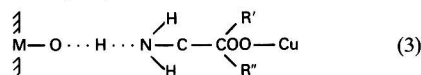
Solid particle	Amino acid	pH	IEA of Cu^{II} / $\mu\text{mol m}^{-2}$	Amino acid- Cu^{II} / mol mol^{-1}	$\nu(\text{OH})^*/\text{cm}^{-1}$		
Illite	Histidine	7.00	15.0	0.06	3441 w	3523 w	—
	Glycine	6.29	16.3	0.06	3441 m	3523 m	—
	Aspartic acid	6.63	17.4	0.06	3441 m	3523 m	—
Montmorillonite	Glycine	8.07	1.57	12.6	3427 s,br	—	—
	Glycine	7.24	6.72	0.06	3427 w	3523 w	—
	Aspartic acid	8.19	1.28	12.6	3427 s,br	—	—
	Aspartic acid	8.02	6.59	0.06	3427 w	3523 w	—
γ -AlOOH	Aspartic acid	2.57	3.33	0.11	3312 m	3427 m	—
	Histidine	4.25	4.09	0.12	3312 w	3427 w	—
	Aspartic acid	3.66	6.79	0.06	3312 m	3427 m	3512 w

* br = Broad, s = strong, m = medium, and w = weak.

surface complex in a solid matrix were obtained by use of the spectral subtraction approach. The resulting spectra are given in Fig. 5 for the amino acid-illite and montmorillonite-copper(II) systems with different IEAs of Cu^{II} , in which bands of $\nu(\text{NH}_3^+)$, $\delta(\text{NH}_3^+)$, $\nu(\text{COO}^-)$, as and $\nu(\text{COO}^-)$, s were assigned and chosen to characterize the interaction among AAs, Cu^{II} and marine solid particles. As shown in Table 5, $\nu(\text{NH}_3^+)$ increases 16–27 cm^{-1} and $\delta(\text{NH}_3^+)$ decreases 34–42 cm^{-1} , while $\nu(\text{COO}^-)$, as increases 15–32 cm^{-1} and $\nu(\text{COO}^-)$, s decreases 10–25 cm^{-1} . However, $\nu(\text{COO}^-)$, as and $\nu(\text{COO}^-)$, s vary less than 4 cm^{-1} as the IEA of Cu^{II} approaches zero, similar to adsorbed amino acids. It can be inferred from Tables 4 and 5 that in the interaction among AAs, clay and Cu^{II} , the amino group of an AA in a solid matrix has the same surface species [eqn. (1)] as the adsorbed AA, which associate with the surface hydroxyl groups on clay, because the variation of $\nu(\text{NH}_3^+)$ and $\delta(\text{NH}_3^+)$ of the copper(II)-amino acid surface complex is sufficiently large to be detected with respect to the resolution of the IR spectrometer. However, unlike the adsorbed AA, the carboxyl group coordinates with Cu^{II} because $\nu(\text{COO}^-)$, as increases 15–32 cm^{-1} and $\nu(\text{COO}^-)$, s decreases 10–25 cm^{-1} , which is greater than the resolution of the spectrometer. If the above mechanism is correct, the Cu–O stretching mode should be detected over the range 250–400 cm^{-1} for the copper(II)-amino acid surface complex.^{3,31,32} Two new bands at 315 and 295 cm^{-1} (Fig. 5) were recognized for the copper(II)-histidine-illite system by comparison with free histidine; the former may be assigned to $\nu(\text{Cu}-\text{O})$, as and the latter to $\nu(\text{Cu}-\text{O})$, s by analogous analysis.^{3,31,32} Similarly, $\nu(\text{Cu}-\text{O})$, as and $\nu(\text{Cu}-\text{O})$, s are 356 and 287 cm^{-1} , respectively, for the histidine-montmorillonite-copper(II) system, and 360 and 314 cm^{-1} , respectively, for the glycine-montmorillonite-copper(II) system. These are all consistent with the values reported previously.^{8,11,12} The change in $\nu(\text{OH})$ of SHHG due to the interaction among amino acids, Cu^{II} and solid particles is shown in Fig. 6. At an IEA of Cu^{II} of 15.0, 16.3 and 17.4 $\mu\text{mol m}^{-2}$, two bands at 3441 cm^{-1} , attributed to the $\nu(\text{OH})$ of SHHG on pure illite, and at 3523 cm^{-1} , were observed for the copper(II)-illite-histidine system. Similarly, at an IEA of Cu^{II} of 1.57 and 1.28 $\mu\text{mol m}^{-2}$, only one band at 3427 cm^{-1} , due to the $\nu(\text{OH})$ of SHHG on pure montmorillonite, was detected,²⁵ while at an IEA of Cu^{II} of 6.59 and 6.72 $\mu\text{mol m}^{-2}$ two bands at 3427 and 3523 cm^{-1} were detected for the glycine-copper(II)-montmorillonite and aspartic acid-copper(II)-montmorillonite systems. When the IEA of Cu^{II} was 3.33 and 4.09 $\mu\text{mol m}^{-2}$ two bands at 3312 cm^{-1} , attributed to the $\nu(\text{OH})$ of SHHG on pure γ -AlOOH,²⁵ and 3427 cm^{-1} were observed, while when the IEA of Cu^{II} increased up to 6.79 $\mu\text{mol m}^{-2}$ three bands at 3312, 3427 and 3512 cm^{-1} were detected for the amino acid-copper(II)- γ -AlOOH system. Consequently, a small change in $\nu(\text{OH})$ of SHHG was observed for copper(II)-amino acid-illite, mont-

morillonite and copper(II)-amino acid- γ -AlOOH systems, analogous to copper(II)-solid particle systems.

The variations of $\nu(\text{NH}_3^+)$, $\delta(\text{NH}_3^+)$, $\nu(\text{COO}^-)$, as and $\nu(\text{COO}^-)$, s and the change in $\nu(\text{OH})$ of SHHG have led to the conclusion that as a 'bridging' reagent the amino acid joins Cu^{II} and the surface hydroxyl group, respectively, through the carboxyl and amino groups:



namely, the Model II of TSC proposed by Leckie and co-workers^{16,18} results from the interaction between AAs, Cu^{II} and clays.

Conclusions

Fourier transform IR spectroscopic studies were carried out in order to characterize the interaction among AAs, Cu^{II} and marine solid particles. The variations of hydroxyl bands show that the ion exchange between Cu^{II} and solid particles and the interaction between AAs, solid particles and Cu^{II} causes a stepwise change in $\nu(\text{OH})$ of SHHG on solid particles with an increase of the IEA of Cu^{II} . However, no change in $\nu(\text{OH})$ of either FSHG on illite, montmorillonite and CaCO_3 or FHG in goethite and γ -AlOOH was observed. This provided the first evidence for the interfacial stepwise ion-exchange theory.

The spectral subtraction approach was used to isolate the main IR bands of adsorbed AAs and copper(II)-amino acid complexes in a solid matrix from the spectra of amino acid-solid particle and amino acid-copper(II)-solid particle systems, respectively. For adsorbed AAs, $\nu(\text{NH}_3^+)$ increases 10–39 cm^{-1} and $\delta(\text{NH}_3^+)$ decreases 13–49 cm^{-1} with respect to free AAs, moderately more than the resolution of the IR spectrometer, whereas variations of $\nu(\text{COO}^-)$, s and $\nu(\text{COO}^-)$, as are less than 4 cm^{-1} , nearly equal to the resolution, indicating that surface hydroxyl groups associate with the amino group of AAs in a solid matrix rather than the carboxyl group. For the copper(II)-amino acid surface complex, $\nu(\text{NH}_3^+)$ increases 10–27 cm^{-1} and $\delta(\text{NH}_3^+)$ decreases 34–42 cm^{-1} , analogous to the adsorbed AA, while $\nu(\text{COO}^-)$, as increases 15–32 cm^{-1} and $\nu(\text{COO}^-)$, s decreases 10–25 cm^{-1} , which are moderately more than the resolution of the IR spectrometer, and bands at 287 to 360 cm^{-1} , due to $\nu(\text{Cu}-\text{O})$, s and $\nu(\text{Cu}-\text{O})$, as, appear. This reveals that as a 'bridging' reagent AAs in a clay matrix join the Cu^{II} and surface hydroxyl group, respectively, through its carboxyl and amino groups.

The author thanks Professor Zhang Zhengbin (Department of Chemistry, Ocean University of Qingdao, China) for helpful suggestions and encouragement, and Associate Professor Xia

Zongfong (of the same address) for assistance with the spectroscopic work.

References

- 1 Huang, J., and Zhang, S., *Haiyang Xeubao*, 1983, **5**, 604.
- 2 Liu, B., *Haiyang Huzhao*, 1981, **2**, 20.
- 3 Zhang, Z., *Estuarine-Marine Chemistry of Huanghe Estuary*, Springer-Verlag, Berlin, 1991, ch. 2.
- 4 Daland, F., Buffle, J., and HaerdI, W., *Environ. Sci. Technol.*, 1984, **18**, 135.
- 5 Wang, X., Zhang, Z., and Liu, L., *Chin. J. Oceanol. Limnol.*, 1988, **6**, 258.
- 6 Zhang, Z., and Liu, L., *Theory of Interfacial Stepwise Ion/Coordination Particle Exchange and Its Application*, Ocean Press, Beijing, 1985, pt. I.
- 7 Zhang, Z., and Liu, L., *Haiyang Yu Huzhao*, 1978, **9**, 51.
- 8 Riley, J. P., and Skirrow, G., *Chemical Oceanography*, Academic Press, London, 1972, vol. 1, ch. 3.
- 9 Zhang, Z., Wang, X., Liu, L., and Liu, X., *Haiyang Yu Huzhao*, 1989, **20**, 34.
- 10 Buckland, A. D., Rochester, C. H., and Topham, S. A., *J. Chem. Soc., Faraday Trans. I*, 1980, **76**, 302.
- 11 Ishikawa, T., Nitta, S., and Konda, S., *J. Chem. Soc., Faraday Trans. I*, 1986, **82**, 2401.
- 12 Lewis, D. G., and Farmer, V. C., *Clay Miner.*, 1986, **21**, 93.
- 13 Marx, U., Sokoll, R., and Hobert, H., *J. Chem. Soc., Faraday Trans. I*, 1986, **82**, 2505.
- 14 Rochester, C. H., and Topham, S. A., *J. Chem. Soc., Faraday Trans. I*, 1979, **75**, 1259.
- 15 Bourg, A. C. M., and Schindler, P. W., *Chimica*, 1978, **32**, 166.
- 16 Davis, J. A., and Leckie, J. O., *Environ. Sci. Technol.*, 1978, **12**, 1309.
- 17 Pleysier, J., and Cremers, A., *J. Chem. Soc., Faraday Trans. I*, 1975, **71**, 256.
- 18 Benjamin, M. M., and Leckie, J. O., *Environ. Sci. Technol.*, 1981, **15**, 1050.
- 19 Bowers, A. R., and Huang, C. P., *J. Colloid Interface Sci.*, 1985, **105**, 197.
- 20 Bowers, A. R., and Huang, C. P., *J. Colloid Interface Sci.*, 1986, **110**, 575.
- 21 Moreals, P. C., Broersm, C., and Badot, C., *Clay Miner.*, 1979, **14**, 307.
- 22 Anderson, M. A., and Rubin, A. J., *Adsorption of Inorganics at Solid/Liquid Interface*, Ann Arbor Science Publishers, Ann Arbor, MI, 1981, pp. 183-217.
- 23 Cambier, P., *Clay Miner.*, 1966, **21**, 191.
- 24 Inskeep, W. P., and Baham, J., *Soil Sci. Soc. Am. J.*, 1983, **47**, 1109.
- 25 Wang, X., Ph.D. Thesis, Ocean University of Qingdao, China, 1989.
- 26 Bellamy, L. J., *The Infrared Spectra of Complex Molecules*, Chapman and Hall, London, 2nd edn., 1980, ch. 4.
- 27 Heiling, A. W., and Long, T. V., *J. Am. Chem. Soc.*, 1970, **92**, 6474.
- 28 Larsson, L., *Acta Chem. Scand.*, 1950, **4**, 27.
- 29 Parker, P. S., and Kirschenbaum, D. M., *Spectrochim. Acta*, 1960, **16**, 910.
- 30 Sokoll, R., and Hobert, H., *J. Chem. Soc., Faraday Trans. I*, 1986, **82**, 1527.
- 31 Misra, B. H., and Kripal, R. K., *Indian J. Pure Appl. Phys.*, 1987, **22**, 430.
- 32 Condrate, R. A., and Nakamoto, K., *J. Chem. Phys.*, 1964, **20**, 2590.

Paper 1/01301G

Received March 18, 1991

Accepted September 17, 1991

Rapid Indirect Method for Determining the Sodium Content of Table Olives

Pedro García, Manuel Brenes and Antonio Garrido*

Instituto de la Grasa y sus Derivados (CSIC), Apartado 1078, 41012 Seville, Spain

Methods for the determination of sodium in olives were studied. Direct measurement by photometric and ion-selective electrode methods did not show systematic errors, with the latter being more precise and easier to apply. The correlation ($p \leq 0.001$) between NaCl concentration in the surrounding brine (calculated using the official Volhard procedure) and Na⁺ content in the olive flesh (determined using an ion-selective electrode, the most practical of the two methods tested) was of particular interest and permitted the determination of the latter from determinations of the former. This indirect measurement enables producers to determine the sodium content in packed olives non-destructively using an established method. It also avoids the problems of obtaining representative samples and the tedium of sample preparation.

Keywords: Sodium determination; ion-selective electrode; flame photometer; table olives

The sodium content in foods is receiving increasing attention because a high sodium intake has been linked with hypertension in certain sensitive individuals.^{1,2} This trend will continue in the future as consumers are becoming more conscious of the close relationship between health and diet. There is concern in some food industries which use salt or fermentation in brine as traditional conservation procedures, where the sodium concentrations in the final products are generally still too high.

Green table olives, Sevillian or Spanish style, are one of these items and the equilibrium percentages of salt in the brines offered to consumers range from 4.0 to 6.0% m/v. In flesh, the corresponding proportion is about 1.2–2.0 g of Na⁺ per 100 g of flesh.^{3,4}

Other types of olive also contain high levels of salt, e.g., natural black olives in brine (about 8% m/v in brine) and natural olives in solid salt (about 10–14% m/v), but their volume in the international market is low. In contrast, the brine of ripe olives (darkened by alkaline oxidation) contains only a low amount of salt (about 2% m/v), which means that the proportion in the flesh could reach 0.4–0.8% m/v, a considerably lower level.⁵ Hence although all table olive products must be carefully monitored for sodium content, green table olives in brine are of most concern.

The Spanish table olive industry is trying to adapt its production methods to this situation and to improve the image of the different packed commercial presentations (plain olives; pitted olives; olives stuffed with pimento, anchovies, almonds, etc.) by the introduction of new packaging technology, a stricter inspection of sodium chloride content and the development of new products with lower sodium contents. Hence simple, rapid, inexpensive and accurate analytical procedures are needed for routine measurements of salt concentrations during the successive phases of production, and control of the sodium level in the packaged olives.

Two procedures, based on the flame photometric determination of sodium and on the determination of sodium or chloride using ion-selective electrodes, have previously been applied successfully to the evaluation of the salt content in table olive brines. Comparison with the Volhard method, the official method prescribed by the International Olive Oil Council, showed that neither of them had constant or proportional systematic errors. Both had the same precision as the reference procedure.⁶ However, when the salt concentration in green table olive brines was determined either by flame photometry or with a sodium ion-selective electrode, a

positive displacement with respect to the Volhard value was observed, owing to an excess of Na⁺ ions with respect to Cl⁻. This additional sodium comes from the preliminary treatment with sodium hydroxide solution^{7,8} to eliminate oleuropein, a polyphenol responsible for the bitter taste of olives, and which also has a certain bactericidal effect that sometimes interferes with the normal lactic fermentative process. Obviously, the deviations observed are caused by the determination of the different ions which form salt, i.e., Na⁺ with photometric and sodium ion-selective methods and Cl⁻ with the chloride ion-selective and Volhard procedures, which in these products are not present in the proportions corresponding to the formula NaCl.

As the determination of salt in olive flesh (the part of the product actually eaten by the consumer) has received little attention until now, investigation of suitable methods would be of interest. Direct analysis by some of the procedures used for brines, including the recently introduced flame photometric and ion-selective electrode methods, is one option. However, another is the use of an indirect measurement that takes advantage of the possible correlation between the sodium content in the flesh and in the surrounding brine. This relationship is very useful as it would provide producers with a non-destructive method that avoids both the problems of obtaining representative samples and the tedium of sample preparation, and would be particularly applicable to packed olives.

The aim of this work was to study and compare the behaviour of flame photometric and sodium ion-selective electrode methods for the determination of sodium in olive flesh. Emphasis is given to the investigation of the correlation between sodium content in the flesh of the final packed product, determined with a sodium ion-selective electrode (the most practical of the two tested procedures) and the salt concentration in the brine determined by the Volhard method, currently used routinely in the industry for fermentation and packing control.

Experimental

Flame Photometry

Apparatus

A Meteor Model NAK-1 flame photometer with a scale reading from 0 to 200 mequiv dm⁻³ (PACISA, Madrid, Spain), an LIC Instruments Model 346 automatic diluter (PACISA), an electric heater plate and an electric oven were used.

* To whom correspondence should be addressed.

Reagents

A standard solution containing 100 mequiv dm^{-3} of sodium (Meteor, Cat. No. 91834; PACISA), a 25% m/v solution of magnesium nitrate [$\text{Mg}(\text{NO}_3)_2 \cdot 6\text{H}_2\text{O}$] in 96% v/v ethanol and 6 mol dm^{-3} hydrochloric acid were used.

Sample preparation

This operation was similar to that described previously for the determination of iron in olives.⁹ A 100 g amount of size-calibrated pitted olives from homogeneous fruits commercially packed (250 g glass containers) was mixed with 100 ml of distilled water and homogenized with a blender. A 4 g amount of the mixture (equivalent to 2 g of fresh) was placed in a quartz capsule containing 0.2 ml of the magnesium nitrate solution. The capsule was heated to 350 °C on an electric heater plate. After 2 h at 350 °C, the capsule was placed in an electric oven and the temperature was first raised rapidly to 250 °C and then slowly to 550 °C, at which it was maintained for 8–10 h.

The greyish white ash was dissolved in three portions of 2 ml of 6 mequiv dm^{-3} HCl, filtering each time through filter-paper of known ash content, using a suction bell. The solubilization of the ash was improved by gentle heating of the capsule after each addition. Finally, the three portions were combined and the volume was made up to 50 ml by addition of distilled, de-ionized water.

Determination

Samples (0.3 ml) were diluted automatically to 10 ml with distilled, de-ionized water and the solution was introduced into the flame photometer.

The apparatus was calibrated to express Na^+ concentration in milligrams per gram of flesh by adjusting the 100 mequiv dm^{-3} solution reading to 57. If the sodium content in flesh was less than 10 mg g^{-1} , the standard sodium solution used was 10 mequiv dm^{-3} . The reading was also adjusted to 57 and the sodium concentration was deduced by dividing the scale readings by 10.

Ion-selective Electrode

Apparatus

An Orion Model 501 specific ion meter with a sodium ion-selective electrode (ref. No. 97–11) and a double-junction reference electrode (ref. No. 90–02), a magnetic stirrer, a 0.001 g precision balance and a mixer were used.

Reagents

In order to prepare an ionic strength adjuster (ISA), analytical-reagent grade NH_4Cl (20 g) was dissolved in about 50 ml of distilled water in a 100 ml calibrated flask, 27 ml of concentrated ammonia solution were added and the mixture was diluted to volume with distilled water.

Standard solutions containing 100, 200, 500 and 1000 ppm of NaCl and with 2 ml of ISA per 100 ml were prepared.

The reference electrode filling solutions were Orion ref. No. 90-00-02 (inner chamber) and 0.1 mol dm^{-3} NH_4Cl (outer chamber).

Electrode storage solution was prepared by adding 2 ml of ISA per 100 ml of 5 mol dm^{-3} NaCl solution. Electrode rinse solution was obtained by diluting 20 ml of ISA to volume in a 1 dm^3 calibrated flask with distilled water.

Sample preparation

The flesh and distilled water were mixed as described previously, then 5 g of the paste were mixed with 195 ml of distilled, de-ionized water and 4 ml of ISA. The mixture was homogenized for 5 min in a magnetic stirrer and assayed immediately.

Determination

Calibration was achieved by verifying the electrode slope with standard solutions. Concentrations in samples were calculated on the basis of a reading of 1000 ppm corresponding, according to the mass of sample and dilutions mentioned, to 31.45 mg g^{-1} of Na^+ per gram of flesh.

For correct working, the electrodes must be rinsed with the electrode rinse solution after each reading and recalibration should be carried out every 2 h.

The Volhard method was applied according to Fernández Díez *et al.*¹⁰

Design of Experiments

The proportional systematic errors of both procedures when used for the determination of sodium in olive flesh were investigated using standard additions experiments. If the confidence interval of the adjusted straight line includes unity it demonstrates the lack of such errors.¹¹

Precision comparisons were made by triplicate analyses of the sodium content in the flesh of green Spanish-style olives and ripe olives (by alkaline oxidation). Standard deviations were calculated from these data and the precisions of the two methods were compared by calculation of the corresponding experimental *F* values and their probabilities.¹¹

Correlation between the sodium contents in flesh and brine was achieved by determination of Na^+ in olives using the ion-selective electrode method, and determining its concentration by the determination of chloride in brine according to the Volhard procedure. In all instances, samples were analysed after 15 d to allow equilibrium of Na^+ between the flesh and the brine to be reached.

Results and Discussion

As mentioned previously, neither procedure showed systematic constant or proportional errors when applied to table olive brines.⁸ In order to investigate the presence of systematic proportional errors if the two assay methods are used to determine sodium in olive flesh, increasing amounts of Na^+ were added to the olive flesh (standard additions experiments). Table 1 shows the average values of the concentration of sodium (*x*) added.

The regression and confidence limits for the slope (*b*) showed they included 1.00 in both instances, thus confirming the absence of systematic proportional errors in the determination of sodium in olive flesh by either the flame photometric or ion-selective electrode method. These results allow the use of either method with this new matrix, and also with the fermentation brine, as has already been demonstrated.⁸

Table 1 Sodium content in olive flesh with different amounts of added Na^+ (*x*) by flame photometric and ion-selective electrode methods

Sodium added/ $\text{mg per 100 g of flesh}$	Na^+ found/ mg g^{-1}	
	Flame photometry	Ion-selective electrode
0	11.66	10.23
3.93	16.00	14.16
7.86	20.00	18.13
15.72	26.33	25.96
23.59	35.33	33.86
Regression parameters		
($y = a + bx$)	$b = 0.9816$	$b = 0.9977$
Confidence limits		
($p \leq 0.05$)	$1.0276 < b < 0.9356$	$1.0022 < b < 0.9931$
* Average of three replicates.		

Table 2 Sodium contents (mg of Na⁺ per gram of flesh) in the flesh of green and ripe olives in brine determined by flame photometric and ion-selective electrode methods. Comparison of the respective precisions

Green olives				Ripe olives			
Flame photometry		Ion-selective electrode		Flame photometry		Ion-selective electrode	
$\bar{x}(1)$	$s \times 10^{-2}$	$\bar{x}(1)$	$s \times 10^{-2}$	$\bar{x}(1)$	$s \times 10^{-2}$	$\bar{x}(1)$	$s \times 10^{-2}$
3.70	10.0	3.75	3.8	8.53	5.7	8.58	7.7
3.21	0	3.36	5.3	7.93	5.7	8.02	4.1
2.60	10.0	2.65	9.2	8.30	10.0	8.24	2.6
2.72	11.0	2.64	0.6	7.33	5.7	7.24	1.7
2.39	0	2.50	0	7.90	10.0	7.94	3.4
2.83	5.7	2.86	4.0	7.56	11.5	7.55	5.3
3.28	10.4	3.29	3.2				
4.16	5.7	4.18	7.6				
Estimated standard errors		$s_1 = 7.86 \times 10^{-2}$ $s_2 = 5.14 \times 10^{-2}$		$s_3 = 8.48 \times 10^{-2}$ $s_4 = 4.59 \times 10^{-2}$			
Variance comparison		$F^* = s_1^2/s_2^2 = 2.34$		$F^{**} = s_3^2/s_4^2 = 3.49$			
One-sided critical values for the F -test		$F(16, 16; 0.05) = 2.33$ $F(16, 16; 0.01) = 3.37$		$F(12, 12; 0.05) = 2.69$ $F(12, 12; 0.01) = 4.16$			

(1) Results are the average of three replicates.

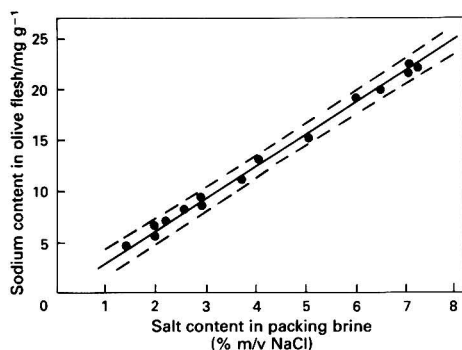
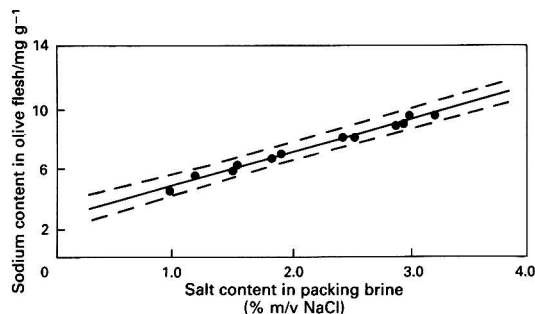
**Fig. 1** Relationship between sodium content in the packing brines (% m/v NaCl) and in the flesh of the corresponding olives (mg of Na⁺ per gram of flesh), and the confidence interval of the regression line for one future determination. Green table olives stuffed with pimento. Regression line equation: $y = -0.13 + 3.17x$ **Fig. 2** Relationship between sodium content in the packing brines (% m/v NaCl) and in the flesh of the corresponding olives (mg of Na⁺ per gram of flesh), and the confidence interval of the regression line for one future determination. Ripe olives. Regression line equation: $y = 2.85 + 2.14x$

Table 2 shows the percentages of sodium in the flesh of green Spanish-style olives and ripe olives and their standard deviations, using both methods. Comparison by F test of the combined variance for each method shows a tendency that was significant at the $p \leq 0.05$ level for the ion-selective electrode, indicating that the results were more precise than the flame photometric results. This fact, together with the simpler procedure, requiring considerably less manipulation and labour, makes the ion-selective electrode method the method of choice. However, flame photometry could also give a sufficient precision for most requirements.

In order to investigate the correlation between the sodium content in brine and in the flesh of the packaged final product, the concentrations of sodium in each medium were determined by the Volhard and ion-selective electrode procedures, respectively. Different types of table olives with a wide range of salt concentrations were examined, although results are given only for pimento-stuffed green olives in 0.3 kg jars, and ripe olives in 0.5 kg cans.

Variance analysis of the corresponding regression demonstrated a significant correlation ($p \leq 0.001$) between both procedures. The adjusted straight lines ($r = 0.998$ and 0.988 , respectively) and their confidence limits for one future

analysis are shown in Figs. 1 and 2. According to the statistical inferences of the confidence intervals, the sodium content in flesh could be determined with a precision of 1 mg of Na⁺ per gram of flesh for stuffed green olives and 0.5 mg of Na⁺ per gram of flesh for ripe olives.

Hence, in spite of the sodium and chloride imbalance in most table olive products, the existence of a good correlation between sodium content in the flesh and chloride in the brine (determined by the Volhard method) permits this to be a useful routine method for sodium monitoring during the production and inspection of the final product for the consumer. Nonetheless, the laboratory must prepare or be provided with adequate correlation graphs or equations for the main variables involved, viz., combined acidity, proportion of juice in olives and fruit-to-brine ratio.

This work was supported by the Spanish Government through the Comisión Interministerial de Ciencia y Tecnología (CICYT) under project Ali-88-0115-CO2-01.

References

- 1 *The Food Labelling Regulations 1984*, SI 1984 No. 1305, HM Stationery Office, London, 1984.
- 2 *Prevention of Coronary Heart Disease*, WHO Technical Report Series, No. 678, World Health Organization, Geneva, 1982.

- 3 Castro Ramos, R., Nosti Vega, M., and Vazquez Ladrón, R., *Alimentaria*, 1980, **115**, 21.
- 4 Nosti Vega, M., Castro Ramos, R., and Vazquez Ladrón, R., *Grasas Aceites*, 1982, **33**, 5.
- 5 Nosti Vega, M., and Castro Ramos, R., *Grasas Aceites*, 1985, **36**, 203.
- 6 *Official, Standardized and Recommended Methods of Analysis*, Society for Analytical Chemistry, London, 1973, pp. 350–351.
- 7 Garrido Fernández, A., and García García, P., *Grasas Aceites*, 1985, **36**, 134.
- 8 García García, P., Brenes Balbuena, M., and Garrido Fernández, A., *Grasas Aceites*, in the press.
- 9 Garrido Fernández, A., Albi Romero, M. A., and Fernández Díez, M. J., *Grasas Aceites*, 1973, **24**, 287.
- 10 Fernández Díez, M. J., Castro Ramos, R., Garrido Fernández, A., González Cancho, F., González Pellissó, F., Nosti Vega, M., Heredia Moreno, A., Mínguez Mosquera, M. I., Sánchez Roldán, F., and Castro Gómez-Millán, A., *Biotecnología de la Aceituna de Mesa*, CSIC, Instituto de la Grasa, Madrid, 1985, p. 414.
- 11 Massart, D. L., Dijkstra, A., and Kaufman, L., *Evaluation and Optimization of Laboratory Methods and Analytical Procedures*, Elsevier, Amsterdam, 1978, p. 39.

Paper 1/024801

Received May 28, 1991

Accepted October 11, 1991

Ion-selective Electrode With Fixed Quaternary Phosphonium Ion-sensing Species

Marie-Josée Rocheleau* and William C. Purdy†

Department of Chemistry, McGill University, Montréal, Québec, Canada H3A 2K6

The response properties and selectivity of polymer membrane electrodes with fixed quaternary phosphonium ion-sensing groups for nitrate are described. A poly(trioctylvinylbenzylphosphonium nitrate) (PTOVBPNO₃) membrane electrode demonstrated a selective response to nitrate in the concentration range 5×10^{-5} – 0.1 mol dm^{-3} , with a slope of $-53.4 \pm 0.5 \text{ mV decade}^{-1}$. The selectivity of this electrode for nitrate ions can be favourably compared to conventional nitrate ion-selective electrodes based on quaternary ammonium ion-exchange sites. Notably, a significant improvement of selectivity for nitrate by two orders of magnitude was obtained in the presence of perchlorate. The PTOVBPNO₃ membrane electrode was used for the determination of nitrate in samples of commercially available fertilizers.

Keywords: *Ion-selective electrode; ionic polymer membrane; fixed ion-sensing species; quaternary phosphonium groups; nitrate determination*

Nitrogen is an essential constituent of natural ecosystems. However, an undesirable level of nitrate in natural waters as a result of man's activities is a serious source of pollution. The extensive use of artificial fertilizers in agriculture has been implicated as a major cause of the increasing concentration of nitrate in natural waters and as an important factor in the growing problem of eutrophication of lakes. This high consumption of artificial fertilizers has stimulated the development of efficient, inexpensive analytical methods for the determination of nitrate.

The use of an ion-selective electrode is the method of choice for measurements of nitrate. This is mainly attributable to the rapidity of the sample preparation and to the simplicity of the potentiometric measurements. Conventional nitrate ion-selective electrodes are based on quaternary ammonium salts entangled in a polymeric matrix.¹ In order to improve the lifetime and robustness of these polymeric ion-selective electrodes, membranes prepared by covalent attachment of the ion-sensing groups to a polymer matrix have been reported.^{2,3} These polymers with fixed ion-sensing groups are commonly referred to as ionic polymers.⁴ The covalent attachment of the ion-sensing species prevents the deterioration of the membrane through the leaching of the ion-sensing groups. Furthermore, membranes with covalently bound ion-sensing species display interesting features such as an enhanced adherence to solid substrates.³ This feature is particularly attractive for the future integration of ionic polymer membranes with semiconductor devices. So far, problems of compatibility between polymeric ion-sensitive membranes and the electronic component have seriously limited the expansion and application of ion-sensitive field effect transistors.⁵

Unfortunately, membranes prepared from covalent attachment of quaternary ammonium groups to a polymeric matrix have demonstrated rather poor selectivity for nitrate ions. Several inorganic anions such as hydroxide and chloride seriously interfere with the measurement of nitrate.² This paper reports the application of quaternary phosphonium functionalized polymer membrane electrodes to the measurement of nitrate. The response properties and selectivity of poly(trioctylvinylbenzylphosphonium nitrate) (PTOVBPNO₃), and poly(triphenylvinylbenzylphosphonium nitrate) (PTPVBPN₃), were investigated.

Experimental

Preparation of Polymeric Membranes

Polymeric membranes were prepared by direct functionalization of poly(vinylbenzyl chloride) (PVBC) with quaternary phosphonium groups. Poly(vinylbenzyl chloride) and triphenylphosphine were obtained from Aldrich (Milwaukee, WI, USA), while trioctylphosphine was obtained from Alfa (Ward Hill, MA, USA). The choice of phosphines was guided by the fact that phosphines with short hydrocarbon chains are pyrophoric. Triphenylphosphine and trioctylphosphine are both stable in air.

In the first reaction scheme, 1.5 g of PVBC were dissolved in 30 ml of a 25% v/v solution of trioctylphosphine in chloroform. The solution was then heated to reflux, to about 70–80 °C. In the second reaction scheme, 1.5 g of PVBC were suspended in 30 ml of a 0.4 mol dm⁻³ solution of triphenylphosphine in methanol. This solution was also heated to reflux. In this instance, the end-point of the reaction was indicated by the dissolution of PVBC, as poly(triphenylvinylbenzylphosphonium chloride) (PTPVBPCl) is soluble in methanol while PVBC is not. Phosphines are characterized by their high nucleophilic reactivity with alkyl halides to produce phosphonium salts. A reflux time of 5–6 h was usually required for completion of the reaction. A quantitative elemental analysis performed on the modified polymers indicated a yield of immobilization of the quaternary phosphonium groups of >80% (mole:mole quaternary phosphonium: benzyl chloride units) in both instances. These analyses were performed by Guelph Chemical Laboratories (Guelph, Ontario, Canada). After quaternization of PVBC with the phosphine, the modified polymers were precipitated and filtered off. The products obtained were redissolved and purified by two successive precipitation steps.

Functionalized PVBC membranes about 100 µm thick were cast on a carbon-support electrode. The construction of the carbon-support electrode has been described previously.⁶ Membranes can be cast easily at room temperature from a solution of the polymer dissolved in a volatile organic solvent. Prior to coating the carbon-support electrode with the polymeric membrane, the counter ions of the bound quaternary phosphonium groups were exchanged for nitrate through a liquid-liquid extraction procedure. Chloroform was used to cast PTOVBPNO₃ membranes, while methanol was used to cast membranes of PTPVBPN₃.

Calibration

The potentiometric measurements were made with a Fisher Accumet Model 805MP pH/ion meter (Fisher Scientific,

* Present address: Department of Chemistry, University of Alberta, Edmonton, Alberta, Canada T6G 2G2.

† To whom correspondence should be addressed.

Montreal, Canada). A Servogor 120 recorder [BBC Goerz Metrawatt (Fisher Scientific)] was used to monitor potential drifts. All potential measurements were made with reference to a saturated calomel electrode (SCE). The temperature of the analyte solutions was maintained at 25 °C with a Heto Type 623 thermostatic bath (Heto Lab. Equipment, Birkerød, Denmark). The membrane electrodes were stored dry and were pre-conditioned in 0.1 mol dm⁻³ potassium nitrate for 30 min prior to reuse.

Results and Discussion

The response of the PTOVBPNO₃ membrane electrode is illustrated in Fig. 1. The linear response of the PTOVBPNO₃ membrane electrode extended from 5×10^{-5} to 0.1 mol dm⁻³ NO₃⁻ with a slope of -53.4 ± 0.5 mV decade⁻¹. Note that each calibration point of Fig. 1 represents the average of three potential readings. The standard solutions were buffered with 0.1 mol dm⁻³ phosphate at pH 7.0. Phosphate ions had no observable effect on the response of the PTOVBPNO₃ membrane electrode. The influence of pH on the potential of this electrode was also investigated. No variation of the electrode potential was measured in the pH range 4–10. Above pH 10, the presence of hydroxide ions interferes with nitrate measurements.

This PTOVBPNO₃ membrane electrode demonstrated an enhanced sensitivity to nitrate ions compared with a membrane electrode prepared from poly(trihexylvinylbenzylammonium nitrate), PTHVBANO₃ (see Fig. 1). Furthermore, the detection limit of the PTOVBPNO₃ membrane electrode for nitrate is significantly improved. The construction and the use of the PTHVBANO₃ membrane electrode are both described in ref. 3. The PTOVBPNO₃ membrane electrode showed a fast response and rapid recovery; the response time is typically <30 s. This membrane electrode continued to function well for several months. Very little deterioration of the membrane response was observed after more than 10 months of use. Comparatively, a typical lifetime of 2–3 months has been reported for a coated-wire electrode based on Aliquat 336S.⁷

The selectivity coefficients for the PTOVBPNO₃ and PTHVBANO₃ membrane electrodes were measured by the fixed interference method; the concentration of interfering anions was fixed at 1 mmol dm⁻³, while the concentration of nitrate was varied from 1×10^{-5} to 0.1 mol dm⁻³. The selectivity coefficients for both electrodes are presented in

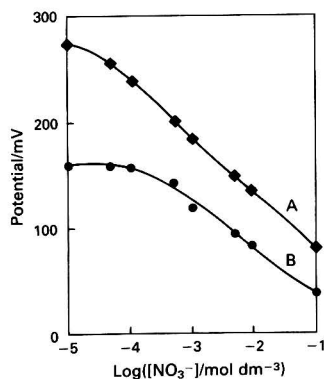


Fig. 1 Potentiometric response of the PTOVBPNO₃ and PTHVBANO₃ membrane electrodes: A, PTOVBPNO₃ membrane (slope = -53.4 ± 0.5 mV decade⁻¹, linear response range = 5×10^{-5} –0.1 mol dm⁻³) and B, PTHVBANO₃ membrane; (slope = -43.2 ± 0.6 mV decade⁻¹, linear response range = 1×10^{-3} –0.1 mol dm⁻³)

Table 1. The PTOVBPNO₃ membrane electrode clearly exhibits an enhanced selectivity for nitrate ions compared with the PTHVBANO₃ membrane in the presence of nitrite ions. The selectivity coefficients of both electrodes in the presence of other anions are comparable.

The performance of this PTOVBPNO₃ membrane electrode and another nitrate ion-selective electrode with covalently bound sites reported by Ebdon *et al.*² were also compared. The latter was prepared from a poly(styrene-*b*-butadiene-*b*-styrene) matrix cross-linked with allyl substituted quaternary ammonium salts (SBS-QAS membrane). This SBS-QAS membrane displayed near-Nernstian response, but poor selectivity for nitrate in the presence of common interfering ions. For example, chloride interferes seriously with the response of the SBS-QAS membrane electrode, $k_{\text{NO}_3^-, \text{Cl}^-} = 0.16$, while the response of the PTOVBPNO₃ membrane is less seriously affected by the presence of chloride, $k_{\text{NO}_3^-, \text{Cl}^-} = 0.008$.

The response properties and the selectivity of the PTOVBPNO₃ membrane can also be favourably compared to conventional nitrate ion-selective electrodes based either on quaternary ammonium¹ or phosphonium^{8,9} ion-sensing species. Perchlorate constitutes one of the most serious interferents of commercially available nitrate ion-selective electrodes based on quaternary ammonium ion-sensing species, typically $k_{\text{NO}_3^-, \text{ClO}_4^-} = 1000$ for a Corning No. 476134 ion-selective electrode (Corning, NY, USA).¹ A significant improvement of selectivity for nitrate in the presence of perchlorate was obtained with the PTOVBPNO₃ membrane electrode, $k_{\text{NO}_3^-, \text{ClO}_4^-} = 10$. This represents an improvement by two orders of magnitude. While the behaviour of a poly(trihexylvinylbenzylammonium chloride) (PTHVBAC) membrane electrode can be related to the lyotropic interactions (Hofmeister series) of the analyte ion with the ion-sensing species and can be described by simple thermodynamics,³ it is not clearly understood why this PTOVBPNO₃ membrane electrode provides such a selective response for nitrate in the presence of perchlorate ions. Unfortunately, very little information is available concerning the selectivity for nitrate of liquid membrane electrodes using phosphonium ion-sensing species. Therefore, their selectivity for nitrate in the presence of interfering ions cannot be compared with the selectivity demonstrated by the PTOVBPNO₃ membrane electrode.

Despite the affinity of quaternary phosphonium sites for nitrate ions, a PTPVBPNO₃ membrane electrode did not demonstrate any sensitivity to nitrate ions. Furthermore, this membrane electrode did not demonstrate any response to other anions such as thiocyanate and salicylate. Not only is selectivity involved in the membrane response mechanism but so is the mobility of the counter ion species within the membrane phase. In conventional polymeric ion-selective membranes, the strong association of an ion-exchange group and a counter ion species results in the formation of a neutral

Table 1 Selectivity coefficients for nitrate ion-selective membrane electrodes with fixed ion-sensing sites

Interfering anion	$k_{i,j}^{\text{pot}}$	
	PTOVBPNO ₃	PTHVBANO ₃
Phosphate	$0.00010 \pm 1 \times 10^{-5}$	$0.00051 \pm 2 \times 10^{-5}$
Acetate	$0.00051 \pm 3 \times 10^{-5}$	$0.00079 \pm 1 \times 10^{-5}$
Sulfate	$0.00320 \pm 1 \times 10^{-5}$	$0.0051 \pm 1 \times 10^{-4}$
Chloride	$0.0081 \pm 1 \times 10^{-4}$	$0.0089 \pm 1 \times 10^{-4}$
Nitrite	0.052 ± 0.001	0.251 ± 0.001
Bromide	0.252 ± 0.003	0.316 ± 0.001
Iodide	3.17 ± 0.07	0.79 ± 0.01
Perchlorate	10 ± 1	15.8 ± 0.8

Table 2 Potentiometric determination of nitrate in commercial fertilizers

Sample	NO ₃ -N (%)	
	Claimed	Found*
RaPidGro evergreen	2.9	2.7 ± 0.1
Jobe's sunsplash	0.4	0.44 ± 0.02

* Average of three measurements ± standard deviation.

pair which is still mobile within the membrane phase because of the presence of a solvent/plasticizer.¹⁰ On the other hand, the more strongly an ion is preferred by the fixed ion-exchange sites in an ionic polymer membrane, the more poorly it moves within the membrane. There are, therefore, opposing effects between affinities and mobilities of ions in ionic polymer membranes, and the strong association of the sensing species with analyte ions constitutes the principal limitation of this membrane system. The lack of sensitivity demonstrated by the PTPVBPN₃ membrane electrodes may also be related to the poor physical properties of the membrane. Membranes prepared from PTPVBPC were found to be porous, hard and brittle.

Determination of Nitrate in Fertilizers

The PTOVBPN₃ membrane electrode was applied to the determination of nitrate-nitrogen in two samples of fertilizers. These fertilizers were obtained from local stores. The RaPidGro evergreen fertilizer (RAPIDGRO, Danville, NY, USA) is a granule concentrate, while the Jobe's sunsplash fertilizer (International Spike, Lexington, KT, USA) is a dilute aqueous preparation. Both contain all three of the main plant nutrients, *i.e.*, nitrogen, phosphate and potassium. They also contain micronutrients such as boron, copper, iron, manganese and zinc.

A 5 g sample of the RaPidGro evergreen fertilizer was finely ground and dried in an oven for 2 h at 100 °C. At this temperature, no degradation of the sample occurs. Three portions of about 0.1 g of the dry sample were then dissolved in 50 ml of 0.1 mol dm⁻³ phosphate buffer, pH 7.0. Three aliquots of the Jobe's sunsplash fertilizer were used without dilution.

An interference suppressor composed of 0.01 mol dm⁻³ aluminium sulfate, 0.01 mol dm⁻³ silver sulfate, 0.02 mol dm⁻³ boric acid and 0.01 mol dm⁻³ sulfamic acid, and adjusted to pH 3.0 with 0.1 mol dm⁻³ sulfuric acid was used. This solution effectively reduces the interfering effect of many common inorganic ions. Chloride ions are quantitatively precipitated as silver chloride. Trace amounts of bromide, cyanide, sulfide and phosphate are also removed by precipita-

tion with Ag⁺. Further, aluminium ion strongly complexes anions of organic acids, and nitrite is quantitatively destroyed by reaction with sulfamic acid. Equal volumes (2 ml) of this interference suppressor and the sample solution were mixed. After precipitation of the interfering species, the solution was filtered and diluted to 50 ml with 0.1 mol dm⁻³ phosphate buffer at pH 7.0. The use of this interference suppressor was found to be particularly useful for the analysis of the Jobe's sunsplash fertilizer. When the suppressor was not used, an unspecified component of the sample caused a positive interference with nitrate measurements.

The nitrate-nitrogen content of three aliquots of each sample was quantified by use of the standard additions method, and the results are reported in Table 2. In both instances, these results are in good agreement with the amount of nitrate-nitrogen guaranteed by the manufacturer. The electrode potential obtained by repeated measurements on a 1 mmol dm⁻³ nitrate solution falls within 1 mV. This variability in the electrode response and sampling errors account for the standard deviation observed. Thus, the electrode described here proved to be a simple, reliable and sensitive means for the determination of nitrate.

The authors are indebted to the Natural Sciences and Engineering Research Council of Canada for financial support of this work.

References

- 1 Davies, J. E. W., Moody, G. J., and Thomas, J. D. R., *Analyst*, 1972, **97**, 87.
- 2 Ebdon, L., King, B. A., and Corfield, G. C., *Anal. Proc.*, 1985, **22**, 354.
- 3 Rocheleau, M. J., and Purdy, W. C., *Electroanalysis*, 1991, **3**, 929.
- 4 *Ionic Polymers*, ed. Holliday, L., Halsted Press-Wiley, New York, 1975, ch. 1.
- 5 Janata, J., and Huber, R. J., in *Ion-Selective Electrodes in Analytical Chemistry*, ed. Freiser, H., Plenum Press, New York, 1980, ch. 3, vol. 2.
- 6 Rocheleau, M. J., and Purdy, W. C., *Talanta*, 1990, **37**, 307.
- 7 James, H., Carmack, G., and Freiser, H., *Anal. Chem.*, 1972, **44**, 856.
- 8 Skobets, E. M., Makovetskaya, L., and Makovetsii, Y., *Zh. Anal. Khim.*, 1974, **29**, 2354; *Chem. Abstr.*, 1975, **82**, 164394a.
- 9 Hopirtean, E., Stefaniga, E., Liteanu, C., and Gusan, I., *Rev. Chim.*, 1976, **27**, 346; *Chem. Abstr.*, 1976, **85**, 153362z.
- 10 Eisenman, G., in *Ion-Selective Electrodes*, ed. Durst, R. A., National Bureau of Standards, Special Publ. 314, US Government Printing Office, Washington, DC, 1969, ch. 1.

Paper 1/02031E
Received May 3, 1991
Accepted October 8, 1991

Determination of Trace Amounts of Estriol and Estradiol by Adsorptive Cathodic Stripping Voltammetry

Shengshui Hu, Qong He* and Zaofan Zhao

Department of Chemistry, Wuhan University, Wuhan, China

Estriol and estradiol are electroinactive in the potential range from -200 to -1000 mV *versus* a silver-silver chloride electrode at a mercury electrode. The conversion of these estrogens into electroactive nitro derivatives of estrogens, which are used for voltammetric determination, was studied. Such nitro derivatives give a well defined cathodic stripping wave at -600 mV in pH 10.5 borate buffer. Estriol and estradiol are determined in the ranges 1×10^{-9} – 1.5×10^{-6} and 5×10^{-9} – 2×10^{-6} mol dm $^{-3}$, respectively, by differential-pulse adsorptive stripping voltammetry at a hanging mercury drop electrode. Some steroids, such as estrone, interfere because the three estrogens have almost the same molecular structure and have similar nitro derivatives, but progesterone does not interfere and is reduced at significantly more negative potentials than the nitrated estrogens. It can be determined simultaneously with estriol or estradiol. A method was developed for the assay of estriol in pharmaceutical preparations.

Keywords: Estriol; estradiol; adsorptive stripping voltammetry

Estriol and estradiol are steroids of importance in biological processes and are substances of pharmaceutical importance. Many methods have been proposed for the determination of trace amounts of steroids, *e.g.*, colorimetric,^{1–4} spectrophotometric,⁵ gas chromatographic^{6–10} and gas chromatographic-mass spectrometric¹¹ techniques. Electrochemical methods have previously been applied to the determination of steroids,^{12–16} but the detection limits are not sufficient for determinations at low concentration levels. Some electroanalytical procedures involve the formation of derivatives to obtain polarographically or voltammetrically usable peaks; for instance, Buecher and Franke^{17,18} converted 17-oxosteroids into the β -vinylhydrazone derivative by heating in 15% hydrochloric acid at 100°C , whereas Starka and Brabencova¹⁹ used oxidation with periodic acid to determine acetaldehyde-steroids in the presence of formaldehyde-steroids in urine.

Estrogens such as estriol and estradiol cannot be reduced at a dropping mercury electrode because they do not contain the ketonic groups or α,β -unsaturated ketonic groups. However, some derivatives of estriol and estradiol enabled these compounds to be determined by polarography or stripping voltammetry. For example, Wolfe *et al.*²⁰ reported that a water-soluble and reducible hydrazone is formed after estrone reacts with trimethylammonium acetohydrazide chloride. An immunoassay of estriol labelled with mercury(II) acetate has been employed for the determination of estriol by electroanalysis.²¹ Wehmeyer *et al.*²² developed another immunoassay system to determine estriol labelled with nitro groups by differential-pulse polarography. Recently, an experimental procedure based on a sensitive polarographic method has been employed for the determination of estrogens at the 4×10^{-8} mol dm $^{-3}$ level by linear-sweep polarography.²³ These estrogens were made electroactive with sodium nitrite, and nitro derivatives of estrogen were obtained.²⁴ These methods have been used to determine estriol in the urine of pregnant women.

Adsorption is often considered a nuisance in an electroanalytical experiment, to be avoided, when possible, by changing the solvent, concentrations, *etc.* However, adsorption of a species is sometimes a prerequisite for rapid electron transfer, and can be of major importance in many processes of practical interest (*e.g.*, the oxidation of aliphatic hydrocarbons or the reduction of proteins). Adsorptive stripping

voltammetry is a very sensitive electroanalytical method for the determination of some compounds that can be adsorbed at the electrode surface by adsorptive accumulation and then reduced. 6-Aminopenicillanic acid has been determined at the 1×10^{-9} mol dm $^{-3}$ level after accumulation for 4 min at a hanging mercury drop electrode.²⁵ The adsorptive stripping voltammetric method was also used for measuring estriol and estradiol in this study. The experiments indicated that nitro derivatives of estriol or estradiol are adsorbed strongly on the mercury electrode and are reduced in the stripping step. By using this phenomenon, extremely sensitive and rapid adsorptive stripping procedures were achieved. Adsorptive deposition periods of 15 min were employed for the determination of estriol and estradiol at the 8×10^{-10} and 2×10^{-9} mol dm $^{-3}$ levels, respectively. This method is also fairly simple because it was unnecessary to separate related compounds and the nitrated estrogen was determined directly in the reaction mixture. In this respect, the method differs from the determination by adsorptive stripping voltammetry of other estrogens such as estrone.²⁶ Nitrosation has also been employed for the determination of 1- and 2-naphthols²⁷ and morphine.²⁸

Experimental

Adsorptive stripping voltammetry was carried out with a Model 174A polarographic analyser [Princeton Applied Research (PAR), Princeton, NJ, USA] with a Model 0089 x-y recorder (PAR). The three-electrode system employed was a Model 303 static mercury drop electrode (PAR), a silver-silver chloride reference electrode and a platinum auxiliary electrode. A medium-sized drop of surface area 0.016 cm 2 was used. pH measurements were made with a Model pHs-203 pH meter (Wuhan Electric and Technical Instrumental Factory, Wuhan, China).

Estriol, estradiol and other biochemicals were obtained from Sigma (St. Louis, MO, USA). The estrogen was dissolved in 100 ml of absolute ethanol to give stock solutions of estriol or estradiol. All chemicals were of analytical-reagent grade or better. All solutions were prepared with doubly distilled water (from quartz).

Borate buffer solutions (0.05 mol dm $^{-3}$) were prepared by dissolving sodium tetraborate in distilled water. A 2 mol dm $^{-3}$ solution of sodium nitrite was prepared by dissolving sodium nitrite in 1×10^{-4} mol dm $^{-3}$ sulfuric acid. Pharmaceutical preparations of estriol were commercially available.

The determination procedures were as follows: 0.2 ml of estriol (or estradiol) was placed in a 10 ml calibrated flask and

* Present address: Department of Chemistry, Qujing Normal School for Professional Training, Yunnan, China.

2 ml of 2 mol dm⁻³ sodium nitrite solution were added. The mixture was heated at 100 °C on a boiling water-bath. After heating for 30 min, the solution was allowed to cool to room temperature, then 2 ml of 0.05 mol dm⁻³ borate buffer solution were added, the pH was adjusted to 10.5 by addition of hydrochloric acid or sodium hydroxide solution and the solution was diluted to 10.0 ml with distilled water. The resulting solution was transferred into an electrolytic cell, the stirrer was started and the solution was purged with nitrogen for 10 min. After forming a new hanging mercury drop, the accumulation potential (-0.10 V) was applied to the working electrode for a selected time while the solution was stirred. At the end of the accumulation period, the stirrer was stopped and 20 s were allowed for the solution to become quiescent. The differential-pulse cathodic stripping scan was then started, the peak height being measured at -0.60 V.

Results and Discussion

The differential-pulse cathodic stripping voltammograms of nitrated estriol and estradiol were investigated at various pH values. The pH-dependent profiles of both estrogens were similar. The maximum height was observed at pH 10.5, but little difference in height was observed at pH >10.8. The peak height obviously decreased between pH 8.5 and 10.0. A small double wave was observed when the pH of the solution was <6.0, and it was not suitable for determining very low concentrations. The use of other buffer solutions that cover this pH range was examined. The best results, with respect to peak enhancement and shape, were obtained using 0.01 mol dm⁻³ borate solution. The effect of the solution pH on the peak potential was also investigated. The results indicate that the peak potential is pH dependent and the peak shifts towards negative potentials with increase in pH.

The accumulation potential applied to the electrode during the period of adsorption strongly affects the peak height obtained, as shown in Table 1. An accumulation potential between -0.05 and -0.1 V is optimum. At more negative potentials the peak height decreases rapidly as the reduction potential of nitrated estrogen is approached. However, at more positive potentials the peak height diminishes because a large amount of mercury(I) hydroxide was deposited on the electrode surface, and this deposited film may inhibit the adsorption of nitrated estrogens and the stripping response by blocking the electrode surface. The greatest peak height was obtained at -0.1 V.

The peak height of nitro derivatives of estriol and estradiol was measured by adsorptive stripping voltammetry as a function of the estrogen concentration. The peak height increased with increasing concentration of estriol and estradiol up to about 2 × 10⁻⁶ mol dm⁻³. At higher concentrations of both estrogens, curvature of the calibration graph occurred.

Table 1 Effect of varying the accumulation potential on peak height of nitrated estrogens at pH 10.5 in 0.01 mol dm⁻³ borate buffer. Accumulation time, 30 s

Potential/V	Peak height/nA	
	5 × 10 ⁻⁷ mol dm ⁻³ estriol	5 × 10 ⁻⁷ mol dm ⁻³ estradiol
+0.5	290	270
0	300	290
-0.05	320	300
-0.1	320	300
-0.2	280	270
-0.3	240	230
-0.4	150	130
-0.5	100	90

The curvature presumably indicates that a limiting value of the amount of nitro derivative on the electrode surface has been achieved under the prescribed conditions. Further increases in concentration did not increase the amount of nitro derivatives at the electrode owing to surface saturation, hence the stripping peak height remained constant. For convenient measurement of concentrations ranging from 1.5 × 10⁻⁶ to 1 × 10⁻⁹ mol dm⁻³ for estriol and from 2 × 10⁻⁶ to 5 × 10⁻⁹ mol dm⁻³ for estradiol, 0.5–10 min is usually sufficient.

Fig. 1 shows the dependence of the adsorptive stripping peak height on the accumulation time for 1 × 10⁻⁷ mol dm⁻³ estriol and estradiol. These profiles represent the corresponding adsorptive isotherms (as the peak height depends on the amount adsorbed). With increasing accumulation time the adsorption of nitro derivatives on the mercury electrode is enhanced. This increased adsorption is non-linear as a function of accumulation time, as the electrode surface rapidly becomes saturated with nitrated estrogens. At adsorption times longer than 4 min, the peak height remains constant. For a 15 min accumulation, the detection limit is 8 × 10⁻¹⁰ and 2 × 10⁻⁹ mol dm⁻³, respectively, based on a signal-to-noise ratio of 3. The sensitivity for the low concentration is improved by increasing the accumulation time, but the linear range is then diminished.

Cyclic voltammograms obtained for a 5 × 10⁻⁷ mol dm⁻³ solution of estradiol at the hanging mercury drop electrode are shown in Fig. 2. Only a cathodic peak appears without the corresponding anodic peak. The measured parameter of these

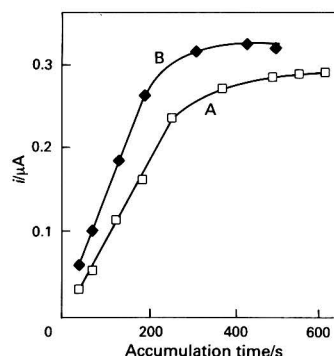


Fig. 1 Effect of accumulation time on the peak height for 1 × 10⁻⁷ mol dm⁻³ estradiol (A) and estriol (B)

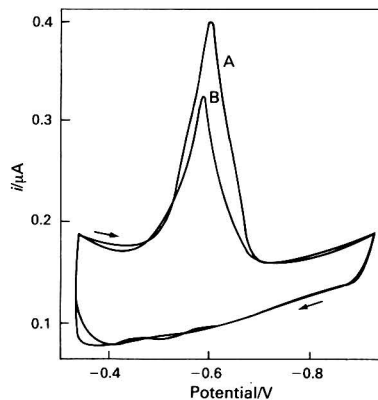
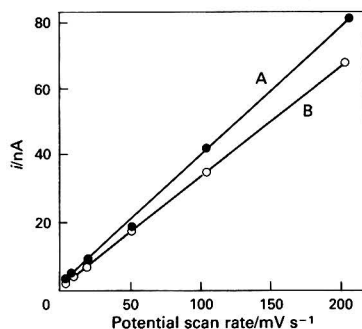
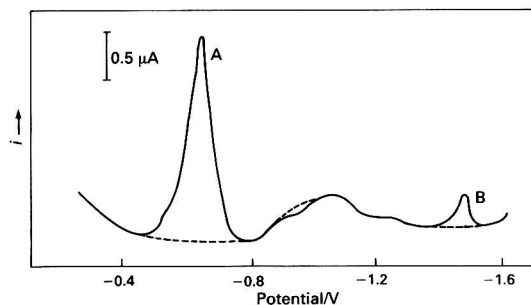


Fig. 2 Cyclic voltammograms of 5 × 10⁻⁷ mol dm⁻³ estradiol at pH 10.5 in 0.01 mol dm⁻³ borate buffer; scan rate = 50 mV s⁻¹. A, First scan, accumulation time = 30 s; and B, second scan, without accumulation

Table 2 Results obtained for estriol in injection samples by the proposed method. Each determination was carried out in triplicate

Sample No.	Estriol content/ μg per ampoule		Recovery experiments		
	Reference value	Proposed method	Estriol added/ $\mu\text{g dm}^{-3}$	Estriol found/ $\mu\text{g dm}^{-3}$	Recovery (%) (mean \pm SD*)
1	500	465	15.0	14.0	93.3 \pm 6.5
2	500	443	18.0	15.9	88.3 \pm 9.6
3	500	448	18.0	16.1	89.4 \pm 4.7

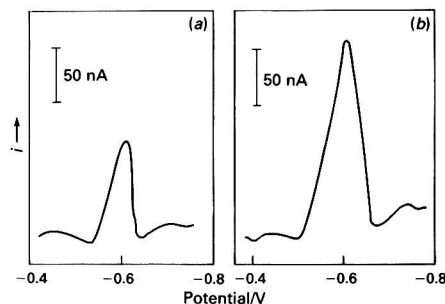
* SD = standard deviation.

**Fig. 3** Effect of varying the potential scan rate on the peak height for $1 \times 10^{-8} \text{ mol dm}^{-3}$ estriol (A) and estradiol (B); accumulation time = 40 s**Fig. 4** Stripping voltammograms for A, $1 \times 10^{-6} \text{ mol dm}^{-3}$ estriol; and B, $5 \times 10^{-7} \text{ mol dm}^{-3}$ progesterone at pH 10.5 in 0.01 mol dm^{-3} borate buffer. Accumulation for 1 min at -0.1 V . The broken line represents the blank at 0.01 mol dm^{-3} borate buffer

i - E curves is the ratio of the peak heights, $i_{p,a}/i_{p,c}$. Deviation of the ratio $i_{p,a}/i_{p,c}$ from unity is indicative of an irreversible electrode process. A large cathodic peak is observed after adsorption accumulation at -0.3 V for 30 s; the second scan without accumulation reveals only a small peak in the cathodic branch and the peak potential shifts towards the positive direction. This is a characteristic feature of adsorption of nitro derivatives. A similar cyclic voltammetric response was observed for estriol.

The effect of varying the potential scan rate on the peak height for $1 \times 10^{-8} \text{ mol dm}^{-3}$ estriol and estradiol is shown in Fig. 3. The cathodic stripping peak height increases rectilinearly with scan rate, as expected for the reduction of an adsorbed species. These results are in agreement with electrochemical theory.^{29,30}

Trace amounts of estrone can interfere if, under the conditions used, a nitrated estrone is formed with sodium nitrite which is adsorbed on the electrode and produces a reduction peak close to that of the nitro derivatives of estriol and estradiol. The nitrated estriol and estradiol have almost the same adsorptive stripping peak potential and cannot be

**Fig. 5** Stripping voltammograms for (a) injection sample; and (b) injection sample plus $5 \times 10^{-8} \text{ mol dm}^{-3}$ estriol. Accumulation time = 2 min. Other conditions as in Fig. 4

determined simultaneously without prior separation. No interference in the determination of $1 \times 10^{-6} \text{ mol dm}^{-3}$ estriol or estradiol was observed when the recommended procedures were applied after the addition of $1 \times 10^{-7} \text{ mol dm}^{-3}$ progesterone, because its reduction is at a more negative potential than the nitrated estrogens; the voltammograms are shown in Fig. 4.

The presence of surfactants may interfere by competitive adsorption, which can diminish the surface area of the electrode available for adsorption of nitro derivatives. It has been shown that the peak height of the nitro derivative was decreased by adding a cationic surfactant (tetrabutylammonium bromide) or an anionic surfactant (sodium lauryl sulfate). However, no interference for $1 \times 10^{-6} \text{ mol dm}^{-3}$ estriol or estradiol was observed with natural organic surface-active materials, such as the non-ionic surfactant poly(vinyl alcohol) (PVA; 2 ppm). This phenomenon may be due to synergistic adsorption or a decrease in the adsorption of non-ionic PVA at this potential.

Because of its high sensitivity, estriol was determined repeatedly in samples of pharmaceutical preparations by using the recommended method. A 0.1 ml estriol injection sample was placed in a 200 ml calibrated flask with 150 ml of ethanol and the flask was stoppered, shaken manually for 2 min and then the contents were diluted to 200.0 ml with distilled water. A 0.2 ml aliquot of the sample solution was transferred into a 10 ml calibrated flask and 2 ml of 2 mol dm^{-3} sodium nitrite solution were added. The mixture was heated on a boiling water-bath for 30 min and the solution allowed to cool to room temperature. Then, 2 ml of 0.05 mol dm^{-3} borate buffer were added, the pH was adjusted to 10.5 and the solution was diluted to 10.0 ml with distilled water. Adsorptive cathodic stripping voltammetry was then applied as described above. The results for the determination of estriol in three injection samples are given in Table 2. The voltammograms from a typical analysis for estriol in an injection solution are shown in Fig. 5.

This work was supported by the National Natural Science Foundation of China.

References

- 1 Forist, A. A., and Theal, S., *J. Am. Pharm. Assoc. Sci. Ed.*, 1958, **47**, 520.
- 2 Mader, W. J., and Buck, R. R., *Anal. Chem.*, 1952, **24**, 666.
- 3 Clarke, I., *Nature (London)*, 1955, **175**, 123.
- 4 Ansari, S., and Khan, R. A., *J. Pharm. Pharmacol.*, 1960, **12**, 122.
- 5 Gross, J. M., Eisen, H., and Kedersha, R. G., *Anal. Chem.*, 1952, **24**, 1049.
- 6 Domskey, I. I., and Perry, J. A., *Recent Advances in Gas Chromatography*, Marcel Dekker, New York, 1971.
- 7 Sanghoi, A., and Wight, C., *Clin. Chim. Acta*, 1974, **56**, 49.
- 8 Gardiner, W. L., and Horning, E. C., *Biochim. Biophys. Acta*, 1966, **115**, 524.
- 9 Horning, M. G., *Anal. Biochem.*, 1968, **22**, 284.
- 10 Wotiz, H. H., *Biochim. Biophys. Acta*, 1963, **69**, 413.
- 11 Stillwell, W. G., and Zlatkis, A., *J. Steroid Biochem.*, 1972, **3**, 699.
- 12 Bond, A. M., Heritage, I. D., and Briggs, M. H., *Anal. Chem.*, 1984, **56**, 1222.
- 13 Wang, J., Farias, A. M., and Mahmoud, S. J., *Anal. Chim. Acta*, 1985, **171**, 195.
- 14 Schaar, J. C., and Smith, D. E., *Anal. Chem.*, 1982, **54**, 1589.
- 15 Fogg, A. G., Fayad, N. M., and Burgess, C., *Anal. Chim. Acta*, 1979, **110**, 107.
- 16 Hu, S.-S., Yan, Y.-Q., and Zhao, Z.-F., *Anal. Chim. Acta*, 1991, **248**, 103.
- 17 Buecher, H., and Franke, R., *Abh. Dtsch. Akad. Wiss. Berlin, Kl. Med. Wiss.*, 1965, **1**, 93.
- 18 Buecher, H., and Franke, R., *Acta Biol. Med. Ger.*, 1965, **14**, 1.
- 19 Starka, L., and Brabencova, H., *Clin. Chim. Acta*, 1960, **5**, 423.
- 20 Wolfe, K. J., Hershberg, B. E., and Fieser, F. L., *J. Biol. Chem.*, 1940, **136**, 653.
- 21 Heineman, W. R., Anderson, C. W., and Halsall, H. B., *Science*, 1979, **204**, 865.
- 22 Wehmeyer, K. R., Halsall, H. B., and Heineman, W. R., *Clin. Chem. (Winston-Salem, N.C.)*, 1982, **28**, 1968.
- 23 Hu, S.-S., He, Q., and Zhao, Z.-F., *Anal. Chim. Acta*, in the press.
- 24 Konyvey, I., and Olsson, A., *Acta Chem. Scand.*, 1964, **18**, 483.
- 25 Hu, S.-S., and Zhao, Z.-F., *Anal. Lett.*, 1991, **24**, 827.
- 26 Hu, S.-S., He, Q., and Zhao, Z.-F., *Chem. J. Chin. Univ.*, in the press.
- 27 Davidek, J., and Seifert, J., *Sb. Vys. Sk. Chem.-Technol. Prazе, E*, 1971, **30**, 7.
- 28 Noninska, K. I., Dryanovska, L., and Iliev, L. S., *Farmatsiya (Sofia)*, 1969, **19**, 24.
- 29 Bard, A. G., and Faulkner, L. R., *Electrochemical Methods*, Wiley, New York, 1980.
- 30 Laviron, E., *J. Electroanal. Chem.*, 1974, **52**, 355.

Paper 1/02388H

Received May 22, 1991

Accepted September 16, 1991

Differential-pulse Polarographic Microdetermination of Reactive Organohalides *via In Situ* Generation of S-Alkylisothiuronium Salts

Wing Hong Chan* and Albert Wai Ming Lee*

Department of Chemistry, Hong Kong Baptist College, 224 Waterloo Road, Kowloon, Hong Kong

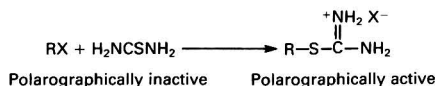
Pei Xiang Cai

Department of Chemistry, Zhongshan University, Guangzhou, People's Republic of China

Reactive organohalides, after *in situ* derivatization to the corresponding S-alkylisothiuronium salts in the presence of an excess of thiourea, were determined in aqueous solution by differential-pulse polarography. A single differential-pulse polarographic peak was obtained at pH 12.6 for all the organohalides under investigation. The calibration graphs were rectilinear over the range from 1×10^{-6} to 1×10^{-4} mol dm $^{-3}$ in the sample solution. Each of the S-alkylisothiuronium derivatives has a characteristic polarographic peak potential, thus allowing the qualitative and quantitative determination of different organohalides. For the microdetermination of reactive organohalides, the method was found to be precise and the detection limit was 1 μ g of halide.

Keywords: Reactive organohalides; differential-pulse polarography; organic analysis; *in situ* S-alkylisothiuronium salt generation

The halide group is one of the most fundamental organic functional groups. Many organohalides are important intermediates in organic reactions and are used extensively in organic synthesis. Other significant uses of this class of compound are as anaesthetics, refrigerants, and grain and fruit fumigants.¹ Although the determination of organohalides has been the focus of many investigations, simple and sensitive methods are still in great demand.²⁻⁴ Many organic substances that are polarographically inactive are amenable to indirect determination by production of an electroactive derivative.⁵ However, few organic reactions give quantitative derivatization; this impedes the application of such a strategy to the polarographic determination of organic species. We previously developed a poly(vinyl chloride) membrane S-alkylisothiuronium-selective electrode for the determination of alkyl halides *via* the generation of the corresponding S-alkylisothiuronium salts.⁶ Smyth and Osteryoung⁷ reported that when subjected to differential-pulse polarographic studies, S-benzylisothiuronium produces a characteristic wave. As the direct polarographic determination of organohalides is sometimes not feasible, this paper describes the development of a sensitive indirect polarographic method for the determination of organohalides *via in situ* generation of their polarographically active derivatives, *viz.*,



Under the defined conditions, all reactive organohalides can be quantitatively converted into water-soluble and electroactive S-alkylisothiuronium salts, thus allowing their analytical determination.

Experimental

Apparatus

Differential-pulse polarographic measurements were made by means of a Metrohm E-506 polarograph coupled with an E-505 polarographic stand. A three-electrode combination was used, consisting of a saturated calomel electrode (SCE) as the reference and platinum as the counter electrode. A Metrohm Model EA-87620 cell equipped with high-purity

nitrogen was used throughout. A pulse amplitude of 40 mV was used with a scan rate of 1.24 mV s $^{-1}$, a force drop time of 2 s, and at a mercury head height of 60 cm.

Reagents

All chemicals were of analytical-reagent grade. S-Benzylisothiuronium chloride was prepared according to the procedure described in the literature⁸ and was recrystallized once from 95% ethanol prior to use. Buffer solutions (pH 11–13), which contained sodium hydroxide, disodium hydrogen phosphate and potassium chloride, as defined by the National Institute of Standards and Technology (formerly the National Bureau of Standards),⁹ were all prepared using distilled water and were used as the background electrolyte.

In Situ Derivatization of Reactive Alkyl Halides

For investigations with large amounts of sample, about 0.5 g of alkyl halides was accurately weighed in a 100 ml round-bottomed flask and 1.3 equiv of thiourea were added. The mixture was dissolved in 25 ml of 95% ethanol and the solution was refluxed for 2 h. After refluxing, the solvent was removed under reduced pressure. The residue was dissolved in distilled water, then made up to 100 ml in a calibrated flask. For the polarographic measurement, 1 ml of the solution was further diluted to the mark with distilled water in a 100 ml calibrated flask.

For the microdetermination study, standard solutions of benzyl chloride and thiourea were prepared separately by dissolving an appropriate amount of the pure substance in 95% ethanol in a calibrated flask. An appropriate amount of each standard solution, such that thiourea is 2–3-fold in excess of the halide, was transferred by pipette and mixed in a 10 ml round-bottomed flask. The mixture was then refluxed for 3 h to effect the formation of the S-alkylisothiuronium salt. The residue was redissolved in distilled water, transferred into a calibrated flask and diluted to the mark with distilled water. Further dilution may be required so that the concentration of the final solution is preferably in the range from 1×10^{-6} to 1×10^{-4} mol dm $^{-3}$.

Determination of Organohalides by Differential-pulse Polarography

A 20 ml volume of supporting electrolyte at pH 12.6 was placed in the cell of the polarograph and flushed with

* Authors to whom correspondence should be addressed.

oxygen-free nitrogen for 5 min. Under a nitrogen atmosphere, a known amount of sample or standard solution was introduced. The mixture was flushed by bubbling nitrogen through the solution for a further 15 s. The cell was attached to the three-electrode assembly and a nitrogen flow maintained over the solution. A potential scan was then performed over the range from -0.40 to -0.80 V versus SCE at a rate of 1.24 mV s $^{-1}$ in order to obtain a differential-pulse polarogram.

Calibration Graphs for the Microdetermination of Benzyl Chloride

A series of samples containing 0.001 – 0.01 mg of benzyl chloride in 1 ml of ethanol was mixed with 2 mg of thiourea. The mixture was refluxed for 3 h. After cooling, supporting electrolyte was introduced and the solution was quantitatively transferred into a 25 ml calibrated flask. A 20 ml aliquot of each of the solutions was then taken for polarographic measurement.

Results and Discussion

In Situ Derivatization Reaction

The conversion of reactive organohalides into *S*-alkylisothiuronium derivatives by refluxing with thiourea has been shown to be quantitative by using the ion-selective electrode method.⁶ In order to determine the time required for the derivatization reaction, the reaction profiles for butyl bromide and benzyl chloride were re-established using the proposed method. By systematically increasing the derivatization time, the peak current of the resulting solution observed in the differential-pulse polarogram gradually increased until a maximum value was reached. The time required to achieve the maximum value of the peak current is likely to be the time needed for the quantitative derivatization

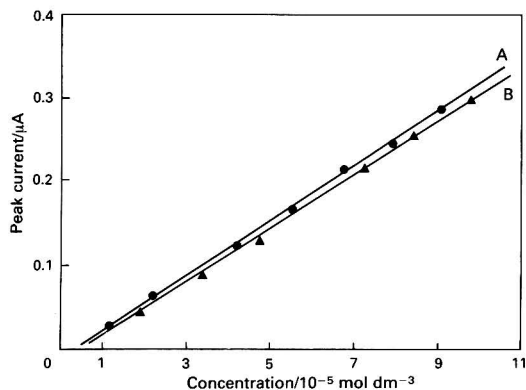


Fig. 1 Calibration graph obtained for *S*-benzylisothiuronium solution prepared from: A, the authentic salt; and B, *in situ* generation

Table 1 *In situ* derivatization conditions for different amounts of benzyl chloride

Mass of benzyl chloride/mg	Molar equivalent of thiourea	Amount of ethanol/ml	Conversion (%)
100–500	1.3	15	100*
10–100	3	10	100*
1–10	5	5	100*
0.1	2 mg	2	75*
			>95†

* Refluxing for 3 h; the extent of the derivatization was assessed by using a standard solution of *S*-benzylisothiuronium.

† Refluxing for 5 h; the extent of the derivatization was assessed by using a standard solution of *S*-benzylisothiuronium.

of the organohalides. By using this assumption, the time required for the quantitative derivatization of benzyl chloride and butyl bromide was found to be very similar in both instances (*i.e.*, 2 h); this is in good agreement with results from previous work.⁶ In order to confirm that the derivatization reaction was quantitative, the differential-pulse polarographic calibration graphs of *S*-benzylisothiuronium solutions prepared both from the authentic salt and the *in situ* generated salt (from benzyl chloride) were constructed and compared. It was found that the two graphs were almost coincident (Fig. 1). Hence, the *in situ* generation of the *S*-benzylisothiuronium salt from benzyl chloride under the proposed conditions is quantitative.

In order to ensure the completion of the derivatization reaction for small sample sizes, a longer reaction time and a greater molar equivalent of thiourea should be used. The derivatization conditions for different amounts of benzyl chloride (*i.e.*, 0.1 – 100 mg) were established (Table 1). Quantitative derivatization could be achieved by refluxing benzyl chloride with an excess of thiourea in ethanol for 3 h. For even smaller amounts of sample (*i.e.*, <0.1 mg), a longer reaction time was required for complete derivatization.

The effect of residual ethanol and thiourea, which act as the solvent and derivatization agent, respectively, on the determination of alkyl halides was also investigated. On the

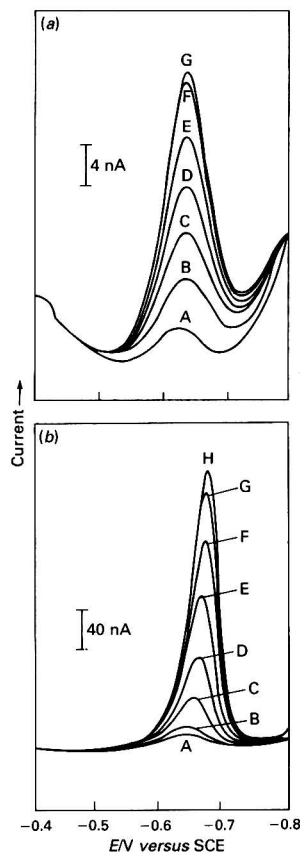
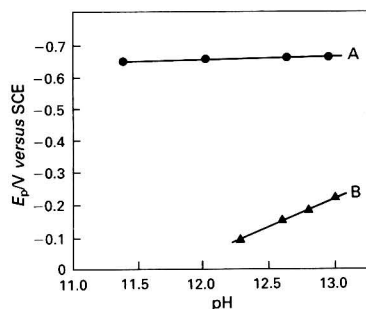


Fig. 2 Typical differential-pulse polarographic responses for the *in situ* determination of butyl bromide (a) at lower concentrations: A, 1.61×10^{-6} ; B, 3.21×10^{-6} ; C, 4.80×10^{-6} ; D, 6.38×10^{-6} ; E, 7.94×10^{-6} ; F, 9.49×10^{-6} ; and G, 1.03×10^{-5} mol dm $^{-3}$. (b) At higher concentrations: A, 1.03×10^{-5} ; B, 1.33×10^{-5} ; C, 2.29×10^{-5} ; D, 3.68×10^{-5} ; E, 5.59×10^{-5} ; F, 7.30×10^{-5} ; G, 8.86×10^{-5} ; and H, 9.82×10^{-5} mol dm $^{-3}$

Table 2 Calibration equations for different alkyl halides (concentration range from 1×10^{-6} to 1×10^{-4} mol dm $^{-3}$) and E_p values of the corresponding *S*-alkylisothiuronium salts

Alkyl halide	Equation*	<i>n</i>	<i>r</i> †	$E_p \pm V$ versus SCE
Allyl bromide	$i = 5.736 \times 10^3 c - 0.020$	11	0.999	-0.582
Benzyl chloride	$i = 2.987 \times 10^3 c - 0.003$	12	0.997	-0.680
Butyl bromide	$i = 3.108 \times 10^3 c - 0.011$	12	0.998	-0.642
Butyl iodide	$i = 3.539 \times 10^3 c - 0.008$	12	0.999	-0.642
Propyl bromide	$i = 3.393 \times 10^3 c - 0.010$	12	0.996	-0.620

* *i* is expressed in μA .† *r* = Correlation coefficient.‡ Concentration 1.0×10^{-5} mol dm $^{-3}$.**Fig. 3** Plot of E_p versus pH for the differential-pulse polarographic wave exhibited by: A, *S*-butylisothiuronium salt; and B, thiourea

systematic addition of up to 1 ml of ethanol and up to 2 mg of thiourea to 25 ml of 1.00×10^{-5} mol dm $^{-3}$ *S*-benzylisothiuronium chloride solution, the peak shape and peak height of the differential-pulse polarographic wave of the solution remained unchanged, *i.e.*, the presence of residual ethanol and thiourea did not affect the polarographic measurement in this determination.

Characteristics of the Differential-pulse Polarographic Wave

Butyl bromide was used as a representative example of an organohalide for detailed studies. Under the derivatization conditions, a single differential-pulse polarographic peak was obtained at 0.64 V versus SCE (for a concentration of 1×10^{-5} mol dm $^{-3}$ butyl bromide). The calibration graphs were rectilinear over the halide concentration range from 1×10^{-6} to 1×10^{-4} mol dm $^{-3}$ (in the sample solution) and the relative standard deviations were good (1.1% for three determinations). Typical differential-pulse polarograms used to obtain a calibration graph are shown in Fig. 2. All the polarograms showed a narrow symmetrical peak which is suitable for quantification. The differential-pulse polarographic waves of the solutions covering the lower concentration range studied [Fig. 2(a)] exhibited some residual current in the pre- and post-wave regions owing to the reduction of thiourea and residual oxygen, respectively. However, this did not affect the accuracy of the determination. On the other hand, the peak current was found to be directly proportional to the square root of the height of the mercury reservoir. This indicated that the polarographic current was diffusion controlled. In addition, the choice of the electrolyte system was adequate for this study. The peak potential (E_p) values of the differential-pulse polarographic wave shifted to more negative values on increasing the concentration of the alkyl halide. A plot of E_p versus $\log [RBr]$ in the concentration range from 8×10^{-6} to 8×10^{-5} mol dm $^{-3}$ was linear with a slope of 29.2 mV.

Owing to the simplicity of the sample treatment procedure, attention was directed initially to the determination of reactive organohalides. When several reactive organohalides were

Table 3 Working calibration graph data for the microdetermination of benzyl chloride (microgram level)

10 μ g level		1 μ g level	
Mass of sample/ μ g	i_p/nA	Mass of sample/ μ g	i_p/nA
20.8	30.6	2.08	2.34
41.6	57.0	4.16	4.14
62.4	87.0	6.24	6.12
83.2	115.2	8.32	7.50
104.0	148.2	10.40	9.96
$r = 0.9993$		$r = 0.9971$	

subjected to the proposed polarographic method, good calibration graphs, covering two orders of magnitude (from 1×10^{-6} to 1×10^{-4} mol dm $^{-3}$), were obtained in all instances. The calibration graphs are described by the equations given in Table 2. The effect of the substituent in the *S*-alkylisothiuronium salt on the E_p is evident (last column of Table 2), thus allowing the qualitative and quantitative determination of different organohalides.

Effect of pH

Under alkaline conditions, the *S*-alkylisothiuronium solution exhibits a well-defined differential-pulse polarographic wave which is amenable to analytical investigation. However, at relatively high concentrations of benzylisothiuronium (*i.e.*, $>1 \times 10^{-4}$ mol dm $^{-3}$), a turbid solution is obtained in a strongly alkaline (pH > 13) medium owing to the hydrolysis of alkylisothiuronium. In order to ascertain the working pH for the determination of alkyl halides, the effect of pH on the E_p values of the differential-pulse polarographic waves exhibited by thiourea and the *S*-butylisothiuronium salt generated *in situ* from butyl bromide was studied. The results are shown in Fig. 3. The difference between the E_p values of the two compounds over the pH range 12–13 is sufficiently large to minimize any possible interference caused by the residual thiourea from the derivatization reaction. In addition, the peak current (i_p) of a standard solution of benzylisothiuronium salt is also constant over this pH range. Hence subsequent polarographic studies of organohalides were arbitrarily carried out at pH 12.6. Also, any interference effect caused by the presence of heavy metal ions will be completely eliminated by the formation of insoluble hydroxides under the alkaline conditions used.

Working Calibration Graphs for the Microdetermination of Benzyl Chloride

Under the described conditions, samples containing as little as 0.001 mg of benzyl chloride can be derivatized satisfactorily to the corresponding isothiuronium salt. The resulting reaction mixtures from different sample sizes were subjected to polarographic measurement after derivatization. Working calibration graphs with good linearity were obtained for halide sample sizes of the order of 1 and 10 μ g (Table 3). These can be

Table 4 Microdetermination of benzyl chloride by *in situ* derivatization to the corresponding isothiuronium salt

Experiment No.	Mass of benzyl chloride used/mg	Mass of benzyl chloride found*/mg	Error (%)
1	536.9	551.7	2.6
2	501.0	511.0	2.0
3	107.1	105.8	-1.3
4	99.4	97.1	-2.3
5	55.2	55.6	0.7
6	46.4	47.5	2.4
7	17.5	16.7	-2.8
8	5.32	5.12	-3.8
9	0.0194	0.0212	9.2
10	0.0416	0.0405	-2.7
11	0.0624	0.0620	-0.6
12	0.0832	0.0812	-2.4
13	0.00194	0.00212	9.2
14	0.00416	0.00412	-1.0
15	0.00832	0.00775	-6.9

* Experiments 1-8 were carried out by using the standard additions method and experiments 9-15 by using working calibration graphs.

Table 5 Reproducibility and precision of the proposed method as illustrated by the determination of benzyl chloride

Experiment No.	Mass of benzyl chloride/mg		Recovery* (%)
	Added	Found	
1	0.1040	0.1002	96.2
2	0.1040	0.1082	104.0
3	0.1040	0.1002	96.3
4	0.1040	0.1041	100.1
5	0.1040	0.1081	103.9
6	0.1040	0.1085	104.3
7	0.1040	0.1002	96.3
8	0.1040	0.1039	99.0
9	0.1040	0.1055	101.4
10	0.1040	0.0984	94.6

* Relative standard deviation = 3.68%.

used as the working calibration graphs for the subsequent microdetermination of benzyl chloride.

Visibility of the Method for the Microdetermination of Reactive Alkyl Halides

For the actual determination of halides, as illustrated by benzyl chloride, two different methods can be used depending

on the size of the sample. For samples on the milligram scale, the standard additions method was found to be suitable (experiments 1-8 in Table 4). For samples on the sub-milligram scale, quantification of benzyl chloride can be achieved by using the working calibration graphs covering the appropriate concentration range (experiments 9-15 in Table 4). In order to demonstrate the reproducibility and precision of the proposed method, ten samples of benzyl chloride were subjected to voltammetric analysis. The average recovery was found to be 99.6% and the relative standard deviation was 3.68% (Table 5).

Conclusion

An indirect polarographic method for the determination of reactive organohalides has been developed. In the presence of thiourea, the quantitative *in situ* generation of the S-alkylisothiuronium salt from the corresponding electroinactive organohalide provides the basis for the viability of the method. The method can be carried out in aqueous solution and can be used to detect as little as 1 µg of halide.

References

- Gessner, G. N., *The Condensed Chemical Dictionary*, Van Nostrand Reinhold, New York, 8th edn., 1971, p. 359.
- Olson, E. C., in *Treatise on Analytical Chemistry*, eds. Kolthoff, I. M., and Elving, P. J., Wiley, New York, 1971, vol. 14, pt. II, p. 1.
- Al-Abachi, M. Q., and Salih, E. S., *Analyst*, 1987, **112**, 485.
- Ware, M. L., Argentine, M. D., and Rice, G. W., *Anal. Chem.*, 1988, **60**, 383.
- Smyth, W. F., *Polarography of Molecules of Biological Significance*, Academic Press, London, 1979, p. 28.
- Chan, W. H., Lee, A. W. M., and Cheung, Y. M., *Analyst*, 1991, **116**, 39.
- Smyth, M. R., and Osteryoung, J. G., *Anal. Chem.*, 1977, **49**, 2310.
- Fumiss, B. S., Hannaford, A. J., Smith, P. W. G., and Tatchell, A. R., *Textbook of Practical Organic Chemistry*, Longman, London, 5th edn., 1989, p. 789.
- Dearr, J. A., *Lange's Handbook of Chemistry*, McGraw-Hill, New York, 13th edn., 1987, pp. 5-101.

Paper 1/03648C

Received July 18, 1991

Accepted September 10, 1991

Application of Ion-exchanger Phase Spectrofluorimetry to the Determination of Micro-amounts of Some Rare Earth Elements by Flow Analysis

Kazuhisa Yoshimura and Shiro Matsuoka

Chemistry Laboratory, College of General Education, Kyushu University, Ropponmatsu, Chuo-ku, Fukuoka 810, Japan

Toyohisa Tabuchi and Hirohiko Waki

Department of Chemistry, Faculty of Science, Kyushu University, Hakozaki, Higashi-ku, Fukuoka 812, Japan

The fluorescence bands originating from d→f electron transitions, which can be used to determine europium, terbium, dysprosium or samarium selectively, were enhanced only if these elements were sorbed in a weak-acid cation-exchange gel, *i.e.*, CM-Sephadex. After a sample solution had been introduced into a fused-silica tube (1.5 mm i.d.) packed with 1 mg of CM-Sephadex, the fluorescence intensity increase, resulting from the rare earth elements sorbed in the ion-exchange gel, could be measured directly with good precision. For europium, the detection limit was 22 ng with an 8.3 cm³ sample solution. The sensitivity of the proposed method depended on the sample volume introduced. The cell could be used repeatedly after desorbing the target element with a solution of nitric acid.

Keywords: Ion-exchanger phase spectrofluorimetry; flow analysis; rare earth element determination; CM-Sephadex sorption

An individual determination of rare earth elements is difficult because of the similarity of their chemical properties. Although the absorption bands or the fluorescence bands originating from f→f or d→f electron transitions are spectrometrically specific for some rare earth elements, they are not very sensitive. One attempt to enhance the sensitivity was to measure directly light absorption by neodymium, which had been preconcentrated onto a cation exchanger.¹ On the other hand, it is known that the sensitivities are enhanced when some rare earth elements form complexes with ligands containing oxygen as the donor atom.^{2,3} Similar phenomena occur for europium, terbium, dysprosium and samarium, but only when they are sorbed in a weak-acid cation-exchange gel, *i.e.*, CM-Sephadex.

Ion-exchanger phase spectrofluorimetry, developed by Waki *et al.*⁴ and used for the determination of trace amounts of beryllium,^{4,5} aluminium,⁶ gallium⁷ and tungsten,⁸ is a very sensitive method consisting of the simultaneous ion-exchange concentration of a target element and direct fluorescence measurements of the ion-exchange gel. This method can be applied to the rare earth element-CM-Sephadex system. However, if the batch concentration method is used, this spectrofluorimetry involves a time-consuming procedure of separating the ion-exchange gel from the bulk solution and packing it into a cell. Moreover, not all of the target element sorbed in the ion-exchange gel can be used for measurement. A more rapid and sensitive way is to use a flow-through cell packed with a much smaller amount of the ion-exchange gel. In this work, this method of spectrofluorimetry was shown to be applicable to the determination of europium, terbium, dysprosium and samarium by flow analysis, using CM-Sephadex gel as the ion-exchange retention medium.

Experimental

Reagents

All of the chemicals used were of analytical-reagent grade. De-ionized water filtered through a 0.45 µm Millipore filter was used for the dilution of samples and reagents.

Each standard solution of europium, terbium, dysprosium and samarium was prepared by dissolving each of the respective

chlorides in 0.1 mol dm⁻³ hydrochloric acid and then standardizing by titration with ethylenediaminetetraacetic acid (EDTA), with Xylenol Orange as the indicator.

A carrier solution was prepared by diluting a mixture of 1.9 g of ammonium acetate, 1.4 cm³ of acetic acid and 0.11 g of calcium chloride with water to a total volume of 1 dm³.

A desorbing agent solution was prepared by diluting 10 cm³ of concentrated nitric acid to 1 dm³ with water.

A cross-linked dextran-type cation-exchange gel, CM-Sephadex C-25, was purchased from Pharmacia in the sodium form.

Apparatus

Fluorescence measurements were made using a Nippon Bunko Model FP-550A, or a Shimadzu Model RF-5000 spectrofluorimeter. The carrier solution was pumped with a medium-pressure pump (GL Sciences, Model MPD-3MG, or Sanuki, Model DM2M-1024).

The flow-through cell shown in Fig. 1 consisted of a fused-silica tube (i.d. 1.5 mm, o.d. 4 mm) with a poly-

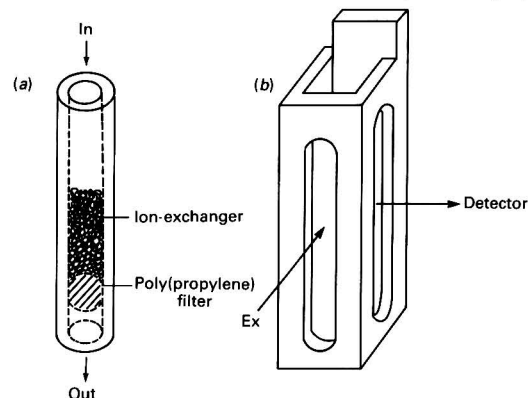


Fig. 1 Flow-through cell for ion-exchanger phase spectrofluorimetry. (a) Flow-through cell: a fused silica tube (1.5 mm i.d.), packed with 1 mg of CM-Sephadex C-25; and (b) micro-cell holder (GL Sciences)

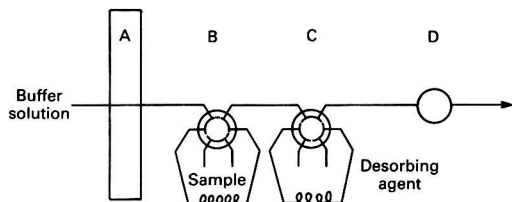


Fig. 2 Schematic diagram of the flow analysis set-up. A, Pump; B and C, six-way rotary valves each with a PTFE tube loop; and D, spectrofluorimetric detector packed with ion-exchanger. Carrier solution, 0.05 mol dm^{-3} acetate (pH = 4.7, 40 mg dm^{-3} calcium); flow rate, $1.5 \text{ cm}^3 \text{ min}^{-1}$; ion-exchanger, CM-Sephadex C-25; flow-through cell, 1.5 mm i.d. ; $\lambda_{\text{ex}} = 395 \text{ nm}$, $\lambda_{\text{em}} = 616 \text{ nm}$

(propylene) filter tip at the bottom, packed with about 1 mg of the ion-exchange gel. The cell, held in an accessory designed for a 3 mm micro-cell (GL Sciences), was placed in such a way that the excitation beam could enter only the ion-exchange gel.

A schematic diagram of the flow analysis set-up is shown in Fig. 2. A sample loop (8.3 cm^3) was made by using a poly(tetrafluoroethylene) (PTFE) tube (1 mm i.d. , 2 mm o.d.). Each of the sample solutions and the desorbing agent solution were introduced into the flow system by means of a six-way rotary valve. The flow rate was maintained constant at $1.5 \text{ cm}^3 \text{ min}^{-1}$. All of the tubing was made of PTFE.

Measurement of Distribution Ratio

After 200 cm^3 of a sample solution containing 4 mg of europium had been equilibrated with 100 mg of CM-Sephadex C-25, the europium concentration of the supernatant solution was measured by the method described below. The distribution ratio, D , of the component is defined by the equation:

$$D = \frac{[(\text{mol of the component sorbed})/(\text{g of ion-exchange gel})]}{[(\text{mol of the component in solution})/(\text{cm}^3 \text{ of solution})]} \quad (1)$$

Procedure for the Determination of Europium

A sample solution containing $0.04\text{--}2 \text{ }\mu\text{g}$ of europium was introduced into the carrier stream. The fluorescence emission intensity was measured continuously at 616 nm (20 nm slit-width) using an excitation wavelength of 395 nm (10 nm slit-width). The emission filter was a Shimadzu O-56 high-path filter; the excitation filter, a Shimadzu B-390. The increase in fluorescence intensity from the background was measured on a chart recorder. After each measurement, the europium in the flow-through cell was desorbed by the introduction of about 3 cm^3 of the desorbing agent solution into the carrier stream.

Procedure for the Determination of Terbium

Terbium ($0.1\text{--}2 \text{ }\mu\text{g}$) was similarly determined. The fluorescence intensity was measured at 544 nm , with an excitation wavelength of 351 nm . The emission filter was a Shimadzu Y-50 high-path filter; the excitation filter, a Shimadzu U-340.

Procedure for the Determination of Dysprosium

Dysprosium ($0.2\text{--}2 \text{ }\mu\text{g}$) was also determined in a similar way. The fluorescence intensity was measured at 573 nm , with an excitation wavelength of 350 nm . The emission filter was a Shimadzu O-56 high-path filter; the excitation filter, a Shimadzu U-340.

Procedure for the Determination of Samarium

The fluorescence intensity of samarium ($0.4\text{--}2 \text{ }\mu\text{g}$) was measured at 596 nm , with an excitation wavelength of 401 nm .

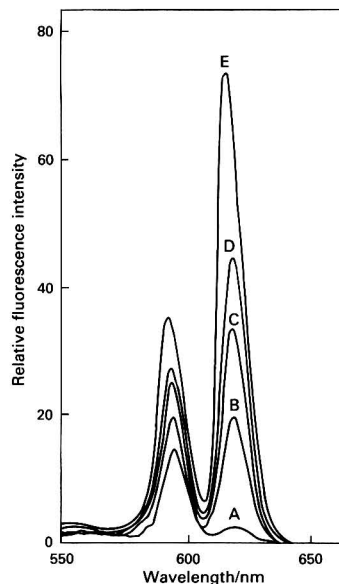


Fig. 3 Emission spectra at an excitation wavelength of 395 nm for acetate buffer solutions containing $1 \times 10^{-3} \text{ mol dm}^{-3}$ europium. A, 0; B, 0.1; C, 0.3; D, 1; and E, 4 mol dm^{-3} acetate (pH 4.7)

The emission filter was a Shimadzu O-56 high-path filter; the excitation filter, a Shimadzu B-390.

Results and Discussion

Fluorescence Spectra of Europium in Ion-exchange Gel and in Solution

The fluorescence spectra of europium in solutions containing different concentrations of acetate (pH 4.7) are shown in Fig. 3. In the visible region, two peaks were observed for each spectrum: the maximum intensities were at an excitation wavelength of 395 nm . The peak at 592 nm is assigned to the $^5\text{D}_0 \rightarrow ^7\text{F}_1$ transition, and the peak at 616 nm to $^5\text{D}_0 \rightarrow ^7\text{F}_2$. With the deviation of europium from octahedral symmetry, the increase in intensity of the $^5\text{D}_0 \rightarrow ^7\text{F}_2$ transition is greater than that of the $^5\text{D}_0 \rightarrow ^7\text{F}_1$ transition.⁹

Europium, to which a large number of ligands containing oxygen donor atoms coordinate, yielded a high fluorescence intensity. By increasing the concentration of acetate, the fluorescence intensity at 616 nm is increased more than that at 592 nm , owing to the complexation of europium with carboxyl groups. Using 0.3 mol dm^{-3} acetate (Fig. 3, curve C), the europium to carboxyl group ratio is estimated to be 1:2 or 1:3, by using reported stability constants of acetate complexes.¹⁰ The spectrum of europium sorbed in the weak-acid cation-exchange gel, CM-Sephadex, which has carboxyl groups as functional groups, is similar to that shown in Fig. 3 curve C, and therefore the degree of complexation in the cation-exchange gel corresponds to that in a 0.3 mol dm^{-3} acetate solution. Also, in the ion-exchange gel phase, excitation at 395 nm gave maximum intensities at two emission peaks.

As shown in Fig. 4(a), the degree of complexation by the fixed functional groups did not change in the ion-exchange gel phase at low europium loadings and, therefore, the emission intensity was proportional to the amount of europium sorbed in the gel. However, the ratio of the fluorescence intensity at 616 nm to that at 592 nm decreased with an increase in europium loading [Fig. 4(b)]: the peak area ratio was 1.35 for curve A and 1.28 for curve D. This means that the degree of complexation is lower at high europium loadings.

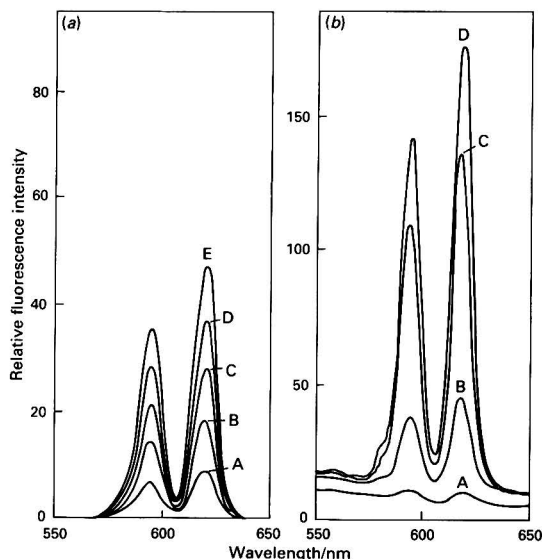


Fig. 4 (a) Net emission spectra at low loadings and (b) emission spectra at high loadings, with an excitation wavelength of 395 nm. Solution, 0.05 mol dm⁻³ acetate (pH 4.7, 100 cm³); ion-exchanger, CM-Sephadex C-25 (100 mg); micro-cell, 3 × 3 × 35 mm. (a) Europium concentration: A, 2; B, 4; C, 6; D, 8; and E, 10 mg dm⁻³. (b) Europium concentration: A, 10; B, 50; C, 100; and D, 200 mg dm⁻³.

Table 1 Relationship between internal diameter of flow-through cell and relative fluorescence intensity

Internal diameter/mm	1.0	1.5	2.0
Relative fluorescence intensity*	2.2	1	0.6

* Normalized value with respect to the intensity using a 1.5 mm diameter cell.

Optimization of Measurements

Geometry of the flow-through cell

The sensitivity was compared using flow-through cells with different internal diameters (Table 1). Ion-exchange gel beads were packed in cells of equal height, and the linear velocity for each cell was kept constant. For a 2.5 mm diameter cell, the intensity was 40% lower than that for a 1.5 mm diameter cell. The intensity for a 1.0 mm diameter cell was about twice that for a 1.5 mm diameter cell, but the measurement time was too long: two samples per hour.

The position of the flow-through cell in the cell compartment is critical, because, when the excitation beam hits the poly(propylene) filter, light scattering increases. As the width of the beam was about 6 mm, the ion-exchange gel column in the flow-through cell had to be about 5 mm in height for the excitation beam to strike the ion-exchange gel beads at the top and to cover the area packed as widely as possible. The change in the shape of the ion-exchange gel beads at the top gave rise to remarkable errors because the light scattering characteristics changed. It might be thought that the precision of ion-exchange phase spectrofluorimetry, which involves an unorthodox solid-phase optical medium, would be inferior to that of conventional solution spectrofluorimetry. However, the errors are not serious for such low sample concentrations, to which the conventional solution method cannot be applied directly.

Selection of ion-exchanger

Four different types of ion-exchanger were tested for polymer matrices, with different functional groups and degree of

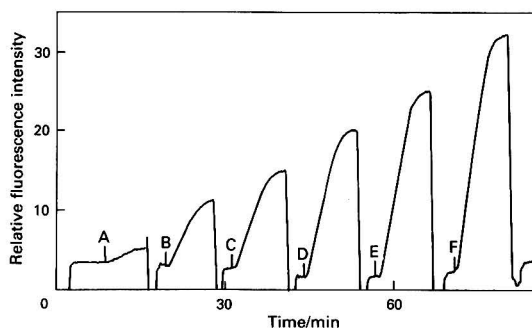


Fig. 5 Fluorescence development profiles of europium obtained using the flow system with ion-exchanger phase spectrofluorimetry. Europium concentration: A, 0; B, 10; C, 20; D, 30; E, 40 and F, 50 µg dm⁻³. Sample volume, 8.3 cm³; carrier solution, 40 mg dm⁻³ Ca in 0.05 mol dm⁻³ acetate (pH 4.7); flow rate, 1.5 cm³ min⁻¹.

cross-linking. Cation-exchange resins of cross-linked polystyrene, for example, Bio-Rad AG 50W-X12 (100–200 mesh, hydrogen form), showed an intense background emission in the visible region because of fluorescent impurities present in the resin. A strong-acid cation-exchange gel of cross-linked dextran, SP-Sephadex C-25, did not increase the sensitivity. Although a weak-acid cation-exchange gel with a low degree of cross-linking, CM-Sephadex C-50, increased the sensitivity for 0.1–1 µg of europium, it was 20% lower than that for CM-Sephadex C-25. Therefore, CM-Sephadex C-25 seemed to be the best choice for this method.

Effect of pH

The relative fluorescence intensity varied at pH values lower than 4.5 owing to shrinkage of the ion-exchange gel and the decrease in the distribution ratio; the intensity was almost constant in the pH range 4.5–7. The pH of the solution was fixed at 4.7. After adjusting the pH of a sample solution, the determination of europium should be made within 1 h, otherwise some loss of europium from the solution, due to its adsorption on glassware vessels, will occur.

Effect of acetate concentration

In order to maintain a constant pH of the sample solution, an acetate buffer solution (0.05 mol dm⁻³) was used. With 0.2 mol dm⁻³ acetate, the fluorescence intensity was 25% lower than with 0.05 mol dm⁻³ acetate. This was because the distribution ratio was lowered owing to the formation of acetato complexes in the solution with high acetate concentration.

Calibration and Sensitivity

Fig. 5 shows typical examples for fluorescence development of europium and continuous measurement of samples. The calibration graph obtained was linear but had a positive blank. Similar results were obtained for the samarium, terbium and dysprosium systems. Relative fluorescence intensity caused by the sorption of each rare earth element is summarized in Table 2; europium could be most sensitively determined.

Enhancement of Ion-exchanger Phase Spectrofluorimetry by Using a Flow-through Cell Packed With Ion-exchange Gel

For an ion-exchange gel layer prepared with m g of ion-exchange gel (previously equilibrated with V cm³ of solution containing a sample component of concentration c_0 mol dm⁻³), the fluorescence intensity, F , can be approximately expressed as:

$$F = kI_0c_0 \times \frac{V}{mv} \times \frac{1}{1 + V/mD} \times \phi a \bar{l} \quad (2)$$

Table 2 Sensitivity and detection limits

Element	Wavelength/nm		Sample volume/ cm ³	RFI*	Detection limit†/ μg dm ⁻³
	Excitation	Emission			
Sm	401	596	4.8	0.41	120 (<i>n</i> = 5)
Eu	395	616	8.3	55.3	2.7 (<i>n</i> = 5)
Tb	351	544	8.3	13.9	5.9 (<i>n</i> = 4)
Dy	350	573	8.3	6.10	9.6 (<i>n</i> = 6)

* Relative fluorescence intensity caused by the sorption of each rare earth element (100 μg dm⁻³).

† The concentration that produces a fluorescence intensity equal to twice the magnitude of the fluctuation in the background fluorescence intensity.

if the concentration of the sample component is sufficiently low and *D* is large.³ The parameter *I*₀ is the excitation beam intensity; φ, the quantum yield of fluorescence; *a*, the absorptivity; *l*, the light path; *v*, the specific volume in the equilibrated state (5 cm³ g⁻¹ for CM-Sephadex C-25); and *k*, an instrumental proportionality constant. (The over-bar refers to the ion-exchange gel phase.)

If $V \ll mD$ as for the present systems [for the europium-CM-Sephadex system, *D* was 2.1 × 10⁵ cm³ g⁻¹ (pH 4.7, 0.05 mol dm⁻³ acetate with 40 mg dm⁻³ calcium)], eqn. (2) can be simplified as follows:

$$F = kI_0c_0 \times \frac{V}{mv} \times \bar{\phi} \bar{a} \bar{l} \quad (3)$$

Eqn. (3) shows that there is a linear relationship between *F* and *c*₀, and that by increasing *V*/*mv* (the solution to ion-exchange gel volume ratio), the present method becomes much more sensitive.

The sensitivity of the proposed method was compared with the solution method as follows. The intensity of the CM-Sephadex C-25 layer (0.1 g of the ion-exchange gel equilibrated with a 100 cm³ solution of 1 mg dm⁻³ europium) was compared with that of a 200 mg dm⁻³ europium solution (0.3 mol dm⁻³ acetate). The concentration of europium in the gel phase was the same as that in the solution. Under such conditions, ion-exchanger phase spectrofluorimetry by the batch method was 200 times more sensitive than the solution method. For the flow method, after packing 1 mg of the ion-exchange gel into the flow-through cell, and loading 10 cm³ of a 0.25 mg dm⁻³ europium solution, the intensity of the ion-exchange gel layer was compared with that of the solution described above: the flow method using a 10 cm³ water sample is much more sensitive than the solution method by a factor of 800.

For the batch method, spectrofluorimetric measurements were made using a micro-cell 3 × 3 × 35 mm, packed with at least 30 mg (0.15 cm³) of the ion-exchange gel and the area where the light beam struck was about 1/4 of the total area of the ion-exchange gel packed in the micro-cell, and, therefore, 0.0375 cm³ of the ion-exchange gel beads in the cell was used for measurements. Therefore, the amount of europium irradiated in the two cells was 7.5 μg for the batch method and 2.5 μg for the flow method. Although the pathlength for the flow method is smaller than that for the batch method, higher sensitivity was obtained: the geometry for fluorescence measurement might be more favourable for the flow method than that for the batch method.

Above all, with a flow-through cell packed with a small amount of ion-exchange gel, the feasibility of much higher volume ratios should greatly increase the sensitivity of ion-exchanger phase spectrofluorimetry.

Detection Limit

The detection limit, defined as the concentration producing a fluorescence intensity equal to twice the magnitude of the

Table 3 Effect of foreign ions on the determination of europium. Sample, 4.8 cm³ (0.200 mg dm⁻³ Eu); carrier, 40 mg dm⁻³ Ca in 0.05 mol dm⁻³ acetate (pH 4.7)

Foreign ion	Concentration/ mg dm ⁻³	Europium found/ mg dm ⁻³	Error (%)
Ca	0	0.214	+7.0
	20	0.204	+2.0
	200	0.189	-5.5
	400	0.161	-19.5
Fe	10	0.213	+6.5
La	2.0	0.211	+5.5
	10	0.233	+11.5
Sm	10	0.206	+3.0
Tb	10	0.209	+4.5
Dy	2.0	0.188	-6.0
	10	0.178	-11.0

Table 4 Determination of samarium, europium and dysprosium in synthetic samples and a mineral

Sample	Concentration found/mg dm ⁻³
<i>Synthetic samples/mg dm⁻³</i>	
Ca 40, Sm 2	Sm 2.00 ± 0.095 (<i>n</i> = 5)
Ca 40, Fe 10, La 2, Sm 2, Eu 0.01, Tb 0.5, Dy 2	Sm 2.14
Ca 40, Eu 0.05	Eu 0.050 ± 0.0038 (<i>n</i> = 5)
Ca 40, Fe 0.5, La 0.05, Sm 0.05, Eu 0.05, Tb 0.05, Dy 0.05	Eu 0.0492
Ca 40, Tb 0.05	Tb 0.050 ± 0.0012 (<i>n</i> = 5)
<i>Yttrium concentrate* (% m/m)</i>	
Y 50.6, La 0.5, Ce 1.2, Pr 0.2, Nd 0.8, Sm 0.9, Eu 0.1, Gd 2.9, Tb 0.8, Dy 6.8, Ho 1.6, Er 5.5, Tm 0.8, Yb 8.3, Lu 0.8	Dy 6.7 ± 0.6 (% m/m) (<i>n</i> = 5)

* Concentrated from xenotime (Shin-etsu Kagaku). Elemental analysis was carried out using X-ray fluorescence spectrometry.

fluctuation in the background fluorescence intensity, is shown in Table 2. For the europium system, the detection limit was 22 ng, i.e., 2.7 μg dm⁻³, with an 8.3 cm³ sample solution.

Effect of Sample Volume

For the present system, *D* is sufficiently large to satisfy eqn. (3). This means that the sensitivity will be increased only by introducing a larger volume of sample solution. A variation in the sample volume from 2.1 to at least 16.6 cm³ resulted in a proportional increase in the fluorescence intensity. Much higher sensitivities can be achieved by employing larger volumes of sample solution.

Effect of Foreign Ions

With 8.3 cm³ sample solutions containing 50 μg dm⁻³ europium, the effects of the concomitant ions of calcium, iron, lanthanum, samarium, terbium and dysprosium were examined. The presence of 40 mg dm⁻³ calcium or 2 mg dm⁻³ dysprosium gave remarkable negative errors, but other ions gave no interference at the 1 mg dm⁻³ level. The ion-exchange gel layer in the flow-through cell became contracted when the loaded ion was converted from a monovalent to a polyvalent cation. Therefore, the error induced by calcium might be due to shrinkage of the ion-exchange gel. In order to eliminate this effect, the counter ion of the ion-exchange gel was changed from ammonium to calcium by adding calcium chloride to a sample and the carrier solution. When 4.8 cm³ of a 0.20 mg dm⁻³ europium solution were introduced, in the presence of 40 mg dm⁻³ calcium, calcium no longer interfered up to 200 mg dm⁻³ (Table 3). The presence of 10 mg dm⁻³ dysprosium gave a negative error; the presence of 10 mg dm⁻³ lanthanum, a positive error.

In addition to europium, samarium, terbium and dysprosium can be determined using the proposed method. Elements that interfered when present at a concentration of less than that of the target element were europium and terbium for the samarium system, samarium for the terbium system and terbium for the dysprosium system.

Determination of Samarium, Europium, Terbium and Dysprosium in Synthetic Samples and a Mineral

With 4.8 or 8.3 cm³ sample solutions, the precision was measured with a Shimadzu Model RF-5000 type spectrofluorimeter. For five determinations, each relative standard deviation was within 10% (Table 4).

The results in Table 4 also show that the method is applicable to the determination of dysprosium in an yttrium concentrate. The value obtained by the proposed method is in close agreement with that obtained by X-ray fluorescence spectrometry.

Conclusion

Although methods such as neutron-activation analysis and inductively coupled plasma optical emission spectrometry have been used for the determination of trace amounts of various rare earth elements, access to the necessary equipment is not always available. Without any fluorescent dyes, the proposed method affords an on-line, simple, rapid and fairly sensitive method to determine europium, terbium, samarium or dysprosium selectively using relatively inexpensive apparatus, because both concentration and spectrofluorimetric measurements are carried out simultaneously.

The fluorescence bands originating from the d→f electron transition can be used to determine individual rare earth elements selectively and can be enhanced in a CM-Sephadex ion-exchange gel phase.

The proposed method is applicable to the determination of trace amounts of a wide variety of target elements by employing the appropriate fluorescent dye.

References

- 1 Yoshimura, K., and Taketatsu, T., *Fresenius Z. Anal. Chem.*, 1987, **328**, 553.
- 2 Chrysochoos, J., and Evers, A., *Chem. Phys. Lett.*, 1973, **18**, 115.
- 3 Bünzli, J.-C. G., and Yersin, J.-R., *Helv. Chim. Acta*, 1982, **65**, 2498.
- 4 Waki, H., Noda, S., and Yamashita, M., *React. Polym.*, 1988, **7**, 227.
- 5 Capitán, F., Manzano, E., Navalón, A., Vilchez, J. L., and Capitán-Vallvey, L. F., *Analyst*, 1989, **114**, 969.
- 6 Capitán, F., Manzano, E., Vilchez, J. L., and Capitán-Vallvey, L. F., *Anal. Sci.*, 1989, **5**, 549.
- 7 Capitán, F., Navalón, A., Vilchez, J. L., and Capitán-Vallvey, L. F., *Talanta*, 1990, **37**, 193.
- 8 Capitán, F., de Gracia, J. P., Navalón, A., Capitán-Vallvey, L. F., and Vilchez, J. L., *Analyst*, 1990, **115**, 849.
- 9 Blasse, G., Bril, A., and Nieuwpoort, W. C., *J. Phys. Chem. Solids*, 1966, **27**, 1587.
- 10 Grenthe, I., *Acta Chem. Scand.*, 1962, **16**, 1695.

Paper 0/055681

Received December 11, 1990

Accepted September 19, 1991

Spectrofluorimetric Determination of the Insecticide Azinphos-methyl in Cultivated Soils Following Generation of a Fluorophore by Hydrolysis

F. García Sánchez and A. Aguilar Gallardo

Department of Analytical Chemistry, Faculty of Sciences, University of Málaga, 29071-Málaga, Spain

A rapid and simple spectrofluorimetric method for determining residues of the pesticide and acaricide azinphos-methyl in soil is described. Soil is extracted with methanol. The method is based on the alkaline hydrolysis of the insecticide to its main metabolite anthranilic acid. A detailed study of the parameters affecting the chemical hydrolysis is presented and the results are discussed. The calibration graphs were linear from 30 to 1000 ng ml⁻¹, with a limit of detection of 8 ng ml⁻¹. The precision of the method is 2% at the 60 ng ml⁻¹ level. Recoveries of spiked soil samples were between 105 and 111%.

Keywords: Azinphos-methyl determination; spectrofluorimetry; soil analysis; insecticide; acaricide

Analysis of pesticides in environmental matrices is of increasing interest because of their widespread use for both agricultural and industrial purposes. Although gas chromatography (GC) remains the major method of determination, high-performance liquid chromatography (HPLC) and discontinuous techniques for pesticides are often used.

Methods for the determination of pesticide residues must offer high sensitivity. Molecular fluorescence is a detection technique that is highly regarded as an analytical tool because of its excellent sensitivity; however, its use has been limited because few pesticides fluoresce naturally and several preliminary derivatizing steps may need to be carried out.

Azinphos-methyl {*S*-(3,4-dihydro-4-oxobenzo[*d*][1,2,3]-triazin-3-ylmethyl) *O,O*-dimethyl phosphorodithioate} is a non-systemic insecticide and acaricide that persists in the environment for long periods of time.¹ It is effective chiefly against biting and sucking insect pests and is used mainly on citrus, cotton, grapes, maize, some ornamental plants, top quality fruit and vegetables. Several workers have reported methods for the determination of azinphos-methyl using a variety of techniques such as titrimetry,² spectrophotometry,³ mass spectrometry⁴ and HPLC⁵⁻⁹ with ultraviolet (UV) detection or GC.^{10,11} The titrimetric method is based on hydrolysing azinphos-methyl in methanol with 3 mol dm⁻³ NaOH in the presence of phenol followed by argentimetric titration of the *O,O*-dimethyl hydrogen phosphorodithioate formed with dichlorofluorescein as indicator. The spectrophotometric method involves the reaction of azinphos-methyl with 4-(4-nitrobenzyl)pyridine and oxalic acid in acetone medium to yield a solution with an absorption maximum at 560 nm.

In a multi-residue method using reversed-phase HPLC with fluorimetric detection,¹² azinphos-methyl spiked in vegetables has been determined at 0.1–5 ppm with recoveries of between 93 and 115%.

In the present paper the utility of spectrofluorimetry to determine the insecticide azinphos-methyl in soil samples by a simple method is described. The proposed method is based on the alkaline hydrolysis of the insecticide to give the fluorophore anthranilic acid, which is monitored at 394 nm with excitation at 314 nm. This provides a sensitive method (limit of detection, 8 ng ml⁻¹) for the determination of azinphos-methyl that is applicable to residues in soils and gives recoveries ranging from 105 to 111%.

Experimental

Apparatus

Emission measurements were carried out with a Perkin-Elmer LS-5 luminescence spectrometer (Perkin-Elmer, Beaconsfield, Buckinghamshire, UK), equipped with a xenon dis-

charge lamp (9.9 W) pulsed at the line frequency, F/3 Monk-Gillieson type monochromators, and 1 × 1 cm quartz cells. The spectrofluorimeter was operated in the computer-controlled mode via the RS232C serial interface by a Perkin-Elmer Model 3600 data station microcomputer. Instrumental control and data collection were achieved by using the commercially available Perkin-Elmer computerized luminescence software (PECLSI). The system enables derivative spectra to be recorded. In order to ensure that all measurements could be compared and that repeatable measurements could be obtained, the LS-5 spectrofluorimeter was checked daily. A fluorescent sample of the polymer *p*-terphenyl (1 × 10⁻⁷ mol dm⁻³) gave a relative fluorescence intensity (RFI) of 90% at $\lambda_{em} = 340$ nm with $\lambda_{ex} = 295$ nm, with a slit-width of 2.5 nm and a sensitivity factor of 0.5973. For graphical recording, an Epson FX-85 printer-plotter (Seiko Epson, Suwa, Japan) was connected to the spectrofluorimeter. All fluorescence spectra are uncorrected because no significant wavelength shifts were observed when the spectra were compared with corrected spectra.

Ultraviolet absorption spectra were recorded with a Shimadzu UV-240 Graphicord recording spectrophotometer (Shimadzu, Kyoto, Japan). A rotary vacuum evaporator (W. Büchi Scientific Apparatus, Flawil, Switzerland) and an Ultrasons Selecta ultrasonic water-bath (Selecta, Barcelona, Spain) were used to homogenize soil samples.

Reagents

Stock solutions of azinphos-methyl [>99% pure (Pestanal quality), Riedel-de-Haën, Seelze, Hannover, Germany] were prepared in ethanol at concentrations of 1.0 mg ml⁻¹. Working solutions at concentrations of 100 µg ml⁻¹ were prepared in ethanol. All solvents used were of analytical-reagent grade and were obtained from Merck (Rahway, NJ, USA).

The NaOH was also of analytical-reagent grade (Merck). The water used was distilled and de-mineralized.

Procedures

Analytical procedure

Transfer aliquots of a standard solution of azinphos-methyl (1 mg ml⁻¹) in ethanol into 10 ml calibrated flasks in order to obtain a final concentration between 0.03 and 1 µg ml⁻¹. Add 6 ml of ethanol and 2.5 ml of 0.2 mol dm⁻³ NaOH (final concentration 5 × 10⁻² mol dm⁻³). Dilute to the mark with de-ionized water. Heat the resultant solutions for 10 min in a water-bath at 85 °C, cool for 3 min under running water and allow to stand for 7 min at room temperature. Measure the

fluorescence intensity at 394 nm with excitation at 314 nm, against a solvent blank. The concentration of azinphos-methyl is determined from the conversion of RFI units by reference to the calibration graph.

Extraction of soil samples

Soil samples were obtained from three cultivated fields in Coin, Algarrobo and Campanillas (Málaga, Spain) by using a V-shaped shovel introduced into the ground to a depth of 20 cm. Twenty sub-samples were taken from different sites of the same field and combined to give a final mass of approximately 2 kg. The sample was spread in a dish, and large pieces and pebbles were removed. The sample was mixed thoroughly and divided into 300 g portions. Each soil sample was air-dried at room temperature and passed through a 2 mm sieve. Volumes of the stock solution of azinphos-methyl in ethanol were added to a 10 g portion of the soil sample in a beaker so that the percentage recovery obtained using the proposed method could be calculated. After thorough mixing, the sample was extracted with methanol in a proportion of 2 + 1 solvent to sample (v/m). In order to achieve a rapid homogenization of the sample with the extracting solvent, the beaker was placed in an ultrasonic bath for 1 min after which the sample was left to stand. The supernatant was filtered through a 30 ml Büchner funnel of medium porosity, and a vacuum was applied. The procedure was repeated three times. The contents of the filter flask were transferred quantitatively into a round-bottomed flask and taken to near dryness on a rotary evaporator at 45 °C. The residue was made up to a final

volume of 10 ml with ethanol. This solution was used for the analytical determination.

Results and Discussion

The alkaline hydrolysis of azinphos-methyl leads to the formation of the metabolite anthranilic acid. The reaction is slow, and essentially depends on the pH of the medium and on the temperature.

The fundamental chemical behaviour of the insecticide azinphos-methyl and its main metabolite anthranilic acid is shown in Scheme 1. This dynamic process is an irreversible hydrolytic process which leads to the generation of a fluorophore, and is a reaction that can be monitored by making fluorescence measurements. This behaviour facilitates the spectrofluorimetric determination of the non-fluorescent reagent.

When the solution of azinphos-methyl is added to a strongly basic medium, the fluorescence emission spectrum observed shows a maximum at 394 nm when excited at 314 nm (Fig. 1). As the reaction is too slow at room temperature, even in basic medium, to be of use, the effect of temperature is significant in the optimization of the experimental procedure.

Effect of the Experimental Variables

The effect of the concentration of NaOH on the rate of hydrolysis was examined by monitoring the fluorescence emission of 3.15×10^{-6} mol dm⁻³ solutions of azinphos-methyl in water-ethanol (40 + 60) at 394 and 314 nm containing 0.01–0.10 mol dm⁻³ NaOH. The solutions were heated to 85 °C for 20 min and, after cooling, the fluorescence was measured.

The results show that constant values of fluorescence intensity were obtained in the range 0.02–0.06 mol dm⁻³ NaOH. Higher concentrations gave a diminution in fluorescence readings, probably because of the decomposition of the hydrolysis products. An NaOH concentration of 0.05 mol dm⁻³ was finally selected for the alkaline working solutions. Under these conditions the hydrolysate of azinphos-methyl is stable for at least 1 h.

Temperature and heating time also have an important influence on the final conditions required for hydrolysis. The effect of these parameters was studied by measuring the fluorescence intensity for the total reaction at two different temperatures (65 and 85 °C) for 0.05 mol dm⁻³ solutions of NaOH for heating periods of between 0 and 50 min. Fig. 2 shows that at lower temperatures longer heating times are

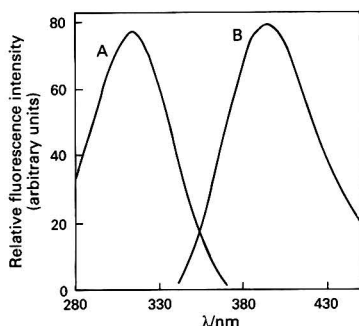
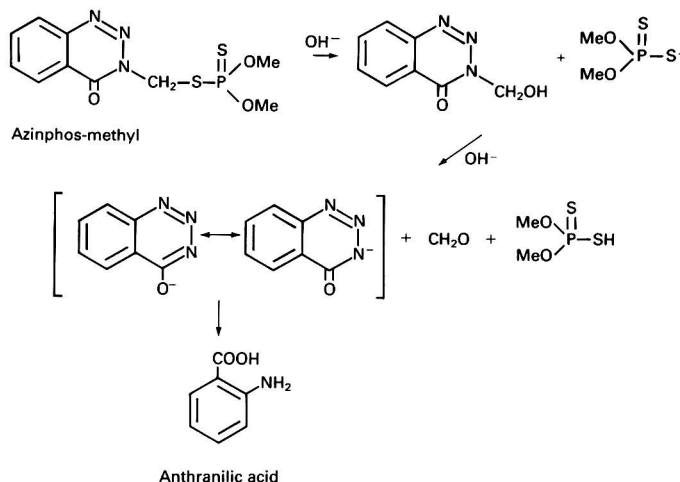


Fig. 1 A, Excitation and B, emission spectra of anthranilic acid in water-ethanol (40 + 60). [Anthranilic acid] = 3.15×10^{-6} mol dm⁻³; λ_{ex} = 314 nm, λ_{em} = 394 nm



Scheme 1

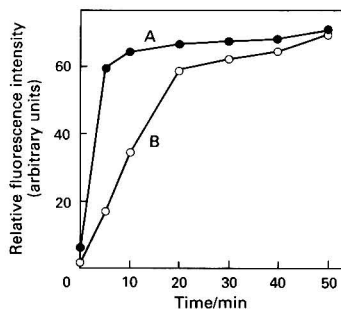


Fig. 2 Effect of temperature on hydrolysis at A, 85 °C and B, 65 °C. [Anthranilic acid] = 3.15×10^{-6} mol dm $^{-3}$; [NaOH] = 0.05 mol dm $^{-3}$; λ_{ex} = 314 nm, λ_{em} = 394 nm

required in order to achieve constant readings in fluorescence intensity. From these experiments, it was deduced that a heating time of 10 min at 85 °C is sufficient to obtain optimum results.

Analytical Parameters

The calibration graphs were prepared using a set of standards individually hydrolysed and measured as described under Analytical procedure and plotting the RFI values against concentration in ng ml $^{-1}$.

Two concentration ranges of azinphos-methyl can be covered by linear calibration graphs, 100–1000 ng ml $^{-1}$ and 20–100 ng ml $^{-1}$, using direct fluorescence intensity measurements. Applying statistical treatment to the analytical data, the linear regression graphs obtained are as follows:

$$I_F = 0.0626 [\text{azinphos-methyl}] + 0.223 \quad r = 0.997$$

$$I_F = 0.3770 [\text{azinphos-methyl}] + 1.390 \quad r = 0.997$$

where I_F is the fluorescence intensity, r the correlation coefficient and [azinphos-methyl] is in ng ml $^{-1}$.

The sensitivity of the method is reported as the analytical sensitivity, $s_A = \sigma/m$, and has a value of 1.23 ng ml $^{-1}$ where σ is the standard deviation of the analytical signal ($n = 7$) and m is the slope of the calibration graph.¹³ The limit of detection, c_L ($K = 3$) and the limit of quantification, c_Q ($K = 10$) are reported as defined by IUPAC¹⁴ and have values of 8.13 and 27.11 ng ml $^{-1}$, respectively; K is a numerical factor chosen in accordance with the confidence level desired. The limit of quantification, c_Q , is employed to establish the lower limit of the linear dynamic range. The relative error of the method was 1.90% and a relative standard deviation (RSD) of 2% was obtained at the 60 ng ml $^{-1}$ level ($n = 7$).

Analysis of Soil Samples

Azinphos-methyl is used for the control of insect pests in fruits and vegetables at rates of 3–4 l ha $^{-1}$; it persists in the soil for about 28 d.

Soil samples from cultivated citrus fields in southern Spain (Coin, Algarrobo and Campanillas, Málaga) were used to demonstrate the applicability of the proposed spectrofluorimetric method.

The first step in the determination of pesticide residues is usually the separation of the residues from the matrix material by solvent extraction. For efficiency, the solvent must remove the pesticide in a reproducible manner without removing large amounts of interfering compounds from the matrix.

One of the most complicated procedures is the extraction from soil, because the extraction efficiency is affected by the type of soil, the properties of the extractant, method of extraction, etc. Ultrasonic techniques are generally preferred as the effect of water in the soil or type of organic matter present in the soil is avoided and the efficiency of the

Table 1 Analysis of azinphos-methyl residues in ground soil; $n = 3$

Type of soil	Azinphos-methyl added/ $\mu\text{g ml}^{-1}$	Azinphos-methyl found/ $\mu\text{g ml}^{-1}$	Recovery (%)	Mean recovery (%)
Ground soil	0.9	0.984	109.3	108.1 \pm 1.1
		0.965	107.2	
		0.970	107.7	
Siliceous	0.9	0.945	105.0	105.6 \pm 0.5
		0.955	106.1	
		0.951	105.6	
Clays	0.9	0.947	105.4	107.7 \pm 3.0
		0.960	106.6	
		1.000	111.1	

extraction is increased. This is due to the breakdown of soil structure, allowing the extractant to work on a larger surface area. Therefore, the ultrasonic technique was selected for the extraction procedure.

With respect to the solvent used to extract the pesticide from soils, a search of the literature showed that most workers have found that higher efficiency is achieved by using methanol as the solvent.^{15–19} Interference problems are generally avoided with soil samples when the proposed extraction procedure is used, except for those interferents that are organic in nature and could fluoresce in an alkaline medium.

The proposed method can be applied to the analysis of soil samples fortified with standard solutions of 0.9 $\mu\text{g ml}^{-1}$ of azinphos-methyl, following the extraction procedure described above.

The concentration of azinphos-methyl found in soil samples and the corresponding percentage recoveries obtained using the proposed method are given in Table 1 ($n = 3$). Blank signals corresponding to untreated soil samples were subtracted from the recovery data.

The measurements obtained show that soil samples containing azinphos-methyl at residue levels may be quantified by the proposed spectrofluorimetric method. No significant differences in the percentage recovery were found for the three types of soils tested.

The recoveries obtained are acceptable. No previous publications reporting recoveries of azinphos-methyl in soils have been found in the literature.

Conclusion

Determination of azinphos-methyl at residue levels in soil samples can be accomplished readily by using hydrolysis-induced fluorescence spectrometry. Despite the widespread use of chromatographic methods in the determination of pesticide residues, the development of alternative methods that are simpler and more rapid than those already in use would be useful to the analytical community. Recovery assays of azinphos-methyl in several soil samples show good results compared with those obtained by use of HPLC.

References

- 1 *Pesticide Manual*, British Crop Protection Council, ed. Worthing, C. R., British Crop Protection Council, Croydon, 7th edn., 1983.
- 2 Muntaz, M., Nasir, N. E. R., and Baig, M. M., *Pak. J. Sci. Ind. Res.*, 1983, **26**, 132.
- 3 Gunther, F. A., Iwata, Y., Papadopoulos, E., Berck, B., and Smith, C. A., *Bull. Environ. Contam. Toxicol.*, 1980, **24**, 903.
- 4 Schulten, H. R., and Sun, S., *J. Environ. Anal. Chem.*, 1981, **10**, 247.
- 5 Bushway, R. J., *J. Liq. Chromatogr.*, 1982, **5**, 49.

- 6 Wilson, A. M., and Bushway, R. J., *J. Chromatogr.*, 1981, **214**, 140.
- 7 Funch, F. H., *Z. Lebensm.-Unters. Forsch.*, 1981, **173**, 95.
- 8 Farran, A., and de Pablo, J., *Int. J. Environ. Anal. Chem.*, 1987, **30**, 59.
- 9 Marutoiu, C., Vlassa, M., Sarbu, C., and Nagy, S., *HRC CC, J. High Resolut. Chromatogr. Chromatogr. Commun.*, 1987, **10**, 465.
- 10 Pressley, T. A., and Longbottom, J. E., *Gov. Rep. Announce. Index (US)*, 1982, **82**, 1544.
- 11 Allmaier, G., Goergl, A., Schmid, E. R., and Wagner, K., *HRC CC, J. High Resolut. Chromatogr. Chromatogr. Commun.*, 1986, **9**, 762.
- 12 Krause, R. T., and August, E. M., *J. Assoc. Off. Anal. Chem.*, 1983, **66**, 234.
- 13 García Sánchez, F., and Cruces Blanco, C., *Anal. Chem.*, 1986, **58**, 73.
- 14 Long, G. L., and Winefordner, J. D., *Anal. Chem.*, 1983, **55**, 712A.
- 15 Klisenko, M. A., *Ser. Fac. Sci. Nat. Univ. Purkynianae Brun.*, 1980, 1068.
- 16 McKone, C. E., *J. Chromatogr.*, 1969, **44**, 60.
- 17 Kahn, S. U., Greenhalgh, R. I., and Cochrane, W. P., *Bull. Environ. Contam. Toxicol.*, 1975, **13**, 602.
- 18 Cotterill, E. G., *Pestic. Sci.*, 1980, **11**, 23.
- 19 Peña-Herasa, A., and Sánchez-Rasero, F., *J. Chromatogr.*, 1986, **358**, 302.

Paper 1/02283K

Received May 15, 1991

Accepted October 8, 1991

Linear Titration Plot for the Determination of Boron in the Primary Coolant of a Pressurized Water Reactor

Derek Midgley and Christopher Gatford

National Power plc, Technology and Environmental Centre, Kelvin Avenue, Leatherhead, Surrey KT22 7SE, UK

A linear titration plot method has been devised for the determination of boron as boric acid in partly neutralized solution, such as occurs in the primary coolant of pressurized water reactors. The total boron and the alkali in the sample are determined simultaneously. Although it is not essential to add mannitol in this method, it is more accurate when the solution is saturated with mannitol. Comparisons are made with other modes of titration: Gran plots, first and second differential potentiometric titrations and indicator titrations. None of these gives the total boron directly in partly neutralized solutions.

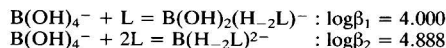
Keywords: Potentiometric titration; Gran plot; linear titration plot; boric acid; pressurized water reactor

Boric acid is added to the primary coolant of pressurized water reactors (PWRs) in nuclear power stations to provide fine control of the reactivity by means of the neutron-absorbing capability of the ^{10}B isotope, which constitutes 20% of natural boron. The boron concentration is reduced from 2000 mg l^{-1} at the start of a fuel cycle to less than 100 mg l^{-1} at the end. Daily analysis of the coolant is required. In addition to providing information on ^{10}B for neutron control, the boric acid concentration also determines the amount of lithium hydroxide to be added to maintain the pH at a level that minimizes corrosion and transport of corrosion products. Other solutions at PWR stations need analysing for boric acid, e.g., in boric acid storage tanks, recovery liquors and auxiliary systems, but these analyses are less critical.

Alkalimetric titration of boric acid is long-established, but in this instance the acid will always be partly neutralized to a small extent ($\approx 1\%$) and some means of correcting for this is required. As the sample will be slightly radioactive, automated procedures with a minimum of sample handling are desirable.

Theory

Boric acid is weakly dissociated ($\text{p}K_a = 9.23$ at 25°C) and conventional titration is impractical, whether using a colorimetric or potentiometric end-point. Adding a polyol that complexes with boric acid, as in eqn. (1), releases protons that can be titrated in the usual way; Belcher *et al.*¹ confirmed that mannitol, $\text{HOCH}_2(\text{CHOH})_4\text{CH}_2\text{OH}$, was the most suitable reagent and the apparent $\text{p}K$ of boric acid in its mixture of complexes is about 5.2. Stability constants in 0.1 mol l^{-1} KCl medium at 25°C have been determined as follows,³ where L represents mannitol:



The above constants are probably averages for a number of steric isomers.

Linear titration plots^{4,5} can cope with acids as weak as boric acid, even without the addition of mannitol and can also be used to calculate the total and neutralized acidity.⁶ Application of the latter plot to data from the literature for boric acid produced results of reasonable but not great accuracy. A disadvantage of linear titration plots, apart from the original Gran plots,⁷ is the necessity of knowing the stability constants relevant to all the equilibria involved. The requirement for computing facilities has also been disadvantageous, but with the availability of personal computers and spreadsheets, this is no longer a problem.

Linear titration plots have not been considered for complex

systems such as borate-mannitol, but examination of the charge and mass balance equations shows that a simple equation is obtained if the mannitol concentration is kept constant. This can be achieved in practice simply by saturating the solution with mannitol. For a volume (V_0 ml) of a solution of boric acid (total boron concentration C_B mol l^{-1}) partly neutralized with C_{Li} mol l^{-1} of lithium hydroxide after the addition of V ml of sodium hydroxide titrant (m mol l^{-1}) in the presence of mannitol:

$$\begin{aligned} \text{total boron, } T_B &= C_B V_0 / (V_0 + V) \\ &= [\text{B}(\text{OH})_3] + [\text{B}(\text{OH})_4^-] \\ &\quad + [\text{B}(\text{OH})_2(\text{H}_{-2}\text{L})^-] + [\text{B}(\text{H}_{-2}\text{L})_2^-] \\ &= [\text{B}(\text{OH})_4^-] \{ \{ \text{H}^+ \} / K_a + 1 \\ &\quad + \beta_1 [\text{L}] + \beta_2 [\text{L}]^2 \} \end{aligned} \quad (1)$$

$$\begin{aligned} \text{total mannitol, } T_L &= [\text{L}] + [\text{B}(\text{OH})_2(\text{H}_{-2}\text{L})^-] \\ &\quad + 2[\text{B}(\text{H}_{-2}\text{L})_2^-] \end{aligned} \quad (2)$$

$$\text{total lithium, } [\text{Li}^+] = C_{\text{Li}} V_0 / (V_0 + V) \quad (3)$$

$$\text{total titrant, } [\text{Na}^+] = mV / (V_0 + V) \quad (4)$$

$$\begin{aligned} \text{charge, } [\text{H}^+] + [\text{Li}^+] + [\text{Na}^+] &= [\text{OH}^-] + [\text{B}(\text{OH})_4^-] \\ &\quad + [\text{B}(\text{OH})_2(\text{H}_{-2}\text{L})^-] \\ &\quad + [\text{B}(\text{H}_{-2}\text{L})_2^-] \\ &= [\text{OH}^-] + T_B - [\text{B}(\text{OH})_3] \end{aligned} \quad (5)$$

where $K_a = \{ \text{B}(\text{OH})_4^- \} \{ \text{H}^+ \} / [\text{B}(\text{OH})_3]$ is the dissociation constant and f is the univalent ion activity coefficient.

If V_e is the volume of titrant required to neutralize the sample,

$$mV_e = V_0(C_B - C_{\text{Li}}) = m(V_B - V_{\text{Li}}), \quad (6)$$

where V_{Li} and V_B are the volumes of titrant equivalent to the lithium hydroxide and total boron, respectively, in the sample. Substituting in eqn. (5),

$$\begin{aligned} \{ \text{H}^+ \} / f + mV_{\text{Li}} / (V_0 + V) + mV / (V_0 + V) &= \\ K_a / \{ \text{H}^+ \} f + mV_B / [(V_0 + V) \times] \\ \{ 1 - [1 + (1 + \beta_1 [\text{L}] + \beta_2 [\text{L}]^2) K_a / \{ \text{H}^+ \} f]^{-1} \} \end{aligned}$$

On re-arrangement,

$$\begin{aligned} (V_0 + V) \{ \{ \text{H}^+ \} - K_a / \{ \text{H}^+ \} \} / mf + V &= \\ V_e - V_B / [1 + (1 + \beta_1 [\text{L}] + \beta_2 [\text{L}]^2) K_a / \{ \text{H}^+ \} f] \end{aligned} \quad (7)$$

The constants K_w , K_a , β_1 and β_2 are known, as are the experimental quantities m , V_0 , V and $\{ \text{H}^+ \}$, so the left-hand side of eqn. (7) can be plotted against $1/[1 + (1 + \beta_1 [\text{L}] + \beta_2 [\text{L}]^2) K_a / \{ \text{H}^+ \} f]$, if $[\text{L}]$ is known, to give a straight line with a slope of $-V_B$ and an intercept on the ordinate of V_e . Hence the original concentrations can be calculated:

$$C_B = mV_B / V_0 \quad \text{and} \quad C_{\text{Li}} = m(V_B - V_e) / V_0$$

If the solution is saturated with mannitol, $[L]$ is constant and the calculation is complicated only by the presence of activity coefficients. The titration can be carried out either at constant ionic strength, with a fixed value of f , or f can be calculated from an equation such as the Davies equation,⁸ with iterative corrections to the ionic strength, I . When I is equal to the left-hand side of eqn. (5), in which $[Na^+]$ is known and $[H^+]$ is initially approximated by $\{H^+\}$; on the first cycle, $[Li^+]$ is neglected. After the first cycle, $[Li^+]$ is known to a good approximation and included in calculations of I until successive iterations agree.

Experimental

Titration were carried out with an Orion 960 titrator operating in Gran mode with approximately 10 mV spacing between points. Standard boron solutions were prepared from Aristar grade boric acid (BDH) and BDH ConvoL sodium hydroxide was used as the titrant. The glass electrode was calibrated each day with standard potassium hydrogen phthalate and KH_2PO_4 - Na_2HPO_4 buffers.

Calculations were carried out using the Microsoft Excel 3.0 spreadsheet, but they are not dependent on any special feature of this product and almost any spreadsheet should suffice.

Results

Boric Acid Solutions

Standard boric acid solutions equivalent to 0.46–9.25 ml of 0.1 mol l^{-1} NaOH were titrated in volumes of 20–25 ml. Results were calculated by the linear titration plot method on a spreadsheet and by the Gran plot software built into the Orion 960 titrator. The Gran weak acid plot, $V\{H^+\}$ versus V , was used for data before the equivalence point and the strong base plot, $(V_0 + V)/\{H^+\}$ versus V , for data after the equivalence point. Segregation of the data was performed automatically by the Orion 960 titrator. The results are shown in Table 1 for boric acid solutions both with and without mannitol. The linear titration plot calculations were carried through with respect to the original volume of solution, *i.e.*, without correction for volume changes produced by the

Table 1 Results for unneutralized boric acid solutions by linear titration plot (LTP) and Gran procedures (25 ml sample, 0.1 mol l^{-1} titrant)

Run	Theoretical V_B/ml	LTP		Gran error in V_B (%)		
		Error in V_B (%)	V_L/ml	Pre-end- point	Post-end- point	Mean
<i>With mannitol—</i>						
1	9.251	-1.89	-0.028	-0.97	-0.30	-0.64
2	9.251	-0.74	-0.023	0.06	0.63	0.35
3	4.626	-0.12	-0.005	0.12	0.57	0.35
4	4.626	-1.27	-0.009	-0.64	-0.01	-0.32
5	2.313	-1.56	-0.004	-0.55	-0.08	-0.32
6	2.313	-2.42	-0.014	-1.37	-0.55	-0.96
7	0.463	4.50	0.013	2.26	3.99	3.12
8	0.463	4.17	0.014	1.39	2.91	2.15
Mean		-0.01	-0.007	0.04	0.89	0.47
<i>Without mannitol—</i>						
9	9.251	0.12	0.008	2.14	-1.46	0.34
10	9.251	0.40	0.039	-11.11	-0.96	-6.04
11	4.626	-1.83	0.026	ND*	ND	ND
12	4.626	1.00	0.064	1.72	-2.54	-0.41
13	2.313	0.87	0.045	2.91	-2.89	0.01
14	2.313	0.76	0.045	1.74	-3.75	-1.01
15	0.463	4.17	0.009	9.61	-2.28	3.66
16	0.463	7.02	0.020	7.88	-0.12	3.88
Mean		1.56	0.032	2.13	-2.00	0.06

* ND = Not detected.

* ND = Not detected.

dissolution of mannitol. The value of $[L]$ was estimated, by interpolation of solubility data,⁹ to be 1.2 mol l^{-1} on this basis, but this tended to produce small positive values of V_L even when only boric acid was present (an average of $0.03 \pm 0.01 \text{ ml}$ for the runs in Table 1). The $[L]$ was adjusted within each run until $|V_L| < 0.0005$; the mean of these optimized concentrations was 1.17 ± 0.02 , which was used to give the results in Table 1, where the mean V_L is $-0.007 \pm 0.015 \text{ ml}$. The plots are not shown here, but would be similar to those shown in Fig. 1 for partly neutralized solutions, except for a displacement on the ordinate. The mean error in V_B was only 0.1% by the linear titration plot, although this was fortuitous to the extent that positive errors at the lowest concentration tested were balanced by negative errors at higher concentrations. The Gran weak acid plot gave still smaller errors, with a smaller spread and the Gran post-end-point plot relatively larger errors.

Repeating the titrations without mannitol shows that the linear titration plot gave fairly good results, whereas those for the Gran weak acid plot were very scattered. The Gran post-end-point plot generally gave a slight underestimate of the titre. In one instance the software failed to find a segment sufficiently linear to qualify as a Gran plot, although the linear titration plot was satisfactory. Linear titration plots for these runs would be similar to those in Fig. 2, but displaced on the ordinate.

In these calculations only one round of iteration was necessary. By working with a constant ionic background of potassium nitrate, iteration was avoided, but without an

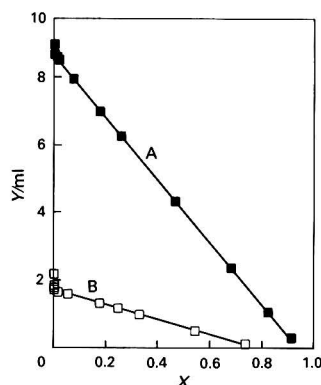


Fig. 1 Linear titration plots for partly neutralized boric acid solutions in the presence of mannitol: A, run 2 and B, run 5 from Table 1. Where $Y = (V_0 + V)/\{H^+\} - K_w/\{H^+\}/mf + V$; and $X = 1/[1 + (1 + \beta_1[L] + \beta_2[L]^2)K_a/\{H^+\}f]$

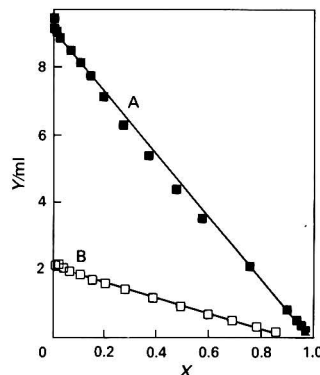


Fig. 2 Linear titration plots for partly neutralized boric acid solutions without mannitol: A, run 9 and B, run 13 from Table 1. X and Y as defined in Fig. 1

improvement in accuracy. The automatic titrator took readings rapidly, but no improvement in accuracy was obtained by slowly adding titrant and judging equilibrium from a display of the potential on a chart recorder.

For titrations in which it is known that no neutralization of the boric acid has occurred, the Gran weak acid procedure would be preferred for its accuracy and simplicity, provided that mannitol is added. Note, however, that the post-end-point plot, in which base is in excess, appears to be better than the Gran weak acid plot itself. The linear titration plot allows the mannitol to be omitted, with little loss of accuracy, whereas the weak acid Gran procedure is rather unreliable in such circumstances.

Partly Neutralized Boric Acid Solutions

The above runs were re-calculated as if the titrations had started after a small volume, V_1 , of titrant had been added. Thus, V_1 is identical with V_{Li} . The results are shown in Table 2. In these titrations, the pH data are the same as for the runs in

Table 2 Results for partly neutralized boric acid solutions by linear titration plot procedure

Run	Theoretical		Found	
	V_B /ml	V_{Li} /ml	Error in V_B (%)	Error in V_{Li} (%)
<i>With mannitol—</i>				
1A	9.251	0.655	−1.71	−2.12
2A	9.251	0.655	−0.52	−0.94
3A	4.626	0.555	0.21	1.41
4A	4.626	0.555	−1.02	0.15
5A	2.313	0.555	−1.22	0.46
6A	2.313	0.504	−2.33	−2.57
7A	0.463	0.302	5.57	5.76
8A	0.463	0.302	5.43	6.47
Mean			0.55	1.08
<i>Without mannitol—</i>				
9A	9.251	0.202	0.22	7.70
10A	9.251	0.202	0.59	26.26
11A	4.626	0.202	−1.35	19.82
12A	4.626	0.202	1.31	37.27
13A	2.313	0.202	1.57	28.48
14A	2.313	0.202	1.42	28.32
15A	0.463	0.202	6.76	9.51
16A	0.463	0.151	7.02	13.47
Mean			2.19	21.36

Table 3 Results for different modes of end-point detection in titrations of boric acid in the presence of mannitol (Orion 960 titrator). All values for the error, within-batch (s_w), between-batch (s_b) and total relative standard deviations (s_t) are given in per cent; degrees of freedom are shown in parentheses

Method		Amount of B/mg (mg l^{-1})				
		10 (1997)	5 (990.4)	2.5 (500.8)	1 (200.4)	0.25 (49.6)
First derivative	Error	0.55	0.92	0.76	3.3	13.7
	s_w (2)	0.05	0.05	4.8	0.1	0.7
Second derivative	Error	−0.60	1.98	0.76	2.79	12.3
	s_w (6)	0.39	0.08	0.38	0.15	1.2
	s_b (2)	NS*	0.44†	NS	0.40†	0
	s_t (8)	0.50	0.45	0.52	0.40	1.2
Gran post-end-point (blank corrected)	Error	0.10	0.07	0.50	0.50	2.82
	s_w (6)	0.10	0.21	0.16	0.45	1.0
	s_b (2)	NS	NS	0	0.50‡	2.4§
	s_t (8)	0.15	0.29	0.16	0.70	2.6
Gran weak acid, pre-end-point	Error	0.10	−0.05	0.38	1.25	9.07
	s_w (6)	0.21	0.36	0.30	0.65	1.2
	s_b (2)	NS	0	0	NS	NS
	s_t (8)	0.29	0.36	0.30	0.65	1.4

* Not significant.

† Significant at the $P = 0.1\%$ level.

‡ Significant at the $P = 5\%$ level.

§ Significant at the $P = 1\%$ level.

Table 1 and the volume data become $V_0' = V_0 + V_1$ and $V' = V - V_1$, where primed symbols refer to Table 2. Data corresponding to $V < V_1$ were omitted. For all but the lowest concentration (well below the normal operating range of the reactor) the accuracy when determining boron was almost the same as for unneutralized solutions. The lithium concentration was also determined with reasonable accuracy. Typical plots are shown in Fig. 1: linearity over most of the plot is excellent, but as the abscissa tends to zero the ordinate increasingly deviates from the ideal value. These deviant points correspond to a pH > 7 and the most likely cause is depression of the pH by the presence of carbon dioxide, whether arising from contamination of the titrant or absorption during the titration. Points with an alkaline pH or abscissa < 0.01 should be excluded from the calculation and these are easily seen on the spreadsheet; no other points needed to be omitted from the data for the above results.

Without mannitol, the boron concentration was still determined fairly accurately, but the errors in the lithium concentration were considerable. Typical linear titration plots are shown in Fig. 2: the scatter is not very large, but greater than when mannitol is present.

Results for Gran and conventional titrations are not shown, as even if perfectly executed they can yield only the boric acid concentration and not the total boron, *i.e.*, they would have given an error in V_B equal to V_{Li} . In these examples the error would be 7% of the greatest boron concentration and 70% for the least. With these traditional titrations, a correction for lithium hydroxide must be made, either by first titrating with acid to pH 7 (before adding mannitol), so that V_B is accurately determined in the subsequent titration with alkali. Alternatively, lithium can be determined by some other method (atomic spectrometry or with an ion-selective electrode) and a correction applied, but this is valid only in highly pure samples such as those used in this work, where it is safe to assume that there are no other sources of lithium or alkali in the boric acid solutions.

Comparison of Conventional Titrations for Boric Acid

Various instrumental methods of end-point detection are available in modern automatic titrators and these were tested for the titration of pure (unneutralized) boric acid solutions in the presence of mannitol. The results in Table 3 show that for the Orion 960 titrator the Gran mode was more accurate than the first and second derivative modes. For comparison, a further series of solutions (Table 4) was analysed with a

Table 4 Boric acid titrations with the Metrohm 682 titroprocessor

B taken/mg	8	4	2	0.8
B taken/mg l ⁻¹	400	200	100	40
Mean error (%)	0.35	0.58	1.6	2.6
s _w * (%)	0.3 (4)	1.0 (4)	0.9 (10)	0.5 (4)

* Within-batch relative standard deviation for a single result, with degrees of freedom in parentheses.

Table 5 Titrations with visual end-point detection

B taken/mg	10	4	1
B taken/mg l ⁻¹	500	200	50
Error (%)	0*	-0.25	1.0
s _w † (%)	0.18	0.35	0.58

* Taken as standard.

† Within-batch relative standard deviation (4 degrees of freedom).

Metrohm 682 titroprocessor, which takes the end-point as the point of inflection of the titration curve and has a syringe burette instead of a calibrated pump, as with the Orion instrument. The precision and accuracy at any concentration were closely comparable for the two titrators. Finally, some titrations were carried out using visual end-point detection with phenolphthalein (Table 5), which produced results equal to those from the titrators.

Tables 3–5 show the expected deterioration of accuracy and precision as the samples become more dilute. This is partly caused by loss of precision and accuracy in delivery of the titrant as the titre becomes smaller, but also by increasing errors in the approximations involved in the Gran functions⁴ or increasing discrepancy between the equivalence point and the point of inflection,¹⁰ however determined. In all of the techniques, the accuracy deteriorates more rapidly than the precision, because of these biases in the calculation of the equivalence point.

Discussion

The linear titration plot gives an accurate measure of the total boron concentration, even in partly neutralized solutions of boric acid, and also gives a good estimate of the amount of alkali added (identified with lithium in the present application). It is still advantageous to add mannitol, although not theoretically necessary. Without mannitol, the error in the estimate of added alkali becomes considerable. The calcula-

tions are easily carried out on a spreadsheet and only one cycle of iteration is required to correct for variations in ionic strength. Alternatively, the ionic strength can be artificially maintained as constant, rendering iteration unnecessary.

If the boric acid is known to be free of alkali, the Gran weak acid procedure is simpler and slightly more accurate than the linear titration plot, but the addition of mannitol is highly desirable. It is particularly convenient when the titrator is programmed to carry out the Gran plot, as in the Orion 960 titrator.

Mannitol is essential for other modes of end-point indication, such as first or second differential potentiometric titrations or the classical visual indicator technique, and these methods are then capable of giving excellent results in simple boric acid solutions. With these, as with both the Gran methods, a second determination is required to detect partial neutralization, necessitating additional sample handling.

The linear titration plot thus provides a one-stop method for partly neutralized boric acid solutions and is particularly suitable when an automated method with minimal handling of samples is required.

Submitted for publication by permission of National Power plc.

References

- 1 Belcher, R., Tully, G. W., and Svehla, G., *Anal. Chim. Acta*, 1970, **50**, 261.
- 2 Dawber, J. G., and Matusin, D. H., *J. Chem. Soc., Faraday Trans.*, 1982, **78**, 2521.
- 3 Antikainen, P. J., and Pitkänen, I. P., *Suom. Kemistil. B*, 1968, **41**, 65.
- 4 Midgley, D., and McCallum, C., *Talanta*, 1974, **21**, 723.
- 5 Midgley, D., and McCallum, C., *Talanta*, 1976, **23**, 320.
- 6 Midgley, D., and McCallum, C., *Fresenius Z. Anal. Chem.*, 1978, **290**, 230.
- 7 Gran, G., *Analyst*, 1952, **77**, 661.
- 8 Davies, C. W., *Ion Association*, Butterworth, London, 1962.
- 9 *International Critical Tables of Numerical Data, Physics, Chemistry and Technology*, McGraw-Hill, New York, 1928, vol. IV.
- 10 Meites, L., and Goldman, J. A., *Anal. Chim. Acta*, 1963, **29**, 472.

Paper 1/04397H

Received August 22, 1991

Accepted October 10, 1991

Complexometric Determination of Copper in Isolation, Alloys and Complexes Using DL-Cysteine as a Selective Masking Agent

B. Narayana

Department of Studies in Chemistry, Mangalore University, Mangalagangothri 574 199, India

M. R. Gajendragad

Kuvempu University, B.R. Project, Shimoga 577 201, India

An accurate, selective and rapid complexotitrimetric method is described for the determination of Cu^{II} in the presence of other metal ions. The method is based on the selective complexing ability of cysteine with Cu^{II}. Copper in the aliquot is initially complexed by the addition of ethylenediaminetetraacetic acid (H₄edta) solution and the excess H₄edta is titrated against Pb(NO₃)₂ solution (pH 5.0–6.0) using hexamine and Xylenol Orange. A known excess of DL-cysteine in water is then added to release the H₄edta from the Cu^{II}–H₄edta complex. This is subsequently titrated against Pb(NO₃)₂ to the same sharp end-point. The amount of H₄edta released from the complex is thus equivalent to the amount of Cu^{II} in the solution. The method works well for Cu in various alloys and metal complexes. Reproducible and accurate results are obtained in the concentration range 3–32 mg per aliquot with a relative error of <0.6% and a standard deviation of <0.04%. The effect of various cations and anions is also studied. The interference of a number of ions, such as Zr^{IV}, Sn^{IV}, Ti^{III}, Hg^{II} and Pd^{II} can be overcome by the use of suitable secondary masking agents.

Keywords: Copper; complexometric titration; cysteine masking agent; alloy analysis; complex analysis

Complexometric methods for the determination of Cu have superseded the classical iodometric method because they are less prone to interference from ions commonly encountered in the analysis of various materials containing Cu. In these methods, the sample is dissolved in a suitable medium, the Cu^{II} is complexed with ethylenediaminetetraacetic acid (H₄edta) and the complex is decomposed by reducing Cu^{II} to Cu^I and stabilized as a Cu^I species. The H₄edta subsequently released from the complex is determined titrimetrically. Many methods have been reported in the literature for the determination of Cu based on the technique of masking. Thus binary or ternary reagent mixtures, such as ascorbic acid and thiocyanate,^{1,2} ascorbic acid and thiourea,³ thiourea, ascorbic acid and thiosemicarbazide⁴ (or a small amount of 1,10-phenanthroline or 2,2'-bipyridyl) or a single reagent serving as a reductant and a complexing agent, such as thiosulfate,⁵ thiourea,⁶ thioglycolic acid,⁷ mercaptopropionic acid⁷ and mercaptosuccinic acid⁸ have been used for decomposing the Cu^{II}–H₄edta complex. The applicability of such a method for the analysis of numerous alloys and ores is also studied and reported.^{2,7,8} Thiols are known to react with Cu^{II} to form a strong Cu^I complex as follows:



In this paper, the results of a study on the feasibility of using DL-cysteine, which can form a strong complex with Cu^{II}, is reported. The reagent is found to be a better chelating agent than those reported earlier.

Experimental

Reagents

Copper(II) standard solution. Prepared by dissolving CuSO₄·5H₂O of analytical-reagent grade in distilled water and standardized by the thiocyanate method.⁹

Ethylenediaminetetraacetic acid solution, ≈ 0.02 mol dm⁻³. Prepared by dissolving the disodium salt of H₄edta in distilled water.

Lead nitrate solution, 0.02 mol dm⁻³. Prepared by dissolving Pb(NO₃)₂ in distilled water and standardized by the chromate method.⁹

DL-Cysteine, 0.5% solution in water.

Xylenol orange, 0.5% solution in water.

Procedure

To a solution containing 3–32 mg of Cu, 0.02 mol dm⁻³ H₄edta solution is added in excess. The solution is diluted to about 100 ml and the pH is adjusted to 5.0–6.0 with hexamine. The excess of H₄edta is titrated with 0.02 mol dm⁻³ Pb(NO₃)₂ solution using Xylenol Orange as indicator. DL-Cysteine solution in water is then added in excess (molar ratio of copper to cysteine of 1 : 3). The change of colour from green to yellow is observed during the addition of the cysteine solution. The solution is left to stand for about 5 min with intermittent shaking. The H₄edta released is then titrated against the Pb(NO₃)₂ solution to the same end-point as before. The results of seven determinations of Cu^{II} are presented in Table 1.

Interference Study

A number of metal ions, rare-earth metal ions and anions are studied for their possible interference in the determination of Cu by this method. Cations such as Zr^{IV}, Sn^{IV}, Ti^{III}, Pd^{II} and Hg^{II} are found to interfere rather severely, but the interferences can be obviated by using suitable secondary masking agents such as fluoride (10% NH₄F, 5–10 ml) for Zr^{IV} (28 mg) and Sn^{IV} (10 mg), hydrazine sulfate (2% solution, 2–5 ml) for Ti^{III} (10 mg) and thiocyanate (5% NH₄SCN, 5–10 ml) for Pd^{II} (5 mg) and Hg^{II} (25 mg). The results are given in Table 2.

Analysis of Alloys

Samples (1.0–1.5 g) of copper-based alloys were dissolved in concentrated HNO₃ and the oxides of nitrogen expelled with the use of concentrated H₂SO₄ until the brown fumes ceased

Table 1 Determination of copper in copper sulfate solution, *n* = 5

Copper taken/mg	Copper found/mg	Standard deviation/mg	Recovery (%)
3.19	3.21	0.02	100.63
6.37	6.36	0.02	99.84
12.74	12.70	0.03	99.67
15.93	15.92	0.02	99.94
19.11	19.19	0.02	100.49
25.48	25.43	0.02	99.80
31.85	31.93	0.04	100.25

Table 2 Determination of copper in the presence of foreign metal ions and anions, $n = 3$. Copper present in the solution = 6.37 mg

Ion	Amount in solution/mg	Amount of Cu found/mg	Mean/mg	Recovery (%)
Zn ^{II}	10	6.38		
	50	6.39	6.39	100.31
Co ^{II}	6	6.36		
	30	6.38	6.37	100.00
Ni ^{II}	6	6.37		
	30	6.36	6.37	100.00
Cd ^{II}	16	6.37		
	32	6.38	6.38	100.16
Mn ^{II}	2.5	6.39		
	5	6.37	6.38	100.16
Fe ^{III}	6	6.39		
	12	6.37	6.38	100.16
Ce ^{III}	14	6.37		
	28	6.41	6.39	100.31
Cr ^{III}	5	6.35		
	10	6.36	6.36	99.84
Al ^{III}	5.5	6.36		
	27.5	6.38	6.37	100.00
Ru ^{III}	4	6.41		
	8	6.88	6.40	100.47
Rh ^{III}	4	6.42		
	8	6.39	6.41	100.62
Au ^{III}	4	6.39		
	8	6.39	6.39	100.31
La ^{III}	14	6.38		
	28	6.39	6.39	100.31
V ^{IV}	5	6.38		
	25	6.36	6.37	100.00
Ti ^{IV}	5	6.34		
	25	6.35	6.35	99.68
U ^{VI}	12	6.34		
	24	6.38	6.36	99.84
Pd ^{II}	1	6.38		
	5	6.39	6.39	100.31
Hg ^{II}	5	6.35		
	25	6.36	6.36	99.84
Tl ^{III}	2	6.41		
	10	6.38	6.40	100.47
Zr ^{IV}	14	6.37		
	28	6.38	6.38	100.16
Sn ^{IV}	5	6.39		
	10	6.37	6.38	100.16
Chloride	50	6.37		
	100	6.41	6.39	100.31
Fluoride	50	6.37		
	100	6.39	6.38	100.16
Acetate	50	6.39		
	100	6.37	6.38	100.16
Citrate	50	6.34		
	100	6.35	6.35	99.68
Tartrate	50	6.38		
	100	6.39	6.39	100.31
Phosphate	50	6.39		
	100	6.41	6.40	100.47

to evolve. The residue was extracted with distilled water and made up to 250 ml in a standard flask. Aliquots (5 ml) were used for titration as per the recommended procedure. For comparison, the Cu content in the alloys was also determined by thiocyanate. The results of the analysis are presented in Table 3.

Analysis of Copper Complexes

Samples (0.1–0.2 g) of the complex were decomposed using *aqua regia* (hydrochloric–nitric acid, 3 + 1) and heated to near dryness and the residue was dissolved in water and made up to 100 ml in a standard flask. Aliquots of 10 ml were used for the determination of Cu by the proposed procedure. The results are presented in Table 4.

Table 3 Analysis of copper alloys

Alloy	Copper found by complexometric titration* (%)	Standard deviation (%)	Copper found by thiocyanate–gravimetric method† (%)	Standard deviation (%)
Cu–Ni	71.22	0.03	71.28	0.06
Bronze	80.90	0.04	80.79	0.04
Brass	67.69	0.02	67.64	0.05
Aluminium–bronze	77.28	0.03	77.19	0.04
Gun-metal	85.10	0.04	84.96	0.05

* Average of four determinations.

† Average of three determinations.

Table 4 Analysis of copper complexes

Complex	Copper found (%)	Copper present (%)
Cu(CH ₃ N ₄ S) ₂ Cl ₂ *	18.20	18.34
Cu(C ₅ H ₈ N ₄ S)†	28.82	28.94
Cu(C ₉ H ₆ N ₄ OS)‡	23.04	22.99
Cu(C ₃ H ₅ N ₄ S)§	33.13	33.00
Cu(C ₁₀ H ₁₁ N ₄ OS)¶	21.36	21.29

* Copper complex of thiocarbohydrazide.

† Copper complex of 4-amino-5-mercapto-3-propyl-1,2,4-triazole.

‡ Copper complex of 4-amino-5-mercapto-3-(*p*-methoxyphenyl)-1,2,4-triazole.

¶ Copper complex of 4-amino-5-mercapto-3-methyl-1,2,4-triazole.

§ Copper complex of 3-(*o*-tolylloxymethyl)-4-amino-5-mercapto-1,2,4-triazole.

Results and Discussion

The quantitative displacement of H₄edta from the Cu–H₄edta complex by cysteine indicates that the Cu–cysteine complex is more stable than the Cu–H₄edta complex at room temperature and that H₄edta is released instantaneously. For the complete release of H₄edta, a slight excess of DL-cysteine above the molar ratio of 1 : 3 is necessary. A larger excess of the reagent does not have any adverse effect on the results of the determination of Cu. It is found that L-cysteine forms a 1 + 1 complex with Cu^{II},¹⁰ but during complexation Cu^{II} is reduced to Cu^I.

Merits of the Method

The merit of the reagent is that it does not form any precipitate with either Cu^{II}, the metal ion to be estimated, or Pb^{II}, the titrant, in the concentration range of Cu studied under the experimental conditions described. This facilitates a sharp end-point. The method works well especially at low concentrations of Cu^{II} in the range 3–32 mg per aliquot with a relative error of <0.6% and a standard deviation of <0.04%.

The main advantage of the proposed method is that heating or cooling is not required before or during the titration. The method does not involve extraction of the Cu–H₄edta complex and hence is simple and can be carried out rapidly in a single step. The H₄edta solution does not require standardization and no pH re-adjustment is required for the final titration.

References

- 1 Kores, E., and Rempert, H., *Chemist-Analyst*, 1957, **56**, 91.
- 2 Rao, B. V., Athavale, S. V., Rao, Y. V., Acharyalu, S. L. N., and Tamhankar, B. V., *Indian J. Technol.*, 1971, **9**, 157.

- 3 Raoot, K. N., Raoot, S., Rao, B. V., and Lahari, D. P., *Indian J. Technol.*, 1976, **14**, 254.
- 4 Singh, R. P., *Talanta*, 1972, **19**, 1421.
- 5 Cheng, K. L., *Anal. Chem.*, 1958, **30**, 243.
- 6 Pribil, R., and Vesely, V., *Talanta*, 1961, **8**, 743.
- 7 Raoot, S., Raoot, K. N., and Rukmani Desikan, N., *Indian J. Technol.*, 1983, **21**, 39.
- 8 Rukmani Desikan, N., and Vijayakumar, M., *Analyst*, 1985, **110**, 1399.
- 9 Vogel, A. I., *A Text Book of Quantitative Inorganic Analysis Including Elementary Instrumental Analysis*, Longmans, London, 4th edn., 1978, pp. 444–462.
- 10 Pierre, L., and Clande, H. J., *Bull. Soc. Chim. Fr.*, 1979, 457.

Paper 1/02681J

Received June 5, 1991

Accepted July 25, 1991

Analysis of Mixtures of Dialkyldithiophosphate, Bis(dialkoxythiophosphinoyl) Disulfide and Elemental Sulfur

Leszek Margielewski and Stanislaw Plaza*

Department of Chemical Engineering and Environmental Protection, University of Łódź, Pomorska 18, 91-416 Łódź, Poland

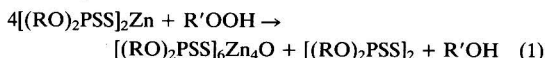
The method presented for the determination of zinc dialkyldithiophosphate, bis(dialkoxythiophosphinoyl) disulfide and elemental sulfur in the presence of each other is based on thiomercurimetric titrations. Zinc dialkyldithiophosphate is determined by titration with *p*-dimethylaminophenylmercury(II) acetate with Michler's thioketone as indicator. The sulfur and bis(dialkoxythiophosphinoyl) disulfide are determined after their reduction. Bis(dialkoxythiophosphinoyl) disulfide is reduced by using tributylphosphine and titration as for zinc dialkyldithiophosphate. The sulfur is treated with bis(2-methoxyethoxy) dihydride and titrated with *o*-hydroxymercuribenzoic acid in the presence of dithiofluorescein as indicator. The method is simple, rapid, reproducible and accurate and samples do not require separation or other preliminary stages prior to their analysis. The method is suitable for monitoring changes in thiophosphorus lubricating oil additives during engine runs.

Keywords: Zinc dithiophosphate; bis(dialkoxythiophosphinoyl) disulfide and elemental sulfur determination; thiomercurimetric titration; lubricating oil additives

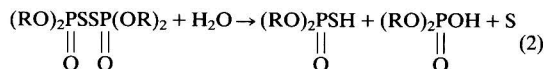
Zinc dialkyldithiophosphate (ZDTP) is added to lubricating oils to serve as an antioxidant. In addition, owing to the formation of protective films on metal surfaces, it prevents the corrosive attack of oxidation products, and also exhibits useful load-carrying properties.

Sodium and potassium dialkyldithiophosphates are used extensively as flotation collectors for sulfide minerals. These salts of dialkyldithiophosphoric acid have also been found to be an important class of analytical reagents for the separation and determination of metal ions.

It is generally accepted that ZDTPs act as both chain-breaking antioxidants (radical scavengers) and preventative antioxidants (hydroperoxide decomposers). Hydroperoxide is decomposed in an oxidation reaction with ZDTP¹ according to the equation



In a further reaction, the basic ZDTP $[(RO)_2PSS]_6Zn_4O$ is oxidized mainly to bis(dialkoxythiophosphinoyl) disulfide, $[(RO)_2PSS]_2$ (DS).² Elemental sulfur is formed in the reaction between DS and hydroperoxide with thionic sulfur elimination.³ Bis(dialkoxyphosphinoyl) disulfide is unstable and hydrolyses to dialkyl- and dialkylthiophosphoric acids and sulfur according to the reaction



It has been shown that the reaction products of ZDTPs formed during oxidation,¹⁻⁶ pyrolysis⁷ and engine runs⁸ include DS and basic ZDTPs as major products, with smaller amounts of the compounds $(RO)_2PSSR$, $(RS)_3PS$, $(RS)_3PO$, $(RS)_3P$, $(RO)_2P(O)SR$ and elemental sulfur.³ These thiophosphorus species were detected by ³¹P nuclear magnetic resonance (NMR) spectrometry. The antiwear and antioxidative behaviour of mixtures of these compounds may be different depending on the amounts of these thiophosphorus species. Hence, a knowledge of the changes in thiophosphorus species in working lubricants is necessary.

A procedure for the analysis of mixtures containing ZDTP, DS and elemental sulfur has not hitherto been reported; ZDTP and DS have been detected and satisfactorily deter-

mined in mixtures using ³¹P NMR spectrometry.^{1,2,4-8} Although the development of ³¹P NMR has opened the way for interesting investigations of lubrication mechanisms with the use of ZDTP, practical difficulties in dealing with very complicated mixtures that also contain elemental sulfur may appear formidable. In spite of an extensive literature on the determination of ZDTP, cited by Hutchings *et al.*,⁹ no one method can be recommended for analysis in the presence of DS and sulfur. Zinc dialkyldithiophosphate in the presence of DS may be determined by a titrimetric method using dimethylaminophenylmercury(II) acetate with Michler's thioketone as an indicator.¹⁰

Bis(dialkoxythiophosphinoyl) disulfide in the presence of ZDTP has been determined by a spectrophotometric method.¹¹ In this method, ZDTP interferes with the determination of DS; in the recommended procedure, ZDTP was separated with an ion-exchange resin, which complicates the analysis. Sulfur dissolved in hydrocarbon solution may be reduced with sodium aluminium bis(2-methoxyethoxy) dihydride to sulfide and determined by titration with *o*-hydroxymercuribenzoic acid.¹²

This paper reports a method for analysing mixtures of ZDTP, DS and elemental sulfur. For the determination of ZDTP and sulfur, the most suitable are thiomercurimetric methods as mentioned above,^{10,12} whereas for the determination of DS, an analytical investigation of the reduction of DS to the dialkyldithiophosphate anion, which can be determined by titration with *p*-dimethylaminophenylmercury(II) acetate, was undertaken.

Experimental

Reagents and Solutions

All chemicals and solvents were of analytical-reagent grade, except for *p*-dimethylaminophenylmercury(II) acetate (APM), zinc diisobutyldithiophosphate and bis(diisobutyloxythiophosphinoyl) disulfide, which were synthesized in this laboratory. Zinc diisobutyldithiophosphate was prepared from butan-2-ol, phosphorus pentasulfide, sodium hydroxide and zinc sulfate.¹³ Bis(*O,O*-diisobutyloxythiophosphinoyl) disulfide was obtained by oxidizing sodium dithiophosphate with iodine.¹⁴ The thiophosphorus compounds prepared were characterized by elemental analysis, and infrared (IR), ¹H and ³¹P NMR spectrometry. Pure APM was synthesized by the procedure developed by Pesci.^{15,16}

*To whom correspondence should be addressed.

Lubricating oils and lubricating oil additives were of technical grade.

A 0.01 mol dm⁻³ APM solution was prepared by dissolving 3.797 g of the reagent in 10 ml of dimethylformamide, adding 2 ml of acetic acid and diluting to 1 dm³ with absolute ethanol. This solution was further diluted with absolute ethanol to obtain the required concentrations. The solution can be used directly as a working standard without standardization. A stock solution of APM is stable for at least 3 months if stored in a dark bottle.

A 0.01% m/v indicator solution of Michler's thioketone (MT) was freshly prepared in absolute ethanol. Solutions of APM and MT are most stable in anhydrous solvents.

A 0.05 mol dm⁻³ solution of *o*-hydroxymercuribenzoic anhydride (HMB) (POCh, Gliwice, Poland) was prepared by dissolving 16 g of the reagent in a mixture of 20 g of diethanolamine and 50 ml of water and then in 200 ml of ethanol and, after standing for 3–4 h, filtering. This solution was standardized with diphenylthiourea.¹⁷ A 2 × 10⁻⁴ mol dm⁻³ solution was prepared by dilution with ethanol-water (9 + 1) containing 1% of diethanolamine. The stock solution was kept in a refrigerator.

A 0.01% m/v indicator solution of dithiofluorescein (POCh) was freshly prepared by dissolving 2 mg of indicator in 1 ml of a solution of 20 g of ethylenediaminetetraacetic acid (EDTA) (disodium salt) and 20 g of triethylamine in 1 dm³ of water and then diluting to 25 ml with water.

A 5 × 10⁻² mol dm⁻³ solution of tributylphosphine in toluene and a 0.01% m/v solution of sulfur in toluene were prepared.

White oil solutions of ZDTP (0.65% m/m), DS (0.65% m/m) and sulfur (0.01% m/m) and lubricating oil additives (the concentrations are given in Table 4) were prepared by dissolving these compounds in a technical-grade oil.

Titration Procedures

Determination of DS and ZDTP in the presence of each other

The procedures were calibrated by titration of various amounts of DS and ZDTP as follows.

To 0.1–2.0 g of oil sample containing more than 50 µg of each compound, which was diluted with chloroform or toluene to a total volume of 5 ml, a few drops of MT were added. The mixture was then titrated with APM, the end-point being indicated by the visual change of the solution from yellow to blue-violet. To the same solution 1 ml of tributylphosphine was added and the colour of the solution returned to yellow after 1 min. A 1 ml volume of sulfur solution was added and the solution was then titrated with APM to a blue-violet colour.

When greater amounts of oil were present in the solution, the mixture became non-homogeneous during titration owing to the formation of an alcoholic solution of the reagent. Further toluene or chloroform was added to obtain a clear solution. In a toluene solution of oils (containing ZDTP and DS to be analysed), the end-point was less sharp than in chloroform.

In the first titration APM was consumed by ZDTP and in the second by *O*,*O'*-diisobutyl hydrogen phosphorodithioate formed in the reduction of DS. In titration with 5 × 10⁻³–2 × 10⁻⁴ mol dm⁻³ reagents, a blank comparison solution of MT must be used, the titration being continued until the colours of both solutions match. The amount of reagent in the blank titration must be subtracted from the amounts of reagent when analysing the ZDTP and DS results.

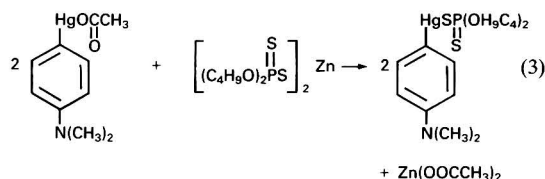
Determination of elemental sulfur in the presence of ZDTP and DS

To another 0.1–2.0 g of oil sample containing ZDTP and DS and sulfur (>0.5 µg), which was diluted with anhydrous, sulfur-free toluene to a total volume of 5 ml, a few drops of

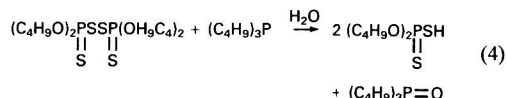
sodium aluminium bis(2-methoxyethoxy) dihydride (SAMD) were added, mixed and then 2 ml of ethanol–1 mol dm⁻³ NaOH (1 + 1 v/v) were added. Before the titration, ethanol was added to give a homogeneous solution and a few drops of dithiofluorescein were added. The solution was titrated with 2 × 10⁻⁴ mol dm⁻³ HMB to the disappearance of the blue colour of the indicator. In the titrations with 2 × 10⁻⁴ mol dm⁻³ HMB the value of the blank titration of the indicator is subtracted from the amount of reagent when analysing the results.

Theory

In samples containing ZDTP and DS, the ZDTP reacts with APM as follows:



One mole of ZDTP consumes 2 mol of APM; DS is reduced with tributylphosphine according to the reaction

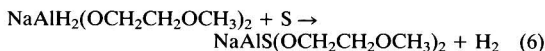


The unreacted tributylphosphine reacts with sulfur:

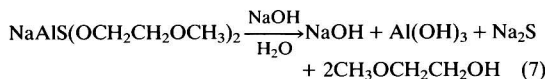


In the second titration 1 mol of DS reacts with 2 mol of APM.

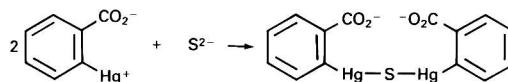
In the second sample elemental sulfur is reduced with SAMD according to



and then the product of reduction is decomposed with water:



Sulfide is determined by titration with HMB:



The reagent SAMD also reduces DS but not quantitatively, and ZDTP and (C₄H₉O)₂DSS⁻ do not interfere in the determination of S²⁻.

Results and Discussion

For the analysis of ZDTP–DS–sulfur mixtures, the determination of DS was the main problem studied. The studies included the choice of reductant, complete recovery and the effects of ZDTP, sulfur and lubricating oil additives on the determination of DS. Of the numerous methods for the reduction of disulfides, the most suitable for the determination of DS in the presence of ZDTP and sulfur is reduction with tributylphosphine. The procedure found to be most suitable is that detailed under Experimental. Table 1 gives the results of the determination of DS. The recovery was nearly 100%. The reproducibility of the determination of DS was good, with a relative standard deviation (RSD) of 2.07% when nine samples with a mean content of 1.255 mg were analysed. The method can be recommended for general use.

The results for the determination of ZDTP and DS in the presence of sulfur are presented in Table 2. The results were in good agreement with the amounts taken for analysis and the average recoveries of ZDTP and DS were near 100%. Further, these results show that ZDTP and DS can be determined in the presence of each other, and sulfur had no effect on the recovery of either compound.

Thiophosphorus compounds, potentially formed in lubricating oils during engine operation, also do not interfere in the

determination of ZDTP and DS. For example, Table 3 gives the results for the determination of ZDTP and DS in the presence of sulfur and (RO)₂PSSR. Good reproducibility of the determination of DS was confirmed, with an RSD of 1.15% ($n = 4$). The apparent increase in the recovery of DS is connected with lower recoveries of ZDTP.

A possible interference from other lubricating oil additives in the determination of DS was also studied. Other additives commonly present in fully formulated lubricating oils were added to the DS solution to determine the effect of each on the

Table 1 Determination of bis(*O,O*-diisobutylthiophosphinoyl) disulfide

Sample No.	Taken/mg	Found/mg	Recovery (%)
1	0.315	0.324, 0.320, 0.309, 0.314	100.5
2	0.945	0.942, 0.972, 0.942, 0.955	100.8
3	1.260	1.325, 1.266, 1.295, 1.325	103.4
4	1.798	1.803, 1.803, 1.805, 1.745	99.6

Table 2 Determination of bis(*O,O*-diisobutylthiophosphinoyl) disulfide and zinc diisobutylthiophosphate in the presence of elemental sulfur (0.01%)

Sample No.	Taken/mg		Found/mg		Recovery (%)	
	ZDTP	DS	ZDTP	DS	ZDTP	DS
1	2.79	2.39	2.80	2.37	100.6	99.2
2	2.79	2.39	2.77	2.41	99.7	100.8
3	2.79	4.78	2.79	4.80	100.0	100.4
4	2.79	4.78	2.73	4.88	97.8	102.1
5	5.58	2.39	5.76	2.35	103.2	98.3
6	5.58	2.39	5.64	2.22	101.1	98.9
7	5.58	4.78	5.42	4.83	97.1	101.1
8	5.58	4.78	5.57	4.91	99.4	102.7
Average					99.8	100.4

Table 3 Determination of bis(diisobutylthiophosphinoyl) disulfide and zinc diisobutylthiophosphate in the presence of (RO)₂PSSR and elemental sulfur (S 0.01%)

Sample No.	Taken/mg		Found/mg		Recovery (%)	
	ZDTP	DS	ZDTP	DS	ZDTP	DS
1	5.58	4.78	5.44	4.86	97.5	101.7
2	5.58	4.78	5.46	4.86	97.8	101.7
3	5.58	4.78	5.46	4.98	97.8	104.2
4	5.58	4.78	5.50	4.90	98.6	102.5
Average					97.9	102.5

Table 4 Effect of other lubricating oil additives on the determination of bis(*O,O*-diisobutylthiophosphinoyl) disulfide

Lubricating oil additive	Concentration (% m/m)	DS taken/mg	DS found/mg			Recovery (%)	
Polyisobutyl succinimide	3.0	1.31	1.26	1.26	1.26	1.26	96.2
		0.655	0.664	0.657	0.652	0.659	100.4
		0.262	0.273	0.242	0.273	0.262	100.2
Octadecylamine	1.0	1.476	1.490	1.471	1.459	1.443	99.3
		0.737	0.735	0.735	0.740	0.741	100.1
		0.295	0.294	0.296	0.290	0.293	99.4
2,6-Di- <i>tert</i> -butyl-4-methylphenol	0.5	1.476	1.520	1.490	1.541	1.530	103.0
		0.947	0.941	0.965	0.953	0.954	100.7
		0.295	0.320	0.320	0.297	0.291	104.1
Poly(methyl methacrylate)	3.0	1.300	1.300	1.290	1.290	1.307	100.1
		0.655	0.660	0.661	0.653	0.651	100.2
		0.262	0.249	0.261	0.266	0.260	98.9
Basic barium sulfonate (TBN-20)	3.0	1.256	1.210	1.220	1.230	1.241	97.6
		1.004	1.020	0.996	1.008	1.006	100.3
		0.502	0.498	0.503	0.498	0.501	99.6

Table 5 Determination of bis(*O,O*-diisobutylthiophosphinoyl) disulfide and zinc diisobutylthiophosphate in a fully formulated mineral oil

Sample No.	Taken/mg		Found/mg		Recovery (%)	
	ZDTP	DS	ZDTP	DS	ZDTP	DS
1	2.745	1.179	2.74	1.18	99.8	100.1
2	2.745	1.179	2.74	1.23	99.8	104.3
3	2.745	1.179	2.69	1.19	97.9	101.0
4	2.745	1.179	2.71	1.21	98.9	102.7
5	2.745	1.179	2.74	1.23	99.8	104.3
Average					99.2	102.5

Table 6 Determination of elemental sulfur in the presence of zinc diisobutylthiophosphate, bis(*O,O*-diisobutylthiophosphinoyl) disulfide and (RO)₂PSSR

Sample No.	Taken/mg	Found/mg	Average recovery (%)	Relative standard deviation (%)
1	12.96	12.39, 12.14, 13.87, 12.14, 13.39	100.0	4.6
2	265.6	263.7, 267.9, 255.3, 251.1, 257.0	97.5	1.7

Table 7 Results of the determination of zinc diisobutylthiophosphate, bis(*O,O*-diisobutylthiophosphinoyl) disulfide and sulfur in mineral oil after four-ball wear test. Load, 30 kg; time, 30 min; temperature of oil, 80 °C

Concentration/10 ⁻³ mol dm ⁻³			
ZDTP		DS	Sulfur
Before test	After test	After test	After test
23.68	17.82	3.96	1.20

recovery of DS. The other lubricating oil additive concentrations were selected for study arbitrarily, but these concentrations may be used in practice. The results for the determination of DS are given in Table 4. Only in the presence of *tert*-butylphenol were the recoveries of DS increased by approximately 3%. No apparent interference from any of the other lubricating oil additives tested was observed in the determination of DS.

Table 5 gives the results of the determination of ZDTP and DS in the presence of sulfur and the composition of lubricating oil additives in mineral oil. The concentrations of lubricating oil additives were as follows: succinimide 2%, viscosity improver 6%, calcium sulfonate 3% and 2,6-di-*tert*-butyl-4-methylphenol 1%. Generally, the results of the recovery of DS are 2.5% high, and all the results for ZDTP are low. The end-point was located visually and because the analysed oil was coloured it was probably responsible for these errors.

Elemental sulfur can be determined in the presence of DS, ZDTP and the other organic thiophosphorus compounds tested by the procedure described under Experimental. Table 6 gives the results of the determination of sulfur. The recoveries and precision of the method were generally good. The results for the determination of sulfur were also not influenced by the other lubricating oil additives.

An application of the proposed method is illustrated in Table 7, which shows the results of a four-ball machine wear test for 30 min with mineral oil containing ZDTP and carbon black; the concentrations of ZDTP, DS and sulfur in the oil were also determined.

The recommended method is generally satisfactory for the determination of more than 1×10^{-7} mol dm⁻³ of ZDTP and DS and more than 0.5 µg of elemental sulfur in the presence of each other. Hence concentrations of ZDTP and DS as low as 0.01% in 1 ml or 1 g samples of used lubricating oil solutions can be determined with good reproducibility.

Some used oils were so dark that the visual location of the end-point was not possible, and the determination of ZDTP and DS was therefore carried out by two-phase titration, in which the end-point was indicated by the visual change in the ethanol layer from yellow to blue-violet. In the determination of ZDTP, DS and sulfur, metal dithiocarbamates interfere, as dithiocarbamates react with APM and *o*-hydroxymercuribenzoic acid.

Conclusions

The proposed procedure for the analysis of mixtures of ZDTP, DS and elemental sulfur is rapid, simple, reproducible and accurate, and samples do not require preliminary separation or another intermediate stage prior to their analysis. In view of the results obtained and the simplicity of the procedure, the method can be recommended for the determination of mixture composites in working lubricating oils.

References

- 1 Paddy, J. L., Brook, P. S., and Waters, D. N., *J. Chem. Soc., Perkin Trans. 2*, 1989, 1703.
- 2 Rossi, E., and Imparato, J., *Chim. Ind. (Milan)*, 1971, **53**, 838.
- 3 Sanin, P. J., Blagovidov, J. F., Vipper, A. B., Kuliev, A. M., Krein, S. E., Ramaya, K. S., Shor, G. J., Sher, V. V., and Zaslavsky, Y. S., *New Concepts of the Mechanism of Action and Depletion of Motor Oil Additives*, 8th World Petrol. Cong., Proc., 5, 91, Applied Science Publishers, London, 1971.
- 4 Burn, A. J., *Tetrahedron*, 1966, **22**, 2153.
- 5 Brunton, G., Gilbert, B. C., and Mawby, R. J., *J. Chem. Soc., Perkin Trans. 2*, 1976, 650.
- 6 Paddy, J. L., Lee, N. C., and Waters, D. N., *Tribol. Trans.*, 1990, **33**, 15.
- 7 Watkins, R. C., *Tribol. Int.*, 1982, **15**, 13.
- 8 Marshall, G. J., *Appl. Spectrosc.*, 1984, **38**, 522.
- 9 Hutchings, M. J., Moody, G. J., and Thomas, J. D. R., *Analyst*, 1987, **112**, 601.
- 10 Plaza, S., *Analyst*, 1984, **109**, 1313.
- 11 Plaza, S., *Microchem. J.*, 1982, **27**, 544.
- 12 Wroński, M., *Talanta*, 1974, **21**, 776.
- 13 Brazier, A. D., and Elliott, J. S., *J. Inst. Pet.*, 1967, **53**, 63.
- 14 Hu, P.-F., and Cheng, W.-Y., *Hua Hsueh Hsueh Pao*, 1956, **22**, 215; *Chem. Abstr.*, 1958, **52**, 7186c.
- 15 Pesci, E., *Gazz. Chim. Ital.*, 1899, **23**, 521.
- 16 Pesci, E., *Chem. Zentralbl.*, 1901, **1**, 452.
- 17 Wroński, M., *Talanta*, 1977, **24**, 347.

Paper 1/04156H

Received August 9, 1991

Accepted October 11, 1991

Spectrophotometric Determination of Quaternary Ammonium Salts by a Flow Injection Method Coupled With Thermochromism of Ion Associates

Tadao Sakai

Department of Chemistry, Asahi University, 1851 Hozumi, Hozumi-cho, Gifu 501-02, Japan

A selective and rapid spectrophotometric method has been established for the determination of cetylpyridinium and benzalkonium chlorides by a flow injection technique coupled with ion-pair extraction and thermochromism of the ion associates. Selectivity can be enhanced because the absorbance of ion association compounds formed between co-existing amines and the anionic tetrabromophenolphthalein ethyl ester disappears at elevated temperatures in the flow cell. Accordingly, interferences due to amine associates can be eliminated by absorbance measurement at 45 °C. The sample throughputs were 60 h⁻¹ for cetylpyridinium and 50 h⁻¹ for benzalkonium. The calibration graphs were linear in the range 5×10^{-7} – 2×10^{-6} mol dm⁻³ for both compounds. The relative standard deviations ($n = 5$) for 1×10^{-6} mol dm⁻³ cetylpyridinium and benzalkonium at 45 °C were both 2.1%. The proposed method was used for the selective and rapid determination of quaternary ammonium compounds in pharmaceuticals.

Keywords: Cetylpyridinium and benzalkonium chloride determination; ion-pair extraction with tetrabromophenolphthalein ethyl ester; flow injection; thermo-spectrophotometry

Although Bromophenol Blue (BPB)¹ and Bromocresol Green² have been commonly used as ion-association reagents for quaternary ammonium salts, these dyes are diprotic acids which show a narrow optimum pH range for extraction and poor extractability of the ion associates into organic solvents. In addition, linearity of the calibration graphs in the lower concentration ranges is poor. Therefore, monoprotic acidic dyes such as Orange II,³ sodium picrate,⁴ 4-(2,6-dibromo-4-hydroxyphenylimino)cyclohexa-2,5-dienone⁵ and tetrabromophenolphthalein ethyl ester (TBPE),⁶ which have a wider optimum pH range compared with diprotic acid dyes were investigated as ion-association reagents for trace amounts of quaternary ammonium salts. Of these reagents, TBPE has the advantages of larger molar absorptivity (1×10^5 l mol⁻¹ cm⁻¹), superior extractability and good reproducibility. However, TBPE is not suitable for the selective determination of quaternary ammonium compounds and amines by the convenient method⁷ at pH 8–9. When the pH is increased, interferences from amines decrease but are not eliminated completely.

Benzethonium has been determined by a solvent extraction–flow injection (FI) method using the coloured BPB–quinine associate.⁸ Although this method has good selectivity, the manifold is complicated and sample throughput low.

It has been observed that the absorbance of ion-association compounds formed between TBPE and amines approaches zero at 60 °C.⁹ It follows that thermochromism of amine associates might be used to eliminate the interference of amines in the determination of quaternary ammonium salts.

This paper describes an FI system with solvent extraction and a temperature-controlled micro-scale flow cell for the selective, sensitive and rapid determination of cetylpyridinium and benzalkonium.

Experimental

Reagents

All reagents were of analytical-reagent grade and were used without further purification.

Stock standard cetylpyridinium solution, 1×10^{-3} mol dm⁻³. Prepared by dissolving 0.0358 g of cetylpyridinium chloride (Kishida Chemical, Tokyo) in distilled water and diluting to 100 ml. Other standards were prepared by appropriate dilution of the stock solution.

Stock standard benzalkonium solution, 1×10^{-3} mol dm⁻³. Prepared by dissolving 0.0354 g of benzalkonium chloride (Nakalai Tesque, Kyoto) in distilled water and diluting to 100 ml. Other standards were prepared by appropriate dilutions.

Amine solution, 5×10^{-3} mol dm⁻³. Prepared by dissolving appropriate amounts of amine hydrochloride or hydromaleate in distilled water.

Buffer solution, pH 3–13.0. Prepared by mixing equal volumes of 0.3 mol dm⁻³ potassium dihydrogen phosphate and 0.1 mol dm⁻³ sodium borate. The pH was adjusted with 1 mol dm⁻³ sodium hydroxide or 0.5 mol dm⁻³ sulfuric acid.

TBPE solution in dichloroethane (TBPE-H), 1×10^{-4} mol dm⁻³. Prepared by adding 0.1 mol dm⁻³ hydrochloric acid to 25 ml of aqueous 4×10^{-4} mol dm⁻³ TBPE potassium solution (TBPE-K) until the colour changed from blue to yellow. The solution was then equilibrated with 100 ml of 1,2-dichloroethane. Working solutions were prepared by appropriate dilutions.

Apparatus

A Hitachi Model 556 double-beam spectrophotometer and a Hitachi Model 057 x-y recorder were used with 10 mm cells for absorption measurements. Extractions were carried out with an Iwaki Model KM shaker. A Hitachi–Horiba pH meter with a combined glass electrode was used.

Procedure for the Batchwise Method

Place an aliquot (0.5–5 ml) of 1×10^{-5} mol dm⁻³ cetylpyridinium or benzalkonium solution and 1 ml of buffer solution (pH 12.8) into a 100 ml separating funnel and dilute the mixture with distilled water to 10 ml. Shake the solution mechanically with 5 ml of 1×10^{-5} mol dm⁻³ TBPE-H solution for 5 min. Transfer the organic phase into a test-tube fitted with a stopper and centrifuge to remove water droplets. Measure the absorbance at 610 nm against a reagent blank as a reference at 25 or 45 °C.

Procedure for the FI Method

A schematic diagram of the flow system used is shown in Fig. 1. The absorbance was measured at 610 nm using a Soma Optics Model S-3250 double-beam spectrophotometer (data

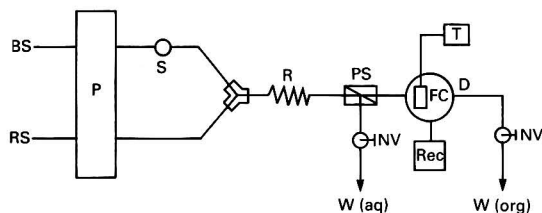


Fig. 1 Schematic diagram of the flow system for the determination of quaternary ammonium salts. BS, buffer solution (pH 12.5); RS, reagent solution (5×10^{-6} mol dm $^{-3}$ TBPE-H in dichloroethane); P, pump (flow rate, 0.8 ml min $^{-1}$); S, sample injector (sample volume 140 μ l); R, reaction tubing (0.5 mm i.d. \times 2 m); PS, phase separator; FC, thermo-controlled micro-scale flow cell; D, spectrophotometric detector; T, thermo-controller; Rec, recorder; NV, needle valve; and W, waste

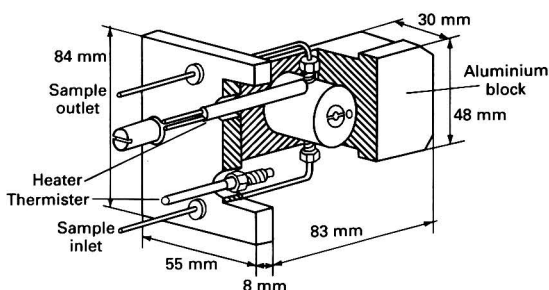


Fig. 2 Cut-away diagram of the thermo-controlled micro-scale flow cell

output, 0–10 mV) with a 10 mm flow cell (8 μ l). The flow cell was a laboratory-made thermo-controlled cell as displayed in Fig. 2. A constant temperature within the range 20–80 °C was maintained by a compact thermocontroller (Shimaden, Tokyo). Signals were recorded using a Toa Electronics FBR-251A recorder. A double-plunger micropump (Sanuki Kogyo, DM2U-1026) was used to propel the carrier solution and the reagent solution. The samples (140 μ l) were injected into the carrier stream by a six-way injection valve (dead volume, 80 μ l) to which a 60 μ l loop was attached. The membrane of the phase separator was made of porous poly(tetrafluoroethylene) (PTFE). Flow lines were of PTFE tubing (0.5 mm i.d.).

Results and Discussion

Effect of pH on Batchwise Extraction of Ion-association Complexes With TBPE-H

The effect of pH on the extraction of cetylpyridinium, procaine, diphenhydramine, chlorpheniramine and methylephedrine was examined in the pH range 3.4–12.8 with 1×10^{-5} mol dm $^{-3}$ TBPE-H in dichloroethane solution. The results are shown in Fig. 3. Absorbance of the blue TBPE-cetylpyridinium associate, which has λ_{\max} at 610 nm, was maximum and constant in the pH range 8.0–12.8. On the other hand, absorbance of the red association complexes formed between TBPE-H and the amines mentioned above was maximum in the pH range 8–10, with the absorbance decreasing markedly at higher pH values. Furthermore, the absorbances of ion association complexes formed with all the amines examined except chlorpheniramine were close to that of the reagent blank. Consequently, interferences due to these amines could be eliminated.

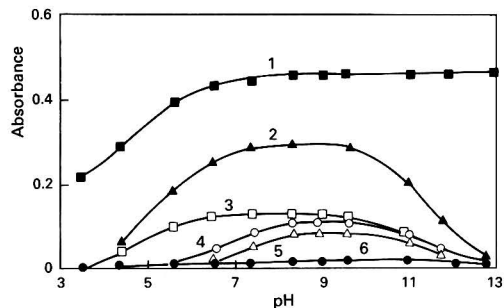


Fig. 3 Effect of pH on batchwise extraction of TBPE associates: 1, 2.5×10^{-6} mol dm $^{-3}$ cetylpyridinium; 2, 2.5×10^{-5} mol dm $^{-3}$ chlorpheniramine; 3, 2.5×10^{-5} mol dm $^{-3}$ diphenhydramine; 4, 2.5×10^{-5} mol dm $^{-3}$ procaine; 5, 2.5×10^{-5} mol dm $^{-3}$ methylephedrine; and 6, reagent blank. TBPE-H, 1×10^{-5} mol dm $^{-3}$; wavelength, 610 nm; and reference, water

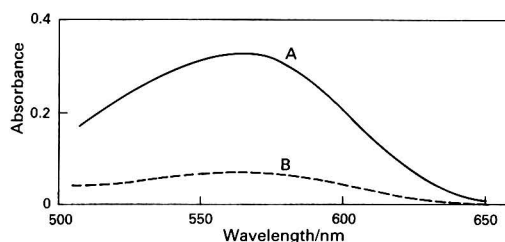
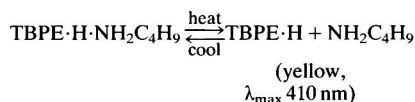
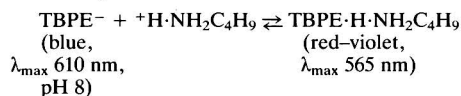


Fig. 4 Effect of temperature on the absorption spectrum of TBPE-H-butylamine associate: A, 20 °C; and B, 45 °C. Butylamine, 2×10^{-5} mol dm $^{-3}$; TBPE-H, 3.2×10^{-4} mol dm $^{-3}$; pH, 8; and reference, water

Thermochromism of Amine Association Complexes With TBPE-H

In a previous paper,⁹ it was reported that TBPE-H-amine association complexes exhibit changes in absorbance with temperature (thermochromism). As can be seen in Fig. 4, absorbance by the TBPE-H-butylamine associate (λ_{\max} , 565 nm) approaches zero when the temperature is increased from 20 to 45 °C. Accordingly, a temperature of 45 °C was chosen to eliminate interferences from amines in the determination of cetylpyridinium and benzalkonium salts. It is assumed that TBPE-H reacts with amines to form ion-association compounds that dissociate at elevated temperatures as shown below for butylamine.



The chemical bond between the proton and butylamine is not strong, hence, increasing the temperature might cause the ion-association compound to dissociate to the free acid and amine. At temperatures over 45 °C, the red colour due to the ion-association compound is seen to disappear completely.

Effect of pH in the FI method

The extraction of cetylpyridinium was examined in the pH range 3–12.5 with 5×10^{-6} mol dm $^{-3}$ TBPE-H in dichloroethane solution. The peak height remained constant at a

maximum over the range pH 7–12.5. This range was much wider than that observed for acetylcholine under similar conditions.¹⁰

Effect of TBPE·H Concentration

Effect of the TBPE·H concentration on the formation of ion association complexes was investigated. The concentration of TBPE·H was varied from 1×10^{-6} to 2×10^{-5} mol dm⁻³. Although a maximum peak height was obtained at concentrations $> 5 \times 10^{-6}$ mol dm⁻³ for 1×10^{-6} mol dm⁻³ cetylpyridinium, at higher TBPE·H concentrations the tolerable concentration of co-existing amines was lower and the baseline was noisier. In this work therefore, 5×10^{-6} mol dm⁻³ TBPE·H solution in dichloroethane was used.

Comparison of Phase Separators

Two kinds of phase separator were compared and the designs are shown in Fig. 5. Type A, designed by Motomizu and Oshima,¹¹ has a sloped groove (membrane chamber depth, 2 mm; membrane chamber width, 2 mm) with a porous PTFE membrane (0.8 µm pore size). Type B, designed by the authors, has a body made of poly(chlorotrifluoroethylene) and a microporous PTFE tube (i.d., 1 mm; thickness 0.5 mm; porosity 60%; length 2.5 cm). With both separators, the organic phase was recovered sufficiently. However, with type B, the peaks were broader and the retention time was longer. For efficient phase separation, type A was used in this work.

Other Variables

In order to examine the efficiency of extraction, the length of the extracting coil was varied from 1 to 4 m. Although the maximum peak height was obtained when the tubing was 3 m in length, 2 m of tubing was chosen. With this length, sample throughput was greater and peak height was only 8% less than that with 3 m of tubing. The effect of the sample injection volume over the range 100–180 µl was investigated; a 140 µl

volume was chosen. Of the extracting solvents, 1,2-dichloroethane, dichloromethane and 1,3-dichlorobenzene, the first was found to be the best for colour stability and reproducibility of extraction. Flow rates of 0.8 ml min⁻¹ were chosen for the reagent and carrier solutions.

Calibration Graphs

At 25 and 45 °C, good linear relationships were found over the range 5×10^{-7} – 2×10^{-6} mol dm⁻³ of cetylpyridinium when 140 µl of the standard solutions were injected. The relative standard deviations ($n = 5$) were 2.0% for 1×10^{-6} mol dm⁻³ cetylpyridinium at 25 °C and 2.1% at 45 °C. The limit of detection [signal-to-noise (S/N) = 3] was 6.1×10^{-8} mol dm⁻³ at 25 °C and 6.3×10^{-8} mol dm⁻³ at 45 °C. The peak height at 45 °C was about 10% less than that at 25 °C.

Similar results were obtained for benzalkonium. The relative standard deviations ($n = 8$) were 1.8% for 1×10^{-6} mol dm⁻³ at 25 °C and 2.1% at 45 °C. The limit of detection (S/N = 3) was 6.3×10^{-8} mol dm⁻³ at 45 °C. The sample throughputs were 60 h⁻¹ for cetylpyridinium and 50 h⁻¹ for benzalkonium.

Table 1 Effect of some amines on cetylpyridinium determination at different temperatures by an FI method: cetylpyridinium concentration, 1×10^{-6} mol dm⁻³; TBPE·H in dichloroethane solution, 5×10^{-6} mol dm⁻³; pH, 12.5; and wavelength, 610 nm

Compound	[Amine]: [cetylpyridinium]	Recovery (%)	
		25 °C	45 °C
Procaine	20	100	—
	30	108	98
	30	100	—
Diphenhydramine	30	100	—
Chlorpheniramine	1	100	—
	2	118	100
	5	142	98
Ephedrine	40	102	—
	80	121	100
Methylephedrine	30	100	—
Eserine	40	103	100
Butylamine	10	110	100
Trimethylamine	10	101	—
Triethylamine	20	106	98
	1	100	—
	2	120	102
Triethanolamine	10	99	—

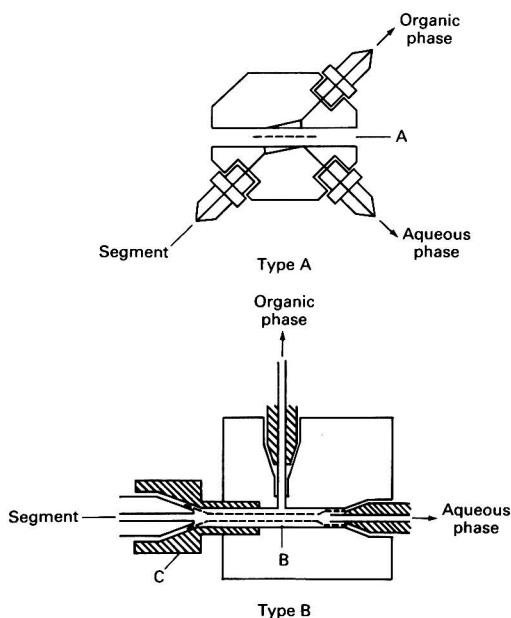


Fig. 5 Phase separators tested. A, PTFE membrane filter (pore size 0.8 µm); B, microporous PTFE tube (1 mm i.d., thickness 0.5 mm, porosity 60%, length 2.5 cm); and C, connector made of Daiflon

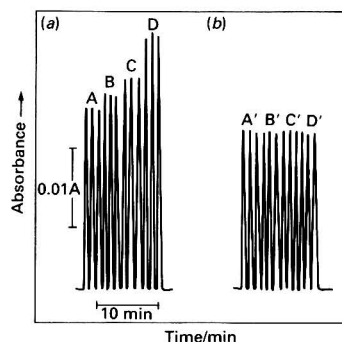


Fig. 6 Flow injection signals of TBPE–cetylpyridinium and a mixture with amine associates at (a) 25 and (b) 45 °C: A and A', 1×10^{-6} mol dm⁻³ cetylpyridinium; B and B', 3×10^{-5} mol dm⁻³ procaine with cetylpyridinium; C and C', 2×10^{-6} mol dm⁻³ chlorpheniramine with cetylpyridinium; and D and D', 5×10^{-6} mol dm⁻³ chlorpheniramine with cetylpyridinium. TBPE·H, 5×10^{-6} mol dm⁻³; pH, 12.5

Table 2 Determination of cetylpyridinium and benzalkonium in commercial samples by the FI method, $n = 3$

Sample	Nominal/ mg	25 °C		45 °C	
		Found/ mg	Recovery (%)	Found/ mg	Recovery (%)
1*	1.00	1.25 ± 0.02	124	0.97 ± 0.03	97.3
2†	4.00	4.37 ± 0.13	109	3.97 ± 0.12	99.2
3‡	1.00	1.46 ± 0.02	145	0.98 ± 0.02	97.9
4§	0.1	0.101 ± 0.01	101	—	—

* Main content: cetylpyridinium chloride; chlorpheniramine maleate (2 mg); naphazoline hydrochloride (1 mg); and iproheptine hydrochloride (3 mg).

† Main content: cetylpyridinium chloride; and dextromethorphan (90 mg).

‡ Main content: cetylpyridinium chloride; chlorpheniramine maleate (5 mg); and procaine hydrochloride (5 mg).

§ Main content: benzalkonium chloride.

Interferences

Various other amines (Table 1) were added to cetylpyridinium and their interferences on the determination were studied. Inorganic compounds including sodium chloride, calcium chloride and sodium acetate had previously been found not to interfere.^{7,9} Aliphatic and aromatic amines (triethylamine, triethanolamine, butylamine, chlorpheniramine and procaine) gave positive errors at 25 °C but their interferences were eliminated by absorbance measurement at 45 °C. Flow injection signals for standard cetylpyridinium and for mixtures with procaine or chlorpheniramine solutions at 25 and 45 °C are shown in Fig. 6.

Application

Practical use of the method was assessed by applying it to the determination of cetylpyridinium and benzalkonium in pharmaceutical preparations. Sample solutions were prepared after filtration and suitable dilution. Table 2 shows the results obtained at 25 and 45 °C with the FI system. Although strong interferences from co-existing amines were observed at 25 °C, the interferences could be satisfactorily eliminated in the determination of cetylpyridinium at 45 °C.

In conclusion, the FI method coupled with solvent extraction and thermochromism of ion associates, described in this paper, has the advantages of sensitivity, selectivity and rapidity for quaternary ammonium salt determinations.

This research was partially supported by a Grant-in-Aid for General Scientific Research, No. 3640503, from the Ministry of Education, Science and Culture (Japan).

References

- 1 Auerbach, E., *Ind. Eng. Chem. Anal. Ed.*, 1943, **15**, 492.
- 2 Irving, H. M. N. H., and Markham, J. J., *Anal. Chim. Acta*, 1967, **39**, 7.
- 3 Scott, G. V., *Anal. Chem.*, 1968, **40**, 768.
- 4 Sakai, T., *Bunseki Kagaku*, 1978, **27**, 444.
- 5 Tsurubo, S., Ohno, N., and Sakai, T., *Nippon Kagaku Kaishi*, 1980, **6**, 828.
- 6 Sakai, T., *Bunseki Kagaku*, 1975, **21**, 199.
- 7 Sakai, T., Hara, I., and Tsubouchi, M., *Chem. Pharm. Bull.*, 1976, **24**, 1254.
- 8 Miyaji, T., Hibi, K., and Sakai, T., *Bunseki Kagaku*, 1990, **39**, 73.
- 9 Sakai, T., and Ohno, N., *Analyst*, 1981, **106**, 584.
- 10 Sakai, T., Gao, Y., Ohno, N., and Ura, N., *Chem. Lett.*, 1991, 163.
- 11 Motomizu, S., and Oshima, M., *Analyst*, 1987, **112**, 295.

Paper 11/04044H

Received August 5, 1991

Accepted October 7, 1991

Micellar Systems in Flow Injection: Determination of Gadolinium With 1-(2-Pyridylazo)-2-naphthol in the Presence of Triton X-100

José Luis Pérez Pavón and Bernardo Moreno Cordero*

Department of Analytical Chemistry, Nutrition and Food Sciences, University of Salamanca, Salamanca, Spain

The optimum conditions for the determination of Gd using the Gd-1-(2-pyridylazo)-2-naphthol (PAN) system in micelles of Triton X-100 have been studied. Under the conditions chosen, the molar absorptivity was $4.8 \times 10^4 \text{ dm}^3 \text{ mol}^{-1} \text{ cm}^{-1}$. It is possible to determine Gd at levels of between 0.9 and $8.8 \mu\text{g ml}^{-1}$ by injection into a stream, buffered at pH 9.2, containing $1.2 \times 10^{-3} \text{ mol dm}^{-3}$ PAN (Triton X-100: PAN = 0.15 g: 1.0 mg). The influence of the presence of electrolytes in the matrix on peak height was studied. The interferences produced by heavy metals were eliminated by extracting their diethyldithiocarbamates into $\text{CHCl}_3\text{-EtOAc}$ (1 + 1).

Keywords: Gadolinium determination; micellar media in flow injection; 1-(2-pyridylazo)-2-naphthol; Triton X-100; rare earths

Various analytical techniques have been used for the determination of rare earths at trace levels such as neutron activation, isotope dilution, mass spectrometry, and X-ray methods. However, most of these techniques require specialized and expensive instruments. The increasing importance of these elements in high technology components and many other fields¹⁻³ has required the development of simple and rapid analytical methods for their determination. Flow injection (FI) is an excellent technique for such purposes owing to its simplicity, versatility and low cost. However, there are few reports on the use of FI for the determination of rare earths.⁴⁻⁶

1-(2-Pyridylazo)-2-naphthol (PAN) has been employed both for spectrophotometric determination⁷ and for the extraction and separation of rare earths.⁸⁻¹⁰ However, both the chromophore and the chelates formed are insoluble in water, necessitating the use of aqueous alcoholic media or other less polar solvents.⁸⁻¹¹

The high solubilization capacity of micellar systems has permitted the modification or the development of analytical procedures in which the extraction process can be avoided and, in many instances, the sensitivity and selectivity of the procedure can be enhanced.^{12,13}

The great analytical potential inherent in the use of organized molecular systems in general, and micellar systems in particular, together with the advantages of these systems, has found application in virtually all analytical techniques, both in the determination of trace elements¹⁴ and in separation.¹⁵ However, there are very few reports concerning the use of these methods in FI.^{4,5}

In the present work, the spectrophotometric behaviour of the Gd-PAN system in the presence of Triton X-100 was studied. A method is proposed for the determination of trace amounts of Gd using an FI technique.

Experimental

Reagents

A standard solution of Gd was prepared by dissolving the appropriate amount of the oxide (99.9%, Sigma) in 1 ml of concentrated HCl and diluting with water. Solutions of PAN were prepared by dissolving appropriate amounts of the product (Merck) in aqueous solutions of Triton X-100.

Apparatus

A Varian Techtron Model 635 spectrophotometer with a Radiometer Rec 61 recorder and 1 cm optical pathlength

cuvettes was used. The pH measurements were performed with a Radiometer PHM 51 pH meter.

The manifold (Fig. 1) was constructed by using Teflon tubing (0.5 mm i.d.) and a Gilson Minipuls (4 channels) peristaltic pump. The sample injector was a Rheodyne 2050 valve with interchangeable loops of different capacities. The absorbance was measured with a Coleman 55 spectrophotometer with a Hellma 178 12-QS flow cuvette with a pathlength of 1 cm and an internal volume of 18 μl .

All statistical parameters were obtained with the 'Statworks' program for an Apple Macintosh computer.

Procedure

In the spectrophotometric determination, the solution of PAN in Triton X-100 (Triton X-100: PAN = 0.15 g: 1.0 mg) and variable amounts of Gd were added to 5.0 ml of a buffer solution (pH = 9.2), bringing the volume up to 50 ml with distilled water. The absorbance was measured at 560 nm against a blank, after 30 min.

In the determinations using FI, 123 μl of Gd solution at pH 2.2 (HCl) were injected in the presence of 0.4 mol dm^{-3} NaNO_3 into a stream of $1.2 \times 10^{-3} \text{ mol dm}^{-3}$ PAN (Triton X-100: PAN = 0.15 g: 1.0 mg), buffered at pH 9.2 ($0.005 \text{ mol dm}^{-3}$ $\text{HBO}_2\text{-BO}_2^-$) and the FI responses were recorded at 560 nm.

Results and Discussion

Spectrophotometric Study of the Gd-PAN-Triton X-100 System

In a buffered medium ($\text{HBO}_2\text{-BO}_2^-$, pH = 9.2) and in the presence of Triton X-100 the Gd-PAN system exhibits two absorption maxima at 535 and 560 nm, respectively (Fig. 2).

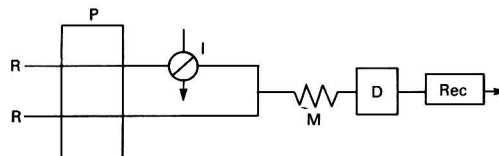


Fig. 1 Schematic diagram of the manifold used for the determination of Gd: R, reagent [$1.2 \times 10^{-3} \text{ mol dm}^{-3}$ PAN; Triton X-100: PAN, 0.15 g: 1.0 mg; pH = 9.2 ($\text{HBO}_2\text{-BO}_2^-$)]; P, peristaltic pump ($q_{\text{total}} = 4.4 \text{ ml min}^{-1}$); I, injection valve (123 μl); D, detector ($\lambda = 560 \text{ nm}$); M, mixing coil (20 cm); and Rec, recorder

* To whom correspondence should be addressed.

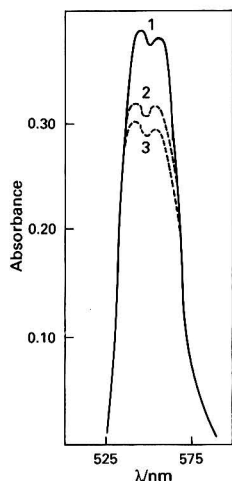


Fig. 2 Absorption spectra of the Gd-PAN system: 8.0×10^{-6} mol dm $^{-3}$ Gd; and 8.0×10^{-5} mol dm $^{-3}$ PAN. 1, Triton X-100: PAN = 0.15 g: 1.0 mg; and 2 and 3, extracts in diethyl ether (recorded after 5 and 30 min)

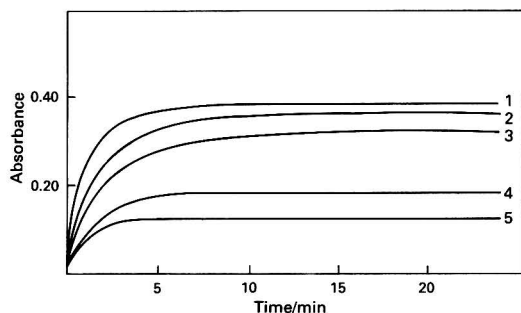


Fig. 3 Variations in absorbance with time and the ratio of Triton X-100: PAN for Triton X-100: PAN ratios (g: mg) of 1, 0.15; 2, 0.25; 3, 0.50; 4, 1.00; and 5, 1.50: 8.0×10^{-6} mol dm $^{-3}$ Gd, 8.0×10^{-5} mol dm $^{-3}$ PAN and pH = 9.2 (0.02 mol dm $^{-3}$ $\text{HBO}_2\text{-BO}_2^-$)

The spectrum obtained is similar to that obtained without using Triton X-100 but extracting with diethyl ether, the most suitable medium according to Shibata⁸ for determination; this extract is, however, not stable.

The time required to reach the maximum response does not depend on the concentration of Triton X-100, but rather on the Triton X-100: PAN ratio; the signal decreases as this ratio increases (Fig. 3) owing to a decrease in the concentration of the chromophore in the micelles as their number increases. Similar effects have been described by other workers.¹⁶

The variation in the absorbance with pH produces a bell-shaped curve (Fig. 4), which exhibits a plateau for pH values between 8 and 10; the working pH chosen was 9.2.

In the presence of Triton X-100, the slope ratio method indicated a stoichiometry of 1:3 (Gd: PAN). This ratio differs from the values reported by other workers.^{8,17}

The system obeys Beer's law at 560 nm in media buffered at pH 9.2 (0.02 mol dm $^{-3}$ $\text{HBO}_2\text{-BO}_2^-$), fitting the equation $A = 4.8 \times 10^4 [\text{Gd}] + 0.006$ ($r = 0.9998$).

The micellization process causes modifications in the pK values of dissociation and protonation of the chromophore¹⁸ as a function of the concentration of the surfactant in solution. However, as the dissociation pK would be shifted towards higher values, under the experimental conditions

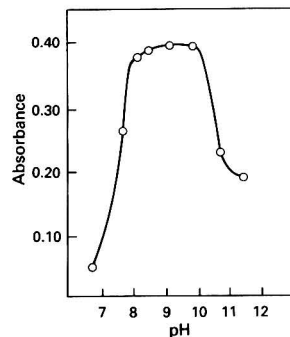


Fig. 4 Variations in absorbance with pH: 8.0×10^{-6} mol dm $^{-3}$ Gd; 8.0×10^{-5} mol dm $^{-3}$ PAN; and Triton X-100: PAN = 0.15 g: 1.0 mg

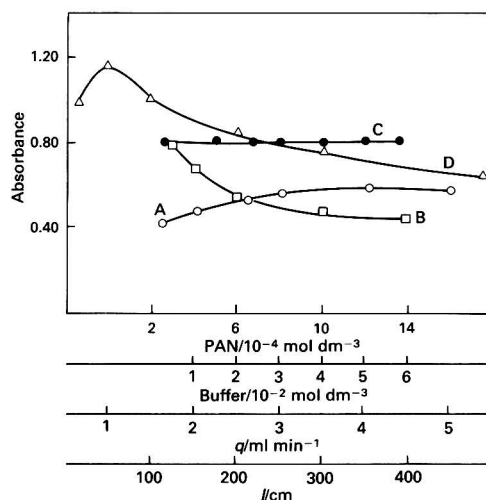
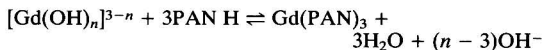


Fig. 5 Influence of manifold and chemical variables on the peak height. A, PAN; B, buffer; C, q (flow rate); and D, l (length of mixing coil). Sample, 8.0×10^{-5} Gd; pH, 4.9, carrier, Triton X-100: PAN = 0.15 g: 1.0 mg; pH, 9.2 ($\text{HBO}_2\text{-BO}_2^-$) and injection volume, 123 μ l

used in this work, PAN must be present mainly in the undissociated form. Moreover, as the lanthanide must be present in the form of a hydroxy complex, the complexing reaction can be expressed as:



Determination of Gd Using FI

The influence that the presence of the surfactant might exert on the shape and the parameters defining the FI response was studied by injecting 123 μ l of Carmoisine (40 ppm) into a simple single channel manifold [length of mixing coil (l) = 50 cm; flow rate (q) = 2.2 ml min $^{-1}$] and into a stream of water in which the concentration of Triton X-100 was varied from 0.001 to 5%. No appreciable changes appeared in the FI responses obtained, indicating that the presence of micelles in the system does not affect the response.

Optimization of the Analytical Parameters

Fig. 5 shows the influence of the concentration of PAN, the flow rate, the length of the reactor and the concentration of buffer solution on peak height.

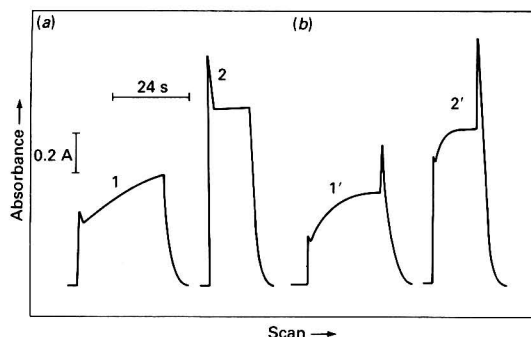


Fig. 6 Stopped flow FI responses. (a) Pump stopped after t (residence time); and (b) pump stopped before t . 1 and 1', pH of the sample = 4.9; 2 and 2', pH of the sample = 2.6

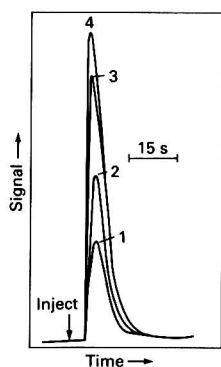


Fig. 7 Variations in peak height 1 and 2, in the presence and absence of NaNO_3 . 1, pH = 4.9; 2, pH = 2.6; 3, pH = 4.9, $0.4 \text{ mol dm}^{-3} \text{ NaNO}_3$; and 4, pH = 2.6, $0.4 \text{ mol dm}^{-3} \text{ NaNO}_3$

Injection volumes greater than $123 \mu\text{l}$ produce double peaks, which are unsuitable for analytical purposes.

The pH of the sample must be between 2 and 3; lower pH values cause double peaks and higher pH values lead to a drop in the signal, owing to a decrease in the rate of exchange of the OH groups by PAN. In order to verify this, stopped-flow FI responses were obtained, halting the pump before and after the residence time (t) for samples at pH 2.6 and 4.9 (Fig. 6).

If the pump is halted after time t it can be seen, at pH 2.6, that the signal does not increase with the reaction time (complete reaction, high ligand exchange rate), whereas at pH 4.9, an increase in the signal takes place, indicating a slower exchange of ligands.

If the pump is stopped before time t , at pH 2.6, the signal is seen to increase faster than at pH 4.9 and reaches constant absorbance in a shorter time.

The presence of electrolytes in solution modifies both the shape and size of the micelles,^{19,20} mainly because of ionic exchange on their surfaces.²¹ Further, electrolytes can modify the initial reaction rates, which causes a large matrix effect in some FI determinations.

Fig. 7 shows the variations in peak height in the presence and absence of $0.4 \text{ mol dm}^{-3} \text{ NaNO}_3$ at two different pH values; higher concentrations of salt increase the blank signal, hindering calibrations. The other electrolytes studied (KCl, KNO_3 , NaCl and NaClO_4) produce similar effects.

Analytical Characteristics of the Method

For the analytical conditions chosen [$\lambda = 560 \text{ nm}$, injection volumes = $123 \mu\text{l}$, flow rate (q) = 4.4 ml min^{-1} and $l = 50 \text{ cm}$],

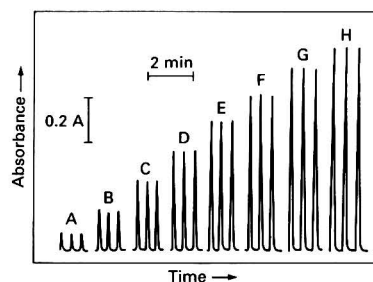


Fig. 8 Calibration peaks for injection of A, 0.9; B, 2.1; C, 3.4; D, 4.6; E, 5.7; F, 6.9; G, 7.8; and H, 8.8 ppm of Gd. Reagent: $1.2 \times 10^{-3} \text{ mol dm}^{-3} \text{ PAN}$; Triton X-100; PAN, 0.15 g; 1.0 mg; pH, 9.2 ($\text{HBO}_2\text{-BO}_2^-$); $q_{\text{total}} = 4.4 \text{ ml min}^{-1}$; $V_i = 123 \mu\text{l}$; $\lambda = 560 \text{ nm}$; and mixing coil, 20 cm

the peak absorbance varies linearly with the concentration of Gd between 0.9 and 8.8 ppm (Fig. 8), and fits the equation $A = 0.06 + 1.6 \times 10^4 [\text{Gd}]$ ($r = 0.9999$). Measurements of ten solutions containing 1.5 ppm of Gd gave a relative standard deviation of 0.48%.

Interferences

Of the anions studied, the following do not interfere (error $\leq 3\%$) at an anion:Gd ratio of 100:1 ($\text{Gd} = 8.0 \times 10^{-6} \text{ mol dm}^{-3}$): F^- , Cl^- , Br^- , I^- , NO_3^- , SO_3^{2-} and CO_3^{2-} . Oxalate, phosphate and citrate interfere and must be absent. The interference produced by heavy metals (except for Ce^{IV}) can be eliminated by extracting their diethyldithiocarbamates with a mixture of $\text{CHCl}_3\text{-EtOAc}$ (1 + 1). The interference produced by Ce^{IV} can be eliminated by precipitating the basic salt formed with KBrO_3 . All the other lanthanides interfere.

References

- Kolbourn, B. T., *J. Less-Common Met.*, 1985, **111**, 1.
- Yoldjian, B., *J. Less-Common Met.*, 1985, **111**, 17.
- Falconnet, P., *J. Less-Common Met.*, 1985, **111**, 9.
- FIAsTAR Flow Injection Analysis Bibliography, 1974–1988.
- Moreno Cordero, B., Pérez Pavón, J. L., and Hernández Méndez, J., *Quim. Anal.*, 1989, **8**, 231.
- Růžička, J., and Hansen, E. H., *Anal. Chim. Acta.*, 1988, **214**, 1.
- Marczenko, Z., *Spectrophotometric Determination of Elements*, Ellis Horwood, Chichester, 1976.
- Shibata, S., *Anal. Chim. Acta.*, 1959, **22**, 470.
- Pustelnik, N., Kuznik, B., and Czakis Sulikowska, D. M., *Anal. Chim. Hung.*, 1985, **118**, 93.
- Czakis Sulikowska, D. M., and Malinowska, A., *Anal. Chim. Hung.*, 1985, **118**, 121.
- Kuznik, B., *Inorg. Nucl. Chem.*, 1981, **43**, 3363.
- Hinze, W. L., in *Solution Chemistry of Surfactants*, ed. Mittal, K. L., Plenum Press, New York, 1979, vol. 1.
- Pelizzetti, E., and Premauro, E., *Anal. Chim. Acta*, 1985, **169**, 1.
- Cline Love, L. J., Habarta, J. G., and Dorsey, J. G., *Anal. Chem.*, 1984, **56**, 133A.
- Armstrong, D. W., *Sep. Purif. Methods*, 1985, **14**, 213.
- Rosendorfova, J., and Cermakova, L., *Talanta*, 1980, **27**, 705.
- Navratil, O., *Collect. Czech. Chem. Commun.*, 1960, **31**, 2492.
- Al'bota, L. A., *J. Anal. Chem. USSR (Engl. Transl.)*, 1985, **40**, 771.
- Díaz García, M. E., and Sanz-Medel, A., *Talanta*, 1986, **33**, 255.
- Chen, J., Su, T., and Mou, Ch. Y., *J. Phys. Chem.*, 1986, **90**, 2418.
- Callahan, J. H., and Cook, K. D., *Anal. Chem.*, 1982, **54**, 59.

Paper 1/03687D

Received July 19, 1991

Accepted September 9, 1991

BOOK REVIEWS

HPLC in Pharmacy and Biochemistry

Edited by Magda Šaršunová, Oldrich Hanč and Bohumil Kakáč. Pp. x + 335. Hüthig. 1990. Price DM98.00. ISBN 3-7785-1699-X.

This book is aimed at chemists interested in the analysis of drugs or in clinical biochemistry and at students, and is said to be suitable for continuing education of pharmacists and clinical biochemists. It is a translation from the original 1984 Czechoslovakian edition, which has been revised to some extent. Despite its 1990 preface, it contains no references beyond 1987.

A short introduction on the development of chromatographic methods is followed by a general section, on the principles of chromatographic methods and a comparison of HPLC with other methods, a theoretical section, and a section covering working techniques including instruments, columns, selection of stationary and mobile phases, detection and quantification. These parts form a minor portion of the book and give brief surveys of the topics covered. Much information is summarized in tables, for example eluotropic series of solvents and available column packings. However, the references are selective and do not appear to date beyond 1981: for example, that for a listing of size-exclusion supports is dated 1980. There is no discussion of microbore HPLC.

The major part, comprising more than three-quarters, of the book summarizes the applications of HPLC in pharmaceutical and toxicological analysis (about half) and in biochemistry and clinical analysis (about one quarter). In this part, sub-sections are devoted to statements of methods and results reported for particular classes of drugs or analytes. A main class, such as drugs acting on the central nervous system, is broken down into separate sections covering groups of anaesthetics, hypnotics and sedatives, antiepileptics, and so on. Many sub-sections cover only one or two pages. Selected chromatograms are reproduced in some sections. A useful feature is the provision of separation data in tabular form which enables the salient characteristics of methods for certain substances to be appreciated rapidly. However, the information is given in the text in a factual manner only and there is little discussion of the relative merits of different analytical systems to guide the reader.

The book concludes with a two-page summary of abbreviations used and an index. It is not clear why the publisher has also included advertisements for other books on chromatography dated no later than 1988.

Although well printed, the text suffers from erratic proof-reading. This book is flawed by the lack of recent references in a rapidly developing field, which means that much of the information presented is out of date, and by the lack of critical assessment of the material included. It cannot be recommended as fulfilling the aims claimed for it.

D. H. Calam

HPLC in Clinical Chemistry

By I. N. Papadoyannis. *Chromatographic Science Series. Volume 54*. Pp. x + 488. Marcel Dekker. 1990. Price \$115.00 (US and Canada); \$138.00 (all other countries). ISBN 0-8247-8139-2.

High-performance liquid chromatography (HPLC) is nowadays widely used in clinical laboratories and there is scope for an up-to-date review of the topic for those training or working as clinical chemists. Unfortunately, Dr. Papadoyannis has missed the mark with this volume. I assume that this is partly

due to ignorance of what clinical chemists actually do. On page 91, for example, we are told that most routine clinical chemistry is now conducted using HPLC. While it is true that an increasing number of specialized assays are performed by HPLC, multichannel autoanalysers still reign supreme as far as 'sample-crunching' is concerned. Indeed, many common analytes (Na^+ , HCO_3^-) are not amenable to HPLC anyway.

Part One (96 pages) aims to cover instrumentation but columns, retention mechanisms and even sample preparation are also discussed. Worthies such as Tswett get a mention but the references stop at 1986; many (most?) are from the 1970s. The mode adopted for reference citation is unhelpful; many are grouped ('18-37'), no titles are given, and 'repeats' later in a chapter are given a new number. The full reference might be repeated in a later chapter. The text itself rambles. For example, three methods for barbiturates are given in Chapter 1 (Basic Principles), yet 20 pages are devoted to this topic in Part Two (Applications). Quaint terminology abounds. Thus, on page 4 we are told that solvent extraction is useful for 'erasing' interfering compounds. The arrangement of Figures is curious: most of the legend to Figure 5.1 (page 55), for example, is situated halfway down page 58. Chapter 8 (General Guide, 4 pages) consists of 2 pages of flow-sheets from Waters publications from 1983 and 1985...

Is Part Two any better? The choice of applications chapters is an odd mixture for a book supposedly concerned with clinical chemistry: amino acids, alkaloids, antibiotics, aflatoxins, barbiturates, carbohydrates, catecholamines, drugs/street drugs, enzyme activity, lipids and lipoproteins, proteins, prostaglandins, steroids, tocopherols and vitamins—were they meant to be ordered alphabetically? Little on nucleosides, organic acids (such as oxalate), porphyrins, or aspects of therapeutic drug monitoring/toxicology (anticonvulsants, antidepressants, cardioactive drugs, cyclosporin, paracetamol, salicylates, theophylline) of concern to clinical chemists. Hopefully someone will find these applications chapters useful, but much of the text and illustrations are lists of what others did with little attempt at interpretation. The references date up to 1988 (1989 for one of the author's papers), although more recent ones cluster at the ends of chapters. Some are inappropriate: in Chapter 13, for example, we are referred to UK Office of Population Censuses and Surveys Mortality Statistics from 1980 for information on sample preparation for barbiturate analysis! There are many spelling and citation errors: ref. 63 (page 388), for example, cites Volume 123 of *Analytical Biochemistry* and then gives up the ghost.

The Index (8 pages) contains the usual vague ('gear box', 'life span', 'liquid chromatograph', 'velocity') and redundant ['adrenaline', 'epinephrine'; 'phenobarbitone' (*sic*), 'phenobarbital'; 'quinalbarbitone', 'secobarbital'] entries; there is also an alphabetical list of the headings of the applications chapters. All this without even bothering to criticize the quality of the information presented in the book: surely a pointer to someone else to do better.

R. J. Flanagan

Biotransformations. Volume 3. A Survey of the Biotransformations of Drugs and Chemicals in Animals

Edited by David R. Hawkins. Pp. 462. The Royal Society of Chemistry. 1991. Price £89.50. ISBN 8-85186-177-G.

This third volume, in what has become an excellent series, more than lives up to expectations. The select group of leading scientists in the field of biotransformation, joined in this volume by Dr. D. Rance, have made another admirable attempt at collating and summarizing the 1989 literature dealing with the metabolism of various chemical entities in vertebrates, particularly mammals.

The format of Volume 3 follows those of Volumes 1 and 2, and appropriately begins with a listing of key functional groups, plus an overview that draws attention to particular findings in investigations that represent more than just straightforward expansion of the general database. This highlighting of results describing novel metabolic pathways and stereoselective/stereospecific processes is to be commended, and is extremely useful to the reader. The overview might be enhanced still further if it were to include the identification of some examples of where particular biotransformations appear to demonstrate genetic polymorphism with important consequences.

The body of the book describes the content of published articles on the biotransformation of chemicals ordered according to their class. In the vast majority the given précis of the results are of an appropriate length and give adequate detail. Whilst there is no doubt that it is the biotransformation data that are of the utmost importance, for some readers it would be additionally helpful if the experimental techniques used were described in a little more detail where they represent an extension of the generic use of the technique or are indeed truly novel. This inclusion would give completeness to the texts in the Volume, even though the reader is fully able to go to the original article if so desired, as the reference is given at the end of each summary.

Volume 3 is a review of 1989 literature. It is, therefore, somewhat surprising to see reference to several articles published in 1988, especially to those appearing in readily accessible journals such as *Xenobiotica*, *Biochemical Society Transactions* and *European Journal of Drug Metabolism and Pharmacokinetics*. (There is even one from 1987, and, strangely enough, one from 1990!)

The editor, and the RSC, are to be particularly congratulated for the additional information given at the back of Volume 3. Thus, there is now a Key Functional Group index, and it, together with the Compound Index, is cumulative across Volumes 1–3. These enhancements greatly improve the usefulness and speed of accessibility of the desired information contained in the Series thus far. Consideration might be given in future volumes to including also an alphabetical, but non-cumulative, list of the references cited. This is partly recommended because certain groups of workers have become associated with certain specialist areas of investigation, and such a list would enable the reader to see quickly whether a contribution of theirs or of interest to them has been included in the volume.

Finally, I would like to echo the thoughts of all scientists to whom biotransformation makes an important contribution to their working lives, by thanking the contributors to Volume 3 for their sterling efforts in its production, and state that we wait with eager anticipation for Volume 4.

C. M. Kaye

Spectroscopy of Biological Molecules

Edited by R. E. Hester and R. B. Girling. *Proceedings of the Fourth European Conference on the Spectroscopy of Biological Molecules, York, UK, September 1–6, 1991*. Pp. xxiii + 464. The Royal Society of Chemistry. 1991. Price £55.00. ISBN 0-85186-437-6.

If you want to find out what is going on at the forefront of research on spectroscopic studies of biological molecules, then this is a good book to browse. There is a lot going on: time-resolved X-ray diffraction, X-ray absorption, picosecond vibrational, and multidimensional NMR spectroscopy combined with molecular graphics, mechanics and dynamics, and more. The systems covered are also wide-ranging—from whole cells, photosystems and lipid membranes, to enzymes,

proteins, DNA, drugs and co-factors. The articles are short conference abstracts, nearly 200 of them in all, many written in the style of papers. I am reading the book only one month after the conference was held—exactly the right timing for publication of material of this type.

As you read the book that familiar conference-eve feeling comes over you: you can sense where the excitement is and your appetite is whetted for the detailed lectures that follow. But as the appendices are not full of videos (could such things be marketed?) all you can do is head for the library. The (camera-ready) papers provide a useful source of references for more detail about particular topics. They are too short themselves to provide it. The style of them is variable; some have no references at all.

The book serves as a reminder that no one technique provides all the information required to solve real biological problems. We should employ a combination of methods with their different time and spatial resolutions. It is all too easy these days, given the sophistication of modern spectroscopic machinery, to become immersed in one's own favourite technique and not appraise critically from time-to-time whether another would be better or add complementary information. This alone is a good reason for reading this book.

The price is high for a book of conference abstracts; a soft cover would have done as the papers will certainly date quickly and be over-written by primary publications from the same authors. If the abstracts had been published as a supplement to an issue of a regular RSC journal they would have been guaranteed a place in all major libraries. At £55 they may not be.

Peter J. Sadler

Effects of Drugs on Clinical Laboratory Tests

By Donald S. Young. Third Edition. Pp. ii + 944. American Association for Clinical Chemistry Press. 1990. Price \$65.00 (AACC Members): \$100.00 (Others). (Outside USA add \$3.00 per book, postage.) ISBN 0-915274-53-1.

The primary function of this directory is to alert the clinical chemist to the possible contribution of drug therapy to abnormal or unexpected test results. The increasing complexity of this subject is clearly illustrated by the major expansion and revision of this third edition compared with the previous lists published in 1975. New drugs and new laboratory tests continue to be introduced and the number of publications highlighting their interaction is also increasing. In an attempt to keep up with these developments the information has been stored on an extensive computer database from which this book has been compiled. It shares a common format with another complementary AACC publication: *Effects of Disease on Clinical Laboratory Tests* (2nd edn.), by R. B. Friedman and D. S. Young, AACC Press, Washington, DC, 1989.

The directory is divided into four alphabetical sections and a numerical list. The first section is an index of laboratory tests and the second an index of drugs cross-referenced to relate generic names to proprietary names. The third section describes the effects by laboratory test and the fourth lists effects by drug. A similar format is used for entries in both of these sections, which form the main body of the work. Each entry lists drug name, body fluid and analyte measured. It also describes the mechanism of the effect where known, listing whether it is physiological, pharmacological or analytical and thereby affects the measurement procedure. Each entry includes a reference number and the fifth section is the list of these references.

The editor is acutely aware of both the need for this information and the limitations of this format. The introduc-

tion draws attention to the contribution of drug metabolites and the parent compound. It notes that drugs are often given in combination, adding to the difficulties of interpretation. It also discusses variations in the metabolic processes of individuals and the possibility that the disease process can modify response. It is also apparent that incomplete information is presented in many of the references, *e.g.*, the concentration of drug at which the effect was observed is not stated, it is unclear if the effect was large enough to have clinical significance or the effects are only reported at non-physiological or inappropriate drug dosage.

Despite these significant limitations, this publication provides a useful, reasonably contemporary, first source of references when laboratory results require cautious interpretation and is particularly relevant for the clinical chemist for whom it was intended. Computer databases are becoming increasingly valuable aids to laboratory and clinical diagnosis, understanding disease processes, and designing and monitoring appropriate therapy. Direct computer access to the database used for this compilation, and its integration into local systems, could make this work even more useful.

Roger S. Ersser

Phosphorimetry. Theory, Instrumentation and Applications

Robert J. Hurtubise. Pp. xii + 370. VCH. 1990. Price DM114.00; £45.00. ISBN 0-89573-749-3 (VCH Publishers); 3-52727-861-3 (VCH Verlagsgesellschaft).

This is an excellent and up-to-date text-book on phosphorimetry. The author has presented a detailed survey of this technique since its inception and has competently discussed modern developments of phosphorimetry, which should be of interest to all researchers working in the field of luminescence spectrometry. This book should be considered as a very useful reference text.

The first chapter presents an historical survey of phosphorimetry and the photophysical phenomena of luminescence are discussed in detail in Chapter 2. Chapter 3 gives a concise coverage of the instrumentation used in phosphorimetry although this subject is also considered in other chapters of the book. A variety of important analytical parameters in phosphorescence measurements are very clearly discussed in Chapter 4. Instrumental aspects, sample preparation and the methodology of low-temperature phosphorimetry are covered in Chapter 5, which includes discussions on phosphorescence line-narrowing spectrometry. Chapters 6–10 discuss various theoretical and practical aspects of room-temperature phosphorimetry (RTP). Chapters 6–8 cover solid-surface RTP, Chapters 9 and 10 present sensitized and quenched RTP. The solid-surface technique is a new development in phosphorimetry and has great potential in analytical science. Chapter 11 presents briefly the applications of phosphorescence of proteins, polypeptides and peptides, and Chapter 12 discusses the use of the technique in polymer research. The final Chapter (13), discusses the future trends in phosphorimetry.

The summary and consolidation of materials presented by the author in this text-book are certainly valuable and the book will be a useful addition to libraries and research workers in this and related fields. Although a few typographical errors appear in some of the common and useful equations, the quality of the book remains high. The publication of the book is timely and is to be welcomed, as is its reasonable price.

R. Narayanaswamy

NMR, NQR, EPR, and Mössbauer Spectroscopy in Inorganic Chemistry

R. V. Parish. *Ellis Horwood Series in Inorganic Chemistry*. Pp. 223. Ellis Horwood. 1990. Price £29.95. ISBN 0-13-625518-3.

This book aims at providing an introduction to the interpretation of four types of spectra that have proved to be particularly useful in inorganic chemistry. The introductory chapter (15 pages) considers the various features that nuclear magnetic resonance, nuclear quadrupole resonance, nuclear gamma resonance (Mössbauer spectroscopy) and electron paramagnetic resonance have in common. The remaining chapters deal with each spectroscopic method in turn (NMR, 85; NQR, 17; Mössbauer, 40; and EPR, 35 pages). The techniques are introduced from scratch and are described primarily from a practical viewpoint. These four chapters follow a similar pattern. A consideration of the experimental conditions is followed by a simplistic account of the fundamentals of the method and a discussion of illustrative applications. Each chapter concludes with a set of problems and answers of graded complexity.

This is a well-written and eminently readable book that will be of considerable value to established workers in the inorganic field and to newcomers in this area. It lives up to its stated aim of providing guidance for the practising inorganic chemist. Its major emphasis is of course on 'first-order' phenomena and how to obtain chemical information from such spectra. The unravelling of more complex spectra receives little attention, but it cannot be otherwise in a treatment of four resonance techniques *ab initio* in 200 pages. Texts giving more comprehensive coverage of these topics are listed in the bibliographies. Relevant properties of NMR and NQR isotopes and of isotopes for Mössbauer spectroscopy are tabulated in appendices.

The book is well produced and is good value for money by present-day standards. I recommend it to inorganic chemists and to teachers looking for advanced material for undergraduate courses.

B. D. Flockhart

Guide to Flow Cytometry Methods

By W. McLean Grogan and James M. Collins. Pp. x + 228. Marcel Dekker. 1990. Price \$99.75 (US and Canada); \$119.50 (All other countries). ISBN 0-8247-8330-1.

Flow cytometry is a fairly recent development in scientific terms and commenced with Coulter producing a device for counting cells, based on differing electrical conductivity between cells and the medium in which they were suspended, some 25 years ago.

This book traces the development of the technique from then to its present state, with its many diverse applications. It is very good in presenting the theory and background to the subject, but the real strength of this book lies in its practical nature with its many applications, and is obviously based on the dedicated experience of the authors themselves. There are chapters on the production of single cell suspensions and DNA analysis with the emphasis on practical detailed methodology.

Theory and application of light scattering and immunofluorescence are described, once again with specific methods. There are also considerations of intracellular pH, calcium and glutathione, followed by cell surface receptors and membrane potentials. For a small book it has a very extensive coverage of the subject and includes many procedures likely to be of use to

workers in flow cytometry laboratories, including clinical and laboratory animal techniques. Indeed our own FACS laboratory is waiting for me to release the book so that they can apply some of the techniques themselves. Being small, the book is essentially brief and it would benefit from a glossary; however, it is well referenced, has a useful appendix and extensive technical data. This, then, is an excellent book providing practical aid for the laboratory worker. It should be in every FACS laboratory but the price may put some people off. Nevertheless it is a book I would highly recommend.

John F. Stevens

Infrared Spectroscopy of Adsorbed Species on the Surface of Transition Metal Oxides

By A. A. Davydov. Pp. xiv + 243. Wiley. 1990. Price £65.00. ISBN 0-471-91813-X.

This is the 1990 translation into English of A. A. Davydov's book first published in Russian in 1984. The book substantially reviews the author's work at the Institute of Catalysis at the USSR Academy of Sciences, Siberian Branch, much of it undertaken over a ten year span from the early 1970s to the early 1980s. As such, the book belies its rather general title, and is perhaps better regarded as a specialist treatise.

The author begins by considering the spectral characteristics of active sites on oxide surfaces—hydroxyl groups, coordinatively unsaturated cations and surface oxygen—and discusses how far infrared spectroscopy can assist us in establishing the chemical properties of these centres by adsorption of simple probe molecules. A lengthy chapter is devoted to the characterization of the oxidation state of surface cations on a range of supported metal catalysts and transition metal exchanged zeolites by adsorption of CO and NO. This is followed by a discussion of the adsorption of alkenes on oxide surfaces, which begins by considering each of the separate structures that can arise on alkene adsorption. Finally, the author considers the applications of infrared spectroscopy to mechanistic studies of heterogeneous catalytic reactions. He succeeds in demonstrating the power of the technique when used in conjunction with other approaches, notably thermal desorption and ESR.

Regarded as a specialist review, this book is valuable; the author's painstaking and high quality work has done much to aid our understanding of the chemical reactivity of oxide surfaces, particularly in catalytic processes. The book contains over 400 references to the literature. Unfortunately, as there is a six year gap between publication of the original manuscript and this translation, most of the citations are to work that is now between 10 and 20 years old, much of it in Russian journals. A large part of the usually cited Western literature, for example on the partial oxidation of alkenes, is not included. Whilst the book will provide an excellent source of reference for the specialist, one wonders why Wiley, in preparing this translation for publication, did not take the opportunity to have the citations updated and widened.

The author states clearly from the outset that he does not intend to discuss the technique of IR itself. However, the age of the original text is exposed by the author's mention of the advent of FTIR in the penultimate paragraph of the book; although it is not stated, presumably all spectra shown were recorded with dispersive instruments. Although this does not detract from the quality of the data included, or the discussion and analysis of it, it adds to the specialist nature of the work.

Viewed in the light of a specialist publication, the cover price is probably reasonable, but this is most certainly not a general text.

Wendy R. Flavell

Carbon, Nitrogen and Sulphur Pollutants and Their Determination in Air and Water

By Jerome Greyson. Pp. xi + 338. Marcel Dekker. 1990. Price \$99.75 (US and Canada); \$119.50 (All other countries). ISBN 0-8247-8235-6.

With such an ambitious title, it might be doubted that a single book could achieve within 376 pages all that is implied. The cover claims, *inter alia*, that in a single volume it highlights new analytical methods, discusses the elementary chemistry of carbon, sulfur and nitrogen, considers the introduction of the elements into the biosphere through industrialization and energy use...and much more!

It is perhaps unfortunate that rather than concentrating on the analytical methods, the author has used the first 120 pages to outline the history, nature and characteristics of carbon, nitrogen and sulfur pollutants in air and water. With such a wide subject area, this is inevitably a selective outline, which even takes the reader into the electron configuration of the elements. I fear that much of the detailed chemistry and biochemistry might make the book less attractive to engineers than the cover suggests.

The target readership is the non-analytical chemist, although analytical chemists are included with a wide range of engineering professions, food scientists and both undergraduate and graduate students in various disciplines. This wide target and the wide scope of the subject matter within the title make it difficult to produce a really useful book for any single group or topic. In my view the book would have been better had the claims been met of being a practical reference detailing procedures available for the monitoring and control of carbon, sulfur and nitrogen pollutants. Although it certainly reviews a range of analytical techniques, including several modern ones, it does not give practical details of procedures. Consequently, unlike other texts it is unlikely to be of use to those involved in the practice of environmental protection and seeking procedural guidelines. The greatest strength of the book is its inclusion of many of the more recent techniques of environmental analysis, such as immunoassays and ion chromatography.

Care must also be taken in reading the book as the following two examples indicate: atmospheric CO₂ is quoted as leading to a rise of about 1 K in the Earth's average temperature; and in the limited section on sampling, despite much detail on the normal distribution, the point is not made that many environmental data are not normally distributed. Such points may limit the confidence of the reader in the content.

A more limited range of content material, with concentration on the traditional and newer analytical methods, would have made this text far more useful in a topical subject.

R. S. Barratt

Pesticide Residues in Food. Technologies for Detection

By US Congress, Office of Technology Assessment, OTA Workshop Participants, March 14–16, 1989. Pp. 230. Technomic Publishing. 1989. Price SwFr108.00. ISBN 0-87762-667-7.

This report by the Office of Technology Assessment (OTA) was designed to provide a brief assessment of existing, new and emerging analytical technologies and methods to detect pesticide residues in foods for the US House Committee on Energy and Commerce.

It consists of an eight chapter review accompanied by an appendix containing 13 specialist papers, grouped under the

heading of Research in Pesticides, which link-in with the main review.

The review chapters are of somewhat mixed value. That on Federal Pesticide Residues in Food Monitoring Programmes makes interesting background reading but is probably of little importance to the majority of European analysts.

The chapter on Contemporary Analytical Techniques makes a good introduction to pesticide residue analysis for non-specialists but contains a number of dubious statements such as: 'the lack of r.r.t. data for capillary columns is a constraint to their use'; and 'HPLC columns usually last longer because they are not subjected to the extremely high temperatures that GC columns are'. Similarly, AFID and NPD are discussed as though they are fundamentally different.

The chapters on Immunoassay and on Automation give good introductions to these topics and the chapter on Pesticide Analytical Methods gives a good overview of the needs of method development.

Although the contents of this book are not what I would have expected for one entitled Technologies for Detection, it will find a useful place in my collection as background reading for non-specialists and for beginners in the art of pesticide residue analysis.

G. M. Telling

Instrumental Effects in Homodyne Electron Paramagnetic Resonance Spectrometers

By R. Czocho and A. Francik. *Ellis Horwood Series in Analytical Chemistry*. Pp. 395. Ellis Horwood. 1990. Price £45.00. ISBN 0-85312-795-6 (Ellis Horwood); 0-470-20897-X (Halsted Press).

The title of this book summarizes its contents well and, implicitly, many of its limitations. These limitations are aggravated somewhat by the delays that have occurred in its publication: a few of the references date from 1983, none is more recent. This is unfortunate, as the last ten years have seen great strides in instrumentation, particularly with regard to the use of computers.

The book is divided into three parts. The first part, of three chapters, covers a brief introduction to the theory and practice of EPR. The first chapter discusses the basic theory of EPR, before going on to cover line profiles. This is followed by a discussion of the various parts of the instrument (and it is noticeable that the products of one manufacturer are featured prominently!). Finally, in the third chapter, there is a brief summary of the factors affecting precision and accuracy in EPR spectrometers.

The second part of the book, consisting of five chapters, is an examination in much greater detail of the matter covered in Chapter 3. This part deals with via-phenomenon instrumental effects; distortions due to the unwanted effects on the signal of sample absorption and dispersion; receiver errors; background; and a miscellany of other factors.

In its two chapters, the third (and last) part of the book considers the choice of operating parameters, and methods of testing the performance of a spectrometer. It is again noticeable that the products of one manufacturer are prominent.

The age of this book is its major defect—it is no longer timely. There is very little on the problems of digitized spectra, or ways of making the most of them. Pulsed EPR has grown up since this book was first conceived; EPR imaging is likewise too modern for it. Most of its material predates the computer revolution, which took place in the 1980s. As far as it goes though, it is useful.

A very important question is, who will want to read this book? The answer is not obvious. It looks the sort of book to find on the shelf next to the instrument, but is it? If the instrument is a workaday spectrometer, then the users will be interested in getting good spectra out of it. They will not be unduly bothered about why the spectra are occasionally distorted—especially not in considerable mathematical detail. If the spectrometer is used more for research into EPR, then the users would probably want a more up-to-date book. Therefore, I suspect that the potential readership is rather limited, which is unfortunate, because there is some useful material in the book. The most-used chapters will, I suspect, be the last two, unless, of course, the system tests just happen to be very similar to those in the instrument manual!

I suspect that the publishers have realized the problems, and have attempted to keep the costs down—at £45 for 400-odd pages it is not unduly expensive. However, cost saving has sometimes gone too far, for instance, why could they not justify the text on both sides of the page throughout, rather than only in the Preface? Furthermore, the binding is poor. I do not see a wide market for this book: I think it has missed its niche by several years.

David Beveridge

The Biochemistry and Uses of Pesticides. Structure, Metabolism, Mode of Action and Uses in Crop Protection

By Kenneth A. Hassall. Second Edition. Pp. xviii + 536. VCH. 1990. Price DM128.00. ISBN 3-527-28151-7 (VCH, Weinheim); 0-89573-976-3 (VCH, New York).

Although recent legislation and registration requirements have improved safety there is currently considerable interest in the use and abuse of pesticides. Media attention has increased public awareness of the dangers of contamination of the environment and the possibility of toxic substances being present in food. This information packed book is a comprehensive treatise on 'The Biochemistry and Uses of Pesticides'. The author has collated and summarized a wealth of information on the structure, metabolism and mode of action of the enormous number of insecticides, fungicides and herbicides currently used in crop protection.

The second edition summarizes the major developments in the biochemistry of pest control revealing the introduction of new groups of pesticides, which offer control where earlier compounds failed. Particular attention is given to recent developments in the understanding of the metabolism and breakdown of pesticides in the target organism, beneficial insects, crop plants and the environment. This information contributes to the selectivity and safety of these compounds and begins to answer the very necessary ecological questions now being posed on the environmentally friendly use of crop protectants.

The book is written in three parts and contains 16 chapters, the first three setting the general scene on pesticide usage, safety, formulation, application and metabolism. The following six consider various aspects of organophosphorus, carbamate, organochlorine and pyrethroid insecticides, including a chapter on the development and management of insect resistance. The next three chapters deal with fungicides and finally the last four chapters with herbicides. The strengths of the book lie in discussing the sheer variety of pesticides, grouping these into chemically similar compounds, comparing their mode of action and considering developments that enhance their effect under various environmental situations. The book considers in detail pesticide metabolism in the target organism, crop plant and soil, indicating the probable routes of degradation. The safety aspect of metabolic selectivity of

recently developed pesticides with the increased knowledge of pest life-cycles is particularly highlighted. Reduced use of chemical pesticides within integrated pest management programmes is now a genuine possibility resulting in a major reduction in input costs. The author rightly points to the difficulties in transferring these integrated systems to developing countries, where it would transform the efficiency and safety of pest control, because of the lack of trained expertise in the field. For this reason alone the book provides a timely addition to the literature as a handbook for anyone involved in crop protection both in research and in the field.

I found this book easy to read and well presented. There is a good balance between the general review and the factual content of the chapters with numerous schematic diagrams indicating the chemical structures and metabolism. It is the sort of book that, after purchase, becomes essential on the bookshelf as a standard reference or textbook.

R. A. Cole

Chromatographic Adsorption Analysis. Selected Works
By Mikhail Semenovich Tswett. *Ellis Horwood Series in Analytical Chemistry*. Pp. 112. Ellis Horwood. 1990. Price £29.95. ISBN 0-13-132069-6.

Chromatography, in its numerous modern variants, is the most widely employed of analytical techniques. By common consent, M. S. Tswett is seen as the inventor and this slim volume consisting of three of his innovative papers published between 1903 and 1906, his monograph of 1910 and brief biographical and historical appreciations by Professor Berezkin leaves us in no doubt of the validity of this attribution. Of no less interest is Tswett's list of relevant literature, which is not only considerable throughout the 19th century but also stretches back even to the work of Senebier (1782) and Lowitz (1790). The intense interest engendered by 19th century advances in recognition and understanding of physical processes capable of providing a basis for analysis can be judged from the fact that among the hundreds of names cited we find such giants of chemistry as Angstrom, Becquerel, Berthelot, Bunsen, Freundlich, Gibbs, Ostwald, Rayleigh, Stokes and Willstätter. Perhaps the most interesting name in the list is that of Borodin, remembered today for very different reasons!

In Chapter II of his monograph Tswett summarizes five techniques for pigment separation that had been developed in the latter half of the 19th century and argues, correctly as we know, that all were inferior to his own 'adsorption analysis', which from about 1906 he had come to call chromatography. In Chapter VI he outlines partition theory in terms of distribution between immiscible phases and comments, *à propos* liquid-liquid distribution, 'the separation of compounds with similar distribution coefficients would require a huge amount of initial solution and liquids, to say nothing of the time'. In subsequent chapters he elaborates on his view, first advanced in 1900, that the use of adsorptive columns gets around these problems, and illustrates his new technique with numerous examples of successful separations.

His inventiveness does not end there, however, as he recognized the possibilities of the displacement in addition to those of the elution mode, he described the procedure of gradient elution, he identified the benefits of narrow columns and recognized that 'fineness of powder is especially important, since band broadening is obtained when grainy material is used...adsorption being coupled with diffusion in wide capillaries'. One could hardly have a clearer instruction on the eventual route to HPLC!

Given that he had provided both a theoretical and a practical basis for the technique it is remarkable that chromatography subsequently lay fallow until its 're-discovery' in 1930. Perhaps Ettré was right in his assessment that Tswett, a botanist by training and repute and hence not part of the (chemical) establishment, was simply ahead of his time, and so (his work was) doomed to non-acceptance.

The volume provides a good read. The reader will learn little more about chromatography but will learn much about early scientists and the rocky path to scientific development and eventual acceptance of ideas and techniques.

J. H. Purnell

Computer Methods in UV, Visible and IR Spectroscopy
Edited by W. O. George and H. A. Willis. Pp. xi + 216. The Royal Society of Chemistry. Price £39.50. ISBN 0-85186-323-X.

This book is a little gem! Of course I may be biased, as it arrived on my desk at a time when I was struggling to convert a database of compressed JCAMP-IR files to a more easily manipulated form, and on leafing through the text it was a pleasure to find two chapters, well written and well presented, on this very topic. A more serious and devoted study of the book confirmed my initial impressions; this is a well prepared book and a delight to read.

The importance and value of computer methods in modern analytical spectroscopy is well recognized and many books have been published in recent years dealing with this wide field of research and application. This book is different in that it is not a mathematical text or a list of algorithms or programs. It consists of 12 chapters, each an essay from different authors on a specific topic, which can be read independently. The material contained in the book is basically the text of lectures presented at the RSC Residential School of Wales in 1989. The main themes covered include computerized identification of materials from IR spectra using database matching and expert systems, data manipulation and combined (hyphenated) techniques, chemometrics and quantitative analysis and, in the final chapter, a discussion of the advantages and pitfalls of user written software.

Chapter 1 provides an interesting historical background to the development of computerized spectroscopic analysis and, in its discussion of the ground rules of digitization of spectral data, should be read by anyone interested in computer interfacing. Chapter 2 moves on to examine data searching techniques. The requirements for a good spectral library are discussed and the problems of defining similarity of chemical structures are clearly explained. The use of a similarity matrix to assess search efficiency is also dealt with. Chapter 3 provides an overview of expert systems in particular EXSPEC, and their potential role in identifying materials from their spectra.

Four further chapters are devoted to data manipulation, chemometrics and quantitative analysis. Simple procedures, such as spectra subtraction and smoothing, through to Fourier deconvolution and maximum entropy methods are all presented.

Spectroscopy and process control, including NIR analysis, has a chapter to itself, as does the topic of spectroscopic databases for HPLC.

The style and presentation of the text in this book make it easy to read. The depth of treatment in all chapters I found to be right for this type of book and I would not hesitate to recommend this book to all students and practitioners of modern spectroscopic analysis.

M. J. Adams

Plasma Source Mass Spectrometry

Edited by K. E. Jarvis, A. L. Gray, I. Jarvis and J. Williams.
The Proceedings of the Third Surrey Conference on Plasma Source Mass Spectrometry, University of Surrey, 16-19 July, 1989. Pp. viii + 172. The Royal Society of Chemistry. Price £35.00. ISBN 0-85186-567-4.

Despite, or perhaps because it is currently one of the most active areas of analytical science, the vast majority of the published information on plasma source mass spectrometry is to be found in conference proceedings, many of which have very limited exposure, and primary journals. Books on the subject are still very scarce, although one or two more are likely to emerge soon. The publication of this slim volume by The Royal Society of Chemistry in its Special Publication series is, therefore, to be welcomed.

The 12 papers it contains are based on nine of the 30 oral presentations and three of the posters given at the third of the highly respected and successful Surrey Conferences on Plasma Source Mass Spectrometry held at the University of Surrey, Guildford, UK, 16-19 July, 1989. Together they illustrate several of the areas in which fundamental research into inductively coupled plasma mass spectrometry (ICP-MS), in particular, is being conducted and give a flavour of the range of applications of this sensitive, multi-element technique.

The first two papers cover different modes of sample introduction, other than the typical nebulization of liquid samples. Both quote experimental data obtained with ICP-AES rather than MS detection, but which will nevertheless be of interest to ICP-MS users. Processes of Laser Ablation and Vapour Transport to the ICP are reviewed by L. Moenke-Blankenburg *et al.*, who provide a useful summary of some of the basic phenomena, such as laser-target interaction, cell design and transport processes, which are important in this attractive but problematic sample introduction technique. K. Dittrich *et al.* briefly discuss the Introduction of Microsamples into Plasmas using electrothermal vaporization (ETV), and compare results with those obtained by their FANES system. An example of the use of ETV as a means of improving the sample introduction efficiency is described by R. J. B. Hall *et al.* in their paper on The Feasibility of the Use of Electrothermal Vaporization Inductively Coupled Plasma Mass Spectrometry for the Determination of Femtogramme Levels of Plutonium and Uranium in urine. From their Evaluation of ICP-MS for the Determination of Trace and Ultra-trace Elements in Human Serum after Simple Dilution, H. Vanhoe *et al.* were convinced that sample introduction using ETV had potential advantages over pneumatic nebulization for several elements *via* the reduction of polyatomic interferences.

Isobaric overlap of analyte ion peaks by polyatomic ions arising from the plasma background and/or sample matrix are a serious limitation in some applications of ICP-MS to the determination of trace amounts of elements such as As, Se and Fe. The addition of a small amount of oxygen or nitrogen to the plasma has been reported to reduce such interferences. Results of their Investigations on Mixed Gas Plasmas Pro-

duced using a Sheathing Device in ICP-MS are reported by D. Beauchemin and J. M. Craig. An alternative, mathematical approach to minimizing the effects of isobaric interferences in The Determination of Titanium, Copper, and Zinc in Geological Materials by Inductively Coupled Plasma Mass Spectrometry with Multivariate Calibration is described by M. E. Ketterer *et al.* They illustrate the use of multiple linear regression with both external calibration and standard additions in the analysis of NIST Standard Reference Materials.

Most of the few typographical errors in this book seem to be concentrated in the paper by R. C. Hutton *et al.* on Analytical Performance of Analogue Detection in ICP-MS and lead, for example, to the unfortunate claim that the upper working range of conventional pulse counting detection is precisely 106 counts s⁻¹. Fallen superscripts aside, the authors make the important point that the performance of some of the latest ICP-MS instruments is such that the very sensitivity that made the reputation of the technique can now be a limitation. They describe the principles of a commercial analogue mode detection system that can be used in conjunction with pulse counting to extend greatly the potential analytical range.

Sample preparation techniques for the analysis of biological material by ICP-MS are emphasized in two papers. E. J. McCurdy examined the use of open-dish digestion with nitric and perchloric acids for The Preparation of Plant Samples and Their Analysis by ICP-MS. T. Cho *et al.* reported A Basic Study on the Application of Tetramethylammonium Hydroxide (TMAH) Alkaline Digestion for the Determination of Some Volatile Elements by ICP-MS in which they established optimum ICP-MS operating conditions for the digested samples and concluded that the reagent had particular advantages in the determination of several volatile elements.

Advantages in terms of speed and simpler sample preparation in The Determination of Actinides in Environmental Samples by ICP-MS rather than by alpha-spectrometry were highlighted by J. Toole *et al.* Improvements in detection limits of about two orders of magnitude were expected by the use of ETV for sample introduction. J. A. F. Moore *et al.* described The Application of Inductively Coupled Plasma Mass Spectrometry to the Analysis of Iron Materials and concluded that, apart from in the determination of germanium, polyatomic interferences derived from the matrix were largely insignificant.

Perhaps the most 'heavyweight' paper in this book is that by J. M. Richardson *et al.* on Re-Os Isotope Ratio Determinations by ICP-MS: a Review of Analytical Techniques and Geological Applications, which discusses many of the sample preparation difficulties and instrumental limitations that have to be overcome to obtain Re and Os isotopic ratios of acceptable precision for geochronological studies.

Reproduction seems to have been largely from the publisher's high quality camera-ready copy and the editors have clearly taken pains to impose some consistency of layout and style across the contributions. The over-all effect is slightly marred by the longest paper being in a markedly different typeface. The inclusion of a subject index is most welcome. At £35 for a 172-page soft-cover book, it is not cheap, but then few things are in ICP-MS!

Douglas L. Miles

CUMULATIVE AUTHOR INDEX

JANUARY–FEBRUARY 1992

- Abdel-Hay, Mohamed H., 157
 Abuirjeie, Mustafa A., 157
 Aguilar Gallardo, A., 195
 Analytical Methods Committee, 97
 Aydin, Hasan, 43
 Barclay, David, 117
 Boomer, Dave, 19
 Bourgoïn, Bernard P., 19
 Brenes, Manuel, 173
 Cacho, Juan, 31
 Cai, Pei Xiang, 185
 Campbell, Milford B., 121
 Chai, Fong, 161
 Chan, Wing Hong, 185
 Chang, Xi-jun, 145
 Chénieux, Jean-Claude, 77
 Coker, Raymond D., 67
 Dinesan, Maravattickal K., 61
 Edgar, Duarte, 19
 El-Din, Mohie Sharaf, 157
 Evans, Don, 19
 Ferreira, Vicente, 31
 Gaind, Virindar S., 9, 161
 Gajendragad, M. R., 203
 Gao, Wen-yun, 145
 García, Pedro, 173
 García Sánchez, F., 195
 Garrido, Antonio, 173
 Gatford, Christopher, 199
 Hall, Tony, 151
 Haswell, Stephen J., 67, 117
 He, Qiong, 181
 Hendrix, James L., 47
 Hirayama, Kazuo, 13
 Hu, Shengshui, 181
 Juretić, Dubravka, 141
 Kageyama, Susumu, 13
 Kalpana, G., 27
 Kanert, George A., 121
 Korošin, Jancz, 125
 Koshy, Valsamma J., 27
 Kožuh, Nevenka, 125
 Lee, Albert Wai Ming, 185
 Levillain, Pierre, 77
 Lu, Jianmin, 35
 Luo, Xing-yin, 145
 Luterotti, Švjetlana, 141
 Margielewski, Leszek, 207
 Matsuoka, Shiro, 189
 Miao-Kang, Shen, 137
 Midgley, Derek, 199
 Milačić, Radmila, 125
 Milosavljević, Emil B., 47
 Momin, Saschi A., 83
 Montagu, Monique, 77
 Moreno Cordero, Bernardo, 215
 Morikawa, Hidehiro, 131
 Nakamura, Toshihiro, 131
 Narayana, B., 203
 Narayanaswamy, Ramaier, 83
 Nawaz, Sadat, 67
 Nelson, John H., 47
 Nerin, Christina, 31
 Nikolić, Snežana D., 47
 Norris, John D., 3
 Novozamsky, Ivo, 23
 Oka, Hideyuki, 131
 Padalikar, Sudhakar V., 75
 Patil, Vitthal B., 75
 Peddy, Rao V. C., 27
 Pérez Pavón, José Luis, 215
 Petit-Paly, Geneviève, 77
 Plambeck, James Alan, 39
 Plaza, Stanislaw, 207
 Powell, Mark J., 19
 Preston, Brian, 3
 Purdy, William C., 177
 Ransirimal Fernando, Angelo, 39
 Rideau, Marc, 77
 Rocheleau, Marie-Josée, 177
 Ross, Lynn M., 3
 Rusterholz, Bruno, 57
 Sakai, Tadao, 211
 Saleh, Hanaa, 87
 Sanyal, Asis K., 93
 Sato, Jun, 131
 Schneckeburger, J., 87
 Seiler, Kurt, 57
 Sevalkar, Murlidhar T., 75
 Simon, Wilhelm, 57
 Štaden, Jacobus F. van, 51
 Štupar, Jancz, 125
 Su, Zhi-xing, 145
 Syed, Akheel A., 61
 Tabuchi, Toyohisa, 189
 Taha, Ziad, 35
 Temminghoff, Erwin J. M., 23
 Unohara, Nobuyuki, 13
 Vohra, Kusum, 161
 Waki, Hirohiko, 189
 Wang, Joseph, 35
 Wang, Kemin, 57
 Warwick, Peter, 151
 Willie, Scott, 19
 Wu, Weh S., 9
 Xiulin, Wang, 165
 Yahaya, Abdul Hamid, 43
 Yin-Yu, Shi, 137
 Yoshimura, Kazuhisa, 189
 Žanić-Grubišić, Tihana, 141
 Zhan, Guang-yao, 145
 Zhao, Zaofan, 181

Advances in Electrochemical Science and Engineering

Edited by
H. Gerischer and C.W. Tobias

Volume 2

1992. IX, 269 pages with 142 figures and 9 tables. Hardcover.
£ 65.00. Series price: £ 59.00.
ISBN 3-527-28273-4

To order please contact your local bookseller or:
VCH, 8 Wellington Court, Cambridge CB1 1HZ, UK
VCH, P.O. Box 10 11 61, D-6940 Weinheim
VCH, Hardstrasse 10, P.O. Box, CH-4020 Basel
VCH, 220 East 23rd Street, New York, NY 10010-4606, USA
(toll free: 1-800-367-8249)

This is the second volume of the new series which continues the highly successful "Advances in Electrochemistry and Electrochemical Engineering". The series covers advanced topics in fundamental and applied electrochemistry and engineering.

The first volume met with great success:

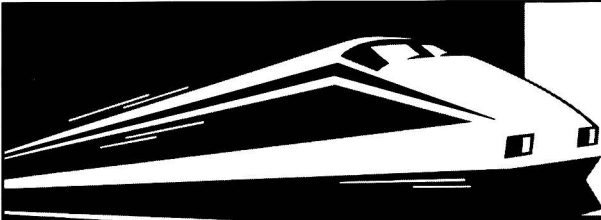
"The editors must be congratulated on the first volume of this reborn series, which will be read with pleasure and profit by many."

Journal of Electroanalytical Chemistry


Volume 1
1990. XI, 296 pages with 163 figures and 15 tables. Hardcover. £ 65.00.
Series price: £ 59.00.
ISBN 3-527-27884-2



Circle 004 for further information



STN Express®: the fast track to searching scientific databases



Easy connection to STN®

Step aboard STN Express® (for the IBM® AT and PS/2 and Apple® Macintosh), the software that will quickly log you on to STN International® and help you prepare your questions *offline*, before online charges are incurred. Then you can upload and execute your search and produce *print-quality output of both text and graphics*.

Easy structure searching

You can draw structures freehand or with templates or venture into molecular modeling. Once you've defined the structure the way you pictured it, *search for it among the 10 million structure diagrams in the CAS Registry file*. Was there a match? If so, that's a valuable piece of information. No match? Knowing that could be *invaluable*.

Let STN Express introduce you to online searching and STN International. They'll take you searching where you've never been before.

YES! Please send me the FREE STN Express evaluation package.

Name

Position

Address

Phone

Enquirers from Eire or UK, please return to: STN International, c/o Royal Society of Chemistry, Thomas Graham House, Science Park, Milton Road, Cambridge CB4 4WF, United Kingdom
STN Help Desk (0223) 420237

Circle 006 for further information

THE ANALYST READER ENQUIRY SERVICE
For further information about any of the products featured in this issue write the appropriate number on the postcard, detach and post.

THE ANALYST READER ENQUIRY SERVICE

FEB'92

Postage paid if posted in the British Isles but overseas readers must affix a stamp.

[illegible]

Valid 12 months

[illegible][illegible]

16

[illegible][illegible][illegible][illegible][illegible][illegible][illegible]

REC'D

--	--	--	--

Postage
will be
paid by
Licensee

Do not affix Postage Stamps if posted in Gt. Britain,
Channel Islands, N. Ireland or the Isle of Man

BUSINESS REPLY SERVICE
Licence No. WD 106

Reader Enquiry Service
The Analyst
The Royal Society of Chemistry
Burlington House, Piccadilly
LONDON
W1E 6WF
England

2

FOURTH SYMPOSIUM ON KINETICS IN ANALYTICAL CHEMISTRY (KAC '92)

**September 27-30, 1992
Erlangen, Germany**

You are cordially invited to participate in the 4th Meeting on Kinetics in Analytical Chemistry (KAC). This conference is intended to continue the series of KAC meetings which started in Cordoba, Spain (1983) and then Preveza, Greece (1986) and Cavtat, Yugoslavia (1989).

The meeting will be particularly important to all scientists involved in kinetic techniques in analytical chemistry and will provide a forum where interesting and useful applications of kinetics can be reported and discussed. In addition to keynote lectures there will be poster sessions and a social programme for delegates and their guests.

The scientific programme will include the following themes:

Kinetic determination of substances because of their catalytic or inhibitory effect
Differential rate methods
Electrochemical methods (e.g., electrocatalysis and chemically modified electrodes)
Flow methods (e.g., flow injection)
Chromatographic methods
Chemical and biochemical sensors
Applications of luminescence
Kinetics in pharmaceutical analysis
Instrumentation
Environmental

Scientific Committee:

Professor K. Cammann (*Munster, Germany*)
Professor U. Nickel (*Erlangen, Germany*)
Professor M. D. Perez-Bendito (*Cordoba, Spain*)

Professor H. A. Mottola (*Stillwater, USA*)
Professor H. L. Pardue (*West Lafayette, USA*)
Professor G. Werner (*Leipzig, Germany*)

Local Organizers:

Professor Dr. U. Nickel (*Erlangen*)
Mrs. B. Thormann (*Erlangen*)

Further information can be obtained from the following address:

**Professor Dr. Ulrich Nickel, Institute of Physical and Theoretical Chemistry, Egerlandstrasse 3,
D-W-8520 Erlangen, Germany.**

**Telephone: +49 9131 857334
Telefax: +49 9131 858307**

The KAC '92 meeting is held in cooperation with the "Fachgruppe 'Analytische Chemie' in der Gesellschaft Deutscher Chemiker".

The Analyst

The Analytical Journal of The Royal Society of Chemistry

CONTENTS

- 117 **On-line Microwave Digestion of Slurry Samples With Direct Flame Atomic Absorption Spectrometric Elemental Detection**—Stephen J. Haswell, David Barclay
- 121 **High-pressure Microwave Digestion for the Determination of Arsenic, Antimony, Selenium and Mercury in Oily Wastes**—Milford B. Campbell, George A. Kanert
- 125 **Critical Evaluation of Three Analytical Techniques for the Determination of Chromium(vi) in Soil Extracts**—Radmila Milačić, Janez Štupar, Nevenka Kožuh, Janez Korošin
- 131 **Determination of Lithium, Beryllium, Cobalt, Nickel, Copper, Rubidium, Caesium, Lead and Bismuth in Silicate Rocks by Direct Atomization Atomic Absorption Spectrometry**—Toshihiro Nakamura, Hideyuki Oka, Hidehiro Morikawa, Jun Sato
- 137 **Determination of Lanthanum in Food and Water Samples by Zeeman-effect Atomic Absorption Spectrometry Using a Graphite Tube Lined With Tungsten Foil**—Shen Miao-Kang, Shi Yin-Yu
- 141 **Rapid and Simple Method for the Determination of Copper, Manganese and Zinc in Rat Liver by Direct Flame Atomic Absorption Spectrometry**—Svjetlana Luterotti, Tihana Žanić-Grubišić, Dubravka Juretić
- 145 **Synthesis of a Morin Chelating Resin and Enrichment of Trace Amounts of Molybdenum and Tungsten Prior to Their Determination by Inductively Coupled Plasma Optical Emission Spectrometry**—Xing-yin Luo, Zhi-xing Su, Wen-yun Gao, Guang-yao Zhan, Xi-jun Chang
- 151 **High-performance Liquid Chromatographic Study of Nickel Complexation With Humic and Fulvic Acids in an Environmental Water**—Peter Warwick, Tony Hall
- 157 **Simultaneous Determination of Theophylline and Guaiphenesin by Third-derivative Ultraviolet Spectrophotometry and High-performance Liquid Chromatography**—Mohamed H. Abdel-Hay, Mohie Sharaf El-Din, Mustafa A. Abuirjeie
- 161 **Determination of Tricarbonyl(2-methylcyclopentadienyl)manganese in Gasoline and Air by Gas Chromatography With Electron-capture Detection**—Virindar S. Gaiind, Kusum Vohra, Fong Chai
- 165 **Fourier Transform Infrared Spectroscopic Studies on the Interaction Between Copper(II), Amino Acids and Marine Solid Particles**—Wang Xiulin
- 173 **Rapid Indirect Method for Determining the Sodium Content of Table Olives**—Pedro García, Manuel Brenes, Antonio Garrido
- 177 **Ion-selective Electrode With Fixed Quaternary Phosphonium Ion-sensing Species**—Marie-Josée Rocheleau, William C. Purdy
- 181 **Determination of Trace Amounts of Estriol and Estradiol by Adsorptive Cathodic Stripping Voltammetry**—Shengshui Hu, Qong He, Zaofan Zhao
- 185 **Differential-pulse Polarographic Microdetermination of Reactive Organohalides via *In Situ* Generation of *S*-Alkylisothiuronium Salts**—Wing Hong Chan, Albert Wai Ming Lee, Pei Xiang Cai
- 189 **Application of Ion-exchanger Phase Spectrofluorimetry to the Determination of Micro-amounts of Some Rare Earth Elements by Flow Analysis**—Kazuhisa Yoshimura, Shiro Matsuoka, Toyohisa Tabuchi, Hirohiko Waki
- 195 **Spectrofluorimetric Determination of the Insecticide Azinphos-methyl in Cultivated Soils Following Generation of a Fluorophore by Hydrolysis**—F. García Sánchez, A. Aguilar Gallardo
- 199 **Linear Titration Plot for the Determination of Boron in the Primary Coolant of a Pressurized Water Reactor**—Derek Midgley, Christopher Gatford
- 203 **Complexometric Determination of Copper in Isolation, Alloys and Complexes Using DL-Cysteine as a Selective Masking Agent**—B. Narayana, M. R. Gajendragad
- 207 **Analysis of Mixtures of Dialkyldithiophosphate, Bis(dialkoxythiophosphinoyl) Disulfide and Elemental Sulfur**—Leszek Margielewski, Stanislaw Plaza
- 211 **Spectrophotometric Determination of Quaternary Ammonium Salts by a Flow Injection Method Coupled With Thermochromism of Ion Associates**—Tadao Sakai
- 215 **Micellar Systems in Flow Injection: Determination of Gadolinium With 1-(2-Pyridylazo)-2-naphthol in the Presence of Triton X-100**—José Luis Pérez Pavón, Bernardo Moreno Cordero
- 219 **BOOK REVIEWS**
- 227 **CUMULATIVE AUTHOR INDEX**

